

UNIVERSIDADE FEDERAL DO RIO GRANDE DO SUL  
Programa de Pós-Graduação em Biologia Celular e Molecular

**Especificidade de substrato e mecanismo cinético da enzima fosforilase de  
nucleosídeos purínicos de *Mycobacterium tuberculosis***

**Rodrigo Gay Ducati**

Tese submetida ao Programa de Pós-Graduação  
em Biologia Celular e Molecular da UFRGS  
como requisito parcial para a obtenção do grau  
de Doutor em Ciências

Orientador: Prof. Dr. Luiz Augusto Basso

Porto Alegre, Março de 2009

Esta Tese foi julgada adequada para a obtenção do grau de Doutor em Ciências, tendo sido aprovada em sua forma final pelo Orientador e pela Banca Examinadora do Programa de Pós-Graduação em Biologia Celular e Molecular da Universidade Federal do Rio Grande do Sul.

**Orientador:**

Prof. Dr. **Luiz Augusto Basso** - Professor do Programa Pós-Graduação em Biologia Celular e Molecular e Professor adjunto da Faculdade de Biociências, Pontifícia Universidade Católica do Rio Grande do Sul (PUCRS / Porto Alegre).

**Banca Examinadora:**

Prof. Dr. **Luiz Juliano Neto** - Professor titular do Departamento de Biofísica da Escola Paulista de Medicina, Universidade Federal de São Paulo (UNIFESP / São Paulo).

Prof. Dr. **Arthur Germano Fett Neto** - Professor do Programa de Pós-Graduação em Biologia Celular e Molecular e Professor titular do Departamento de Botânica, Universidade Federal do Rio Grande do Sul (UFRGS / Porto Alegre).

Prof. Dr. **André Arigony Souto** - Professor do Programa Pós-Graduação em Biologia Celular e Molecular e Professor adjunto da Faculdade de Química, Pontifícia Universidade Católica do Rio Grande do Sul (PUCRS / Porto Alegre).

Prof. Dr. **Osmar Norberto de Souza** (suplente) - Professor do Programa Pós-Graduação em Biologia Celular e Molecular e Professor adjunto da Faculdade de Informática, Pontifícia Universidade Católica do Rio Grande do Sul (PUCRS / Porto Alegre).

O presente trabalho foi integralmente desenvolvido no Centro de Pesquisas em Biologia Molecular e Funcional (CPBMF) do Instituto de Pesquisas Biomédicas (IPB) da PUCRS, sendo financiado com recursos do Instituto do Milênio - CNPq/MCT, da Coordenação de Aperfeiçoamento de Pessoal de Nível Superior (CAPES) e do Conselho Nacional de Desenvolvimento Científico e Tecnológico (CNPq).

Dedico este trabalho aos meus pais, Maria Beatriz de Leone Gay e Jorge Ricardo Ducati, aos quais admiro pelo empenho e ética no desenvolvimento da pesquisa científica no Brasil. Serei eternamente grato pelo constante incentivo e apoio.

## AGRADECIMENTOS

Ao Prof. Dr. Diógenes Santiago Santos, por me aceitar como estudante do grupo de pesquisa que lidera e me dar a oportunidade de realizar este trabalho em um laboratório de alto nível.

Ao Prof. Dr. Luiz Augusto Basso, por me ensinar a fazer ciência no sentido pleno da palavra.

Ao Prof. Dr. André Arigony Souto pela revisão da Tese, e aos demais membros da Banca Examinadora pela importante contribuição para a melhor avaliação deste trabalho.

Ao Programa de Pós-Graduação em Biologia Celular e Molecular da UFRGS pela oportunidade da realização desta etapa.

Ao Prof. Dr. Arthur Germano Fett Neto e ao Prof. Dr. Giancarlo Pasquali, membros da Comissão de Acompanhamento, pelo monitoramento do trabalho desenvolvido.

À Sílvia Regina Centeno e ao Luciano Saucedo, pelo exemplar profissionalismo e eficiência no auxílio em questões burocráticas e logísticas.

Ao amigo e colega Dr. Rafael Guimarães da Silva pelos valiosos conselhos e, principalmente, incentivos, além da amizade.

Aos demais colegas, funcionários e técnicos do laboratório pela amizade, irrestrita ao ambiente de trabalho.

Ao meu irmão, Gabriel Gay Ducati, pela amizade e companheirismo.

À CAPES e, posteriormente, ao CNPq, pela concessão da bolsa de estudos e ao Instituto do Milênio - CNPq/MCT pelo importante apoio financeiro.

## ÍNDICE

<b>APRESENTAÇÃO DA TESE</b> .....	8
<b>ABREVIATURAS</b> .....	10
<b>RESUMO</b> .....	12
<b>ABSTRACT</b> .....	13
<b>1. INTRODUÇÃO</b> .....	14
<b>1.1. Histórico</b> .....	15
<b>1.2. Ressurgimento e epidemiologia</b> .....	19
<b>1.3. Transmissão, infectividade e imunopatologia</b> .....	21
<b>1.4. O bacilo de Koch</b> .....	24
<b>1.4.1. A parede celular micobacteriana</b> .....	26
<b>1.4.2. Análise genômica de <i>Mycobacterium tuberculosis</i></b> .....	27
<b>1.5. Latência e reativação</b> .....	29
<b>1.6. Tuberculose resistente a drogas</b> .....	30
<b>1.7. O sinergismo entre TB e AIDS</b> .....	31
<b>1.8. Métodos de diagnóstico</b> .....	32
<b>1.9. Desenvolvimento de vacinas</b> .....	34
<b>1.10. Quimioterapia</b> .....	35
<b>1.11. A busca de alvos para o desenvolvimento de novas drogas</b> .....	37
<b>1.11.1. Rota de salvamento de purinas e fosforilase de nucleosídeos purínicos</b> .....	39
<b>2. OBJETIVOS</b> .....	46
<b>2.1. Objetivo geral</b> .....	46
<b>2.2. Objetivos específicos</b> .....	46

<b>3. ARTIGO 1:</b> DUCATI, R. G.; RUFFINO-NETTO, A.; BASSO, L. A. & SANTOS, D. S. The resumption of consumption - a review on tuberculosis. <i>Mem. Inst. Oswaldo Cruz</i> , 101(7): 697-714, 2006. ....	47
<b>4. ARTIGO 2:</b> DUCATI, R. G.; SANTOS, D. S. & BASSO, L. A. Substrate specificity and kinetic mechanism of purine nucleoside phosphorylase from <i>Mycobacterium tuberculosis</i> . <i>Arch. Biochem. Biophys.</i> (no prelo). ....	48
<b>5. DISCUSSÃO</b> .....	49
<b>6. CONCLUSÕES E PERSPECTIVAS</b> .....	61
<b>7. REFERÊNCIAS BIBLIOGRÁFICAS</b> .....	63
<b>8. APÊNDICES</b> .....	69
<b>8.1. ARTIGO 3:</b> TIMMERS, L. F.; CACERES, R. A.; VIVAN, A. L.; GAVA, L. M.; DIAS, R.; DUCATI, R. G.; BASSO, L. A.; SANTOS, D. S. & DE AZEVEDO, W. F., JR Structural studies of human purine nucleoside phosphorylase: towards a new specific empirical scoring function. <i>Arch. Biochem. Biophys.</i> , 479(1): 28-38, 2008. ....	70
<b>8.2. ARTIGO 4:</b> DUCATI, R. G.; BASSO, L. A. & SANTOS, D. S. Mycobacterial shikimate pathway enzymes as targets for drug design. <i>Curr. Drug Targets</i> , 8(3): 423-435, 2007. ....	71
<b>9. CURRICULUM VITAE resumido</b> .....	72

## APRESENTAÇÃO DA TESE

A presente Tese de doutorado foi desenvolvida no período de Março de 2005 à Fevereiro de 2009 sob orientação do Prof. Dr. Luiz Augusto Basso. A seção de Introdução contém uma revisão bibliográfica abrangente sobre a tuberculose humana, de forma a apresentar a atual condição desta doença no mundo. Os dados apresentados evidenciam a urgente necessidade da geração de novos agentes quimioterápicos com atividade seletiva contra o *Mycobacterium tuberculosis*. Um dos alvos de estudo, a enzima fosforilase de nucleosídeos purínicos, constitui o tema principal desta Tese.

As seções de Materiais e Métodos e Resultados estão apresentadas na forma de uma coletânea de trabalhos, desenvolvidos durante o período supracitado, que reportam as análises teóricas e resultados experimentais de maior relevância para o foco principal desta Tese. Os trabalhos aqui apresentados são os seguintes: “The resumption of consumption - A review on tuberculosis”, uma revisão da literatura, com uma abordagem e cobertura mais ampla, no que se refere ao conhecimento existente sobre a tuberculose; este Artigo (Artigo 1) foi publicado no periódico “*Memórias do Instituto Oswaldo Cruz*” em Novembro de 2006. “Substrate specificity and kinetic mechanism of purine nucleoside phosphorylase from *Mycobacterium tuberculosis*”, um trabalho que aborda o estudo da especificidade de substrato e do mecanismo cinético e químico da reação catalisada pela enzima fosforilase de nucleosídeos purínicos de *M. tuberculosis*; este Artigo (Artigo 2) foi recentemente aceito para publicação no periódico “*Archives of Biochemistry and Biophysics*”.

A seção de Discussão é centrada na descrição simplificada e interpretação dos resultados obtidos no trabalho referente ao Artigo 2. A seção de Conclusões e Perspectivas



apresenta uma avaliação sintética final sobre o conjunto de resultados que integram o referido Artigo e os futuros estudos que podem contribuir para a continuação do trabalho.

Por fim, após a seção de Referências Bibliográficas, estão apresentados, como Apêndices, os trabalhos desenvolvidos durante o período supracitado que não fazem parte do corpo principal da Tese. Os Artigos publicados que estão nesta seção resultaram de atividades realizadas pelo presente autor em projetos paralelos. Os trabalhos aqui apresentados são os seguintes: “Structural studies of human purine nucleoside phosphorylase: Towards a new specific empirical scoring function”, um trabalho que propõe uma nova função escore empírica específica para a família de PNPs com o intuito de avaliar a afinidade de ligação do complexo proteína-ligante, como também dos resultados de simulações de *docking* rígido. Como objeto de estudo, foi utilizada a enzima fosforilase de nucleosídeos purínicos humana; este Artigo (Artigo 3) foi publicado no periódico “*Archives of Biochemistry and Biophysics*” em Novembro de 2008. “Mycobacterial shikimate pathway enzymes as targets for drug design”, uma revisão da literatura que estuda o potencial das enzimas que compõem a via do chiquimato como alvos promissores para o desenvolvimento de novos agentes antimicobacterianos; este Artigo (Artigo 4) foi publicado no periódico “*Current Drug Targets*” em Março de 2007.

## ABREVIATURAS

As abreviaturas usadas na Tese foram mantidas segundo o padrão do Artigo 2, que compõe o corpo principal da mesma, estando presentes ao longo do texto e/ou nas legendas das figuras.

**2dGuo:** 2'-desoxiguanosina

**2dIno:** 2'-desoxiinosina

**7mGuo:** 7-metilguanina

**ADD:** adenosina desaminase

**Ade:** adenina

**Ado:** adenosina

**ADOK:** adenosina quinase

**AIDS:** síndrome da imunodeficiência adquirida (*acquired immune deficiency syndrome*)

**APRT:** adenina fosforribosiltransferase (*adenine phosphoribosyl transferase*)

**BCG:** bacilo de Calmette e Guérin

**DNK:** desoxinucleosídeo quinase

**DOTS:** terapia de curta duração de observação direta (*directly observed treatment short-course*)

**Gua:** guanina

**Guo:** guanosina

**HGPRT:** hipoxantina-guanina fosforribosiltransferase (*hypoxanthine-guanine phosphoribosyl transferase*)

**HIV:** vírus da imunodeficiência humana (*human immunodeficiency virus*)

**HsPNP:** PNP humana

**Hx:** hipoxantina

**ImmH:** Imucilina-H (*Immucillin-H*)

**Ino:** inosina

**IPTG:** isopropil  $\beta$ -D-tiogalactopiranosídeo (*isopropyl  $\beta$ -D-thiogalactopyranoside*)

**$k_{cat}$ :** constante catalítica

**$K_d$ :** constante de dissociação global

**$K_M$ :** constante de dissociação global (*Michaelis constant*)

**MDR-TB:** tuberculose resistente a múltiplas drogas (*multidrug-resistant tuberculosis*)

**MESG:** 7-metil-6-tio-guanosina

**MtPNP:** PNP de *M. tuberculosis*

**pb:** pares de bases

**$P_i$ :** fosfato inorgânico

**PNP:** fosforilase de nucleosídeos purínicos (*purine nucleoside phosphorylase*)

**ppGpp:** guanosina 3',5'-bis(difosfato)

**R1P:** ribose 1-fosfato (*ribose 1-phosphate*)

**RelA:** (p)ppGpp sintetase I

**RR:** ribonucleotídeo redutase

**SPR:** ressonância plasmônica de superfície (*surface plasmon resonance*)

**TB:** tuberculose humana

**Th:** T auxiliar (*T helper*)

**XDR-TB:** tuberculose extensivamente resistente a drogas (*extensively drug-resistant tuberculosis*)

**XOX:** xantina oxidase

## RESUMO

A tuberculose humana (TB), causada pelo *Mycobacterium tuberculosis*, continua sendo uma ameaça à saúde pública no mundo, tendo resistido às tentativas da história da humanidade em derrotar a consumição. A emergência de cepas resistentes a drogas levaram à urgente necessidade do desenvolvimento de novos compostos anti-TB. Estes agentes quimioterápicos podem ser desenhados baseados em vias metabólicas que sejam essenciais ao patógeno. Há uma necessidade contínua de estudos do metabolismo micobacteriano, como tentativa de identificar enzimas de relevância biológica, uma vez que estas podem representar alvos promissores para o desenvolvimento de novos agentes anti-TB. A fosforilase de nucleosídeos purínicos de *M. tuberculosis* (MtPNP), uma enzima chave da rota de salvamento de purinas, foi recentemente proposta como sendo essencial para a sobrevivência micobacteriana. Foi sugerido que esta enzima possa desempenhar um papel no processo de latência. Entretanto, não houve nenhum relato sobre o mecanismo enzimático e especificidade de substrato de MtPNP. No presente trabalho, demonstramos que MtPNP é mais específica por 2'-desoxiguanosina (2dGuo) e não catalisa a fosforólise de adenosina. Dados de velocidade inicial, inibição por produto e ligação em equilíbrio sugerem que MtPNP catalisa a fosforólise de 2dGuo por um mecanismo cinético ordenado em estado estacionário do tipo bi bi, onde o fosfato inorgânico liga-se primeiro, seguido pela ligação de 2dGuo para formar o complexo ternário cataliticamente competente, e ribose 1-fosfato é o primeiro produto a se dissociar, seguido pela guanina. Dados de cinética em estado pré-estacionário indicam que a liberação de produto é o passo limitante da velocidade para a reação catalisada por MtPNP. Os resultados aqui descritos deverão ser úteis para o desenho de inibidores de MtPNP com potencial ação contra *M. tuberculosis*.

## ABSTRACT

Human tuberculosis (TB), caused by *Mycobacterium tuberculosis*, remains a public health threat worldwide, resisting through the historic attempts of humanity on defeating consumption. The emergence of drug-resistant strains has led to an urgent need for the development of new anti-TB compounds. These chemotherapeutic agents can be designed based on metabolic pathways which are essential for the pathogen. There is a continuous requirement for studies on mycobacterial metabolism, as an attempt to identify enzymes of biological significance, as these might represent promising targets for the development of new anti-TB agents. *M. tuberculosis* purine nucleoside phosphorylase (MtPNP), a key enzyme of the purine salvage pathway, has been recently proposed to be essential for mycobacterial survival. It has been suggested that this enzyme may play a role in the latency process. However, there has been no report on MtPNP enzyme mechanism and substrate specificity. In the present work, we demonstrate that MtPNP is more specific to 2'-deoxyguanosine (2dGuo) and does not catalyze the phosphorolysis of adenosine. Initial velocity, product inhibition and equilibrium binding data suggest that MtPNP catalyzes 2dGuo phosphorolysis by a steady-state ordered bi bi kinetic mechanism, in which inorganic phosphate binds first followed by 2dGuo binding to form the catalytically competent ternary complex, and ribose 1-phosphate is the first product to dissociate followed by guanine. Pre-steady-state kinetic data indicate that product release is the rate-limiting step for MtPNP-catalyzed reaction. The results described here should be useful to the design of MtPNP inhibitors with potential action against *M. tuberculosis*.

## 1. INTRODUÇÃO

A tuberculose humana (TB) é uma doença infecto-contagiosa causada principalmente pelo *Mycobacterium tuberculosis*, uma bactéria patogênica aeróbica que estabelece sua infecção preferencialmente em macrófagos alveolares do sistema pulmonar. O desenvolvimento da doença é fundamentalmente regulado pela integridade do sistema imune do hospedeiro, que pode determinar a imediata eliminação do microrganismo, ou mesmo condicioná-lo a um estado de latência. A incapacidade imunológica em conter a evolução da infecção primária provê ao patógeno condições ideais de crescimento, de forma que este, por sua vez, passa a desencadear, conseqüentemente, a doença ativa em seu hospedeiro.

Esta doença tem acompanhado e afligido a humanidade ao longo de séculos de sua história, sendo responsável pela morte de milhões de pessoas, devido principalmente à carência de métodos adequados para o tratamento de enfermos. Apesar de a TB ter sido considerada erradicada a partir da segunda metade do século XX, devido à introdução de drogas para combater o patógeno e vacinas para prevenir o estabelecimento de sua infecção, reconhece-se hoje que esta doença é responsável pela maior parte das mortes humanas causadas por um único agente infeccioso. A ressurgência desta doença em países desenvolvidos se deve a fatores essencialmente antrópicos, como a recente pandemia de HIV/AIDS e o desenvolvimento de linhagens resistentes a drogas, resultantes de tratamentos inapropriados e/ou ineficientes.

Desta forma, faz-se necessário um maior investimento na pesquisa, de maneira a controlar a doença a partir do desenvolvimento de novas drogas a serem introduzidas no

tratamento de pacientes com TB ativa, e da otimização de vacinas de ação profilática ou mesmo terapêutica, de forma a atuar especificamente contra o bacilo causador da TB.

## 1.1. Histórico

A partir da segunda metade do século XVII, a grande peste branca conquistou o título de “capitã de todas as mortes humanas” por John Bunyan, quando esta já atingia substanciais índices de mortalidade no continente europeu. A mesma doença que dizimou populações no final do século XIX e início do século XX, é hoje a principal infecção causadora de mortes em adultos no mundo devido a um único agente patogênico (DANIEL, 1997). Apesar de ter sido provavelmente descrita pela primeira vez em textos indianos, a TB pulmonar é conhecida desde os tempos de Hipócrates como tísica, termo de origem grega utilizado para referir-se ao enfraquecimento ou desgaste corpóreo (CASTIGLIONI, 1993). O efeito devastador desta patologia tem sido acompanhado durante séculos pela humanidade, ao longo dos quais serviu de inspiração para a realização de fantásticas descobertas científicas e para a produção de magníficas obras de arte.

Em 1680, o pesquisador francês Franciscus Sylvius (Figura 1A) realizou estudos anátomo-patológicos da doença em nódulos pulmonares de vítimas de TB, aos quais denominou de tubérculos (origem do nome da doença), observando sua evolução para úlceras pulmonares. Muitos dos grandes patologistas da época acreditavam se tratarem de tumores ou glândulas anormais, descartando qualquer possível origem infecciosa. Entretanto, a primeira especulação confiável quanto à sua natureza infecciosa foi inferida somente 42 anos mais tarde, quando o médico britânico Benjamin Marten propôs que a TB seria transmitida pela exalação de uma pessoa doente, inalada por uma pessoa sadia,

tornando-a então doente (CASTIGLIONI, 1993). Finalmente, em 1865, o cirurgião militar francês Jean-Antoine Villemin (Figura 1C) demonstrou formalmente a propriedade infecto-contagiosa da doença em modelos animais. Apesar desta demonstração científica, estes resultados experimentais foram ignorados por seus colegas durante muitos anos (VILLEMIN, 1865).



**Figura 1.** Cinco pesquisadores que realizaram importantes descobertas sobre a TB, em ordem cronológica, respectivamente. A. Franciscus Sylvius - 1680; B. Richard Morton - 1689; C. Jean-Antoine Villemin - 1865; D. Robert Koch - 1882; E. Albert Calmette - 1908/1921.

Com a doença definitivamente estabelecida entre todas as classes de cidadãos europeus e afligindo muitos dos intelectuais e artistas do continente na metade do século XIX, a TB viveu uma época de “romantização”, quando sintomas enfêrmicos clássicos, como a esqualidez e palidez passaram a ser considerados sinais de beleza e status (DANIEL, 1997); esta renovação conceitual foi claramente retratada em pinturas da época, como na obra de William Morris (Figura 2A), que esboça toda a beleza da lendária Guinevere, esposa do Rei Arthur, que já apresentava os sintomas iniciais da doença. Outro famoso exemplo é o da bela e jovem Simonetta Vespucci (Figura 2B), vitimada pela TB ainda aos 23 anos, após ter posado para Sandro Botticelli; o artista se inspirou na modelo,



produzindo uma de suas obras mais célebres, de caráter profano e mitológico, O nascimento de Vênus (Figura 2C), onde a retrata sobre uma concha, emergindo da espuma do mar, para simbolizar o nascimento da beleza a partir do nu feminino.

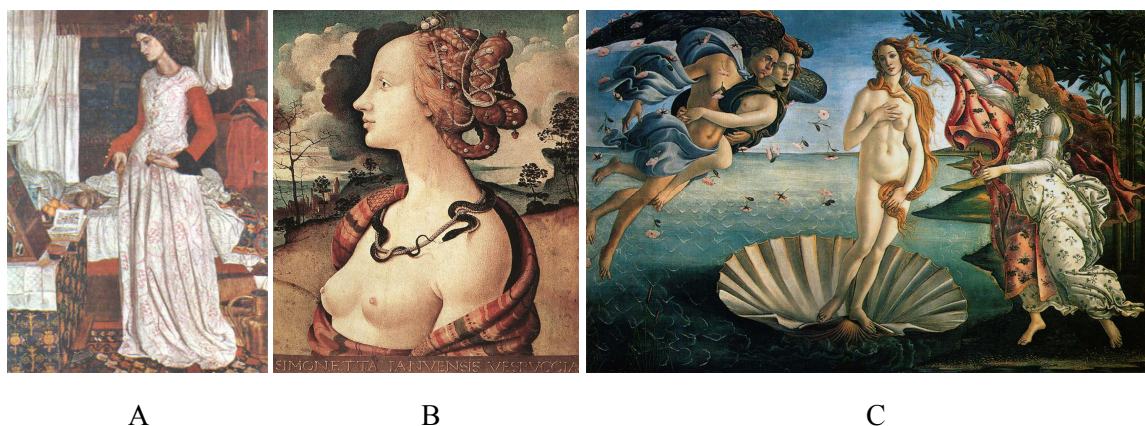


**Figura 2.** Representativas obras de arte da época de romantização da TB. A. Guinevere, de William Morris; B. Simonetta Vespucci; C. O nascimento de Vênus, de Sandro Botticelli.

Um dos trabalhos de maior prestígio na pesquisa sobre a TB foi realizado por um dos grandes cientistas do século XIX, o médico e bacteriologista alemão Robert Koch (Figura 1D), que conseguiu isolar e cultivar *M. tuberculosis*, identificando-o como o agente etiológico da doença, no ano de 1882 (KOCH, 1882). Oito anos de dedicação à pesquisa experimental resultaram, em 1890, na produção de um filtrado de cultura denominado tuberculina, para o qual atribuiu propriedades de cura da doença; entretanto, seu otimismo exagerado o condenou a uma profunda frustração, da qual nunca viria a se recuperar. Alguns anos mais tarde, após ser parcialmente purificado, este mesmo filtrado tornou-se a principal ferramenta utilizada no diagnóstico deste tipo de infecção, sendo atualmente conhecido como teste dermatológico de reatividade à tuberculina (DANIEL, 1997).

Em 1896, o bacteriologista americano Theobald Smith demonstrou que a tuberculose bovina parecia não ser causada pelo *M. tuberculosis*, mas por uma outra espécie micobacteriana, *M. bovis* (DANIEL, 1997). Em 1908, o casal Albert Calmette (Figura 1E) e Camille Guérin isolou esta variante a partir de tubérculos bovinos e a cultivou experimentalmente. A análise da 39ª geração revelou a existência de uma variante morfológica avirulenta em modelos animais, e que os imunizava a desafios contra *M. tuberculosis*. Treze anos de pesquisa possibilitaram a obtenção da 231ª geração, a qual foi administrada pela primeira vez como vacina em humanos para imunizar uma criança cuja mãe havia morrido durante o parto, vítima de TB (CALMETTE, 1927). Esta vacina, posteriormente denominada de bacilo de Calmette e Guérin (BCG), passou a ser utilizada mundialmente no combate à TB, a partir da administração infantil profilática de bacilos atenuados vivos (DANIEL, 1997).

A partir da descoberta do bacilo de Koch, instituir-se-iam diversas terapias visando o tratamento de tuberculosos. Uma das primeiras investidas em combater a doença foi realizada em 1884 por Edward Livingston Trudeau, que, após se recuperar da doença, estabeleceu o primeiro sanatório norte-americano, baseado no descanso, ar fresco e dieta equilibrada. Visto que os índices de recuperação jamais foram representativos, fez-se necessária a instituição de drogas terapêuticas. A introdução de antibióticos como estreptomicina, isoniazida e ácido para-amino-salicílico revolucionaram a quimioterapia contra a doença ativa, reduzindo consideravelmente a mortalidade por TB. Posteriormente, surgiram outras drogas, como etambutol e rifampicina (BLOOM & MURRAY, 1992; DANIEL, 1997).

## 1.2. Ressurgimento e epidemiologia

No ano de 1993, a TB foi declarada uma questão de urgência à saúde pública global pela Organização Mundial da Saúde, sendo a única doença a receber esta designação até então. No entanto, a mesma pôde ser considerada reemergente apenas em alguns países desenvolvidos (europeus e norte americanos), visto que esta constitui um problema presente a longo prazo em nações subdesenvolvidas como o Brasil (RUFFINO-NETTO, 2002). Seu gradual ressurgimento em países desenvolvidos tem sido atribuído principalmente a fatores como: o aumento na incidência de cepas resistentes a drogas; a epidemia de HIV/AIDS surgida no início da década de 1980; a baixa adesão dos pacientes ao tratamento; o aumento no número de usuários de drogas injetáveis; mudanças na estrutura social; o aumento no número de imigrantes oriundos de países com uma alta prevalência da doença; o envelhecimento da população mundial; o aumento do número de ambientes de aglomeração humana, onde o bacilo é facilmente transmitido; e a deterioração dos sistemas de saúde (BLOOM & MURRAY, 1992; FÄTKENHEUER *et al.*, 1999).

Apesar de terem sido criados hospitais e instituídas quimioterapias para o combate à TB, que reduziram consideravelmente sua incidência em países de primeiro mundo, dados históricos calculados pela Organização Mundial da Saúde indicam que estes esforços não têm surtido grandes efeitos no problema global desde a época de Koch (BLOOM & MURRAY, 1992). Esta doença é responsável pela maior parte da mortalidade humana causada por um único agente infeccioso, representando 26% das mortes possíveis de se prevenir e 7% de todas as mortes no mundo. Dados epidemiológicos baseados em testes dermatológicos de reatividade à tuberculina indicam que aproximadamente um terço da

população mundial esteja infectada com *M. tuberculosis*, estando sob risco de desenvolver a doença, e estima-se que ocorram cerca de 8 a 10 milhões de novos casos e 3 milhões de mortes anualmente, atingindo principalmente os adultos mais jovens e economicamente produtivos (ENARSON & MURRAY, 1996). Segundo a Organização Mundial da Saúde, a TB vitima mais pessoas que a malária e a síndrome da imunodeficiência adquirida (AIDS) juntas, sendo responsável pela morte de 100.000 crianças anualmente. Espera-se mais de 1 bilhão de novos casos de infecção para as duas próximas décadas deste milênio, dos quais 200 milhões virão a desenvolver a doença, e 70 milhões morrerão de TB, caso o controle não seja reforçado (PASQUALOTO & FERREIRA, 2001).

A TB apresenta-se, até certo ponto, sob controle em países como Japão e Estados Unidos, mas prolifera-se descontroladamente no sudeste da Ásia, África e partes da região do Pacífico, principalmente em função das complicações geradas pela epidemia do vírus da imunodeficiência humana (HIV) e pela geração de cepas resistentes a drogas (BRENNAN, 1997). Estudos econômico-geográficos demonstraram que cerca de 95% dos casos de TB ocorrem em países em desenvolvimento (ou subdesenvolvidos), para os quais atribuem-se 98% dos óbitos mundiais causados pela doença (WHO, 1998), reflexos trágicos de uma realidade em que poucos recursos estão disponíveis para garantir um tratamento adequado e onde a infecção pelo HIV pode ser comum (YOUNG, 1998). Segundo a relação da Organização Mundial da Saúde de 1998, o Brasil já alcançou o décimo terceiro lugar dentre 22 países onde a TB apresenta-se mais disseminada (RUFFINO-NETTO, 2002). A tuberculose resistente a múltiplas drogas (MDR-TB), definida pela resistência a pelo menos isoniazida e rifampicina, duas das drogas de primeira linha utilizadas no tratamento da doença ativa (TELENTI & ISEMAN, 2000), tem apresentado alta incidência, de forma crescente, na Letônia, Índia, Estônia, República Dominicana e Argentina, e baixa

incidência na maioria dos países da Europa Ocidental, África e América do Norte (FÄTKENHEUER *et al.*, 1999), e estima-se que cerca de 50 milhões de pessoas estejam infectadas pela cepa multi-resistente (PASQUALOTO & FERREIRA, 2001). Mais recentemente, o Centro de Controle e Prevenção de Doenças dos Estados Unidos da América reportou a emergência de casos de tuberculose extensivamente resistente a drogas (XDR-TB), cujos isolados são MDR-TB e também resistentes a todas as fluoroquinolonas e a pelo menos uma das três drogas de segunda linha injetáveis, amicacina, canamicina ou capreomicina (CDCP, 2006; CDCP, 2007). A presença de linhagens resistentes está diretamente relacionada à disponibilidade de medicamentos para combater a doença e inversamente relacionada à eficácia do tratamento. A partir de um projeto global de vigilância de MDR-TB, realizado em 35 países, demonstrou-se que, durante o período de 1994 a 1997, todas as regiões analisadas apresentavam cepas resistentes a pelo menos uma das drogas anti-TB, sendo geralmente à isoniazida ou estreptomicina, o que revela a doença como um problema global (PABLOS-MENDEZ *et al.*, 1998).

### **1.3. Transmissão, infectividade e imunopatologia**

A TB pode ser causada por algumas micobactérias do “complexo *M. tuberculosis*”, sendo transmitida principalmente por meio de partículas infectivas. A tosse de pacientes com a doença ativa, que caracteriza o sintoma de inflamação pulmonar crônica, constitui o principal mecanismo de disseminação do organismo para novos (e susceptíveis) hospedeiros (GLICKMAN & JACOBS, 2001). Estas partículas, resultantes da formação de aerossóis de secreções respiratórias, são propelidas do pulmão para o ar, podendo permanecer em suspensão durante horas, o que justifica sua propriedade altamente

contagiosa (*NSB EDITORIAL COMMENT, 2000; PASQUALOTO & FERREIRA, 2001*). Dentre os principais determinantes de risco de infecção estão a concentração de organismos presentes na partícula exalada e a duração da exposição à mesma (*BLOOM & MURRAY, 1992*).

Uma vez inalados, os bacilos são ingeridos por macrófagos alveolares fagocíticos, residindo dentro de um vacúolo ligado à membrana, o fagossomo (*BLOOM & MURRAY, 1992; GLICKMAN & JACOBS, 2001*); estes microrganismos podem, então, seguir dois caminhos: serem imediatamente eliminados ou crescerem intracelularmente em lesões localizadas (tubérculos). Geralmente 2 a 6 semanas após a infecção, ocorre o estabelecimento de imunidade celular, seguida de infiltração de linfócitos e macrófagos ativados na lesão, resultando na eliminação da maior parte dos bacilos e o término da infecção primária, geralmente sem a apresentação de sintomas (*BLOOM & MURRAY, 1992; YOUNG, 1998*). Entretanto, o bacilo pode algumas vezes persistir e coexistir pacificamente em seu hospedeiro na forma de uma infecção quiescente em macrófagos alojados em estruturas calcificadas ou cicatrizadas resultantes da tentativa do indivíduo em isolar a área infectada, os chamados tubérculos (*NSB EDITORIAL COMMENT, 2000*), estabelecendo um grande reservatório bacteriano. Indivíduos nesta condição apresentam um risco de desenvolver a doença ativa de aproximadamente 5% após o primeiro ano e de 10% ao longo da vida; portanto, o estado de latência representa um estágio de equilíbrio entre a persistência do patógeno e a resposta imune do hospedeiro (*BLOOM & MURRAY, 1992*).

Assim como a maior parte dos bacilos que são eliminados, uma grande proporção de fagócitos infiltrantes e células do parênquima pulmonar também são mortas, produzindo uma estrutura necrosante sólido-esponjosa denominada granuloma, onde alguns bacilos

podem se refugiar (BLOOM & MURRAY, 1992; YOUNG, 1998). No pulmão, onde a carga bacteriana é constantemente alta, observa-se uma evidente patologia crônico-progressiva; pode ocorrer fibrose intersticial, havendo substituição gradual de grande parte do espaço aéreo do pulmão por tecido fibroso denso separando grupos de sacos alveolares, dando ao pulmão a aparência de um “favo de mel” (EHLERS, 1999). Estas estruturas podem causar a desestabilização e destruição de tecidos adjacentes, podendo ocorrer necrose e, conseqüentemente, formação de cavidades (JAGIRDAR & ZAGZAG, 1996), sendo geralmente resultantes de reações de hipersensibilidade do tipo tardia mediada por células CD4 em tecidos parenquimais. Portanto, basicamente o mesmo sistema envolvido na redução do crescimento bacteriano é também responsável pela formação de granulomas (EHLERS, 1999). Desta forma, muitos dos sintomas da TB, incluindo a destruição tecidual que eventualmente liquefaz porções infectadas do pulmão, são primariamente mediados pela resposta imune do hospedeiro contra o bacilo, ao invés da virulência bacteriana propriamente dita (GLICKMAN & JACOBS, 2001). O predomínio da resposta imune do hospedeiro pode conter a lesão, permanecendo apenas danos residuais no pulmão. Em contraposição, a expansão da reação necrosante pode evoluir a cavidades pulmonares, o que possibilita a disseminação de muitos bacilos para o ambiente externo por meio da tosse (BLOOM & MURRAY, 1992; YOUNG, 1998). Desta forma, pode-se dizer que a resposta imune do hospedeiro constitui seu principal mecanismo de defesa contra a infecção pelo bacilo da TB (DANIEL, 1997), ainda que esta esteja intrinsecamente associada a danos teciduais, pela formação de granulomas e necrose (EHLERS, 1999).

O processo patológico-inflamatório pulmonar induz sintomas tais como enfraquecimento, febre, perda de peso, sudorese noturna, consternação torácica, insuficiência respiratória e tosse, ou mesmo hemoptíase (expectoração de sangue a partir

de alguma via do trato respiratório, formando escarro sanguinolento) (BLOOM & MURRAY, 1992). Estes sintomas justificam o antigo termo “consumição”, utilizado no final do século XVII pelo médico inglês Richard Morton (Figura 1B) para referir-se especificamente à TB (CASTIGLIONI, 1993), visto que esta doença se desenvolve lentamente e com múltiplos sintomas, levando à gradativa debilidade e exaustão física.

#### 1.4. O bacilo de Koch

Dentro do gênero *Mycobacterium* existem cerca de 60 espécies conhecidas, sendo a grande maioria bactérias saprofitas de solo. Entre as poucas espécies deste gênero com patogenicidade suficiente para desenvolver TB estão *M. tuberculosis*, *M. bovis* e *M. africanum*; o desenvolvimento de lepra, uma outra enfermidade micobacteriana, ocorre somente a partir de infecção por *M. leprae* (JARLIER & NIKAIDO, 1994). O principal agente etiológico da TB, o *M. tuberculosis* (Figura 3), pertencente à família Mycobacteriaceae, é uma bactéria considerada fracamente Gram-positiva, em forma de bastão, que não possui flagelos, não forma esporos, não produz toxinas e não possui cápsula. O bacilo tem uma variação na largura de 0,3 a 0,6  $\mu\text{m}$ , e na altura de 1 a 4  $\mu\text{m}$ , e caracteriza-se por apresentar um crescimento muito lento (tempo de geração de 24 horas), envelope celular complexo, homogeneidade genética e parasitismo intracelular obrigatório (COLE *et al.*, 1998).



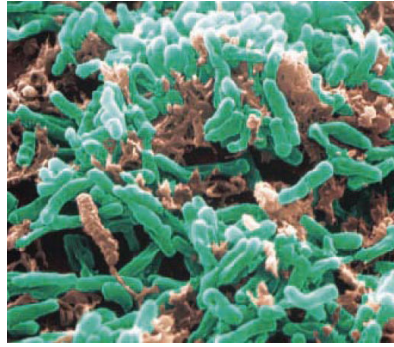


**Figura 3.** Análise por microscopia eletrônica de bacilos do *M. tuberculosis*, o agente etiológico da TB (adaptado de [YOUNG, 1998](#)).

A TB, como qualquer outra doença infecciosa, apresenta ciclos epidêmicos que podem, ainda que raramente, levar séculos para encerrar seu curso. Tem sido demonstrado historicamente que a virulência de organismos patogênicos pode sofrer uma gradual redução; além disto, pode ocorrer o favorecimento (seleção natural) de hospedeiros geneticamente menos susceptíveis à doença ([BLOOM & SMALL, 1998](#)). Ainda que os genes não influenciem o risco de infecção à exposição, eles determinam o risco de doença e de seu curso ([DANIEL, 1997](#)), e ainda que evidências de variabilidade genética na susceptibilidade humana à esta doença sejam difíceis de se obter, tem-se observado que a severidade da TB é maior entre negros do que brancos, há uma maior concordância entre gêmeos monozigóticos do que dizigóticos, e populações mais recentemente expostas ao bacilo têm maior propensão a desenvolver a doença em relação a populações que convivem com a mesma há séculos. A análise destes estudos indica que *M. tuberculosis* continua sendo um extraordinário patógeno, que exerce uma poderosa pressão seletiva no genoma humano ([BLOOM & SMALL, 1998](#)).

### 1.4.1. A parede celular micobacteriana

As diferentes espécies do gênero produzem o mesmo tipo de parede celular, sendo esta de estrutura extremamente incomum (Figura 4). A camada de peptídeoglicano contém ácido *N*-glicolilmurâmico ao invés de ácido *N*-acetilmurâmico, encontrado na maioria das outras bactérias. Uma característica ainda mais distinta é que cerca de 60% da parede celular micobacteriana é constituída de lipídeos que consistem basicamente em ácidos graxos de cadeia longa incomuns, denominados ácidos micólicos (BRENNAN & NIKAIKO, 1995). Uma terceira propriedade que as distingue das demais bactérias é o fato de sua parede celular reter fucsina básica (corante) mesmo na presença de álcool e ácido (método de coloração de Ziehl-Nielsen). A partir desta técnica, pode-se decorar a parede celular de qualquer tipo de bactéria, exceto a micobacteriana; esta propriedade categorizou o gênero como sendo do tipo bacilo álcool-ácido resistente (GLICKMAN & JACOBS, 2001).

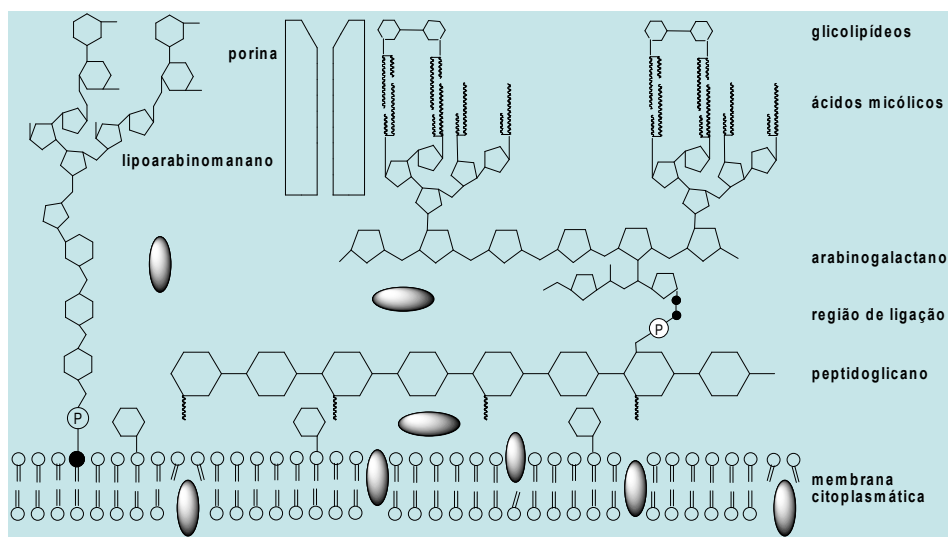


**Figura 4.** Esquema ilustrativo da parede celular micobacteriana, detalhando sua estrutura extremamente incomum (adaptado de SCHROEDER *et al.*, 2002).

A incomum parede celular apresentada por este bacilo permite que o mesmo sobreviva dentro de macrófagos fagocíticos, além de conferir resistência a uma série de antibióticos (NSB EDITORIAL COMMENT, 2000). Uma vez que este patógeno é relativamente resistente à dessecação, álcalis e certos desinfetantes químicos, torna-se difícil prevenir a transmissão do mesmo em instituições e meios urbanos em geral. Pode-se alegar, portanto, que esta resistência, assim como a resistência a alguns agentes terapêuticos, estão intrinsecamente relacionadas à distinta estrutura da parede celular micobacteriana. A parede celular do *M. tuberculosis* tem atraído o interesse das mais recentes pesquisas direcionadas ao mecanismo de ação de várias drogas antigas e da busca de alvos para novas drogas (BRENNAN & NIKAIDO, 1995).

#### **1.4.2. Análise genômica de *Mycobacterium tuberculosis***

Baseados na análise do seqüenciamento completo do genoma da cepa micobacteriana mais bem caracterizada, o *M. tuberculosis* H37Rv (Figura 5), Stewart Cole e colaboradores caracterizaram a mesma por possuir um cromossomo circular com 4.411.529 pares de bases (pb), ao longo dos quais observa-se um conteúdo de G+C de 65,6%, porcentagem consideravelmente alta em relação a maioria das bactéria. Desde seu isolamento, em 1905, esta linhagem tem tido grande aplicação mundial na pesquisa biomédica devido à total retenção de virulência em modelos animais, além de ser susceptível a drogas e amena à manipulação genética (COLE *et al.*, 1998).

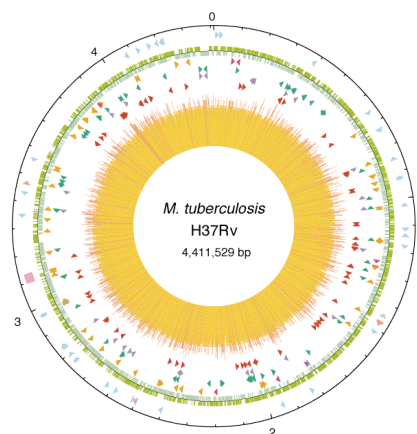


**Figura 5.** Representação esquemática do genoma circular de *M. tuberculosis* H37Rv, com 4.411.529 pb e um conteúdo de G+C de 65,6% (adaptado de COLE *et al.*, 1998).

Apesar de seu genoma ser menor que o de *Escherichia coli*, é bastante versátil, codificando enzimas envolvidas na maioria das rotas anabólicas e catabólicas características das bactérias e na síntese e degradação de aminoácidos. Este aprofundado estudo genômico permitiu que fossem identificadas singularidades deste organismo, como a existência de 4.000 genes, majoritariamente destinados à codificação de enzimas envolvidas em lipólise e lipogênese; em questão, trata-se da degradação de lipídeos para sobrevivência intracelular, e da biossíntese de lipídeos destinados à construção do envelope celular, respectivamente. Cabe salientar que cerca de 59% dos genes deste microrganismo são transcritos no mesmo sentido da replicação, porcentagem consideravelmente menor que os 75% em *Bacillus subtilis*, o que provavelmente justifica seu crescimento lento e infreqüentes ciclos de replicação. A partir da inspeção genômica identificou-se que, além das várias funções envolvidas no metabolismo de lipídeos, estão também presentes enzimas envolvidas em glicólise, rota das pentoses, e ciclos do ácido tricarbóxico e glioxilato, o que evidencia, portanto, o metabolismo dinâmico desta bactéria (COLE *et al.*, 1998).

## 1.5. Latência e reativação

A TB latente constitui uma síndrome clínica decorrente de exposição ao *M. tuberculosis*, seguido do estabelecimento da infecção e geração de resposta imune celular do hospedeiro para controlar o bacilo, reduzindo seu metabolismo e forçando-o a um estado de quiescência no tecido infectado; em geral, o sistema imunológico humano está capacitado para conter, mas não para eliminar, a infecção. Entretanto, ao contrário da doença ativa, a TB latente não constitui uma doença infecciosa e, portanto, não representa um risco de saúde pública.

A sobrevivência intracelular do patógeno está baseada na capacidade do mesmo em lidar com a acidificação fagossômica de macrófagos infectados e prevenir a fusão fagossomo-lisossomo. Na maioria dos indivíduos imunocompetentes infectados, ocorre o recrutamento de linfócitos T e macrófagos, e o estabelecimento de resposta imune secundária, resultando no controle da infecção. Porém, condições de imunossupressão oportunizam a reativação do bacilo dormente, possibilitando o desenvolvimento de TB ativa em seu hospedeiro, geralmente muitas décadas após a infecção inicial. Dentre os fatores responsáveis pela reativação de infecções latentes estão: co-infecção por HIV, subnutrição, aumento da idade, uso de drogas, câncer, diabetes, insuficiência renal crônica e quimioterapia imunossupressiva (PARRISH *et al.*, 1998).

## 1.6. Tuberculose resistente a drogas

A era dos antibióticos tem sido constantemente marcada por ciclos, consistindo na introdução de novos agentes antimicrobianos e uma subsequente emergência de resistência a estas drogas (SWARTZ, 2000). A história da resistência a drogas como um problema no tratamento de TB é quase tão antiga quanto a introdução das primeiras drogas anti-TB no tratamento da doença. Sabe-se que os fenótipos resistentes e multi-resistentes são causados por mutações cromossômicas randômicas espontâneas (“resistência natural”) em diferentes genes deste microrganismo (PETRINI & HOFFNER, 1999). As taxas de mutação são diferentes para cada droga, equivalendo a  $10^{-6}$  para isoniazida e  $10^{-8}$  para rifampicina. Uma vez que uma lesão pulmonar cavitária pode abrigar até  $10^9$  organismos, é matematicamente possível ou mesmo provável que existam bacilos resistentes a pelo menos uma destas drogas. No entanto, o fato de a taxa de mutação para ambas as drogas ser de  $10^{-14}$  impossibilita virtualmente que o patógeno se torne espontaneamente resistente às duas drogas em pacientes corretamente tratados (RILEY, 1993). Uma vez tendo sido estabelecido que a monoterapia induz à seleção de populações resistentes à droga (“resistência adquirida”), torna-se necessária a utilização de terapias combinadas, visto que a probabilidade de uma linhagem bacteriana desenvolver resistência a duas ou mais drogas simultaneamente é extremamente baixa (PETRINI & HOFFNER, 1999).

A taxa de mortalidade por MDR-TB está estimada em 40-60%, equivalente à mortalidade entre pacientes com TB não tratada (BLOOM & MURRAY, 1992). Manifestações clínicas têm demonstrado que XDR-TB está associada à morbidade e mortalidade maiores que casos não-XDR-TB (JASSAL & BISHAI, 2008). Dentre os fatores responsáveis pelo aumento na incidência de MDR-TB estão a pandemia de

HIV/AIDS e o aumento na incidência de TB, especialmente entre populações de países desenvolvidos com fácil acesso a medicamentos (RILEY, 1993). Nestas nações podem ser algumas vezes identificados tratamentos completamente inadequados, baseados na utilização de uma única droga, combinações equivocadas de drogas, curtos períodos de tratamento devido à baixa adesão de pacientes, e à baixa absorção das drogas administradas. Estas condições expõem o patógeno a concentrações antibacterianas subletais, selecionando o crescimento de bacilos resistentes dentro de uma população originalmente susceptível (PETRINI & HOFFNER, 1999).

### 1.7. O sinergismo entre TB e AIDS

A ligação entre a TB e a AIDS foi bem documentada pela primeira vez em Nova Iorque, onde foi estimado que o risco de desenvolvimento da doença ativa entre indivíduos co-infectados com HIV e *M. tuberculosis* era de 8% ao ano, comparado com 10% de risco ao longo da vida para indivíduos infectados apenas pelo bacilo latente (BLOOM & MURRAY, 1992); estes dados alarmantes são resultantes do considerável enfraquecimento imunológico proporcionado pelo HIV, sendo responsável pelo aumento na probabilidade de desenvolvimento da TB em até 30 vezes (PASQUALOTO & FERREIRA, 2001). O aumento na susceptibilidade à TB está associado aos primeiros estágios da infecção por HIV, que por sua vez passa a acelerar a progressão da segunda para AIDS (YOUNG, 1998). Cabe destacar que, entre indivíduos soropositivos, podem ocorrer infecções oportunistas causadas pelas chamadas “micobactérias atípicas”, que incluem o complexo *M. avium*, *M. kansasii*, *M. fortuitum* e *M. chelonae*, ainda que estas espécies sejam essencialmente saprofíticas (BRENNAN & NIKAIIDO, 1995).

A incidência de casos de dupla infecção ocorre principalmente entre trabalhadores em idade de alta produtividade, abrangendo idades entre 15 e 59 anos (NARAIN *et al.*, 1992). Nas últimas décadas, tem-se observado um dramático aumento na incidência de TB na África, causado principalmente pela epidemia de HIV. Um estudo realizado neste continente identificou evidências que sugerem uma grande associação entre as duas infecções, como: a TB é a principal doença associada ao HIV, sendo a maior responsável pela mortalidade de pacientes soropositivos em hospitais; o aumento na incidência de TB coincidiu em época, local e população com o surgimento da AIDS; e, finalmente, a TB ativa está mais presente entre indivíduos soropositivos que negativos (FÄTKENHEUER *et al.*, 1999). Segundo a Organização Mundial da Saúde, um terço do aumento na incidência de TB nos últimos seis anos pode estar atribuído à co-infecção por HIV; portanto, o sinergismo existente entre o *M. tuberculosis* e o HIV representa um problema de efeito devastador tanto para pacientes infectados como para a população em geral. Entre pacientes soropositivos co-infectados por MDR-TB, observam-se índices de mortalidade freqüentemente superiores a 80%, sendo o intervalo entre o diagnóstico e a morte de 4 a 16 semanas (RILEY, 1993); em função disto, MDR-TB passou a ser conhecida como “a mais maligna infecção oportunista associada à infecção por HIV” (NOLAN, 1997).

### **1.8. Métodos de diagnóstico**

Dentre as técnicas utilizadas no diagnóstico da TB, o teste dermatológico de reatividade à tuberculina, monitoramento epidemiológico mundialmente disseminado, constitui o principal método capaz de identificar um possível contato prévio entre este patógeno e seu hospedeiro (BLOOM & MURRAY, 1992), evidenciando a infecção latente



pelo bacilo de Koch a partir da indução de hipersensibilidade do tipo tardia contra antígenos micobacterianos (GLICKMAN & JACOBS, 2001). Entretanto, a vacinação por BCG também produz reatividade ao teste dermatológico de reatividade à tuberculina, fazendo com que a utilização e confiabilidade do mesmo diminuam com o aumento de crianças vacinadas (BLOOM & MURRAY, 1992). Diferentemente das cepas sensíveis, o diagnóstico de MDR-TB requer a execução de testes de sensibilidade bacilar às drogas anti-TB, para os quais são utilizadas concentrações estabelecidas de fármacos. Alternativamente, o método de proporção identifica quais drogas e em que concentrações mínimas ocorre a inibição de pelo menos 99% do crescimento bacteriano (PETRINI & HOFFNER, 1999).

Ainda que o pequeno prestígio do diagnóstico molecular seja uma realidade, há uma clara tendência na direção de métodos moleculares de detecção de doenças humanas. Este direcionamento molecular se deve à era genômica, que disponibilizou a sequência genética de organismos importantes, e ao descobrimento de alvos relevantes ao diagnóstico (FARKAS, 2002). O progresso destas técnicas permitirá o desenvolvimento de testes mais sensíveis e rápidos na detecção, identificação e monitoramento epidemiológico de micobactérias; muitas destas tecnologias já estão disponíveis no mercado, propondo uma sensibilidade e especificidade superior a 90%. Entretanto, o alto custo destas técnicas torna seu estabelecimento desfavorável, restringindo seu uso a países desenvolvidos (BLOOM & MURRAY, 1992; CAWS & DROBNIOWSKI, 2001; GILBERT, 2002).

## 1.9. Desenvolvimento de vacinas

O sistema imunológico mamífero pode atuar por intermédio de uma resposta celular ou humoral, mas, ainda que ambas envolvam células T auxiliares (Th), são guiadas por diferentes regras. A resposta imune do tipo Th-1 envolve linfócitos T CD4+, sendo de natureza celular. Ela atua contra doenças crônicas como parasitismo intracelular e câncer a partir da ativação de macrófagos, facilitando a detecção e lise de células doentes; este processo resulta na formação de um granuloma não-necrosante, que representa o paradigma da imunidade de proteção em doenças intracelulares, como um sinal de morte bacteriana e regressão da doença. Em contraposição, a resposta do tipo Th-2 envolve um conjunto diferente de linfócitos T CD4+, sendo de natureza humoral; pode tornar-se necessária para eliminar antígenos e parasitas extracelulares. Esta resposta pode também causar destruição tecidual e necrose, representando o fracasso da resposta imune em muitas doenças (LABIDI *et al.*, 2001).

Esforços têm sido focados no isolamento e desenvolvimento de antígenos ou epitopos individuais em vacinas (LABIDI *et al.*, 2001). Com o intuito de se induzir uma imunidade de proteção duradoura, novas vacinas deverão combinar antígenos selecionados com potentes adjuvantes, além de estimular rotas apropriadas do sistema imune (GRANGE *et al.*, 1995). Para tanto, faz-se necessário um adjuvante micobacteriano capaz de induzir um aumento da resposta Th-1 e uma inibição da resposta Th-2. Desta forma, considera-se como vacina ideal aquela que contenha imunógenos capazes de induzir a formação de granulomas não-necrosantes.

Atualmente, a vacina mais utilizada no mundo para combater a TB é a BCG; a mesma oferece uma série de vantagens, uma vez que pode ser administrada via oral; requer

uma única imunização, sendo geralmente eficaz na prevenção de TB meningeal infantil; e tem um baixo custo de produção (LABIDI *et al.*, 2001; ORME, 2001). Apesar das vantagens, sua eficácia varia entre 0 e 80% (COLDITZ *et al.*, 1994), além de não conferir proteção à TB pulmonar em adultos (ORME, 2001), fato que tem incentivado muitos grupos de pesquisa a investir esforços no âmbito da produção de vacinas de maior imunogenicidade a partir do desenvolvimento de adjuvantes, induzindo uma maior hipersensibilidade mediada por células CD4+ (EHLERS, 1999).

Muitos tipos de vacinas têm sido testadas em camundongos e cobaias com o intuito de substituir a BCG em humanos, como vacinas recombinantes e vacinas auxotróficas, entre outras; entretanto, nenhuma destas têm apresentado resultados melhores que a própria BCG (ORME *et al.*, 2001). Outra área alternativamente explorada é a de vacinas de DNA, a partir da qual seqüências microbianas podem ser utilizadas como vacinas alvo (ORME, 2001); o volumoso esforço que tem sido investido nesta estratégia tem gerado uma grande expectativa de resultados promissores. De qualquer forma, visto que um terço da população mundial está infectada com *M. tuberculosis*, faz-se necessário o desenvolvimento de dois tipos de vacinas: um para prevenir a invasão do patógeno e outro para erradicar infecções já estabelecidas (latentes) (HESS & KAUFMANN, 1999).

### **1.10. Quimioterapia**

Estima-se que aproximadamente metade dos novos casos de TB sejam inevitáveis, uma conseqüência da história natural da doença e da co-infecção pelo HIV. Entretanto, muitos dos casos excedentes, resultantes do aumento de transmissão ativa, poderiam ter sido evitados a partir da implementação de programas efetivos de tratamento (BLOOM &

MURRAY, 1992). A TB é uma doença grave, porém curável na maioria dos casos, desde que, uma vez diagnosticada, seja tratada com o emprego de uma quimioterapia adequada, visto que um dos maiores riscos de mortalidade resulta da instituição tardia do tratamento.

O tratamento quimioterápico padrão atualmente recomendado pela Organização Mundial da Saúde para o controle e/ou erradicação da TB no mundo, conhecido como terapia de curta duração de observação direta (DOTS), consiste na administração combinada de quatro drogas, isoniazida, rifampicina, pirazinamida e estreptomicina (ou etambutol), durante 2 meses, seguida da combinação de duas drogas, isoniazida e rifampicina, por pelo menos mais 4 meses (NSB EDITORIAL COMMENT, 2000). Inicialmente, objetiva-se uma ação bacteriostática, inibindo a síntese de parede celular, ácidos nucleicos e proteínas micobacterianas, e eliminando rapidamente a maior parte dos bacilos infectantes. Posteriormente, objetiva-se uma ação bactericida, a partir da consolidação do tratamento pela eliminação dos bacilos remanescentes (TELENTI & ISEMAN, 2000). No entanto, a natural relutância humana em cumprir com o requisito de tratamento intensivo de 6 meses, resultante da longa duração quimioterápica e dos desagradáveis efeitos colaterais ocasionados pelas drogas administradas, conduziram a Organização Mundial da Saúde a investir em medidas de adesão universal ao tratamento. A versão mais atualizada de DOTS, que combina comprometimento político, serviços de microscopia, suprimentos de drogas e sistemas de monitoramento e observação direta do tratamento previne a ocorrência de novas infecções e inviabiliza completamente o desenvolvimento de MDR-TB (PASQUALOTO & FERREIRA, 2001). Casos clínicos comprovam que MDR-TB requer a extensão do período de tratamento para cura, quando esta é possível, e a utilização de drogas de segunda ou até terceira linha, ainda que a maior toxicidade seja um fator limitante (TELENTI & ISEMAN, 2000), tornando o tratamento

mais difícil e dispendioso. Em países industrializados, o tratamento completo da doença tem um custo de aproximadamente US\$ 2.000 por paciente, valor substancialmente menor que os US\$ 250.000 investidos em pacientes com MDR-TB (PASQUALOTO & FERREIRA, 2001).

Segundo a Organização Mundial da Saúde, nenhum tipo de tratamento tem esboçado resultados melhores que DOTS entre pacientes com TB ativa e no controle de MDR-TB. Análises recentes apontam que os índices de cura pós-DOTS apresentados por pacientes co-infectados com HIV e *M. tuberculosis* e por pacientes infectados apenas pelo bacilo de Koch são muito semelhantes (FÄTKENHEUER *et al.*, 1999). Entretanto, estes mesmos resultados animadores não se aplicam à MDR-TB, visto que a simples confirmação de suspeita de resistência requer 8 semanas para ser diagnosticada, período maior do que o tempo médio de sobrevivência destes pacientes co-infectados (RILEY, 1993); um estudo realizado na Flórida com pacientes soropositivos revelou que a duração média de sobrevivência é de aproximadamente 45 dias entre casos de co-infecção por MDR-TB e de 430 dias entre casos de co-infecção por TB susceptível a drogas (FISCHL *et al.*, 1992).

### **1.11. A busca de alvos para o desenvolvimento de novas drogas**

Um estudo realizado entre 1972 e 1998, que analisou o número de agentes antimicrobianos descritos na revista *Antimicrobial Agents and Chemotherapy*, publicada pela Sociedade Americana de Microbiologia, apresentou as seguintes porcentagens entre as categorias: 46% antibacteriana, 24% antiviral, 13% antiparasitária, 9% antifúngica e 8% antimicobacteriana. Ainda que a categoria de agentes antimicobacterianos possa estar sub-

representada, uma vez que foram incluídas somente drogas descritas em artigos relacionando seu uso contra micobactérias, percebe-se que esta categoria tem tido o menor desenvolvimento ao longo dos anos (SWARTZ, 2000). De fato, não houve qualquer descrição na literatura reportando a identificação de novas drogas de primeira linha capazes de substituir as atualmente utilizadas no combate ao bacilo causador da TB desde a metade da década de 80 (PETRINI & HOFFNER, 1999). O baixo interesse da indústria farmacêutica nesta área não se deve necessariamente ao alto investimento necessário para desenvolver um novo composto anti-TB, mas ao pequeno retorno financeiro esperado, visto que a grande maioria dos casos de TB ocorrem em países subdesenvolvidos (RUFFINO-NETTO, 2002).

A atual realidade epidemiológica e quimioterápica tem revelado uma urgente necessidade do desenvolvimento de agentes antimicobacterianos mais eficientes. Estes devem apresentar uma toxicidade seletiva, sendo ativos contra cepas resistentes e não-resistentes a drogas, assim como infecções latentes; além disto, devem requerer uma menor duração do tratamento para aumentar a adesão dos pacientes à quimioterapia.

Em princípio, a seqüência genômica de *M. tuberculosis* inclui informações sobre todos os possíveis alvos aos quais possam se direcionar novos agentes antimicobacterianos. Uma maneira de explorar informações em programas de desenvolvimento de drogas é clonando e expressando genes que codificam enzimas biossintéticas específicas do patógeno, assim como validando a sua atividade biológica que havia sido inferida apenas por homologia de seqüência e não por demonstração experimental. As proteínas recombinantes podem ser usadas em ensaios funcionais na procura de inibidores, e, ao mesmo tempo, possibilitar a geração de informações estruturais para o desenvolvimento de drogas (YOUNG, 2001).

### 1.11.1. Rota de salvamento de purinas e fosforilase de nucleosídeos purínicos

Em *E. coli* e *Salmonella typhimurium*, a rota de salvamento das purinas desempenha um papel fundamental, atuando na captação de bases e nucleosídeos exógenos para a biossíntese de nucleotídeos e na reutilização de bases e nucleosídeos gerados pela reciclagem intracelular de nucleotídeos (ZALKIN & NYGAARD, 1996). Apesar de homólogos às enzimas da rota de salvamento de purinas terem sido identificados no genoma de *M. tuberculosis* (COLE *et al.*, 1998) e atividades correspondentes às de enzimas desta via já terem sido detectadas em extratos celulares micobacterianos (WHEELER, 1987; BARCLAY & WHEELER, 1989), poucos genes e proteínas desta via metabólica foram aprofundadamente estudados, e o conhecimento da preferência de substratos destas enzimas e como elas diferem de seus homólogos em humanos ainda é consideravelmente escasso. A Figura 6 apresenta as principais enzimas envolvidas no metabolismo de purinas em células micobacterianas. Adenina (Ade) e adenosina (Ado) são convertidas a AMP por adenina fosforribosiltransferase (APRT) e adenosina quinase (ADOK), respectivamente, e hipoxantina (Hx) e guanina (Gua) são convertidas a IMP e GMP, respectivamente, por hipoxantina-guanina fosforribosiltransferase (HGPRT). Estes nucleotídeos são então convertidos a todos os nucleotídeos trifosfatados naturais que, por sua vez, servem de substrato para a síntese de DNA e RNA.

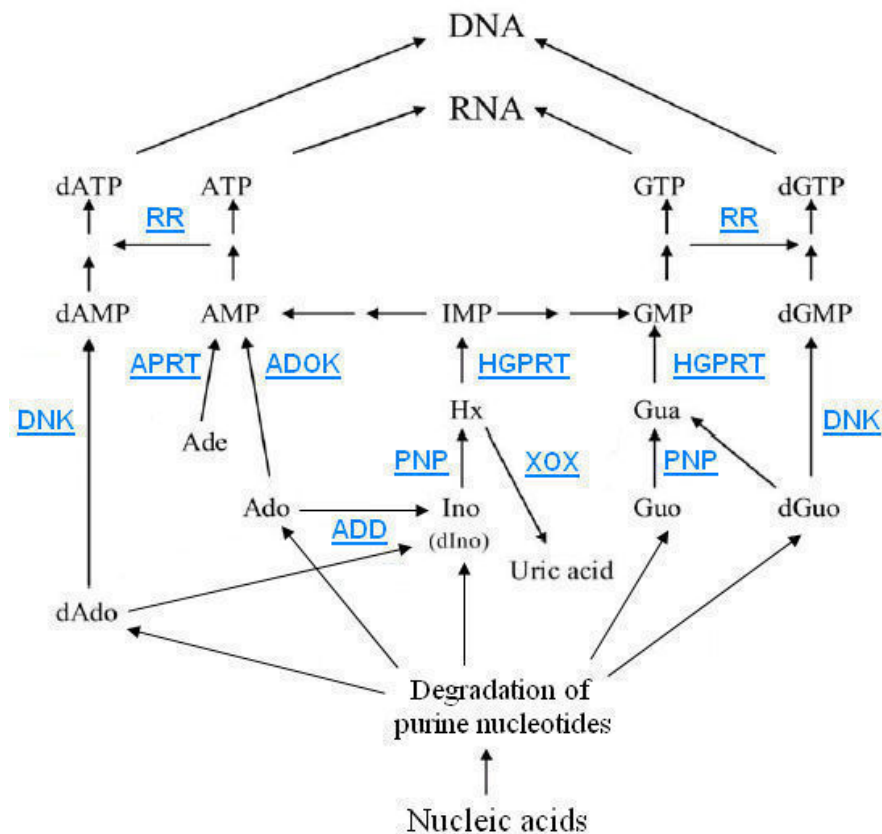


**Figura 6.** Esquema proposto da rota de salvamento de purinas micobacteriana (adaptado de PARKER & LONG, 2007). Abreviaturas utilizadas na Figura: ADD, adenosina desaminase; Ade, adenina; Ado, adenosina; ADOK, adenosina quinase; APRT, adenina fosforribosiltransferase; dAdo, 2'-desoxiadenosina; dGuo, 2'-desoxiguanosina; desoxinucleosídeo quinase, DNK; Gua, guanina; Guo, guanosina; Hx, hipoxantina; HGPRT, hipoxantina-guanina fosforribosiltransferase; Ino, inosina; PNP, fosforilase de nucleosídeos purínicos; RR, ribonucleotídeo redutase.

A sobrevivência a longo prazo de células não-replicantes de *M. tuberculosis* é assegurada pelo desligamento coordenado de seu metabolismo ativo a partir de um amplo programa transcricional denominado resposta severa (*stringent response*). A resposta severa consiste em um conjunto de adaptações fisiológicas, mediado por ppGpp, que se



caracteriza pela súbita repressão da síntese de ácidos nucleicos e proteínas e a simultânea ativação da degradação de proteínas e síntese de aminoácidos (CASHEL *et al.*, 1996; CHATTERJI & OJHA, 2001). A síntese e degradação de guanosina 3',5'-bis(difosfato) (ppGpp) e pppGpp são catalisadas pela enzima (p)ppGpp sintetase I (RelA; *relA*, Rv2583) utilizando GTP como substrato (AVARBOCK *et al.*, 1999). O acúmulo de guanosina hiperfosforiladas é a característica mais marcante da resposta severa, a partir da qual as bactérias entram em estado de latência em resposta à deficiência de aminoácidos e outros nutrientes, bem como a situações ambientais que temporariamente interrompem o crescimento bacteriano (CASHEL *et al.*, 1996; MAGNUSSON *et al.*, 2005; BRAEKEN *et al.*, 2006). Em condições “normais”, onde o crescimento bacteriano é considerado favorável, o nível basal de pppGpp e ppGpp é mantido em estado estacionário nas células bacterianas, pela atividade das enzimas RelA e SpoT - ou, em certas espécies, somente por RelA (CHATTERJI & OJHA, 2001). Em condições de estresse nutricional, pppGpp é convertido em ppGpp, iniciando efeitos regulatórios globais que levam a uma resposta adaptativa e permitem às células bacterianas resistir ao estresse (BRAEKEN *et al.*, 2006).

Os mecanismos pelos quais ppGpp exerce seus efeitos regulatórios ainda não são totalmente conhecidos, mas sabe-se que, em *E. coli*, as moléculas de ppGpp se ligam a subunidades da RNA polimerase, afetando, portanto, a transcrição gênica. Assim, genes relacionados ao crescimento são reprimidos (regulação negativa) e genes relacionados à sobrevivência ao estresse são ativados (regulação positiva) (MAGNUSSON *et al.*, 2005).

O acúmulo de ppGpp resultante de estresse nutricional em *M. smegmatis* (OJHA *et al.*, 2000) pode indicar que a resposta severa poderia ser importante processo de latência de *M. tuberculosis* no hospedeiro humano. Foi demonstrado experimentalmente que um mutante de *M. tuberculosis* deficiente na produção de RelA havia perdido a capacidade de

acumular ppGpp; este mutante era muito menos apto que a linhagem selvagem a sobreviver a estresse nutricional *in vitro* por longos períodos, indicando que a resposta severa era, de fato, importante à latência do patógeno (PRIMM *et al.*, 2000). Foi demonstrado que esta cepa mutante apresentava capacidade diminuída de manter uma infecção crônica em um modelo murino de TB persistente (DAHL *et al.*, 2003). Uma análise genômica comparativa recentemente realizada entre *M. tuberculosis* H37Ra (avirulenta) and H37Rv (virulenta) identificou, entre outras mudanças, uma mutação *missense* em uma proteína regulatória da resposta severa (ZHENG *et al.*, 2008). Na síntese *de novo* de ribonucleotídeos purínicos, a formação de AMP e GMP a partir de IMP é irreversível, mas bases, nucleosídeos e nucleotídeos purínicos podem ser interconvertidos a partir das atividades de fosforilase de nucleosídeos purínicos (PNP; *deoD*, Rv3307), adenosina desaminase (ADD; *add*, Rv3313c) e HGPRT (*htp*, Rv3624c). Havia sido anteriormente sugerido pelo nosso grupo que a inibição *in vivo* da PNP de *M. tuberculosis* (MtPNP) levaria ao acúmulo de nucleotídeos de guanina, visto que os genes da guanilato quinase (*gmk*, Rv1389) e da nucleosídeo difosfato quinase (*ndkA*, Rv2445c) estão presentes no genoma do bacilo (BASSO *et al.*, 2001), prejudicando, assim, seu metabolismo celular.

Como no interior dos granulomas, durante a fase de latência, a disponibilidade de nutrientes (e, conseqüentemente, energia) é menor, muitas vias anabólicas se encontram total ou parcialmente reprimidas, obrigando o bacilo a fazer uso de reservas e rotas de reciclagem que não exijam etapas enzimáticas complexas. Desta maneira, a inibição da PNP, com conseqüentes efeitos sobre a via de salvamento das purinas, poderia interferir no estado de latência de *M. tuberculosis*, em maior ou menor grau. De qualquer forma, o papel fisiológico de MtPNP ainda não foi experimentalmente demonstrado.

A PNP (EC 2.4.2.1) desempenha um papel central na rota de salvamento das purinas, catalisando a fosforólise reversível da ligação *N*-glicosídica de (desoxi)ribonucleosídeos purínicos, na presença de fosfato inorgânico (P<sub>i</sub>), gerando (desoxi)ribose 1-fosfato e a base purínica correspondente (KALCKAR, 1947; PORTER, 1992), invertendo a configuração de β-(desoxi)nucleosídeo para α-(desoxi)ribose 1-fosfato (STOECKLER *et al.*, 1980). A reação catalisada pela PNP está apresentada na Figura 7. Ainda que o equilíbrio da reação seja termodinamicamente favorecido no sentido da síntese de nucleosídeos, a fosforólise *in vivo* é consideravelmente favorecida devido ao acoplamento com as enzimas xantina oxidase (XOX) e HGPRT (PARKS & AGARWAL, 1972).

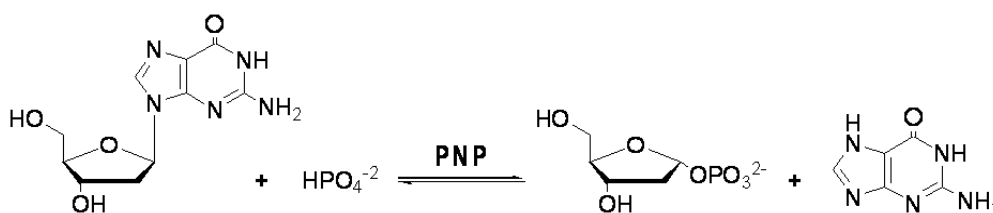


**Figura 7.** Reação catalisada pela PNP.

A enzima MtPNP, codificada pelo gene *deoD* (Rv3307, 807 pb), é uma proteína de 268 aminoácidos e massa molecular de 80 kDa (massa molecular da subunidade de 27437 Da), sendo um homotrímero em solução (BASSO *et al.*, 2001), à semelhança da enzima humana (HsPNP), mas em contraste com as enzimas de *E. coli* e *S. typhimurium*, de estrutura homohexaméricas (JENSEN, 1978; TRAUT, 1994; BZOWSKA *et al.*, 2000).

Um recente trabalho do nosso grupo empregou o método de mutagênese por troca alélica de *deoD* selvagem por uma versão mutante para avaliar a possível relação de MtPNP à mecanismos que participam na regulação do processo de latência micobacteriano

e a sua importância na rota de salvamento de purinas. Os resultados deste experimento sugerem que o gene *deoD* é essencial à viabilidade de *M. tuberculosis* (C. Z. Schneider *et al.*; dados não publicados), sendo fundamental, dentro da própria rota de salvamento de purinas, na reciclagem e interconversão das bases purínicas para garantir a baixa atividade metabólica do bacilo durante a fase de latência, quando a disponibilidade de nutrientes é extremamente baixa e o mesmo encontra-se sob intensa pressão do sistema imune do hospedeiro. Além disso, há indicativos de que esta enzima participa de algum mecanismo, ainda desconhecido, que liga o catabolismo de purinas à resposta severa. Dessa forma, o acúmulo de guanosina hiperfosforilada teria efeitos tóxicos ou mesmo letais ao *M. tuberculosis*. Visto que níveis elevados de guanosina hiperfosforilada desencadeiam a repressão da transcrição de genes envolvidos na replicação de DNA e na síntese de RNAs estáveis, é possível que a ausência de atividade de PNP produza uma condição fatal ao *M. tuberculosis*.

O desenvolvimento de eficientes drogas quimioterápicas pode ser executado mesmo para atividades enzimáticas que são compartilhadas entre humanos e seus agentes infecciosos. O estudo das diferenças existentes entre MtPNP e HsPNP pode ser importante no sentido do desenho racional de drogas, capazes de interagir especificamente com a enzima bacteriana. Imucilina-H (ImmH), um análogo ao estado de transição, demonstrou ser um inibidor do tipo *slow-onset* (associação lenta) de MtPNP, com uma constante de inibição global na escala de pM (BASSO *et al.*, 2001). A estrutura tridimensional de MtPNP complexada com ImmH mostrou que a extremidade lateral do anel fenólico de Tyr188 está orientado perpendicularmente ao plano da base de ImmH e forma uma ligação de hidrogênio de 2,8 Å com o grupo hidroxil 5' do análogo ao estado de transição (SHI *et al.*, 2001). Este é o único resíduo que interage diretamente com o inibidor ligado que não

está conservado nas PNPs de mamíferos e, portanto, é provável que modificações 5' de ImmH possam gerar inibidores mais específicos à MtPnP. A possibilidade do desenho de inibidores capazes de distinguir proteínas homólogas foi recentemente demonstrada para PNP; o referido trabalho mostra que, mesmo que as enzimas bovina e humana compartilhem de 87% de identidade e apresentem conservação total de resíduos no sítio ativo, é possível desenhar inibidores com especificidade diferencial (TAYLOR RINGIA *et al.*, 2006).

A revolução genômica tem sido fundamental ao investimento do desenho racional de drogas baseado em alvos específicos, que inclui abordagens estruturais e funcionais. Ao combinar grupos químicos protéicos e de substratos no estado de transição, as enzimas são capazes de catalisar reações químicas de diversos passos e a atingir velocidades fenomenais de aceleração. Os inibidores que se utilizam destas interações químicas estão entre as drogas mais potentes e eficientes conhecidas até o presente (ROBERTSON, 2007). Portanto, análises mecanísticas deveriam sempre representar a principal forma de estudo em programas de desenvolvimento de drogas para alvos enzimáticos, de forma a permitir o desenho de potentes inibidores baseados na função protéica. Neste sentido, o presente trabalho descreve estudos cinéticos da reação catalisada pela enzima MtPnP, a partir de análises de especificidade de substrato, parâmetros cinéticos em estado estacionário, inibição por produto, perfis de pH, energia de ativação, efeitos isotópicos de deutério de solvente e inventário de prótons, espectroscopia de fluorescência em equilíbrio, ressonância plasmônica de superfície (SPR) da formação de complexo binário e cinética em estado pré-estacionário da formação de produto.

## 2. OBJETIVOS

### 2.1. Objetivo geral

Combinar os campos da biologia funcional para investigar a participação desta enzima no processo de latência em *Mycobacterium tuberculosis*.

### 2.2. Objetivos específicos

Determinar os mecanismos cinético e químico da reação catalisada por MtPNP, a partir de análises de:

- especificidade de substrato;
- velocidade inicial;
- inibição por produto;
- estudos de ligação;
- perfis de pH;
- efeitos isotópicos de solvente;
- inventário de prótons;
- efeitos de temperatura.

**3. ARTIGO 1:** DUCATI, R. G.; RUFFINO-NETTO, A.; BASSO, L. A. & SANTOS, D. S. The resumption of consumption - a review on tuberculosis. *Mem. Inst. Oswaldo Cruz*, 101(7): 697-714, 2006.

## The resumption of consumption – A review on tuberculosis

Rodrigo Gay Ducati\*\*, Antonio Ruffino-Netto\*, Luiz Augusto Basso<sup>+ / ++</sup>,  
Diógenes Santiago Santos<sup>+ / ++</sup>

Faculdade de Farmácia, Faculdade de Biociências, Centro de Pesquisas em Biologia Molecular e Funcional, Pontifícia Universidade Católica do Rio Grande do Sul, Av. Ipiranga 6681, Tecnopuc-Prédio 92A, 90619-900 Porto Alegre, RS, Brasil

\*Departamento de Medicina Social, Faculdade de Ribeirão Preto, Universidade de São Paulo, Ribeirão Preto, SP, Brasil

\*\*Programa de Pós-graduação em Biologia Celular e Molecular, UFRGS, Porto Alegre, RS, Brasil

*Among all infectious diseases that afflict humans, tuberculosis (TB) remains the deadliest. At present, epidemiologists estimate that one-third of the world population is infected with tubercle bacilli, which is responsible for 8 to 10 million new cases of TB and 3 million deaths annually throughout the world. Approximately 95% of new cases and 98% of deaths occur in developing nations, generally due to the few resources available to ensure proper treatment and where human immunodeficiency virus (HIV) infections are common. In 1882, Dr Robert Koch identified an acid-fast bacterium, *Mycobacterium tuberculosis*, as the causative agent of TB. Thirty-nine years later, BCG vaccine was introduced for human use, and became the most widely used prophylactic strategy to fight TB in the world. The discovery of the properties of first-line antimycobacterial drugs in the past century yielded effective chemotherapies, which considerably decreased TB mortality rates worldwide. The later introduction of some additional drugs to the arsenal used to treat TB seemed to provide an adequate number of effective antimicrobial agents. The modern, standard short-course therapy for TB recommended by the World Health Organization is based on a four-drug regimen that must be strictly followed to prevent drug resistance acquisition, and relies on direct observation of patient compliance to ensure effective treatment. Mycobacteria show a high degree of intrinsic resistance to most antibiotics and chemotherapeutic agents due to the low permeability of its cell wall. Nevertheless, the cell wall barrier alone cannot produce significant levels of drug resistance. *M. tuberculosis* mutants resistant to any single drug are naturally present in any large bacterial population, irrespective of exposure to drugs. The frequency of mutants resistant to rifampicin and isoniazid, the two principal antimycobacterial drugs currently in use, is relatively high and, therefore, the large extra-cellular population of actively metabolizing and rapidly growing tubercle bacilli in cavitary lesions will contain organisms which are resistant to a single drug. Consequently, monotherapy or improperly administered two-drug therapies will select for drug-resistant mutants that may lead to drug resistance in the entire bacterial population. Thereby, despite the availability of effective chemotherapy and the moderately protective vaccine, new anti-TB agents are urgently needed to decrease the global incidence of TB. The resumption of TB, mainly caused by the emergence of multidrug-resistant (MDR) and extensively drug-resistant (XDR) strains and HIV epidemics, led to an increased need to understand the molecular mechanisms of drug action and drug resistance, which should provide significant insight into the development of newer compounds. The latter should be effective to combat both drug-susceptible and MDR/XDR-TB.*

Key words: *Mycobacterium tuberculosis* - epidemiology - chemotherapy - vaccine - drug action - mechanism of resistance

*There is a dread disease which so prepares its victim, as it were, for death; which so refines it of its grosser aspect, and throws around familiar looks, unearthly indications of the coming change – dread disease, in which the struggle between soul and body is so gradual, quiet, and solemn, and the result so sure, that day by day, and grain by grain, the mortal part wastes and withers away, so that the spirit grows light and sanguine with its lightning load, and, feeling immortality at hand, deems it but a new term of mortal life; a disease in which death takes the glow and hue of life, and life the gaunt and grisly form of death; a disease which medicine never cured, wealth warded off, or poverty could boast exemption from; which sometimes moves in giant strides, and sometimes at tardy pace; but, slow or quick, is ever sure and certain.*

Charles Dickens, 1870, in Nicholas Nickleby, Wiendenfeld and Nicholson, London, p. 243.

Human tuberculosis (TB) is a contagious-infectious disease mainly caused by *Mycobacterium tuberculosis*, which is an aerobic pathogenic bacterium that establishes its infection usually in the lungs. Progression of TB infection is fundamentally regulated by host's immune system integrity, which may succeed through microbial immediate elimination and/or latency conditioning, or fail resulting in development of active disease.

TB was responsible for millions of human deaths in the past, when there were no adequate treatment methods for infected patients. Introduction of chemotherapy and prophylactic measures led to drastic death reduction, which was maintained for various decades. However, the "good times" waned, as this disease became worldwide recognized as the one responsible for most human deaths caused by a single infectious agent. TB resumption is basically a consequence of anthropic factors, such as the recent HIV/AIDS pandemic and the development of drug-resistant strains (stemmed from inappropriate treatments and/or patient non-compliance). It thus appears to be of fundamental importance to increase investment in research, as disease control can hopefully be reached

Financial support: Fapergs, CNPq, Pronex, Instituto do Milênio

<sup>+</sup>Corresponding authors: diogenes@puers.br; luiz.basso@puers.br

<sup>++</sup>Research fellow CNPq

Received 18 May 2006

Accepted 9 August 2006



through new drug development (to be introduced in the treatment of patients with active TB), and through prophylactic and/or therapeutic vaccine optimization.

### Looking the past

*The captain of all these men of death that came against him to take him away, was the consumption, for it was that brought him down to the grave.*

John Bunyan, 1680, in *The Life and Death of Mr. Badman*, Dent, London, 1928, p. 282.

TB, also known as the white plague, received the title of “captain of all these men of death” by John Bunyan in the second half of the XVII century, when the disease reached a high level of death rates in Europe. This malady became the principal cause of death by the end of the XIX and beginning of the XX century, and among its various victims were worldwide known people, such as Frédéric Chopin, Paganini, St. Francis of Assisi, Charlotte Brontë (and most of the Brontë family), John Keats, Lord Byron, George Orwell, Castro Alves, Alvarez de Azevedo, Cruz e Souza, Augusto dos Anjos, Noel Rosa, Eleanor Roosevelt, and Vivian Leigh, among many others. Currently, this disease still represents a global threat, as it stands as the leading cause of death due to an infectious agent among adults worldwide.

Although it was probably described for the first time in Indian texts, pulmonary TB is known since the time of Hippocrates as phthisis, which is derived from the Greek for “wasting away”. Scrofula, a rare manifestation form of TB that affects the lymph nodes, especially of the neck, most commonly found in children and usually spread by unpasteurized milk from infected cows, was well documented during the European Middle-Age, when it was believed that cure resulted from the power of the divine touch of the kings. Pott’s disease or Gibbous deformity, a rare TB manifestation, revealed only among several antique Egyptian mummies, is a destructive form of TB that leads to serious spine deformities and subsequent member paralysis.

In 1680, the French Franciscus Sylvius carried out anatomic-pathologic studies in pulmonary nodules from TB patients, which he named as “tubercula” (small knots), observing their evolution to lung ulcers (cavities). However, most of the great pathologists of his time believed these knots were some type of tumor or abnormal gland, rejecting any probable infectious origin. The first credible speculation of the infectious nature of TB was performed by the British Doctor Benjamin Marten, who proposed in 1722 that TB could be transmitted through the “breath” of a sick person, inhaled by a sound one, and thereby turning her ill. In 1689, the English Doctor Richard Morton used the term “consumption” to specifically denote TB, and finally, in 1819, the inventor of the stethoscope, the French Doctor René Laennec identified for the first time the TB manifestation unit.

As the disease became completely established among every European social level, afflicting many of the intellectual and artists of the continent by the half of the XIX century, TB was romanticized, as typical symptoms like thin and pale faces of the infected ones became signs of beauty. The romantic Era of TB can also be recognized in

fine pieces of art, such as in the famous painting of William Morris, which exhibits all the splendor of the legendary Guinevere, King Arthur’s wife, already displaying typical symptoms of the active disease.

In 1865, the Military Surgeon Jean-Antoine Villemin demonstrated formally that TB is a contagious disease; although his experimentation could be effectively reproduced in rabbits, the finding was ignored by his contemporaries for a long time.

One of the greatest works on TB was performed in 1882 by Robert Koch, an esteemed scientist of his time. Koch isolated and cultured *M. tuberculosis* from crushed tubercles. His experimental work identified the bacterium as the TB etiological agent (Bloom & Murray 1992, Daniel 1997). In August of 1890, during The First Ordinary Session of the International Medical Congress, in Berlin, he announced the discovery of a TB therapeutic drug. Three months later, the “Deutsche Medizinische Wochenschrift”, in extraordinary edition, published a new statement of Koch, revealing that although interested in the therapeutic properties of his findings, he observed that the referred liquid, named tuberculin, could be useful as a diagnostic tool to detect the disease due to the intensified reaction developed by sick animals inoculated with this drug, as no measurable effect was ever observed in healthy ones. This concept was perpetuated for several years, until it was observed that even healthy animals could react to the drug. The veterinarians of his time clarified the fact by demonstrating that the healthy ones could be simply infected, although not ill. As a result, it was established that *M. tuberculosis*-infected animals will react to tuberculin infusion, whereas the non-infected ones will not. This drug, the first industrialized one, was called old tuberculin; subsequently, other tuberculins were produced, such as purified protein derivate (PPD), PPD-S, and PPD RT23, among others (Vaccarezza 1965, Ruffino-Netto 1970). The tuberculin skin test became the principal tool for infection diagnosis. In the same period, Koch developed staining methods for the identification of the bacillus; these techniques were subsequently improved by the German Doctor and bacteriologist Paul Ehrlich, whose method for detection of the bacillus provided the basis for the development of the Ziehl-Nielsen staining, which still is an important tool to diagnose TB.

Koch’s discovery allowed researchers to focus efforts on the development of new and more efficient therapies to treat TB patients. One of the first attempts to fight the disease was performed by Edward Livingston Trudeau, who suffered from TB and was subsequently cured. Trudeau established the first sanatorium in the United States in 1884. This institution received only TB patients, and invested in a treatment based on rest, fresh air and a healthy diet.

In 1896, the American bacteriologist Theobald Smith demonstrated that bovine TB was not caused by *M. tuberculosis*, but rather by another species, *M. bovis*. Twelve years later, the scientist-couple Albert Calmette and Camille Guérin isolated the bovine variant from its host and grew the bacilli in dispersed culture containing ox bile. By the 39th passage they observed a morphological variant that was avirulent in several animal models and

which conferred immunological protection against subsequent challenges with virulent *M. tuberculosis*. Thirteen years of experimentation led to the obtaining of the 231st passage, the variant that was administered for the first time in humans (orally), as an attempt to immunize a child whose mother died in childbirth victim of TB. Currently known as BCG (bacille Calmette-Guérin), the (intra-dermal) vaccine has become widely used to combat TB; it relies on a prophylactic administration of live attenuated bacilli to children.

The introduction of antibiotics, such as streptomycin (1947), isoniazid (synthesized in 1912, but introduced 40 years later) and *p*-aminosalicylic acid, led to a TB chemotherapy revolution, as TB mortality rates were considerably reduced (Bloom & Murray 1992, Daniel 1997). Subsequently, other anti-TB drugs were also developed, such as ethambutol and rifampicin, among others. Since the mid 1980s, however, there has been no new first-line drug development to fight the TB causing bacilli (Petrini & Hoffner 1999).

In Brazil, it is believed that the disease was introduced by the Portuguese and Jesuit missionaries since 1500. Oral BCG was administered for the first time by Arlindo de Assis in 1927 to newborn, and intradermal vaccination was implemented in 1973, becoming obligatory for one year minors since 1976. Brazilian TB mortality rates were drastically reduced due to introduction of tuberculostatic drugs by the 1940s, including streptomycin (1948), *p*-aminosalicylic acid (1949), and isoniazid (1952). The standard chemotherapy treatment recommended by the World Health Organization (WHO) to control or eradicate TB worldwide, which is based on a short-course therapy that combines the use of four anti-TB drugs, currently known as directly observed treatment short-course (DOTS), seems to be used in Brazil since 1962 by the Fundação de Serviço Especial de Saúde Pública (Sesp) in units of all complexity levels (Ruffino-Netto 2002).

### Tuberculosis resumption

In 1993 the WHO declared TB a global public health emergency, being the only disease so far to warrant that designation. Although hospitals have been established and chemotherapy has been developed to combat TB, which have brought considerable reduction in incidence to developed nations, historical data calculated by the WHO indicate that there have not been great effects on the global problem since the time of Koch (Bloom & Murray 1992). Currently, TB is responsible for more human deaths than any other single infectious agent, standing for 26% of all preventable deaths and 7% of all deaths (Enarson & Murray 1996).

TB resumption has been attributed to several factors, such as the increase in drug resistance; the HIV/AIDS pandemic (in the beginning of the 1980s); the increase of injectable drug users; changes in social structure; the increase of immigrants from high prevalence nations to developed ones; the aging of the world population; the active transmission amongst environments of human accumulation (such as prisons, hospitals, and homeless shelters); and the degradation of health care systems (Fätkenheuer et al. 1999). Although TB became a reemerg-

ing disease to European and North-American nations, TB is not an emergent nor reemerging public health problem in developing countries such as Brazil, but rather a long lasting one (Ruffino-Netto 2002).

In order to facilitate the comprehension of the various components involved in the interaction between these factors, Ruffino-Netto (2004) proposed an "equation" which expresses the TB charge, represented as follows:

$$TbB \approx \frac{(SIN).(PHIV).(PDEF).(PR).(MIG).(OLDP)}{(AHS).(DOTS).(EDU).(NUT).(HRTb).(DPP)}$$

where SIN: social inequality; PHIV: prevalence of HIV-positive; PDEF: percentual default of treatment; PR: prevalence of primary resistance + acquired resistance; MIG: migrations; OLDP: age of the population; AHS: adequate health services; DOTS: directly observed treatment short-course; EDU: educational level; NUT: nutrition level; HRTb: human resources for TB control; DPP: degree of political participation of the population.

Among all the components, social inequality should be emphasized as the most important one, since it generates poverty and, consequently, leads to malnutrition, ill-provided living conditions and education, among others, thereby influencing practically all other components. It should also be pointed out that the prevalence of primary resistance (whose definition is given below) stands as an aggravating epidemiological factor more important than acquired resistance (subsequently defined under treatment section). According to Ruffino-Netto (2004), the above-mentioned expression does not represent a mathematical equation and, therefore, will not yield predictable numeric solutions, but rather facilitates to wonder about the problem (TB charge analysis). One should notice that it contains variables of qualitative nature.

In nations such as India, China, Indonesia, Pakistan, Nigeria, Philippine, South Africa, Ethiopia, Vietnam, Russian Federation, Democratic Republic of Congo, Brazil, United Republic of Tanzania, Kenya, Thailand, Myanmar, Afghanistan, Uganda, Peru, Zimbabwe, and Cambodia, it is estimated an occurrence of up to 80% of world TB cases. It can be immediately perceived that, among the above-mentioned nations, the problem may be located either at the level of the numerator, denominator, or both within the expression. In Russia, for example, the multidrug-resistance prevalence problem is prominent and severe. In African nations, all the numerator and denominator components have a strong influence. Brazil might represent an intermediate condition, as it displays a (yet) small multidrug-resistance prevalence problem, but deals with major social inequality and has all remaining components in a phase of organization.

It is possible that a more elaborated reflection of this new "formula" might allow one to perceive that at the same time technical, biological, clinical, and epidemiological knowledge on TB advances, its social dimension should be remembered, valorized and used as an indicator of poor living conditions in other discussion forums such as The World Health Assembly, The International Labour Organization, and The World Trade Organization, among others.

Antibiotic treatment efficacy against Koch's bacillus

has had some hindrances, in part, owing to human natural reluctance in complying with the 6 month-intensive treatment required, and more recently, owing to development of drug-resistant strains of the bacillus (Young 1998). In 1969, the Medic Chief of the National Institute of Health declared in congress that "it was time to close the books about infectious diseases" (Bloom & Murray 1992). With a similar point of view, the TB problem was considered to be "resolved" by authorities, as the malady, physiopathology, diagnostic methods, therapeutic strategies and pharmaceutical resources were already well known (Ruffino-Netto 2002). Arrogant and low-priced behaviors like these have severe consequences, as millions of people suffer daily from the various diseases (infectious or not) that afflict humans.

### *M. tuberculosis*

*M. tuberculosis* is the principal TB etiological agent in humans; it is a weak Gram-positive rod-shaped bacterium that has no flagellum, does not form spores nor produces toxins and has no capsule. The microbe's width and height vary from 0.3 to 0.6 and 1 to 4 µm, respectively, and it presents a complex cellular envelope, considerably slow growth, and genetic homogeneity. It is a macrophage intracellular pathogen that establishes its infection preferentially to the pulmonary system, where it is usually conditioned into a dormancy state as long as host's immune system prevails. The generation time is around 24 h in both synthetic medium and on infected animals (Cole et al. 1998). Bacterial growth at laboratory environment permits visual colony formation; these have a dry and wrinkled surface, and requires 3 to 4 weeks of growth on solid media to become visible (Bloom & Murray 1992). Owing to its pathogenicity and aerosol transmission, there are specific biosafety guidelines that demand the use of laminar-flow hoods and level 3 facility equipments for *M. tuberculosis* laboratorial work.

Currently, there are 60 known species among the *Mycobacterium* genera, most of them being saprophytic soil bacteria; and a minority of these species is pathogenic to humans, causing TB (*M. tuberculosis*, *M. bovis*, and *M. africanum*) and leprosy (*M. leprae*) (Jarlier & Nikaido 1994). The *M. tuberculosis* complex consists of *M. tuberculosis*, *M. bovis*, *M. bovis* BCG, *M. africanum*, and *M. microti*; and it is believed that their ancestral is a bacterium from soil, and that the human bacillus may have been derived from the bovine form (*M. bovis*), probably through cattle domestication by the pre-dynastic Egyptians. *M. tuberculosis* genomic studies indicate that horizontal transference of genetic material to a free living ancestral from the *M. tuberculosis* complex might have occurred in nature before the bacillus adopted its specialized intracellular niche (Cole et al. 1998, Daniel 1997).

There is a great variability in the infection rates among people exposed to different infection sources, and among infected ones, approximately 90% will never develop the disease at all. There are also differences in the capacity to transmit the infection among patients due to exhaled bacterial charge variability. Experimental evidence also suggests that the observed variation in transmission potential might be attributed to pathogenic features. *M. tuber-*

*culosis* can have virulence variations among different strains; the more virulent ones present higher pathogenicity or capacity to develop active disease. However, it should be pointed out that it is fundamental to have a clear distinction between the capacity a strain has to cause infection and its capacity to develop the disease (Bloom & Small 1998).

Like many other infectious diseases, TB presents epidemic cycles that might, although rarely, take centuries to end its course. History has proved that pathogenic virulence suffers considerable reduction along time, and natural selection takes place upon its hosts, as only the more genetically resistant ones survive. Since untreated TB patients have mortality rates ranging from 40 to 60%, one can consider the possibility of human selection occurrence in favor to the ones with increased genetic resistance (Bloom & Small 1998). Although genes will not influence the risk of infection upon exposure, they might determine the risk of disease development and its course (Daniel 1997). Furthermore, although genetic variability evidence on TB human susceptibility is very difficult to be determined, several studies revealed a greater disease severity among black than white people, there is a greater TB course agreement between monozygotic than heterozygotic twins, and populations more recently exposed to the TB bacillus have a greater propensity to develop the disease when compared to others that coexist with TB for centuries. As one gathers all these data, he can suppose that *M. tuberculosis* still is an extraordinary pathogen which exerts a powerful selective pressure on the human genome (Bloom & Small 1998).

### *M. tuberculosis* genome

The complete genome sequencing of the best characterized *M. tuberculosis* strain, H37Rv, allowed the identification of unique microbial features. This pathogen has a circular chromosome with 4,411,529 base pairs with a 65.6% G+C content. Since its isolation in 1905, this strain has had a great application worldwide in biomedical research due to total TB virulence retention in animal models, and also because it is susceptible to drugs and amenable to genetic manipulation (Cole et al. 1998). *M. tuberculosis* sequence determination establishes a new phase in the battle against one of the more successful predators of the human race (Young 1998).

Although *M. tuberculosis* genome is smaller than *Escherichia coli*, it is very versatile, coding for most of the typical bacterial anabolic and catabolic pathways and amino acid synthesis/degradation. However, it is important to point out that a feature that differentiates *M. tuberculosis* from any other bacteria is the presence of a genome with approximately 4000 genes, mostly coding for enzymes involved in lipolysis (for bacterial survival inside its host) and lipogenesis (for cellular envelope synthesis). This microbe has around 250 enzymes involved in fatty acid metabolism. The genome is rich in repetitive DNA, especially insertion sequences, inserted in intergenic or non-coding regions, frequently close to tRNA genes. These are usually clustered, indicating the existence of insertion hot spots, which may prevent gene inactivation. There have been at least two prophages detected

in its genome, which can be involved with the fact that *M. tuberculosis* has a low lysis level in culture. Interestingly, about 59% of the genes are transcribed in the same direction as the replication; once compared to the 75% of *Bacillus subtilis*, one can probably relate this feature to the peculiar slow growth and infrequent replication cycles of the former one. Data comparative analyses allowed the precise function attribution to 40% of the proteins identified, and some information or similarities to another 44%. The remaining 16% have no similarity to any known protein, being probably involved in specific mycobacterial functions. Among secreted proteins that were identified in the mycobacterial genome sequence that could act as virulence factors are phospholipases C, lipases and esterases, which might attack cellular or vacuolar membranes, as well as several proteases. One of these phospholipases is involved in bacterial persistence in the nutrient-limited phagosome environment.

Stewart Cole et al. (1998) made an important contribution as they identified a group of variable elements, the polymorphic G+C-rich sequences, which correspond to a family of sequences that encode proteins with small peptide motifs, PE and PPE, which are organized as common repetitive domains. These proteins represent approximately 10% of the genome coding capacity and seem to be remnants of the ones related to antigenic variation in other bacteria. Through protein expression pattern alternation, these pathogens can be presented to their host's immune system as a moving target, interfering in the immunological response by antigen processing inhibition, and thereby, ensuring a greater survival probability to the bacteria.

*M. tuberculosis* proteome determination and its comparison with that of other microorganisms whose sequences are available revealed a significant statistical preference for the amino acids alanine, glycine, proline, arginine, and tryptophan, which are all encoded by G+C-rich codons, and a comparative reduction in the use of amino acids encoded by A+T-rich codons, such as asparagine, isoleucine, lysine, phenylalanine, and tyrosine. By means of mycobacterial genomic inspection, it became clear that besides the various functions involved in lipid metabolism, the enzymes required for glycolysis, the pentose phosphate pathway, and the tricarboxylic acid and glyoxylate cycles are also present, thereby evidencing the dynamic metabolism of the bacillus (Cole et al. 1998).

### **Mycobacterial cellular envelope**

Mycobacteria produce an extremely uncommon cell wall structure; the peptidoglycan contains *N*-glycolylmuramic acid instead of the usual *N*-acetylmuramic acid, found amongst most other bacteria. A far more distinctive feature is that up to 60% of the mycobacterial cell wall is composed of lipids that consist basically of uncommonly long-chain fatty acids with 60 to 90 carbons, denominated mycolic acids (Brennan & Nikaido 1995). Mycolic acids are branched fatty acids that have a short and a long branch, with 22 to 24 and 40 to 64 carbons, respectively (Jarlier & Nikaido 1994); they are covalently linked to the polysaccharide that composes the cell wall, the arabinogalactan, which in turn is attached to pepti-

doglycan by a phosphodiester link (Brennan & Nikaido 1995). Approximately 10% of the arabinose residues in the arabinogalactan are substituted by mycolic acids (McNeil & Brennan 1991). The cell wall also contains several other free lipid species, which are not covalently attached to this basal skeleton (the mycolylarabinogalactan-peptidoglycan complex). These lipids can act as antigens in the host (Brennan & Nikaido 1995).

In 1982, Minnikin proposed a new cell wall model where the mycolic acid chains are packed side by side perpendicular to the cell surface, and this inner leaflet of long-chain fatty acids is covered by an outer leaflet composed of extractable lipids, thereby reproducing an asymmetric lipid bilayer. Recently, this model was updated by mycobacterial cell wall X-ray diffraction studies. In the arabinogalactan polysaccharide, both galactan main chain and arabinan side branches are designed in a manner that would ensure maximum mobility between sugar residues. The mycolic acid residues are esterified to approximately two-thirds of the non-reducing termini of this highly branched polysaccharide (McNeil & Brennan 1991), as shown in Fig. 1.

Another distinguishing property shared among mycobacteria is the fact that their cell wall retain carbol fuchsin dye even in the presence of acidic alcohol, for this reason the rod-shaped mycobacteria are also known as acid fast bacilli (Glickman & Jacobs 2001). *M. tuberculosis* produces a considerably diverse array of lipophilic molecules, which range from simple fatty acids, such as palmitate and tuberculostearate, to long-chain complex molecules, such as mycolic acids and phenolphthiocerol alcohols (mycoside attachment) (Cole et al. 1998). Although mycobacteria have various cell wall lipid types, some are limited to specific species, such as sulfolipids, solely present in *M. tuberculosis* and which are involved in its pathogenicity (Brennan & Nikaido 1995). Furthermore, the mycobacterial cell wall fluidity gradient appears to have an opposite orientation to all Gram-negative bacteria, as the more external regions are more fluid than the internal ones (Brennan & Nikaido 1995).

Mycobacteria possess membrane proteins that form selective cationic channels called porins that control or retard the diffusion of small hydrophilic molecules, thereby conferring low cell wall permeability to hydrophilic solutes (Jarlier & Nikaido 1994). Amongst mycobacterial species, *M. tuberculosis* is one of the more permeable to hydrophilic antimycobacterial agents, and, thereby, less resistant to such drugs (for instance, ethambutol) (Brennan & Nikaido 1995). In principle, lipophilic molecules should be able to easily cross any biological membrane, dissolving itself in the hydrocarbon interior of the lipid bilayer. However, factors such as low fluidity of the mycolic acid leaflet and the bilayer's uncommon thickness result in reduction of this process in the mycobacterial cell wall. The inner leaflet presents a low fluidity, indeed a nearly crystalline structure; since the diffusion of lipophilic solutes through a lipid bilayer requires a fluid interior, this structure should act as an excellent barrier against the penetration of lipophilic antibiotics. Notwithstanding, the more lipophilic derivatives of chemotherapeutic agents are often more active against mycobacteria,

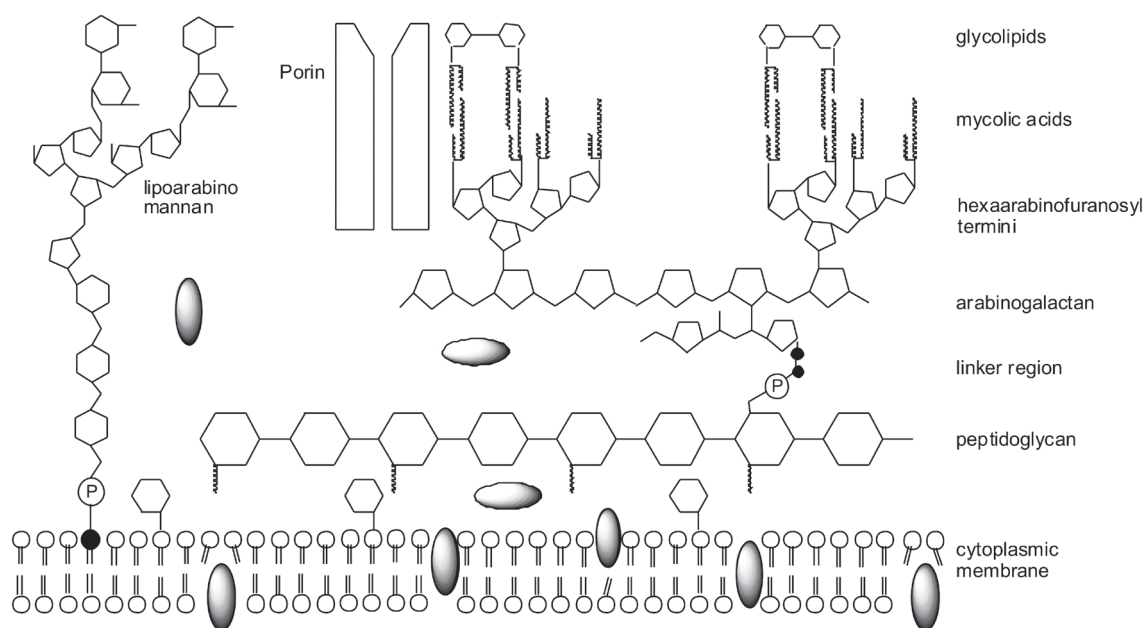


Fig. 1: schematic representation of the mycobacterial cell wall.

suggesting contribution of a lipophilic pathway to lipophilic solute transport (Jarlier & Nikaido 1994).

Since mycobacteria are relatively resistant to drying, alkali, and many other chemical disinfectants, it is thus very difficult to prevent *M. tuberculosis* transmission in urban institution environments. This resistance, and the resistance to therapeutic agents, are both basically conferred by the extremely uncommon mycobacterial cell wall structure (Brennan & Nikaido 1995). The unusual cell wall also permits the microorganism to survive inside the macrophage, which would usually destroy phagocytosed pathogens (NSB Editorial Comment 2000).

Although the cell wall acts as an exceptional permeable barrier, resistance to drugs in mycobacteria normally requires the participation of additional mechanisms, such as the removal of incorporated antibiotic molecules through chemical modification by  $\beta$ -lactamases that, synergistically, confer significant resistance levels (Jarlier & Nikaido 1994). Thereby, since *M. tuberculosis* has a cell wall with a relatively high permeability, the inactivation of the second factor in synergism may allow an effective chemotherapy. *M. tuberculosis* cell wall has become a target of the more recent researches towards the elucidation of the mechanism of action of many old drugs and the search of targets for the design of new ones (Brennan & Nikaido 1995). New data on genes specifically involved in its synthesis may represent potential drug targets (Young 1998).

### Epidemiology and disease properties

Based on tuberculin skin test reactivity, epidemiologists estimate that around one third of the world population (1.7 billion people) is infected with *M. tuberculosis*, and at risk of developing active TB. Statistical data indicate the occurrence of 8 to 10 million new TB cases and 3

million deaths annually, afflicting mostly the young and productive adults. Under the current conditions, it is expected for this decade that 90 million people will develop the disease and 30 million will die from TB (Enarson & Murray 1996).

TB seems, to a certain point, under control in developed countries such as Japan and United States, but detains a violent manifestation in other places like south-eastern Asia, Africa, and some regions of the Pacific, mostly due to complications of HIV infection and drug resistance (Brennan 1997). Approximately 95% of TB cases occur in developing nations, where 98% of the world TB death cases happen. According to the WHO databank, in 1998 Brazil occupied the 13th position among 22 countries where TB was well disseminated. In 1999, an interesting study of the distribution of TB notified cases among Brazilian states revealed a decreasing ordered incidence among São Paulo, Rio de Janeiro, Bahia, Minas Gerais, and Rio Grande do Sul (Ruffino-Netto 2002).

Currently, multidrug-resistant (MDR) TB presents a high incidence, in an increasing order, in Latvia, India, Estonia, Dominican Republic, and Argentina, and low incidence in most occidental European and African countries and United States (Fätkenheuer et al. 1999). The presence of resistant strains has a direct relation to drug availability and an inverse relation to treatment efficacy. A WHO and International Union Against Tuberculosis and Lung Disease (IUATLD) anti-TB drug-resistance global surveillance project made among 35 nations of 5 continents with standardized methods showed that during the 1994-1997 period, all the countries and regions analyzed presented *M. tuberculosis* strains resistant to at least one drug, usually isoniazid or streptomycin, suggesting that the disease represents a global problem (Pablos-Mendez et al. 1998).

Human TB is an infectious disease caused by some mycobacteria of the "*M. tuberculosis complex*", including *M. bovis*, *M. africanum*, and prevalently *M. tuberculosis*. According to the WHO, TB kills more people than malaria and AIDS together. Annually, TB is responsible for the death of 100,000 children worldwide, and 161,800 new cases occur only in Brazil. From now until 2020, it is estimated that 1 billion more people will be infected, 200 million will develop the disease, and 70 million will die in case surveillance and control strategies continue as they are (Pasqualoto & Ferreira 2001).

The principal means of transmission occurs by infective particles. Active TB patients will usually cough, as a result of typical chronic pulmonary inflammation, which constitutes the main dissemination mechanism for the pathogen to new hosts (Glickman & Jacobs 2001). The released particles from an ill patient are exhaled from the infected lungs into the air, being able to remain in suspension for hours, representing a highly contagious disease (NSB Editorial Comment 2000). Infection usually occurs from person to person through the inhalation of the infective particles (Pasqualoto & Ferreira 2001). Experiments with animal models demonstrate that particles in suspension containing 1 to 10 bacilli are enough to cause an infection. The main determinants of risk of infection are the concentration of bacilli in an exhaled particle from a source, its aerodynamic features, the ventilation rate, and the exposure period (Bloom & Murray 1992).

Usually, upon infection, inhaled bacilli are ingested by phagocytic alveolar macrophages, and can either be immediately eliminated or grow in the intracellular environment in localized lesions called tubercles. Two to six weeks past infection are usually followed by the establishment of cellular immunity, and subsequent lymphocyte and activated macrophage infiltration into the lesion, which leads to the elimination of most portion of the bacilli and the end of the primary infection, commonly without symptom presentation. The sole evidence of previous infection in these cases can be identified by the tuberculin skin test reactivity, or, in some cases, evidences of calcified lesions by X-ray.

In most cases, however, the bacilli can coexist peacefully within its human host as a quiescent or dormant form of infection, establishing a large bacterial reservoir among infected individuals. People harboring latent infection have an active TB developing risk of approximately 5% after the first year and 10% during their life-time.

Although much of the bacterial load is usually eliminated, a great proportion of the infiltrating phagocytes and lung parenchymal cells are also killed, which produces a characteristic solid caseous necrosis (granuloma or Gohn complex) where some bacilli have the opportunity to hide. In case host immune response predominates, the lesion is contained, causing simply residual damage to the lungs. However, in case the necrosis reaction expands, breaking into a bronchus, a lung cavity can be formed, which may allow a massive bacterial dissemination into the air through coughing. There can be even worse cases, such as when inflammatory cells liquefy the solid necrosis, creating a rich environment for bacillary proliferation

(Bloom & Murray 1992, Young 1998).

Approximately 15% of the patients with the active disease present extra-pulmonary TB, which is caused by granuloma evolution due to excessive bacterial growth, invading the blood stream and disseminating the bacilli to various parts of the body. Also called miliary TB, it frequently occurs in the pleura, lymph nodes, liver, spleen, bones and joints, heart, brain, genital-urinary system, meningis, peritoneum, and skin.

The pathological and inflammatory processes produce typical TB symptoms such as weakness, fever, weight loss, night sweat, chest pain, respiratory insufficiency, and cough; advanced pathology may also cause blood vessel disruption, which leads to hemoptysis (Bloom & Murray 1992). For this reason, TB was also known as consumption, since the disease is developed at a leisurely pace and with multiple symptoms which lead to gradual debilitation and physical exhaustion.

### Immune system in tuberculosis

Following intravenous mycobacterial infection in mice, the bacilli present (initially) a very short replication time in vivo, when macrophage activation begins by macrophage-derived pre-inflammatory cytokines, such as inter-leukin 6 (IL-6), IL-12, and tumor necrosis factor (TNF), besides the involvement of gamma interferon (INF- $\gamma$ ), initially derived from natural killer (NK) cells, in order to contain or inhibit bacterial growth. Approximately 2 weeks after initial infection, there is a considerable reduction of bacterial growth (representing a plateau in a growth plot) due to the activation and differentiation of specific lymphocytes, which are able to supply the lack of INF- $\gamma$  required to increase the initial innate response, activating macrophages that induce the nitric oxide synthase 2 (iNOS) to produce nitric oxide, one of the main myco-bacteriostatic mediators or effector molecules in mice. Following infection with *M. tuberculosis*, there is a significant reduction of bacterial load in the liver, and also in the spleen (to a lesser extent). The remaining bacilli enter into a state of non-replicating persistence, although these still are fully viable (Ehlers 1999). Although the bacillus charge in this phase of the infection in mice does not mimic the latent state in the human host, it represents an equilibrium between the pathogen's persistence and the host's immune response (Glickman & Jacobs 2001). This dormant but yet viable bacillary form can re-establish its replication and develop the active disease in certain conditions of immune suppression, such as aging, corticosteroid therapy, CD4 cell charge reduction or treatments with iNOS inhibitors. Unfortunately, total bacillary elimination is improbable solely through the immune system, and considerably difficult to be reached by chemotherapy (Ehlers 1999).

Although most inhaled bacilli are usually rapidly destroyed by the host immune system, some will eventually establish infection, primarily in macrophages, inhabiting inside a membrane-bound vacuole, the phagosome (Glickman & Jacobs 2001). These can sometimes remain in a dormant form inside lung macrophages lodged in the calcified structures called tubercles (which gave origin to the disease's name), resultant of an attempt to isolate the

infected area (NSB Editorial Comment 2000). Granuloma formation might sometimes occur at the moment where the above-mentioned plateau is reached, causing destabilization and destruction of adjacent tissues, and possibly necrosis, followed by cavity formation (Jagirdar & Zagzag 1996). Granulomas are a result of CD4-mediated delayed-type hypersensitivity reaction within parenchymal tissues. Accordingly, the same system that is responsible for bacterial growth decrease (host defense) is also intrinsically associated with tissue damage through granuloma formation and necrosis (Ehlers 1999). Many TB symptoms, including tissue destruction which eventually liquefies lung infected portions, are preferentially mediated by the host's immune response against the bacillus instead of the bacterial virulence itself (Glickman & Jacobs 2001).

Depending on the bacterial charge that persists in the primary lesions, there can be granuloma development and differentiation. Owing to an efficient systemic antibacterial response, liver-localized granulomas will frequently suffer size reduction and can sometimes disappear. In the lungs, where bacterial charge is constantly high, it can be observed evident chronic-progressive pathology. Progressive interstitial fibrosis can eventually occur, gradually replacing most of the lung airspaces with dense fibrotic tissue separating groups of alveolar sacs, giving the entire lung a honeycomb appearance (Ehlers 1999).

#### ***M. tuberculosis* latency and reactivation**

Latent TB is a clinical syndrome caused by exposure to *M. tuberculosis*, followed by establishment of infection and host's immune response to control bacillary growth, forcing it into a quiescent state in the infected tissue. It is characterized by a reduction of bacterial metabolism, as a consequence of the action of cellular immune response, and which can, to a certain point, contain, but not eradicate, the infection. Contrary to active TB, latent TB is not an infectious disease and, therefore, does not represent a public health threat. Since latent TB is not presented as a clinical illness, the sole form to be diagnosed is by tuberculin skin tests. A positive result indicates that the patient has already had contact with the microbe. The method relies on the intradermal inoculation of PPD. In certain cases, the infection can be identified through a chest X-ray radiography that demonstrates scars of an old infection.

The bacterial intracellular survival is based on its capacity to deal with the phagosome acidification in infected macrophages and prevent the phagosome-lysosome fusion. In most immunocompetent infected patients, there is the occurrence of T-cell and macrophage recruitment, and the establishment of secondary immune response, resulting in infection control. As the immune system begins to fail, latent infection can be reactivated, leading to the development of active TB, frequently several decades after initial infection. Reactivation can be induced by various factors, all of which compromise the immune system's efficacy, such as HIV co-infection, malnutrition, aging, drug use, cancer, diabetes, chronic renal insufficiency and immunosuppressive drug therapy (Parrish et al. 1998).

It is well known that the conventional treatment can

reduce active TB risk in patients recently infected by the bacillus. Since 90% of the infected people develop immune response against the microorganism, it becomes interesting to establish an effective protection mechanism that complements the immune system action, curbing disease development through drugs or recombinant strain vaccines. Antigenic expression induction during latent infection can optimize immune system activation against microorganisms that insist in persisting (Young 2001).

#### **Tuberculosis and AIDS**

The connection between TB and the human HIV was well documented for the first time in New York, where it was estimated that the risk of developing active TB among HIV and *M. tuberculosis* co-infected people was approximately 8% per year, compared to 10% risk throughout life-time for people infected solely with the bacillus (Bloom & Murray 1992). As the immune system withers due to HIV infection, the probability to develop the disease increases up to 30 times (Pasqualoto & Ferreira 2001). An increase in TB susceptibility is associated to the first HIV infection stages, accelerating its progression to acquired immune deficiency syndrome (AIDS) (Young 1998). The incidence of double infection cases occurs mainly among workers in high productivity age, such as 15 to 59 years old (Narain et al. 1992). Among patients with AIDS (immune suppressed) there can be opportunistic infections, caused by the so called "atypical mycobacteria", which include the *M. avium* complex, *M. kansasii*, *M. fortuitum*, and *M. chelonae*, although these species are essentially saprophytic (Brennan & Nikaido 1995).

Currently, HIV infection represents the major risk for the progression of a latent infection into the active disease. Furthermore, TB induces AIDS development in HIV-positive patients by the production of stimulatory cytokines and a decrease in CD4 cell charge. Therefore, HIV-*M. tuberculosis* co-infection represents a devastating problem to both, infected patients and the global population. In the last decades, a dramatic increase in TB incidence in Africa has been observed, as a consequence mainly of HIV epidemic, reaching alarming rates and leading people to question whether "Africa can still be saved". A study performed in this continent demonstrated that there are several evidences that demonstrate the strong association between these two infections, as: TB is the most important disease associated to HIV and AIDS-defining disease; TB is the principal cause of mortality among patients HIV-infected in hospitals; TB incidence increase coincides within period, region and population with the appearance of AIDS; HIV is more present among people with TB than within the whole population; active TB is more common between HIV-positive individuals than negative ones. There are approximately 20 million people infected with HIV in sub-Saharan Africa, and half of these are co-infected with TB. According to the WHO, one third of the increase in TB incidence in the last 6 years was attributed to HIV co-infection. In Brazil, it is estimated that 200,000 people are co-infected with TB and HIV. The synergism established between these two infections rendered them the designation of "cursed duet".

HIV infection has drastically changed TB's epidemiology and "natural" history, causing an increase in its transmission dynamic, morbidity and mortality. TB diagnosis among HIV-positive patients became more difficult to be performed due to various factors, such as: false negative tuberculin skin tests; pulmonary TB with atypical chest X-ray findings or with sputum smears negative for acid fast bacilli; and extra-pulmonary TB (Fätkenheuer et al. 1999). It is evident that HIV epidemic favors the emergence of drug-resistant strains of the TB bacillus in co-infected patients since, in these cases, there is a higher treatment abandon rate (Brennan 1997). Mortality rates among HIV-positive patients infected with MDR-TB frequently exceed 80%, and the period between the diagnosis and death usually ranges from 4 to 16 weeks (Riley 1993). For these reasons, MDR-TB is currently known as "the most malignant opportunistic infection yet associated with HIV infection" (Nolan 1997).

### Diagnosis

The tuberculin skin test is the epidemiological surveillance method currently disseminated throughout the world, and can be used to detect infections from many years past or even very recent ones (Bloom & Murray 1992), and it is the only way to detect a latent infection by the Koch's bacillus, through delayed type hypersensitivity against mycobacterial antigens (Glickman & Jacobs 2001). However, BCG vaccination also produces reactivity to PPD, making the use and trustworthiness of this method gradually lower as child BCG vaccination increases (Bloom & Murray 1992). It was demonstrated by an animal model experiment that there is a great discrepancy between immunological, bacteriological and microscopic methods for the detection of latent TB in infected animals, which suggests that none of these techniques is 100% sensitive. Based on this fact, it can be inferred that the tuberculin skin test used to detect latent TB in humans gives distrustful results (Ehlers 1999).

Diagnosis and treatment of pediatric TB have several difficulties due to various factors, since young children rarely expectorate, tuberculin skin tests are not always easily interpreted, as false positive results can occur due to BCG vaccination, which is routinely given at birth; and false negative results can frequently occur in immune suppressed patients (Fätkenheuer et al. 1999). In order to diagnose MDR-TB, it is necessary to perform bacillary sensibility tests for anti-TB drugs (Bactec system), using established drug concentrations, and a control without drugs (as a reference). Another technique is the proportion method, in which it is defined which drugs and at what minimal concentrations occurs inhibition of at least 99% of bacterial growth (Petrini & Hoffner 1999). The progress of molecular techniques allowed the development of more sensitive and rapid methods for the detection and identification of mycobacteria. Many of these methods are commercially available, with sensitivity and specificity usually superior to 90%. However, one of the main problems here relies on the cost of these methods, restricting their use to developed nations. Molecular detection methods usually initiate with genomic sequence amplification, generally through polymerase chain reac-

tion (PCR), which uses specific repetitive or DNA single copy sequences, and can give a specific and sensitive diagnosis in a few hours (Bloom & Murray 1992, Caws & Drobniowski 2001). In vitro amplification of specific sequences in the pathogen's genome allows a rapid diagnosis with a greater sensitivity and specificity degree than standard traditional methods that have been established along the past years. In a few hours, it is possible to identify relevant pathogenic clinical features, either directly in samples or in precocious cultures, and detect antimicrobial resistance markers directly on samples. Thereby, TB diagnosis can now be confirmed in a single day instead of a 1 to 2 month period as in the past.

There are many mycobacterial genes that confer resistance to drugs caused by specific mutations. After the sequencing of these genes and the identification of their mutations, one can use several molecular detection methods for drug resistance. Although the ideal one would be DNA sequencing, it is sometimes impracticable, forcing the option for alternative techniques, such as PCR single-strand conformation polymorphism analysis, heteroduplex analysis, mutation-specific priming, restriction enzyme analysis, and solid-phase hybridization methods. Other rapid detection systems have recently been developed as an alternative based on phenotypic methods, which can be adapted for use in susceptibility tests. One of these techniques uses mycobacteriophages with the *lux* gene inserted in the genome, for example; other methods include flow cytometry and reverse transcriptase PCR (Caws & Drobniowski 2001).

Molecular methods tend to have their use gradually increased in order to perform rapid diagnosis, pathogenical studies and epidemiological distribution of infectious diseases. The availability of genomic sequences from a great number of microbial pathogens will provide a better understanding of their evolutive genetics, virulence and interactions with its host (Gilbert 2002). Although molecular diagnosis has a modest prestige, human disease diagnosis is clearly tending towards these innovative methods. According to Daniel Farkas, this molecular trend is due to the genomic Era, which turned available genomic sequences from important organisms, and also to the discovery of relevant targets to diagnose (Farkas 2002).

In order to have a better understanding of pathogenicity, it becomes necessary to know the classes or groups of proteins and their variants. Therefore, proteomic use and development becomes necessary in order to explain complex disease phenotypes. The identification of all protein variants, their inter-relations, and the functional consequences generated by changes in their levels should be considered to understand the clinical presentation of complex diseases. There are some barriers to be overcome before there can be an implementation of molecular diagnostic tests in clinical laboratories, such as: which test to be applied, the technology and equipment to be chosen, and factors like cost-effectiveness, precision, and staff training, among others (Fortina et al. 2002).

It is already known that drug efficacy or toxicity varies among medicated patients and, since these differences are greater among people with no sort of kinship than



between monozygotic twins, it is believed that some of these differences in drug response are inherited. It is supposed that this can be attributed to polymorphisms in genes encoding drug-metabolizing enzymes, drug transporters and/or drug targets. However, it is recognized that many non-genetic factors influence the effects of medications in patients, including the nature and the severity of the disease that is being treated, the patient's age, sex, and ethnicity, among others. The utility of pharmacogenetics in diagnosis will come from the ability to determine, based on genetic tests, the probability of a specific medication to produce the desired therapeutic effects (the efficacy) or the risk of an adverse response to the drug (the toxicity). It can divide a population of patients with the same diagnostic into sub-groups that have genetic differences in their metabolism and/or drug response susceptibility.

Chemotherapy efficacy rates to most diseases vary from 25 to 80%. Therefore, the ability to predict an efficient response based on genetic tests, performed before the beginning of therapy, has the potential to be of great clinical value. Since all drugs that produce an efficient response can, in specific conditions, induce adverse effects, the availability of genetic tests that can identify the patients at risk of developing the rare, but still severe, adverse effect seems particularly attractive. These genetic determinants of drug effects remain stable during the patient's lifetime, and, therefore, require a single measurement. At birth the child can have a blood sample collected in order to have the genome determined, which can be used throughout life to guide primary prevention strategies, make diagnoses on a molecular basis, and establish particular drug therapy, that is, translate functional genomics into personalized medicine. It seems inevitable that, in the future, pharmacogenomics will come up to be an important part in the process of drug development (Johnson & Evans 2002).

## Treatment

*It happens then as it does to physicians in the treatment of Consumption, which in the commencement is easy to cure and difficult to understand; but when it has neither been discovered in due time nor treated upon a proper principle, it becomes easy to understand and difficult to cure. The same thing happens in state affairs; by foreseeing them at a distance, which is only done by men of talents, the evils which might arise from them are soon cured; but when, from want of foresight, they are suffered to increase to such a height that they are perceptible to everyone, there is no longer any remedy.*

Niccolò Machiavelli, in The Prince, Luigi Ricci, Ed. (English edition, Oxford University Press, Oxford, 1933), chap. 3, p. 153.

About half of the new TB cases would be inevitable, as a consequence of the disease's natural history and HIV co-infection. However, many of the exceeding cases, which result from the increase in active transmission, could be prevented by effective treatment program implementation (Bloom & Murray 1992). In the XIX century, common "treatments" for TB included lung collapse and thoracoplasty (mutilating surgery where a few ribs were removed from the patient with cavitary TB), besides the isolation of infected patients to institutions, where the air

was thought to be cleaner (NSB Editorial Comment 2000). Previously, in the classic period of the Roman Empire, Clarissimus Galenus, son of the great mathematician and architect Nikon, used to prescribe to his patients treatments based on fresh milk, pure air, maritime trips, horse-back rides, and much rest in dry environments of higher altitude. TB treatment has evolved throughout time, from magical potions to rational drug use (Daniel 1997).

The principal objective of chemotherapy in TB patients is the eradication of the whole bacillary load (Petrini & Hoffner 1999). The disease is caused by a well studied pathogen, against which there can be "magic bullets" – drugs that eliminate the bacteria without causing damage to man (Daniel 1997). Modern therapy relies on a combination of potent bactericidal agents, such as isoniazid, rifampicin and pyrazinamide, in a treatment with six month duration. Sometimes during treatment, there can be an initial resistance of the bacillus to isoniazid, making it necessary to add other first-line drugs to the treatment, such as ethambutol and streptomycin. Whenever there is resistance to at least rifampicin and isoniazid, which characterizes MDR-TB (Telenti & Iseman 2000) it becomes necessary to extend the treatment period, and frequently rely on the use of second- or even third-line drugs, even though the increased toxicity stands as a negative factor. Very recently the Center for Diseases Control, CDC-USA, defined a new class of MDR, which was named extensively drug-resistant (XDR) TB, whose isolates were resistant to isoniazid and rifampicin and at least three of the six main classes of second line drugs (aminoglycosides, polypeptides, fluoroquinolones, thioamides, cycloserine and para-aminosalicylic acid) (CDC 2006). In extreme cases, when an infection involves MDR or XDR strains (or when there is a portion of an organ considerably damaged), it becomes sometimes necessary to resort to surgical removal of granulomas, as an attempt to increase the likelihood of cure (Telenti & Iseman 2000).

First-line drugs are mainly bactericidal, and combine a high degree of efficacy with a relative toxicity to the patient during treatment; these include isoniazid, rifampicin, streptomycin, ethambutol, pyrazinamide, and fluoroquinolones (Fig. 2). Second-line drugs are mainly bacteriostatic, which have a lower efficacy and are usually more toxic; these include para-aminosalicylic acid, ethionamide, and cycloserine (Fig. 3), among others (Goodman et al. 1996). Effective TB chemotherapy must include early bactericidal action against rapidly growing organisms and subsequent sterilization of dormant populations of bacilli. The first-line drugs exhibit early bactericidal activity against actively metabolizing bacilli and the bacteriostatic second-line drugs are reserved to strengthen the treatments with the presence of resistance (NSB Editorial Comment 2000). Among all first-line anti-TB agents, isoniazid has the greatest bactericidal activity against microorganisms growing actively in cavities, followed by rifampicin, streptomycin and quinolones. However, isoniazid can frequently cause fever, and is one of the drugs with the highest degree of toxicity (Morehead 2000).

Although TB is a serious illness, it can still be cured in most new cases as long as, once diagnosed, appropriate

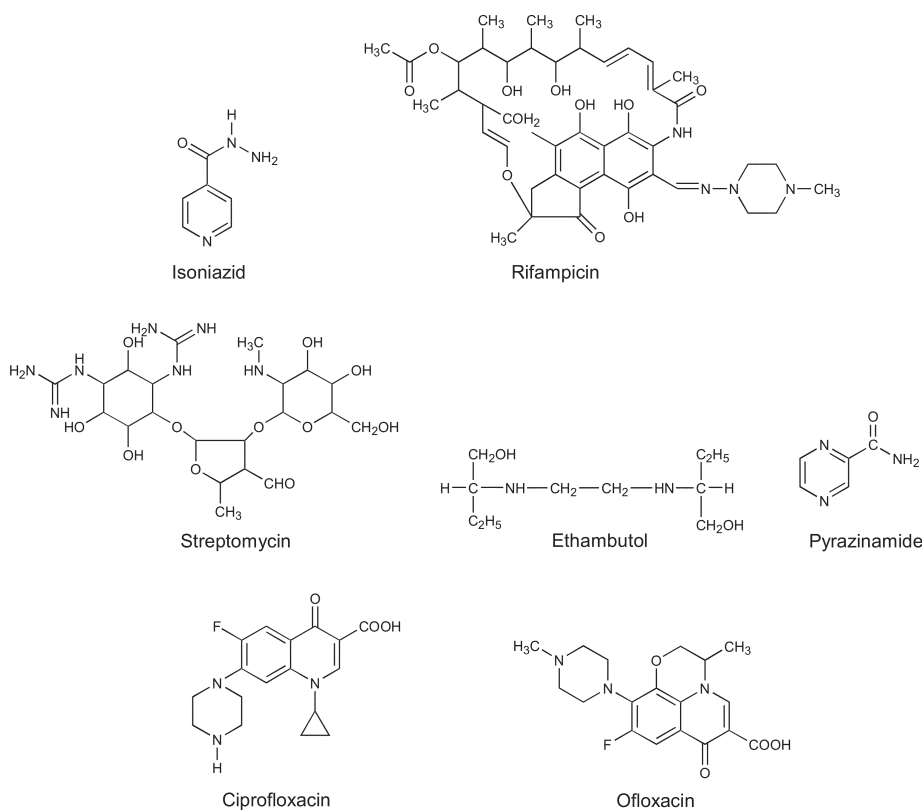


Fig. 2: first-line drugs are mainly bactericidal, combining a high efficacy with a relative low toxicity to patients undergoing treatment.

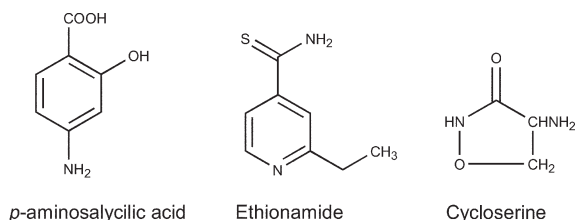


Fig. 3: second-line drugs are usually more toxic than first-line ones, have a lower efficacy and are mainly bacteriostatic.

chemotherapy is employed, since one of the greatest risks of mortality in TB is the delayed treatment. The treatment is normally consists of a medicinal association of regular use for a period long enough to avoid bacterial resistance and persistence. The treatment currently recommended by the WHO consists of the combined administration of isoniazid, rifampicin, pyrazinamide and streptomycin (or ethambutol) during the first 2 months, followed by the combination of isoniazid and rifampicin for at least 4 additional months. However, the long treatment period involves undesirable side effects to the administered drugs, leading patients to “give up” chemotherapy. The patient non-compliance led the WHO to invest in universal treatment adherence programs, through a process currently known as the directly observed treatment short-course (DOTS), where health care workers counsel patients, perform progress surveillance, and make sure that each medi-

cation dose is correctly taken (NSB Editorial Comment 2000).

This revolutionary treatment aims initially at a bacteriostatic action, inhibiting the synthesis of cell wall, nucleic acids and mycobacterial proteins, and, thereby, leading to a rapid elimination of most part of the infecting bacilli. The therapy also aims at a subsequent bactericidal action to consolidate the treatment through the elimination of all remaining bacilli. DOTS combines five fundamental elements: political commitment, microscopic services, drug supplies, surveillance systems and direct treatment observation. This strategy prevents the occurrence of new infections and, more importantly, makes MDR/XDR-TB generation impracticable (Pasqualoto & Ferreira 2001).

Patients with latent TB can also be treated on a chemotherapeutic basis; this treatment is based solely on isoniazid (monotherapy) and works only for patients with the latent infection that have not developed the active disease yet. According to the pediatrician Edith Lincon, inventor of this treatment in 1954, the therapy relies on the prophylactic administration of isoniazid for 6 to 9 months; this treatment makes disease development unlikely due to dormant bacilli elimination. The patients that most benefit from this kind of therapy are the ones more recently infected and not at advanced age. Although this chemotherapy has reached excellent results in the United States, where it is currently widely used, this type of prevention was not adopted by practically any other nation

as part of the TB national control program (Daniel 1997).

HIV-positive patients treated according to the WHO recommendations (DOTS) have sputum conversion and cure rates similar to HIV-negative treated patients. According to the WHO, there are no treatments currently available that have yielded definitive cure results for active TB patients and MDR/XDR-TB control better than DOTS (Fätkenheuer et al. 1999). Even though the efficacy of the treatment for HIV-positive and negative patients is quite similar when dealing with drug-susceptible *M. tuberculosis* infection, the choice for an appropriate TB treatment when drug resistance is suspicious can frequently be affected by the lack of rapid diagnosis tests. Drug-susceptibility tests require approximately 8 weeks to be concluded, a period usually greater than co-infected patient's survival mean time (Riley 1993). Primary or initial resistance is defined by the identification of tolerance in individuals without previous medication; and acquired or secondary resistance is defined as the resistance resultant from previous inefficient treatments (Telenti & Iseman 2000). Usually, nations with a high primary resistance rates indicate the inefficiency of previous national TB control programs to curb the occurrence of transmission of resistant strains; secondary resistance to at least one drug is likely to reflect problems in programs in progress (Petrini & Hoffner 1999).

Curiously, the recognition of TB as a global threat and the interest in tackling this problem do not derive primarily from public health institutions, but rather from the World Bank and, most of all, by the IUATLD, which annually invests 4 million dollars in the establishment of control programs that detect approximately two-thirds of all cases, treat 65,000 cases, and provide cure rates ranging from 80 to 85% in some developing nations (Bloom & Murray 1992). However, this investment is still considerably below what is considered as necessary.

Since TB mortality is mainly attributed to the delayed detection of the disease, and is also associated to drug resistance and HIV co-infection, among others, it is expected that patients without these factors will survive. However, the treatment of patients infected with drug-susceptible *M. tuberculosis* that have developed active disease with sub-therapeutic drug doses can easily lead to death, as the bacilli have a favorable condition to expand infection and cause active disease (Morehead 2000).

### Mechanism of drug action and MDR/XDR

*M. tuberculosis* is naturally resistant to many antibiotics and chemotherapeutic agents, such as  $\beta$ -lactams, owing to the presence of hydrolytic and drug-modifying enzymes, such as periplasmic  $\beta$ -lactamases and aminoglycoside acetyltransferases, and drug efflux systems, besides the fact that they possess a highly hydrophobic cell wall that acts as a contention barrier that makes treatment more difficult. This bacterium is only susceptible to isoniazid, ethambutol, aminoglycosides (such as streptomycin) and rifamicins (such as rifampicin), among antibiotics, and to fluoroquinolones (Fig. 2) among general chemotherapeutic agents (Brennan & Nikaido 1995). Within the same genus, obligatory parasite species such as *M. tuberculosis* have a relatively high permeability as

compared to soil mycobacterial species that have developed a protection mechanism through the production of a cell wall with extremely low permeability, and, therefore, naturally more resistant (Jarlier & Nikaido 1994).

Many pathogenic bacteria possess resistance plasmids, which can effect a rapid MDR transition to drug-susceptible wild-type strains, and might confer resistance to many antibacterial substances at once. This has never been observed in *M. tuberculosis*, but it is known that the resistant and multi-resistant phenotypes are caused by random chromosomal mutations in different genes of this organism, such as nucleotidic insertions, deletions, or substitutions (Petrini & Hoffner 1999).

The drug resistance in TB treatment is almost as old as the introduction of the first anti-TB drugs (Petrini & Hoffner 1999). After 4 to 6 weeks of treatment, the physical debilitation symptoms begin to disappear, inducing many of the patients to interrupt the therapy. However, many of them end up developing the disease recurrently, making it necessary to initiate a new treatment, in case they are diagnosed, which creates favorable conditions for the selection of drug-resistant organisms (Bloom & Murray 1992). The first step towards the development of molecular detection methods of drug-resistance was the identification of genes and mutations involved in this process. Mycobacteria develop resistance to drugs spontaneously ("natural resistance"), and present different mutation rates for each drug. In the TB bacillus, these rates are equivalent to 1 in  $10^5$  to  $10^6$  for isoniazid, 1 in  $10^8$  for rifampicin (Riley 1993), 1 in  $10^8$  to  $10^9$  for streptomycin, 1 in  $10^7$  for ethambutol, and 1 in  $10^9$  for cycloserine (Gangadharam 1984). A cavitary lung lesion can shelter up to  $10^9$  organisms, and, thereby, it is probable that there exists isoniazid or rifampicin resistant organisms. Mutation rates for both drugs is 1 in  $10^{14}$ , so it is virtually impossible for *M. tuberculosis* to become spontaneously resistant to both drugs in patients correctly treated (Riley 1993). As monotherapy induces the selection of drug-resistant populations ("acquired resistance"), it becomes necessary to use a combined therapy, since the probability of a bacterial strain to develop resistance to two or more drugs at the same time is extremely low (Petrini & Hoffner 1999).

The first biochemical effect of isoniazid occurs in the first stages of mycolic acid synthesis. Isoniazid is a synthetic pro-drug that requires the product of the *katG* structural gene for its activation (Telenti & Iseman 2000); this drug becomes an active compound once it is metabolized by the *M. tuberculosis* catalase-peroxidase enzyme, and inhibits the activity of the enoyl-ACP (CoA) reductase enzyme (encoded by the *inhA* gene) in the presence of NADH or NAD<sup>+</sup> (reviewed in Basso & Blanchard 1998, Schroeder et al. 2002, Basso & Santos 2005). Resistance to isoniazid is more complex, as it involves at least 4 genes: *katG*, which mediates both susceptibility and resistance to isoniazid, and encodes the catalase-peroxidase enzyme; *inhA*, which is involved in the elongation of fatty acids (Zhang et al. 1992); *ahpC*, which encodes the hydroperoxide alquil reductase C; and *oxyR*, which is an important regulator of oxidative stress (Telenti & Iseman 2000).

Rifampicin interacts specifically with the  $\beta$  subunit

of the RNA polymerase enzyme from prokaryotic organisms to inhibit transcription, leading to bacterial death. Molecular detection of resistance is relatively easy to be analyzed, since about 96% of the rifampicin-resistance cases involve specific mutation in the *rpoB* gene, which codes for the enzyme's beta chain, producing resistance to the drug through the decrease in binding affinity of rifampicin to the polymerase (Telenti et al. 1993). The mutation rate responsible for isoniazid resistance is 100 times greater than the one responsible for rifampicin resistance, and is usually the first modification in the susceptibility of wild-type *M. tuberculosis* (Petriani & Hoffner 1999). Since, in the United Kingdom, 90% of the rifampicin-resistant isolates are also isoniazid-resistant, a single positive resistance result to the former can be considered a strong indicator of MDR-TB (Caws & Drobniowski 2001).

Streptomycin acts as an inhibitor of prokaryotic protein synthesis initiation. Two genes were identified as being involved with the resistance to this drug: *rrs*, which encodes the rRNA 16S; and *rpsL*, which encodes the ribosomal protein S12 (Telenti & Iseman 2000). Resistance to ethambutol is determined by mutations in the *embA*, *embB* and *embC* genes, which encode enzymes involved in the synthesis of arabinan (Alcaide et al. 1997). Pyrazinamide is a drug that functions only against *M. tuberculosis*, and no other mycobacterial species. Pyrazinamide resistance appears to be conferred by mutations in the *pncA* gene, which encodes pyrazinamidase, an enzyme that hydrolyses the drug to turn it active (Telenti & Iseman 2000). Current experimental evidence indicates that pyrazinamide enters *M. tuberculosis* by passive diffusion, is converted to pyrazinoic acid by pyrazinamidase/nicotinamidase enzyme activity, and is excreted by a weak efflux pump (Zhang & Mitchison 2003). Protonated pyrazinoic acid is then reabsorbed into the bacilli under acidic conditions and accumulates due to the inefficiency of the efflux pump, leading to cellular damage. Pyrazinoic acid and pyrazinamide could de-energize the membrane by collapsing the membrane potential and affect the membrane transport function at acidic pH. Unlike other anti-tubercular agents, PZA has no defined target of action. The mode of action of fluoroquinolones is on enzymes responsible for DNA topological conformation, topoisomerases, mainly DNA girases. Resistance to ciprofloxacin, one of the most active fluoroquinolones against *M. tuberculosis*, is conferred by mutations to *gyrA*, *gyrB* and *lfrA* genes, which encode the subunits A and B of DNA girase, and an efflux protein, respectively. Like most wild-type *M. tuberculosis* strains, many of the multi-resistant strains are susceptible to fluoroquinolones, since these bactericidal compounds increase the activity of isoniazid and rifampicin (Telenti & Iseman 2000). Some second line drugs, such as cycloserine, should be used in the lack of alternatives, as these present greater toxicity and, thereby, can cause dangerous psychic collateral effects (Petriani & Hoffner 1999).

The rate of MDR-TB mortality is estimated to range from 40 to 60%, which is similar to the mortality of patients with untreated TB (Bloom & Murray 1992). Among some of the factors responsible for the increase in MDR/

XDR-TB incidence, there is the HIV/AIDS epidemic and the increase in TB incidence, especially in populations with easy access to anti-TB medication. The principal risk factors that contribute for MDR/XDR-TB emergence are patient noncompliance with the treatment and the inappropriate administration of drugs by clinicians (Riley 1993). The Era of antibiotics has been constantly marked by cycles, which consist on the introduction of new antimicrobial agents and the subsequent emergence of resistance to these drugs (Swartz 2000).

Although MDR/XDR-TB patients manifest the disease in a more aggressive form, there is no evidence that these patients, HIV co-infected or not, are more prone to transmit the infection than patients with drug-susceptible TB, nor that these drug-resistant strains are more infectious than drug-susceptible ones. In HIV-negative patients, MDR/XDR-TB frequently leads to considerable loss of weight, respiratory insufficiency, and the formation of lung cavitory lesions. In contrast, in HIV-positive patients, MDR/XDR-TB is more aggressively developed, leading to high mortality rates (Riley 1993). A study performed in Florida with HIV-positive patients revealed that, since diagnosis, the mean duration of survival is approximately 45 days for MDR-TB co-infected patients and 430 days for drug-susceptible TB co-infected ones (Fischl et al. 1992).

The WHO estimates that around 50 million people are infected with MDR-TB, which is more difficult and expensive to be treated, and more likely to be fatal. In industrialized nations, the complete treatment costs about US\$ 2,000 per patient, much cheaper than the US\$ 250,000 required to treat an MDR-TB patient (Pasqualoto & Ferreira 2001). *M. tuberculosis* resistant strains are usually scarce in regions where there is little availability of drugs to fight the disease, since non-treated TB patients either die, get spontaneously cured, or become chronic bacilli disseminators, but, in any case, their infecting bacteria will rarely develop any kind of drug-resistance. In contrast, easy drug access and inappropriate chemotherapy conditions will always inevitably lead to drug-resistance (Petriani & Hoffner 1999). Therefore, MDR/XDR-TB is less common in developing nations, although high TB rates are usually present, owing to the lack of medications. However, among developed nations, where there is a greater availability of anti-TB medications, the MDR/XDR-TB rates tend to be much higher (Riley 1993). Inappropriate chemotherapy is defined as the use of a single drug, inappropriate combinations of drugs, short treatment periods resultant of patient noncompliance, and low absorption of the administered drugs. In these conditions, *M. tuberculosis* will be exposed to sub-lethal antibacterial concentrations, which impose a selection favorable to the growth of resistant bacilli among an originally susceptible population. When dealing with the detection or suspicion of resistance, one should avoid the addition of a single drug into the treatment, even though it shows an initial activity, as this situation resembles a monotherapy, which allows the development of resistance to a drug to a bacterial strain already resistant to a different agent (Petriani & Hoffner 1999).

In principle, *M. tuberculosis* genomic sequence includes information about all the possible targets to which

new antimycobacterial agents might be directed. Structural and functional information about a particular protein target can be, to a certain point, deduced by the sequence of the respective encoding gene. A way to exploit these information for drug development programs is by cloning and expressing genes that encode specific biosynthetic enzymes. The recombinant proteins can be used in functional assays for inhibitor search, and, at the same time, allow the generation of structural information for the development of drugs (Young 2001).

The *inhA*-encoded 2-*trans* enoyl-acyl carrier protein reductase enzyme (InhA) has been shown through biochemical and genetic studies to be the primary target for isoniazid. In agreement with these results, mutations in the *inhA* structural gene have been found in isoniazid-resistant clinical isolates of *M. tuberculosis*. In addition, the isoniazid-resistant InhA mutants were shown to have higher dissociation constant values for NADH and lower values for the apparent first-order rate constant for isoniazid inactivation as compared to wild-type InhA (Basso et al. 1998). More recently, an understanding of isoniazid drug resistance mechanism in *M. tuberculosis* was revealed by our group (Oliveira et al. 2006) through crystallographic and pre-steady-state kinetics studies on binding of NADH to wild-type and isoniazid-resistant enoyl-ACP(CoA) reductase enzymes from *M. tuberculosis*. In this work, in an attempt to identify structural changes between wild-type and isoniazid-resistant InhA enzymes, we have solved the crystal structures of tetrameric wild-type, S94A, I47T and I21V InhA proteins in complex with NADH to resolutions of, respectively, 2.3 Å, 2.2 Å, 2.0 Å, and 1.9 Å (Fig. 4). These InhA mutants were identified in isoniazid-resistant clinical isolates of *M. tuberculosis* (Basso et al. 1998). The more prominent structural differences are located in, and appear to indirectly affect, the dinucleotide binding loop structure. Moreover, studies on pre-steady-state kinetics of NADH binding have been carried out. The results showed that the limiting rate constant values for NADH dissociation from the InhA-NADH binary complexes ( $k_{off}$ ) were 11-, 5-, and 10-fold higher for, respectively, I21V, I47T, and S94A isoniazid-resistant mutants of InhA as compared to isoniazid-sensitive wild-type InhA. Accordingly, these results are proposed to be able to account for the reduction in affinity for NADH for the isoniazid-resistant InhA enzymes. These results are in agreement with our molecular dynamic simulation studies that show a higher flexibility of pyrophosphate moiety of NADH and a lower occupancy of conserved direct bonds between the coenzyme and protein residues in isoniazid-resistant mutant than in wild-type InhA (Schroeder et al. 2005).

As one analyzes the pharmacodynamic parameters for anti-TB drugs, it becomes clear that isoniazid and rifampicin are considerably more potent than the other available drugs used. Clinical data proved that MDR/XDR-TB requires a period considerably longer to cure. Ethionamide can be considered the least potent drug among all, and considering the fact that its use tends to cause gastrointestinal irritation, this second-line drug is usually used as a last option. There are other factors that can affect the selection of anti-TB drugs, such as pregnancy and lacta-

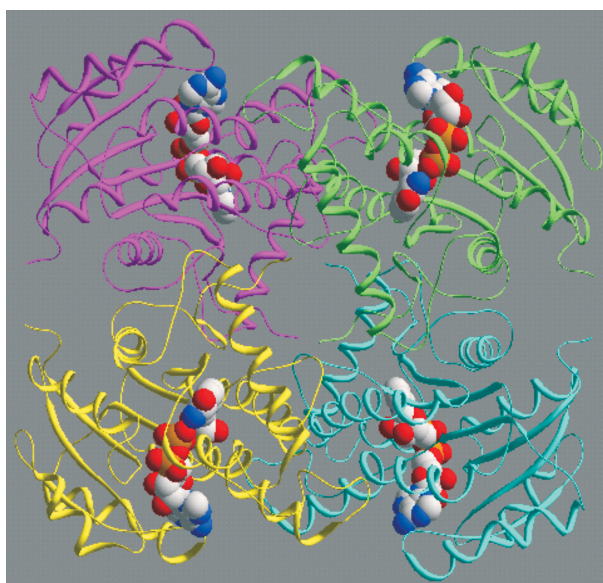


Fig. 4: three-dimensional structure of tetrameric wild-type enoyl-ACP reductase from *Mycobacterium tuberculosis* in complex with NADH (CPK model) refined to 1.92 Å (PDB access number 2AQ8, released on May 23rd, 2006).

tion, which are situations where the toxicity should be considered. Ethionamide is known to be teratogenic, and the aminoglycosides have been associated with decreased hearing in newborns. Accordingly, these agents should be avoided during pregnancy unless the survival of the mother depends of its use.

For a drug treatment, there is no “right” dose for all patients. Usually, dosage of a particular drug is based on clinical considerations as a function of the patient’s needs for the drug. The initial dosage regimen can then be tested in the patient, and the serum concentration can be measured. Subsequently, the doses can be adjusted as a function of the patient’s needs. The pharmacodynamic relationship between the serum drug concentration and the probability of therapeutic response is described mathematically by the equations of Hill. Fig. 5 shows a graphic representation of the concentration and response curves. The response corresponds to the curve of probability of an efficient therapy, and the toxicity corresponds to the curve of probability of drug adverse reactions. In the lower-left corner of the curve, there is no sufficient drug present to produce an observable response. Subsequently, there is a modest change in serum concentration, which produces a considerable change in the response. These drugs are usually denominated “concentration-dependent” with respect to their activity. This is the case for quinolones, aminoglycosides, and rifampicins. When the concentrations reach a plateau (in the upper-right portion of the curve), the addition of drugs seem to produce no greater increases in the response. Drugs that operate in this part of the curve are usually called “concentration-independent” with respect to their activity. The toxicity profile dictates where on the curve we must operate. The separation between both curves along the x-axis defines

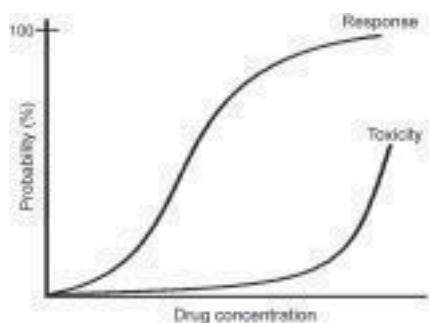


Fig. 5: graphical representation of the curves of concentration and response to drugs.

the “therapeutic range” of the drug. The maximum dose for any patient is the one that produces the desired therapeutic effect with an acceptable level of toxicity. However, when the disease reaches a life-threatening threshold to a patient, it might be necessary to accept an additional toxicity to attain cure (Peloquin 2001).

#### Vaccine development

The mammalian immunological system acts either by a cellular or humoral response, and although both responses involve helper T lymphocyte (Th) cells, the outcome of the immune response depends on which subclass is involved. Helper T lymphocytes are produced by two maturation pathways (Th-1 and Th-2) and are grouped according to cluster differentiation (CD4 and CD8) and secrete different cytokines. Th-1 type immune response involves CD8<sup>+</sup> and CD4<sup>+</sup> helper T lymphocytes and is cellular in nature; it acts against chronic diseases, such as intracellular parasitism and cancer, through macrophage activation, and detection and lysis of affected cells. This process leads to granuloma formation, which is the paradigm of protective immunity in intracellular diseases. In contrast, Th-2 type immune response involves different subsets of CD8<sup>+</sup> and CD4<sup>+</sup> T lymphocytes and is humoral in nature. It may be required to eliminate extra-cellular antigens and parasites. However, this response can also cause tissue destruction and necrosis, which represents immune response failure in many diseases. Cells of the Th-2 maturation pathway secrete cytokines such as IL-4, IL-5, IL-6, IL-9, IL-10, and TNF; these cytokines inactivate macrophage proliferation, and TNF causes tissue inflammation and necrosis when released at high levels. Antibodies are produced due to interaction between B cells and activated CD4<sup>+</sup> T lymphocytes. These antibodies can be effective in the neutralization of infectious agents, but are not able to eliminate all the infected cells, and, thereby, the host will depend on cellular immune response to protect itself from pathologies that initiate in the intracellular environment. Cellular immune response involves Th lymphocytes produced by the Th-1 maturation cell pathway. These cells secrete cytokines such as IL-2, IL-12, IL-15, INF- $\gamma$ , lymphotoxins, and granulocyte macrophage colony stimulating factor, which activate macrophage (Labidi et al. 2001).

As an attempt towards human immunization, the first vaccines were produced aiming at protection against acute infections, where Th-2 type immune responses can be efficient. These vaccines were composed of a variety of crude antigens, including dead or attenuated cells, toxins, and other structural components derived from the pathogen (Grange et al. 1995). More recently, efforts have been focused on isolating and developing single antigens or epitopes into vaccines (Labidi et al. 2001). In order to have a long-lasting protective immunity, new vaccines should combine selected antigens with potent adjuvants, and stimulate the appropriate immunological pathway (Grange et al. 1995). The ideal mycobacterial adjuvant would be the one that induces an increase in Th-1 response and a concomitant inhibition of Th-2 response. The mycobacterial material is selected based on its lack of pathogenicity in humans and animals, and its capacity of association with mammal cells, being in the form of live or dead mycobacterial cells from strains derived from non-pathogenic species. The ideal vaccine would be the one that contains immunogens that induce the formation of granulomas without necrosis. The latter is the paradigm of protective immunity, as a sign of bacterial death and regression of the disease. TB immunity is local, which means that the consequences of a lesion (where the first invasive bacteria remained) depend on the nature of T cells that are attracted to the lesion. If the attracted immune cells are Th-2, there is a lesion-necrosis evolution and disease progression; if, however, the attracted cells are Th-1, the bacteria are destroyed, there is granuloma formation, and both lesion and disease suffer regression.

BCG is currently the most widely used vaccine in the world against TB. It has been administered to 2 to 3 billion people (since 1948) without serious complications, is of easy inoculation and can also be administered as an oral vaccine, requires a single immunization and can confer immunity for a long period, is a very efficient adjuvant for immunity induction, and has a low cost of production (Labidi et al. 2001). However, recent molecular analysis have revealed that genetic modifications formed substrains along time, and a complete avirulence acquisition is also suspected for the vaccine, making immunization impracticable. Another problem is that many years after BCG immunization, there can be a gradual loss of T memory cell population (Orme 2001). Since the efficacy of this vaccine varies from zero to 80% (Colditz et al. 1994), scientists are in a constant search for vaccines with some kind of modification, such as recombinant and other attenuated live mycobacterial strains. Although BCG has been effective to prevent meningeal TB in children, it does not confer protection to pulmonary TB in adults (Orme 2001). Thereby, it is necessary to turn BCG or mycobacterial molecules more immunogenic through the development of adjuvants, in order to induce a greater hypersensitivity mediated by CD4<sup>+</sup> cells (Ehlers 1999). Even though BCG was originally developed for oral immunization, this delivery route was gradually replaced to its current intradermal use among most nations ever since the Lubeck (Germany) disaster, where a great number of children died from or developed active TB as a result of vaccine contamination with *M. tuberculosis*.

However, despite the great resistance, the Atauilpho de Paiva Foundation (Brazil) has retained efforts on research and production-distribution of the BCG Moreau Rio de Janeiro oral vaccine, as some physicians still recommend its use. Recent results of a phase I clinical trial have suggested that this strain is extremely immunogenic and causes negligible side effects as compared to any other BCG strain (Benevolo-de-Andrade et al. 2005). Anyhow, in order to develop alternative mycobacterial vaccines to BCG, it becomes necessary to identify all species of the *Mycobacterium* genera that can induce an appropriate immune response and be genetically favorable to cloning and expression of a wide spectrum of antigens. This requires a global knowledge and comprehension of the chemical structure of the cell wall and the genetics of each member of the genera (Labidi et al. 2001).

Currently, DNA vaccine is a widely explored area, where microbial DNA sequences can be used as target vaccines. The strategy consists on identifying immunogenic proteins, isolate its encoding gene, clone it into an expression vector that has a strong promoter, transform bacterial cells with the recombinant plasmid, and use the vector as a vaccine. Once injected into animal muscle cells, the plasmid is transcribed to RNA, and the cells express the recombinant protein (Orme 2001). DNA vaccines have used the mycolyl-transferase Ag85 enzyme, which has demonstrated promising results in short and long term assays, and the hsp60 heat shock protein, which, when derived from *M. leprae*, showed to be effective in both prophylactic and immunotherapeutic form (Young et al. 1988, Lowrie et al. 1999), but when derived from *M. tuberculosis*, showed no protection, besides producing inflammatory reactions in the bronchi airways (Orme et al. 2001). However, since one third of the world population is infected with *M. tuberculosis*, two types of vaccines seem to be necessary: one to prevent the invasion of the pathogen (two thirds of the population) and the other to eradicate the already established infection (one third of the population) (Hess & Kaufmann 1999).

### Perspectives

As the genome sequencing of *M. tuberculosis* H37Rv was completed, it was estimated that approximately 16% of its genome is dedicated to the codification of unknown proteins, which might be involved in specific mycobacterial functions, and can be interesting as potential drug targets and as antigens in vaccines. Strategies based on the discovery of new targets require the identification of specific biochemical pathways from mycobacteria and related organisms. Many of these metabolic processes occur during the biosynthesis of mycobacterial cell wall components, and some new attractive targets have appeared. The comprehension of the synthesis of the characteristic mycobacterial cell wall through the use of mycolic acids synthesis inhibitors can possibly lead to the development of new antimycobacterial agents.

The availability of three-dimensional structures of a biomolecule by X-ray diffraction crystallography and/or nuclear magnetic resonance spectroscopy introduces the possibility to design drugs based on a detailed model of the target binding site. Molecular modeling can also be

employed to gather information for drug design. The rational design of new agents using computer assisted molecular modeling (CAMM), based on *M. tuberculosis* enzymes involved in essential biosynthetic pathways that are not present in humans is a promising alternative for anti-TB drug design. The currently available drugs used to fight TB were identified in the period of 1945 to 1967 by traditional prospection, that is, by chance. Considering that X-ray crystallography can determine a crystalline structure in nearly atomic resolutions for any protein of therapeutical interest, the detailed knowledge of the target protein both wild-type and mutant can assist in the design of a new ligand for the receptor binding site that blocks essential pathways in sensible and resistant strains.

Anyway, it is fundamental to perform the diagnosis of TB infected patients as soon and efficiently as possible in order to avoid active disease development and the dissemination of infective organisms into the population. It thus becomes extremely important to standardize the treatment method to which infected and/or actively ill patients should be submitted, as it is of vital priority to avoid the possibility of already established host infective bacteria to develop resistance to the drugs used in chemotherapy. We would like to suggest that a greater investment in the establishment of DOTS into all possible regions, as the development of drug-resistant mycobacterial strains in appropriately treated patients has been proven to be statistically improbable. Notwithstanding, identification of new targets and the development of new antimycobacterial agents are urgently needed to combat the drug resistant strains of *M. tuberculosis*, and to strengthen the current treatment and to shorten the "short-course" treatment to improve patient compliance.

### REFERENCES

- Alcaide F, Pfyffer G, Telenti A, Amalio I 1997. Role of *embB* in natural and acquired resistance to ethambutol in mycobacteria. *Antimicrob Agents Chemother* 41: 2270-2273.
- Basso LA, Blanchard JS 1998. Resistance to antitubercular drugs. *Adv Exp Med Biol* 456: 115-44.
- Basso LA, Santos DS 2005. Drugs that inhibit mycolic acid biosynthesis in *Mycobacterium tuberculosis* – An update. *Medicinal Chemistry Reviews – Online* 2: 393-413.
- Basso LA, Zheng R, Musser JM, Jacobs Jr WR, Blanchard JS 1998. Mechanism of isoniazid resistance in *Mycobacterium tuberculosis*: enzymatic characterization of enoyl reductase mutants identified in isoniazid-resistant clinical isolates. *J Infect Dis* 178: 769-75.
- Benevolo-de-Andrade TC, Monteiro-Maia R, Cosgrove C, Castello-Branco LRR 2005. BCG Moreau Rio de Janeiro – An oral vaccine against tuberculosis – Review. *Mem Inst Oswaldo Cruz* 100: 495-465.
- Bloom BR, Murray CJL 1992. Tuberculosis: commentary on a reemergent killer. *Science* 257: 1055-1064.
- Bloom BR, Small PM 1998. The evolving relation between humans and *Mycobacterium tuberculosis*. *N Engl J Med* 338: 677-678.
- Brennan PJ 1997. Tuberculosis in the context of emerging and reemerging diseases. *FEMS Immunol Med Microbiol* 18: 263-269.

- Brennan PJ, Nikaido H 1995. The envelope of mycobacteria. *Annu Rev Biochem* 64: 29-63.
- Caws M, Drobniowski FA 2001. Molecular techniques in the diagnosis of *Mycobacterium tuberculosis* and the detection of drug resistance. *Ann NY Acad Sci* 953: 138-145.
- Center for Diseases Control – CDC-USA (MMWR) 2006. Emergence of *Mycobacterium tuberculosis* with extensive resistance to second-line drugs worldwide, 2000-2004, p. 301-305.
- Colditz GA, Brewer TF, Berkey CS, Wilson ME, Burdick E, Fineberg HV, Mosteller F 1994. The efficacy of bacillus Calmette Guérin vaccination in the prevention of tuberculosis: meta-analysis of the published literature. *JAMA* 271: 698-702.
- Cole ST, Brosch R, Parkhill J, Garnier T, Churcher C, Harris D, Gordon SV, Eiglmeier K, Gas S, Barry CE 3rd, Tekaia F, Badcock K, Basham D, Brown D, Chillingworth T, Connor R, Davies R, Devlin K, Feltwell T, Gentles S, Hamlin N, Holroyd S, Hornsby T, Jagels K, Barrell BG 1998. Deciphering the biology of *Mycobacterium tuberculosis* from the complete genome sequence. *Nature* 393: 537-544.
- Daniel TM 1997. *Captain of Death: the Story of Tuberculosis*, University of Rochester Press, New York.
- Ehlers S 1999. Immunity to tuberculosis: a delicate balance between protection and pathology. *FEMS Immunol Med Microbiol* 23: 149-158.
- Enarson DA, Murray JF 1996. Global epidemiology of tuberculosis. In WM Rom, S Garay (eds) *Tuberculosis*, Little, Brown and Co., Boston, p. 57-75.
- Farkas DH 2002. Molecular diagnostics: the best is yet to come. *Trends Mol Med* 8: 245.
- Fätkenheuer G, Taelman H, Lepage P, Schwenk A, Wenzel R 1999. The return of tuberculosis. *Diagn Microbiol Infect Dis* 34: 139-146.
- Fischl MA, Daikos GL, Uttamchandani RB, Poblete RB, Moreno JN, Reyes RR, Boota AM, Thompson LM, Cleary TJ, Oldham SA, et al. 1992. Clinical presentation and outcome of patients with HIV infection and tuberculosis caused by multiple-drug-resistant bacilli. *Ann Intern Med* 117: 184-190.
- Fortina P, Surrey S, Kricka LJ 2002. Molecular diagnostic: hurdles for clinical implementation. *Trends Mol Med* 8: 264-266.
- Gangadharam PRJ 1984. *Drug Resistance in Mycobacteria*, CRC Press, Boca Raton, FL.
- Gilbert GL 2002. Molecular diagnostics in infectious diseases and public health microbiology: cottage industry to postgenomics. *Trends Mol Med* 8: 280-287.
- Goodman LS, Ruddon, RW, Gilman AG, Milinoff PB, Limbird, LE 1996. *Goodman & Gilman's The Pharmacological Basis of Therapeutics (International Edition)*, 9th ed., McGraw Hill, New York.
- Glickman MS, Jacobs Jr WR 2001. Microbial pathogenesis of *Mycobacterium tuberculosis*: dawn of a discipline. *Cell* 104: 477-485.
- Grange JM, Stanford JL, Rook GA 1995. Tuberculosis and cancer: parallels in host responses and therapeutic approaches. *Lancet* 345: 1350-1352.
- Hess J, Kaufmann SHE 1999. Development of novel tuberculosis vaccines. *Life Sci* 322: 953-958.
- Jagirdar J, Zagzag D 1996. Pathology and insights into pathogenesis of tuberculosis. In WM Rom, S Garay (eds) *Tuberculosis*, Little, Brown and Co., Boston, p. 467-482.
- Jarlier V, Nikaido H 1994. Mycobacterial cell wall: structure and role in natural resistance to antibiotics. *FEMS Microbiol Lett* 123: 11-18.
- Johnson JA, Evans WE 2002. Molecular diagnostics as a predictive tool: genetics of drug efficacy and toxicity. *Trends Mol Med* 8: 300-305.
- Labidi AH, Estes RC, David HL, Bollon AP 2001. *Mycobacterium* recombinant vaccines. *Tunis Med* 79: 65-81.
- Lowrie DB, Tascon RE, Bonato VLD, Lima VMF, Faccioli LH, Stavropoulos E, Colston MJ, Hewinson RG, Moelling K, Silva CL 1999. Therapy of tuberculosis in mice by DNA vaccination. *Nature* 400: 269-271.
- McNeil M, Brennan PJ 1991. Structure, function and biogenesis of the cell envelope of mycobacteria in relation to bacterial physiology, pathogenesis and drug resistance. *Res Microbiol* 142: 451-463.
- Morehead RS 2000. Delayed death from pulmonary tuberculosis: unsuspected subtherapeutic drug levels. *South Med J* 93: 507-510.
- Narain JP, Raviglione MC, Kochi A 1992. HIV-associated tuberculosis in developing countries: epidemiology and strategies for prevention. *Tuber Lung Dis* 73: 311-321.
- Nolan CM 1997. Nosocomial multidrug-resistant tuberculosis: global spread of the third epidemic. *J Infect Dis* 176: 748-751.
- NSB Editorial Comment 2000. Taming tuberculosis-again. *Nat Struct Biol* 7: 87-88.
- Oliveira JS, Pereira JH, Canduri F, Rodrigues NC, De Souza ON, De Azevedo Jr WF, Basso LA, Santos DS 2006. Crystallographic and pre-steady-state kinetics studies on binding of NADH to wild-type and isoniazid-resistant enoyl-ACP(CoA) reductase enzymes from *Mycobacterium tuberculosis*. *J Mol Biol* 359: 646-666.
- Orme IM 2001. The search for new vaccines against tuberculosis. *J Leukoc Biol* 70: 1-10.
- Orme IM, McMurray DN, Belisle JT 2001. Tuberculosis vaccine development: recent progress. *Trends Microbiol* 9: 115-118.
- Pablos-Mendez A, Raviglione MC, Laszlo A, Binkin N, Rieder HL, Bustreo F, Cohn DL, Lambregts-van Weezenbeek CS, Kim SJ, Chaulet P, Nunn P 1998. Global surveillance for antituberculosis-drug resistance, 1994-1997. *N Engl J Med* 338: 1641-1649.
- Parrish NM, Dick JD, Bishai WR 1998. Mechanisms of latency in *Mycobacterium tuberculosis*. *Trends Microbiol* 6: 107-112.
- Pasqualoto KFM, Ferreira EI 2001. An approach for the rational design of new antituberculosis agents. *Curr Drug Targets* 2: 427-437.
- Peloquin CA 2001. Pharmacological issues in the treatment of



- tuberculosis. *Ann NY Acad Sci* 953: 157-64.
- Petrini B, Hoffner S 1999. Drug-resistant and multidrug-resistant tubercle bacilli. *Int J Antimicrob Agents* 13: 93-97.
- Riley LW 1993. Drug-resistant tuberculosis. *Clin Infect Dis* 17: 442-446.
- Ruffino-Netto A 1970. *Epidemiologia da Tuberculose - Estudo de Alguns Aspectos Mensuráveis na Prova Tuberculínica*, PhD Thesis, Faculdade de Medicina de Ribeirão Preto, Universidade de São Paulo, São Paulo, 55 pp.
- Ruffino-Netto A 2002. Tuberculosis: the neglected calamity. *Rev Soc Bras Med Trop* 35: 51-58.
- Ruffino-Netto A 2004. Carga da tuberculose: reflexões sobre o tema. *J Bras de Pneumol* 30: 307-309.
- Schroeder EK, Basso LA, Santos DS, De Souza ON 2005. Molecular dynamics simulation studies of the wild-type, I21V and I16T mutants of isoniazid resistant *Mycobacterium tuberculosis* enoyl reductase (InhA) in complex with NADH: towards the understanding of NADH-InhA different affinities. *Biophys J* 89: 1-9.
- Schroeder EK, de Souza ON, Santos DS, Blanchard JS, Basso LA 2002. Drugs that inhibit mycolic acid biosynthesis in *Mycobacterium tuberculosis*. *Curr Pharm Biotechnol* 3: 197-225.
- Swartz MN 2000. Impact of antimicrobial agents and chemotherapy from 1972 to 1998. *Antimicrob Agents Chemother* 44: 2009-2016.
- Telenti A, Iseman M 2000. Drug-resistant tuberculosis: what do we do now? *Drugs* 59: 171-179.
- Telenti A, Imboden P, Marchesi F, Lowrie D, Cole ST, Colton MJ, Matter L, Schopfer K, Bodmer T 1993. Detection of rifampin-resistant mutations in *Mycobacterium tuberculosis*. *Lancet* 341: 647-650.
- Vaccarezza RF 1965. *Robert Koch - La Etiologia de la Tuberculosis y Otros Trabajos*, Eudeba, Buenos Aires, p. 109-124.
- Young D 2001. Letting the genome out of the bottle: prospects for new drug development. *Ann NY Acad Sci* 953: 146-150.
- Young DB 1998. Blueprint for the white plague. *Nature* 393: 515-516.
- Young D, Lathigra R, Hendrix D, Sweetser D, Young RA 1988. Stress proteins are immune targets in leprosy and tuberculosis. *Proc Natl Acad Sci USA* 85: 4267-4270.
- Zhang Y, Mitchison DA 2003. The curious characteristics of pyrazinamide: a review. *Int J Tuberc Lung Dis* 7: 6-21.
- Zhang Y, Heym B, Allen B, Young D, Cole ST 1992. The catalase-peroxidase gene and isoniazid resistance of *Mycobacterium tuberculosis*. *Nature* 358: 591-593.

**4. ARTIGO 2:** DUCATI, R. G.; SANTOS, D. S. & BASSO, L. A. Substrate specificity and kinetic mechanism of purine nucleoside phosphorylase from *Mycobacterium tuberculosis*. *Arch. Biochem. Biophys.* (no prelo).



Contents lists available at ScienceDirect

## Archives of Biochemistry and Biophysics

journal homepage: [www.elsevier.com/locate/yabbi](http://www.elsevier.com/locate/yabbi)

## Substrate specificity and kinetic mechanism of purine nucleoside phosphorylase from *Mycobacterium tuberculosis* <sup>☆</sup>

Rodrigo G. Ducati, Diógenes S. Santos <sup>\*</sup>, Luiz A. Basso <sup>\*</sup>

Centro de Pesquisas em Biologia Molecular e Funcional (CPBMF), Instituto Nacional de Ciência e Tecnologia em Tuberculose (INCT-TB), Pontifícia Universidade Católica do Rio Grande do Sul (PUCRS), 6681/92-A Av. Ipiranga, 90619-900 Porto Alegre, RS, Brazil

## ARTICLE INFO

## Article history:

Received 26 March 2009  
and in revised form 23 April 2009  
Available online xxxx

## Keywords:

Purine nucleoside phosphorylase  
PNP  
Substrate specificity  
Initial velocity  
Product inhibition  
Fluorescence titration  
pH-rate profiles  
Solvent isotope effects  
Pre-steady-state kinetics  
Enzyme kinetic mechanism

## ABSTRACT

Purine nucleoside phosphorylase from *Mycobacterium tuberculosis* (MtPNP) is numbered among targets for persistence of the causative agent of tuberculosis. Here, it is shown that MtPNP is more specific to natural 6-oxopurine nucleosides and synthetic compounds, and does not catalyze the phosphorolysis of adenosine. Initial velocity, product inhibition and equilibrium binding data suggest that MtPNP catalyzes 2'-deoxyguanosine (2dGuo) phosphorolysis by a steady-state ordered bi bi kinetic mechanism, in which inorganic phosphate ( $P_i$ ) binds first followed by 2dGuo, and ribose 1-phosphate dissociates first followed by guanine. pH-rate profiles indicated a general acid as being essential for both catalysis and 2dGuo binding, and that deprotonation of a group abolishes  $P_i$  binding. Proton inventory and solvent deuterium isotope effects indicate that a single solvent proton transfer makes a modest contribution to the rate-limiting step. Pre-steady-state kinetic data indicate that product release appears to contribute to the rate-limiting step for MtPNP-catalyzed reaction.

© 2009 Elsevier Inc. All rights reserved.

Tuberculosis (TB)<sup>1</sup> remains a serious health threat worldwide, even though there are effective drugs [1] and an efficient chemotherapeutic treatment [2] against its causative agent, *Mycobacterium tuberculosis*. The emergence of acquired immunodeficiency syn-

drome (AIDS) caused by human immunodeficiency virus (HIV) infection and the poor access to drugs in developing nations [3] are among the factors that contribute to our failure to control the disease. Moreover, the Center of Disease Control and Prevention of USA has reported the worldwide emergence of extensively drug-resistant (XDR) TB cases, defined as cases in persons with TB whose isolates are multidrug-resistant as well as resistant to any one of the fluoroquinolone drugs and to at least one of the three injectable second-line drugs, amikacin, kanamycin or capreomycin [4,5]. Clinical manifestations have shown that XDR-TB is associated with greater morbidity and mortality than non-XDR-TB [6]. *M. tuberculosis* has been considered the world's most successful pathogen and this is largely due to its ability to persist in host tissues, where drugs that are rapidly bactericidal *in vitro* require prolonged administration to achieve comparable *in vivo* effects [7]. Approximately 2 billion individuals are believed to harbor latent TB [3], and its resumption of growth in a proportion of individuals sustains the pandemic of active TB [8]. Hence, more effective and less toxic anti-tubercular agents are needed to shorten the duration of current treatment, improve the treatment of drug-resistant TB, and to provide effective treatment of latent TB infection.

Long-term survival of nonreplicating *M. tuberculosis* is ensured by the coordinated shutdown of active metabolism through a broad transcriptional program called the stringent response. The synthesis and degradation of guanosine 3',5'-bis(diphosphate) (ppGpp)

<sup>☆</sup> This work was supported by Millennium Initiative Program and National Institute of Science and Technology Program, MCT-CNPq, Ministry of Health – Department of Science and Technology (DECIT) – Secretary of Health Policy (Brazil) to D.S.S. and L.A.B. D.S.S. (CNPq, 304051/1975-06) and L.A.B. (CNPq, 520182/99-5) are Research Career Awardees of the National Research Council of Brazil (CNPq). R.G.D. is a postdoctoral fellow of CNPq.

<sup>\*</sup> Corresponding authors. Fax: +55 51 33203629.

E-mail addresses: [diogenes@pucrs.br](mailto:diogenes@pucrs.br) (D.S. Santos), [luiz.basso@pucrs.br](mailto:luiz.basso@pucrs.br) (L.A. Basso).

<sup>1</sup> Abbreviations used: TB, tuberculosis; AIDS, acquired immunodeficiency syndrome; HIV, human immunodeficiency virus; XDR, extensively drug-resistant; ppGpp, guanosine 3',5'-bis(diphosphate); PNP, purine nucleoside phosphorylase; MtPNP, PNP from *Mycobacterium tuberculosis*; ImmH, immucillin-H; SPR, surface plasmon resonance; Guo, guanosine; 7mGuo, 7-methylguanosine; Ino, inosine; 2dIno, 2'-deoxyinosine; Gua, guanine; 2dGuo, 2'-deoxyguanosine; R1P, ribose 1-phosphate; MESG, 2-amino-6-mercapto-7-methylpurine ribonucleoside; HPLC, high performance liquid chromatography; FPLC, fast performance liquid chromatography; LB, Luria-Bertani; IPTG, isopropyl β-D-thiogalactopyranoside; Tris, tris(Hydroxymethyl)aminomethane; MWCO, molecular weight cutoff; SDS-PAGE, sodium dodecyl sulfate-polyacrylamide gel electrophoresis; HEPES, N-2-hydroxyethylpiperazine-N'-2-ethanesulfonic acid; 7mGua, 7-methylguanine;  $P_i$ , inorganic phosphate; MES, 2-(N-morpholino)ethanesulfonic acid; CHES, 2-(N-cyclohexylamino)ethanesulfonic acid; RU, response units; HsPNP, human PNP.

and pppGpp are catalyzed by (p)ppGpp synthase I (*relA*, Rv2583) using GTP as substrate [9]. Increased concentration of hyperphosphorylated guanosine moieties is a central feature of pleiotropic physiological response of the stringent response, through which bacteria enter a latent state in response to nutritional stress [10]. The accumulation of ppGpp has been implicated in the latency of *Mycobacterium smegmatis* [11]. A *rel*-deficient mutant of *M. tuberculosis* was shown no longer be capable of ppGpp synthesis and this mutant had impaired long-term survival during *in vitro* starvation, indicating that ppGpp concentration may control mycobacterial adaptation to growth-limiting condition, allowing for long-term survival [12]. It has been shown that the *rel*-deficient *M. tuberculosis* mutant strain has impaired ability to sustain chronic infection in a murine model of persistent TB [13]. More recently, a comparative genomic analysis between *M. tuberculosis* H37Ra (avirulent) and H37Rv (virulent) identified, among other changes, a missense mutation in a regulatory protein of stringent response [14]. In the *de novo* synthesis of purine ribonucleotides, the formation of AMP and GMP from IMP is irreversible, but purine bases, nucleosides, and nucleotides can be interconverted through the activities of purine nucleoside phosphorylase (PNP; *deoD*, Rv3307), adenosine deaminase (*add*, Rv3313c), and hypoxanthine–guanine phosphoribosyl transferase (*htp*, Rv3624c). We have previously suggested that inhibition of *M. tuberculosis* PNP (MtPNP) could potentially lead to the accumulation of guanine nucleotides since a putative guanylate kinase (*gmk*, Rv1389) and nucleoside diphosphate kinase (*ndkA*, Rv2445c) are encoded in the genome of *M. tuberculosis* [15]. Accordingly, the *deoD* gene product (PNP) has been numbered among the top 100% persistence targets by the TB Structural Genomics Consortium ([www.webtb.org](http://www.webtb.org)). However, the physiological role of PNP in *M. tuberculosis* remains to be demonstrated.

PNP plays a key role in purine salvage pathway. PNP (EC 2.4.2.1) catalyzes the reversible phosphorolysis of *N*-glycosidic bond of  $\beta$ -purine (deoxy)ribonucleosides to generate  $\alpha$ -(deoxy)ribose 1-phosphate and the corresponding purine bases [16,17] (Fig. 1). Immucillin-H (ImmH), a transition state analogue, has been shown to be a slow-onset inhibitor of MtPNP with an overall inhibition constant in the pM range [15]. The three-dimensional structure of MtPNP:ImmH:P<sub>i</sub> ternary complex showed that the edge of the phenolic ring in Tyr188 is oriented perpendicular to the plane of the ImmH base and also forms a 2.8 Å hydrogen bond with the 5'-hydroxyl group of the transition state analogue [18]. Tyr188 is the only residue that interacts directly with bound inhibitor that is not conserved in the mammalian PNPs and it is thus likely that 5'-modifications of ImmH may yield inhibitors more specific for MtPNP. In addition, it has recently been shown that even though bovine and human PNPs share 87% sequence identity and have totally conserved active site residues, inhibitors with differential specificity can be designed [19].

Here, we describe MtPNP substrate specificity, steady-state kinetic parameters, product inhibition, pH-rate profiles, energy of activation, solvent kinetic isotope effects and proton inventory, equilibrium fluorescence spectroscopy upon binary and ternary complex formation, surface plasmon resonance (SPR) measurements upon binary complex formation, and pre-steady-state kinet-

ics of product formation. The results described here should be useful to the design of MtPNP inhibitors with potential action against *M. tuberculosis* growth.

## Materials and methods

### Materials

All chemicals used were of analytical or reagent grade and required no further purification. Adenosine, guanosine (Guo), 7-methylguanosine (7mGuo), inosine (Ino), 2'-deoxyinosine (2dIno), guanine (Gua), and lysozyme were from Sigma. Adenine was from MP Biomedicals. 2'-Deoxyguanosine (2dGuo) and ribose 1-phosphate (R1P) were from Fluka BioChemika. 2-Amino-6-mercapto-7-methylpurine ribonucleoside (MESG) is commercially available in the Enzchek phosphate assay kit from Molecular Probes. Complete protease inhibitor cocktail tablets were from Boehringer (Mannheim, Germany). Protein assay kit was from Bio-Rad. Deuterium oxide (99.9 atom% D<sub>2</sub>O) was from Cambridge Isotope Laboratories. Amicon stirred ultrafiltration cell, regenerated cellulose ultrafiltration membranes, and Centricon centrifugal filter devices were all from Millipore. High performance liquid chromatography (HPLC) assays (25 °C) and fast performance liquid chromatography (FPLC) protein purification (4 °C) were carried out in an Äkta purifier from GE Helthcare; all chromatographic columns were also from GE Helthcare. All steady-state activity assays were carried out in an UV-2550 UV-Visible Spectrophotometer (Shimadzu), and fluorescence binding experiments were carried out in a RF-5301PC Spectrophotometer (Shimadzu). SPR measurements were carried out in a BIA-Core X equipment using a carboxymethyl-dextran coated gold surface (Sensor Chip CM5), both from Biacore AB. Pre-steady-state measurements were performed using an Applied Photophysics (London, UK) SX.18MV-R stopped-flow spectrofluorimeter on absorbance mode.

### Recombinant enzyme expression and purification

Recombinant MtPNP expression was as previously described [15], with some modifications. The pET-23a(+):*deoD* recombinant expression plasmid [15] was transformed into *Escherichia coli* BL21(DE3)NH [20] competent cells. The cells were grown in Luria-Bertani (LB) medium pH 7.2 containing 50  $\mu\text{g mL}^{-1}$  ampicillin at 37 °C to an OD<sub>600nm</sub> of 0.5, induced by 0.5 mM isopropyl  $\beta$ -D-thiogalactopyranoside (IPTG) [21], and allowed to grow for additional 50.7 h. All subsequent steps were performed at 4 °C, unless stated otherwise. Approximately 20 g of cells were harvested by centrifugation (6000g for 30 min) from 9 L of LB media, washed with 50 mM Tris(Hydroxymethyl)aminomethane (Tris) pH 7.6, and stored at –20 °C. Frozen cells (20 g) were thawed and suspended in 40 mL of 50 mM Tris pH 7.6 (buffer A1) containing a cocktail of protease inhibitors (Complete) and 0.2 mg mL<sup>-1</sup> lysozyme, and the mixture was stirred for 30 min. Cells were disrupted by sonication, and centrifuged (40,000g for 1 h) to remove cell debris. The supernatant was incubated with 1% streptomycin sulfate (final concentration) for 40 min to precipitate nucleic acids and

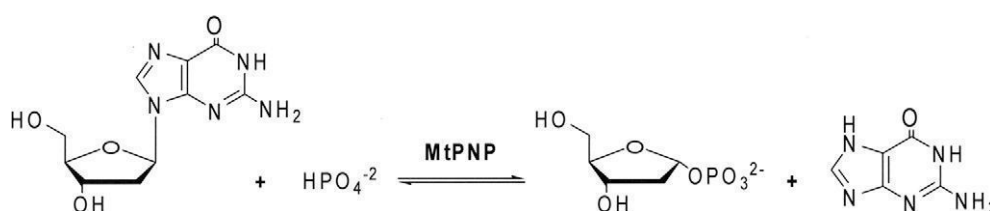


Fig. 1. Reaction catalyzed by MtPNP with 2'-deoxyguanosine, a natural substrate.

centrifuged (48,000g for 1 h). The supernatant was dialyzed (12–14 kDa molecular weight cutoff – MWCO – dialysis tubing) against  $2 \times 2$  L (2.5 h each) of buffer A1, and clarified by centrifugation (48,000g for 30 min). The supernatant was loaded on a  $2.6 \text{ cm} \times 8.2 \text{ cm}$  Q-Sepharose Fast Flow column, pre-equilibrated with buffer A1, washed with 10 column volumes of buffer A1, and the adsorbed proteins eluted with a 10 column volume linear gradient (0–100%) of 50 mM Tris 0.5 M NaCl pH 7.6 (buffer B1). All fractions were analyzed by sodium dodecyl sulfate–polyacrylamide gel electrophoresis (SDS–PAGE) [22], and the fractions containing the target protein were pooled, concentrated using an Amicon stirred ultrafiltration cell with a regenerated cellulose ultrafiltration membrane (10 kDa MWCO), centrifuged (48,000g for 30 min), and the supernatant was loaded on a  $2.6 \text{ cm} \times 60 \text{ cm}$  Sephacryl S-200 High Resolution column, pre-equilibrated with buffer A1. The column was eluted with buffer A1, the fractions containing the target protein were pooled, ammonium sulfate was added to a final concentration of 1.0 M and centrifuged (48,000g for 30 min). The supernatant was loaded on a  $1.6 \text{ cm} \times 10 \text{ cm}$  HighLoad Phenyl Sepharose High Performance column, pre-equilibrated with 50 mM Tris 1.0 M  $(\text{NH}_4)_2\text{SO}_4$  pH 7.6 (buffer A2). The column was washed with 5 column volumes of buffer A2, and the adsorbed proteins were eluted along a 15 column volume linear gradient (0–100%) of buffer A1. The fractions containing the target protein were pooled, dialyzed against  $2 \times 2$  L (2.5 h each) of buffer A1, and centrifuged (48,000g for 30 min). The supernatant was loaded on a  $1.0 \text{ cm} \times 10 \text{ cm}$  Mono Q High Resolution column, pre-equilibrated with buffer A1. The column was washed with 5 column volumes of buffer A1, and the adsorbed proteins were eluted with a 27 column volume linear gradient (0–100%) of buffer B1. The active fractions exhibiting a single band on SDS–PAGE were pooled, protein concentration determined by the Bradford's method [23] using the Bio-Rad protein assay kit and bovine serum albumin as the standard, and stored in 85%  $(\text{NH}_4)_2\text{SO}_4$  solution at 4 °C.

#### Substrate specificity

MtPNP in 85%  $(\text{NH}_4)_2\text{SO}_4$  solution was centrifuged (20,800g for 30 min), the pellet was suspended in 500  $\mu\text{L}$  of 100 mM Tris pH 7.5, dialyzed against  $2 \times 250 \text{ mL}$  (2.5 h each) of 100 mM Tris pH 7.5, centrifuged (20,800g for 30 min), and the protein concentration determined. Determination of apparent steady-state kinetic parameters was carried out under initial rate conditions at 25 °C in 100 mM *N*-2-hydroxyethylpiperazine-*N'*-2-ethanesulfonic acid (Hepes) pH 7.5 (500  $\mu\text{L}$  total reaction volume) to determine MtPNP substrate specificity. Phosphorolysis of MESG to 2-amino-6-mercapto-7-methylpurine was monitored at 360 nm ([24];  $\epsilon = 11,000 \text{ M}^{-1} \text{ cm}^{-1}$ ); phosphorolysis of Guo and 2dGuo to Gua was monitored by time-dependent decrease in absorbance at 258 nm ([25];  $\epsilon = 5,500 \text{ M}^{-1} \text{ cm}^{-1}$ ); phosphorolysis of Ino and 2dIno to hypoxanthine was monitored at 280 nm ([15,26];  $\epsilon = 1000 \text{ M}^{-1} \text{ cm}^{-1}$ ); and phosphorolysis of 7mGuo to 7-methylguanine (7mGua) was monitored at 260 nm ([27];  $\epsilon = 4,600 \text{ M}^{-1} \text{ cm}^{-1}$ ). The concentration ranges were as follows: varying MESG concentration (5–300  $\mu\text{M}$ ) at fixed-saturating inorganic phosphate ( $\text{P}_i$ ) concentration (2 mM) and varying  $\text{P}_i$  concentration (20–2000  $\mu\text{M}$ ) at fixed-saturating MESG concentration (300  $\mu\text{M}$ ); varying Guo concentration (2–100  $\mu\text{M}$ ) at fixed-saturating  $\text{P}_i$  concentration (20 mM) and varying  $\text{P}_i$  concentration (400–20,000  $\mu\text{M}$ ) at fixed-saturating Guo concentration (100  $\mu\text{M}$ ); varying 2dGuo concentration (2–100  $\mu\text{M}$ ) at fixed-saturating  $\text{P}_i$  concentration (20 mM) and varying  $\text{P}_i$  concentration (200–20,000  $\mu\text{M}$ ) at fixed-saturating 2dGuo (100  $\mu\text{M}$ ); varying Ino concentration (10–400  $\mu\text{M}$ ) at fixed-saturating  $\text{P}_i$  (15 mM) and varying  $\text{P}_i$  concentration (200–15,000  $\mu\text{M}$ ) at fixed-saturating Ino concentration (400  $\mu\text{M}$ ); varying 2dIno concentration (10–400  $\mu\text{M}$ ) at fixed-satu-

rating  $\text{P}_i$  concentration (20 mM) and varying  $\text{P}_i$  concentration (200–20,000  $\mu\text{M}$ ) at fixed-saturating 2dIno (400  $\mu\text{M}$ ); varying 7mGuo concentration (12–100  $\mu\text{M}$ ) at fixed-saturating  $\text{P}_i$  concentration (20 mM) and varying  $\text{P}_i$  concentration (200–20,000  $\mu\text{M}$ ) at fixed-saturating 7mGuo concentration (100  $\mu\text{M}$ ). Phosphorolysis of adenosine to adenine and R1P was monitored by HPLC. The assay reaction mixture (1.0 mL) containing adenosine (100  $\mu\text{M}$ ) and  $\text{P}_i$  (50 mM) was incubated for 12 h at 25 °C. The reaction mixture was boiled (100 °C) for 1 min to extinguish MtPNP activity, and precipitated protein was removed by a Centricon centrifugal filter device (10 kDa MWCO; 5000g). The protein-free reaction mixture (500  $\mu\text{L}$ ) was loaded on a  $4.6 \text{ mm} \times 250 \text{ mm}$  5  $\mu\text{m}$  ST Sephasil Peptide C18 column and elution monitored at 260 nm using 50 mM Ammonium Dihydrogen Phosphate 5% Acetonitrile pH 4.5 as the mobile phase and a flow rate of  $1 \text{ mL min}^{-1}$  at 25 °C [28]. This protocol proved to be able to separate adenosine (retention time: 15.5 min) from adenine (retention time: 6.7 min) when pre-mixed.

#### Initial velocity and product inhibition patterns

Enzyme activity assays were performed under initial rate conditions at 25 °C in 100 mM Hepes pH 7.0 in 500  $\mu\text{L}$  total reaction volumes, unless stated otherwise, and each individual initial rate datum is the average of duplicate or triplicate measurements. To determine the true steady-state kinetic parameters and initial velocity patterns, MtPNP activity was measured in the presence of varying concentrations of 2dGuo (2–100  $\mu\text{M}$ ) and several fixed-varied  $\text{P}_i$  concentrations (200–20,000  $\mu\text{M}$ ). Product inhibition patterns were determined by measuring initial rates at varying concentrations of one substrate, fixed non-saturating concentration of the co-substrate, and fixed-varying levels of product (either Gua or R1P). The concentrations employed in product inhibition studies were as follows: varying 2dGuo (8–160  $\mu\text{M}$ ) at fixed  $\text{P}_i$  concentration (1 mM) and fixed-varying Gua concentration (0–15  $\mu\text{M}$ ); varying 2dGuo (28–160  $\mu\text{M}$ ) at fixed  $\text{P}_i$  concentration (1 mM) and fixed-varying R1P concentration (0–80  $\mu\text{M}$ ); varying  $\text{P}_i$  (0.6–20 mM) at fixed 2dGuo concentration (44  $\mu\text{M}$ ) and fixed-varying Gua concentration (0–18.75  $\mu\text{M}$ ); and varying  $\text{P}_i$  (0.6–250 mM) at fixed 2dGuo concentration (44  $\mu\text{M}$ ) and fixed-varying R1P concentration (0–832  $\mu\text{M}$ ).

#### pH-rate profiles

To determine the dependence of the kinetic parameters on pH, initial velocities were measured in the presence of varying concentrations of one substrate and a saturating level of the other in a buffer mixture of 2-(*N*-morpholino)ethanesulfonic acid (MES)/Hepes/2-(*N*-cyclohexylamino)ethanesulfonic acid (CHES) over the following pH values: 6.0, 6.5, 7.0, 7.5, 8.0, 8.5, 9.0, and 9.5 [29]. The substrate, 2dGuo, has no ionizable groups over the pH range studied. MtPNP was incubated over a broader pH range and assayed under standard conditions to identify denaturing values and ensure enzyme stability over the pH range studied. The pH profile studies have identified a range of pH values in which the kinetic parameters are pH-independent, and solvent kinetic isotope effects were thus assessed in this pH range.

#### Energy of activation

To determine the energy of activation of the MtPNP-catalyzed reaction, initial velocities were measured in the presence of varying concentrations of one substrate and a saturating level of the other, at temperatures ranging from 15 to 35 °C. MtPNP was incubated for several minutes in all of the temperatures tested and assayed under standard conditions to ensure enzyme stability under all conditions.

### Solvent kinetic isotope effects and proton inventory

Solvent kinetic isotope effects were determined by measuring initial velocities using a saturating level of one substrate and varying concentrations of the other in either H<sub>2</sub>O or 90 atom% D<sub>2</sub>O. The proton inventory on the catalytic constant ( $k_{cat}$ ) was determined using saturating concentrations of both substrates (2dGuo and P<sub>i</sub>) at various mole fractions of D<sub>2</sub>O.

### Fluorescence spectroscopy

Fluorescence titration was performed to study the interaction at equilibrium between MtPnP and either substrate(s) or product(s) at 25 °C. P<sub>i</sub>, 2dGuo, R1P and the enzyme were dissolved in 100 mM Hepes pH 7.0, and Gua in water titrated to pH 3.0 with diluted solution of HCl. Fluorescence titration with P<sub>i</sub> was carried out by making microliter additions of 100 mM and 500 mM NaH<sub>2</sub>PO<sub>4</sub> (49.98–6607.98 μM final concentration) to 2 mL of 3 μM MtPnP, keeping the dilution to a maximum of 2.15%. Fluorescence titration with 2dGuo was carried out by making microliter additions of 3 mM 2dGuo (1.50–156.43 μM final concentration) to 2 mL of 3 μM MtPnP, keeping the dilution to a maximum of 5.5%. Fluorescence titration with R1P was carried out by making microliter additions of 2 mM and 4 mM R1P (1.0–151.93 μM final concentration) to 2 mL of 3 μM MtPnP, keeping the dilution to a maximum of 4.0%. Fluorescence titration with Gua was carried out by making microliter additions of 0.5 mM Gua (0.25–6.66 μM final concentration) to 2 mL of 3 μM MtPnP, keeping the dilution to a maximum of 1.35%. Fluorescence titration of pre-formed MtPnP:Gua binary complex with P<sub>i</sub> and ensuing ternary complex formation was carried out by making microliter additions of 100 and 500 mM NaH<sub>2</sub>PO<sub>4</sub> (49.98–25,118.31 μM final concentration) to 2 mL of 3 μM MtPnP in the presence of 10 μM Gua, keeping the dilution to a maximum of 5.5%. Fluorescence titration of ternary complex formation upon binding of Gua to pre-formed MtPnP:P<sub>i</sub> binary complex was carried out by making microliter additions of 0.5 mM Gua (0.25–4.71 μM final concentration) to 2 mL of 3 μM MtPnP in the presence of 20 mM P<sub>i</sub>, keeping the dilution to a maximum of 0.95%. The pH of the binding mixture in the cuvette was measured to ensure that it remained constant. Measurements of intrinsic protein fluorescence of MtPnP employed excitation wavelengths at 300 nm in binding experiments with the substrates and at 296 nm with the products, and the emission wavelength ranged from 320 to 400 nm (maximum MtPnP  $\lambda_{EM}$  = 334 nm). In equilibrium binary complex formation studies, the slits for excitation and emission wavelengths were, respectively, 1.5 and 10 nm. In equilibrium ternary complex formation experiments, the slits for excitation and emission wavelengths were, respectively, 3 and 5 nm. Control experiments were employed to both determine the maximum ligand concentrations to be used with no inner filter effect and dilution effect on protein fluorescence.

### SPR measurements

Interaction of 2dGuo with MtPnP was also studied by SPR titration of the enzyme at 25 °C. A solution of 40 μg mL<sup>-1</sup> MtPnP in 10 mM sodium acetate pH 4.5 was injected at 10 μL min<sup>-1</sup> in a carboxymethyl-dextran coated gold surface (Sensor Chip CM5), previously activated with *N*-ethyl-*N'*-(3-dimethylaminopropyl)carbodiimide and *N*-hydroxysuccinimide. Protein injections were repeated until the desired response level was reached. Ethanolamine was subsequently used to block all possible remaining reactive sites on the surface. A reference cell was prepared through the same steps except protein injection. The initial response units (RU) of the immobilized protein was 9108 RU, which dropped to a stable 6003 RU level after 30 h under a flow rate of 30 μL min<sup>-1</sup>, probably

due to the removal of the non-covalently attached subunits of each trimer from the surface. Several concentrations of 2dGuo (in 100 mM Hepes pH 7.0) were injected at a flow rate of 30 μL min<sup>-1</sup>, and the response was measured for each concentration. The value of the blank (100 mM Hepes pH 7.0) was subtracted from all values obtained with each substrate concentration.

### Pre-steady-state kinetics

Pre-steady-state kinetic measurements of product formation by MtPnP were carried out to assess whether product release is the rate-limiting step. The decrease in absorbance upon 2dGuo conversion to Gua product was monitored at 258 nm (1 mm slit width = 4.65 nm spectral band), at 25 °C, using a split time base (0.5–5 s; 200 data points for each time base). The experimental conditions were 20 μM MtPnP, 20 mM P<sub>i</sub> (14 ×  $K_M$ ), and 150 μM 2dGuo (3 ×  $K_M$ ) in 100 mM Hepes pH 7.0 (mixing chamber concentrations). The dead time of the stopped-flow equipment is 1.37 ms.

### Data analysis

Kinetic parameter values and their respective standard errors were obtained by fitting the data to the appropriate equations by using the nonlinear regression function of SigmaPlot 2004 (SPSS, Inc.). Hyperbolic saturation curves [30,31] at a single concentration of the fixed substrate and varying concentrations of the other were fitted to Eq. (1).

$$v = VA/(K_a + A) \quad (1)$$

Intersecting initial velocity patterns were fitted to Eq. (2), which describes a sequential mechanism.

$$v = VAB/(K_{ia}K_b + K_aB + K_bA + AB) \quad (2)$$

For Eqs. (1) and (2),  $v$  is the measured reaction velocity,  $V$  is the maximal velocity,  $A$  and  $B$  are the concentrations of the substrates (2dGuo and P<sub>i</sub>),  $K_a$  and  $K_b$  are their respective Michaelis constants, and  $K_{ia}$  is the dissociation constant for substrate  $A$ .

Competitive and noncompetitive inhibition data were fitted to Eqs. (3) and (4), respectively, where  $I$  is the inhibitor concentration, and  $K_{is}$  and  $K_{ii}$  are the slope and intercept inhibition constants, respectively.

$$v = VA/[K_a(1 + I/K_{is}) + A] \quad (3)$$

$$v = VA/[K_a(1 + I/K_{is}) + A(1 + I/K_{ii})] \quad (4)$$

pH-rate profiles data were fitted to Eq. (5) for a bell-shaped curve, in which  $y$  is the apparent kinetic parameter,  $C$  is the pH-independent plateau value of  $y$ ,  $H$  is the proton concentration, and  $K_a$  and  $K_b$  are, respectively, the apparent acid and base dissociation constants for ionizing groups.

$$\log y = \log[C/(1 + H/K_a + K_b/H)] \quad (5)$$

Temperature effect data were fitted to Eq. (6), where  $k$  is the maximal reaction rate,  $E_a$  is the energy of activation,  $T$  is the temperature (in Kelvin),  $R$  is the gas constant (1.987 cal mol<sup>-1</sup>), and  $A$  is a pre-exponential factor that correlates collision frequency and the probability of the reaction occurring when reactant molecules collide.

$$\log k = (-E_a/2.3R)(1/T) + \log(A) \quad (6)$$

Kinetic isotope effect data were fitted to Eq. (7), which assumes isotope effects on both  $V/K$  and  $V$ . In this equation,  $E_{V/K}$  and  $E_V$  are the isotope effects minus 1 on  $V/K$  and  $V$ , respectively, and  $F_i$  is the fraction of isotopic label (solvent).

$$v = VA/[K(1 + F_iE_{V/K}) + A(1 + F_iE_V)] \quad (7)$$

Data from equilibrium fluorescence spectroscopy were fitted to Eq. (8), the Hill equation [32], in which  $F$  is the observed fluorescence signal,  $F_{\max}$  is the maximal fluorescence,  $F/F_{\max}$  ratio is the degree of saturation,  $n$  represents the total number of binding sites, and  $K'$  is the mean dissociation constant for MtPNP:ligand binary complex formation, which is comprised of interaction factors and the intrinsic dissociation constant. The equilibrium fluorescence data representing the fractional saturation (0.10–0.90) for the trimeric form of MtPNP were fitted to Eq. (9) (the Hill plot), in which  $Y$  is the fraction of substrate binding sites occupied by the substrate, and  $h$  is the Hill coefficient.

$$F/F_{\max} = A^n / (K' + A^n) \quad (8)$$

$$\log[Y/(1 - Y)] = h \log A - \log K' \quad (9)$$

The pre-steady-state time course of product formation was fitted to Eq. (10) for a single exponential decay, in which  $A$  is the absorbance at time  $t$ ,  $A_0$  is the absorbance at time zero, and  $k$  is the apparent first-order rate constant for product formation.

$$A = A_0 e^{-kt} \quad (10)$$

## Results and discussion

### Recombinant enzyme expression and purification

Maximal expression of recombinant MtPNP was achieved at 50.7 h of cell growth in LB medium after IPTG induction (0.5 mM) of *E. coli* BL21(DE3)NH cells harboring pET-23a(+):*deoD* vector. Recombinant MtPNP was purified to homogeneity by a four-step purification protocol, yielding 140 mg of active MtPNP from 20 g of cell culture, which represents a ~600% increase in protein recovery as compared to a previously published protocol that yielded ~23 mg from 20 g of cells [15].

### Substrate specificity

The apparent steady-state kinetic parameters and catalytic efficiencies for natural and synthetic compounds are summarized in Table 1. It is noteworthy that kinetic curves for either  $P_i$  or any of the nucleosides in the concentration ranges tested here were best fitted to a Michaelis–Menten hyperbolic function. Non-hyperbolic kinetics and allosteric regulation of PNP with  $P_i$  as well as nucleoside substrates have been described [33–35]. The largest  $k_{\text{cat}}$  values were for MESH and 7mGuo (Table 1), and the reaction with these two substrates is essentially irreversible in favor of phosphorolysis [24,36]. The specificity for  $P_i$  is one order of magnitude larger for these two substrates and this is due to increased values for the catalytic constant and lower overall dissociation constant val-

ues (lower  $K_M$  values). MtPNP was more specific to MESH and 7mGuo than any natural nucleoside tested, which is largely due to increased catalytic constant values since  $K_M$  values were of similar magnitude. These results are in contrast with results obtained for human PNP (HsPNP), which was shown to be more specific for natural substrates such as Ino and Guo than MESH [37]. In addition, the HsPNP  $K_M$  value for MESH (358  $\mu\text{M}$ ; [37]) is ~12-fold larger than that for MtPNP. These differences imply that enzyme inhibitors more specific for MtPNP may be designed based on the chemical functional group substitutions of MESH, in particular the sulfur at the sixth position of the purine base.

Homotrimeric PNPs are known to be highly specific for catalysis of natural 6-oxopurines, their nucleosides (Ino, 2dIno, Guo, and 2dGuo), and some analogues, whereas homohexameric PNPs additionally accept 6-aminopurine (adenine), their nucleosides and many analogues [38]. Among trimeric PNPs, the rates of phosphorolysis and/or synthesis of adenosine, when detectable, are negligible or extremely low [39,40]. Although MtPNP has been clearly classified among the homotrimeric enzymes, there have been no reports describing either adenosine metabolism in *M. tuberculosis* cells [41] or experimental data probing MtPNP specificity for adenosine. MtPNP has been shown to be trimeric [15], similar to mammalian PNP's but unlike hexameric prokaryotic enzymes [42,43]. However, it remains to be shown on whether or not MtPNP catalyzes the phosphorolysis of adenosine (a 6-aminopurine nucleoside). We have thus investigated MtPNP specificity for adenosine as a possible substrate, and our results indicate that the rate of phosphorolysis of adenosine by MtPNP is undetectable or, at the most, negligible. These results are in agreement with trimeric PNP enzymes not being able to catalyze the phosphorolysis of 6-aminopurine nucleosides to an appreciable extent. Moreover, these results show that MtPNP, as other homotrimeric PNPs, catalyzes the phosphorolysis of nucleosides having a 6-oxo substituent (or other substituents with analogous electronic properties, such as S or Se) [34] and a protonated N at position 1. Also, the Guo N7 methyl analogues (7mGuo and MESH) were, as expected [27], excellent substrates in the direction of phosphorolysis, although synthetic. All subsequent experiments here described were performed with a substrate having high catalytic efficiency (2dGuo) and that was deemed more appropriate for enzyme activity assays.

### Initial velocity patterns and kinetic constants

Initial velocity patterns were determined using either 2dGuo or  $P_i$  as the variable substrate to distinguish between sequential and ping-pong mechanisms. Double-reciprocal plot [44] analysis revealed intersecting patterns for both substrates (Fig. 2), which is consistent with ternary complex formation and a sequential mechanism. The existence of ternary complexes has also been described for other trimeric PNPs, such as from calf spleen, human erythrocyte, and *Cellulomonas* sp. [45–47]. A rapid equilibrium ordered mechanism could also be ruled out, since in this mechanism the family of lines for the second substrate to bind to the enzyme should intersect on the y axis. The data were fitted to Eq. (2), and yielded the following values for the true steady-state kinetic constants:  $k_{\text{cat}} = 4.4 \pm 0.1 \text{ s}^{-1}$ ,  $K_{2\text{dGuo}} = 47 \pm 4 \mu\text{M}$ ,  $K_{P_i} = 1372 \pm 105 \mu\text{M}$ ,  $k_{\text{cat}}/K_{2\text{dGuo}} = 9.4 (\pm 0.8) \times 10^4 \text{ M}^{-1} \text{ s}^{-1}$ ,  $k_{\text{cat}}/K_{P_i} = 3.2 (\pm 0.3) \times 10^3 \text{ M}^{-1} \text{ s}^{-1}$ . The  $k_{\text{cat}}$  value for MtPNP using 2dGuo as substrate is approximately sixfold lower than that for HsPNP using Guo as substrate; however, their  $K_M$  values are similar [48].

### Product inhibition patterns

Product (Gua and R1P) inhibition studies were carried out to elucidate the order of substrate addition to the enzyme. The data were fitted to equations for competitive (Eq. (3)) or noncompeti-

**Table 1**  
Substrate specificity apparent kinetic parameters and catalytic efficiencies.<sup>a</sup>

Substrate pair	$k_{\text{cat}}$ ( $\text{s}^{-1}$ )	$K_M$ ( $\mu\text{M}$ )	$k_{\text{cat}}/K_M$ ( $\text{M}^{-1} \text{s}^{-1}$ )
$P_i$	$17.9 \pm 0.8$	$427 \pm 52$	$4.2 (\pm 0.5) \times 10^4$
MESH	$17.3 \pm 0.7$	$29 \pm 5$	$6.0 (\pm 1.1) \times 10^5$
$P_i$	$3.5 \pm 0.1$	$1345 \pm 206$	$2.6 (\pm 0.4) \times 10^3$
Guanosine	$4.0 \pm 0.2$	$12 \pm 2$	$3.3 (\pm 0.6) \times 10^5$
$P_i$	$4.9 \pm 0.2$	$2349 \pm 329$	$2.1 (\pm 0.3) \times 10^3$
2'-Deoxyguanosine	$5.1 \pm 0.2$	$15 \pm 2$	$3.4 (\pm 0.5) \times 10^5$
$P_i$	$4.9 \pm 0.2$	$583 \pm 108$	$8.4 (\pm 1.6) \times 10^3$
Inosine	$5.4 \pm 0.1$	$40 \pm 3$	$1.4 (\pm 0.1) \times 10^5$
$P_i$	$6.9 \pm 0.1$	$1131 \pm 66$	$6.1 (\pm 0.4) \times 10^3$
2'-Deoxyinosine	$7.5 \pm 0.3$	$68 \pm 7$	$1.1 (\pm 0.1) \times 10^5$
$P_i$	$13.3 \pm 0.1$	$427 \pm 23$	$3.1 (\pm 0.2) \times 10^4$
7-Methylguanosine	$18.0 \pm 0.9$	$33 \pm 4$	$5.5 (\pm 0.7) \times 10^5$

<sup>a</sup> At 25 °C and 100 mM Hepes pH 7.5.

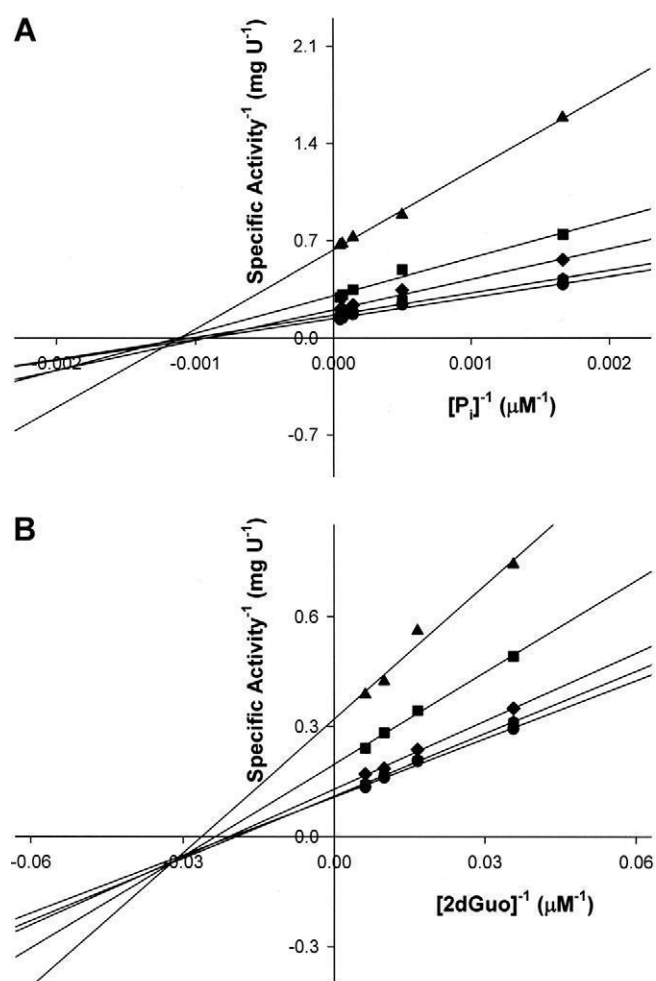


**Fig. 2.** Intersecting initial velocity patterns for MtPNP with either  $P_i$  (A) or 2dGuo (B) as the variable substrate. Each curve represents varied-fixed levels of the co-substrate. One unit of enzyme activity (U) is defined as the amount of enzyme that catalyses the phosphorolysis of 1  $\mu$ mol of 2dGuo per minute in a 1 cm optical path.

tive (Eq. (4)) inhibition. The results (Table 2) showed a pattern of three noncompetitive and one competitive inhibition, which is consistent with a steady-state ordered bi bi kinetic mechanism [49,50] in which  $P_i$  binds first to the enzyme, followed by the binding of 2dGuo to form the catalytically competent ternary complex.

#### Equilibrium binding of ligands to MtPNP

Binding experiments were employed to confirm, or refute, the proposed kinetic mechanism. In equilibrium binary complex formation experiments, the intrinsic MtPNP fluorescence enhanced upon binding of either  $P_i$  or Gua. Titration of MtPNP with  $P_i$  was

**Table 2**  
Product Inhibition Patterns for MtPNP.<sup>a</sup>

Varied substrate	Product inhibitor	Inhibition type <sup>b</sup>	$K_{is}$ ( $\mu$ M) <sup>c</sup>	$K_{ii}$ ( $\mu$ M) <sup>d</sup>
2dGuo	Gua	NC	$6 \pm 1$	$15 \pm 3$
$P_i$	Gua	NC	$5 \pm 1$	$21 \pm 2$
2dGuo	R1P	NC	$70 \pm 14$	$333 \pm 150$
$P_i$	R1P	C	$60 \pm 11$	–

<sup>a</sup> At 25 °C and 100 mM Hepes pH 7.0.

<sup>b</sup> NC, noncompetitive; C, competitive.

<sup>c</sup>  $K_{is}$  is the slope inhibition constant.

<sup>d</sup>  $K_{ii}$  is the intercept inhibition constant.

hyperbolic (Fig. 3A) and with Gua was sigmoidal (Fig. 3B). Fitting the data of the former to a hyperbolic function (Eq. (1)) and the latter to the Hill equation (Eq. (8)) yielded values of  $2232 \pm 86 \mu$ M for the overall dissociation constant of  $P_i$  ( $K_d$ ) and of  $11 \pm 1 \mu$ M for Gua ( $K'$ ). The  $P_i$  overall dissociation constant value for MtPNP is 12-fold larger than that for HsPNP [48]. The value for  $K'$  represents a mean dissociation constant for MtPNP:Gua binary complex formation, which is comprised of interaction factors and the intrinsic dissociation constant [51,52]. A Hill plot of the data (Fig. 3C) fitted to Eq. (9) yielded a value of  $11 \pm 1 \mu$ M for  $K'$  and a value larger than one for  $h$  ( $3.2 \pm 0.2$ ). The latter value indicates strong positive homotropic cooperativity on Gua binding to trimeric MtPNP, which is further supported by the upward-curved double-reciprocal plot (inset in Fig. 3C). A value of  $0.4 \mu$ M has been determined for Gua binding to HsPNP [48]. It should be pointed out that titration of a chromophore-free HsPNP (in which the tryptophan residues at positions 16, 94 and 178 were replaced with tyrosines) with Gua showed similar overall dissociation constant value as compared to wild-type HsPNP [48]. Accordingly, the titration of MtPNP with Gua here presented clearly demonstrates binding of the base to free enzyme. No intrinsic protein fluorescence change upon addition of either 2dGuo or R1P to MtPNP could be observed, suggesting that neither of these compounds could bind to free MtPNP enzyme.

In equilibrium ternary complex formation studies, the intrinsic fluorescence of MtPNP:Gua binary complex decreased upon binding of  $P_i$ , whereas the fluorescence of MtPNP: $P_i$  binary complex enhanced upon binding of Gua. Similarly to the binary complex formation at equilibrium, titration of MtPNP:Gua with  $P_i$  was hyperbolic (Fig. 4A), and titration of MtPNP: $P_i$  with Gua was sigmoidal (Fig. 4B). Fitting the data of the former to a hyperbolic function (Eq. (1)) and the latter to the Hill equation (Eq. (8)) yielded values of  $8380 \pm 600 \mu$ M for the overall dissociation constant of  $P_i$  ( $K_d$ ) and of  $2.6 \pm 0.3 \mu$ M for Gua ( $K'$ ) upon ternary complex formation. The  $P_i$  overall dissociation constant value for MtPNP:Gua: $P_i$  ternary complex formation is approximately fourfold larger than that for MtPNP: $P_i$  binary complex formation. On the other hand, the Gua overall dissociation constant value from MtPNP: $P_i$ :Gua ternary complex is approximately fourfold smaller than that for MtPNP:Gua binary complex formation. These results suggest a positive free energy coupling ( $\Delta G_{coop} = 3.3 \text{ kJ mol}^{-1}$ ) for  $P_i$  binding to MtPNP:Gua, and a negative free energy coupling for Gua binding to MtPNP: $P_i$  as compared to binary complex formation ( $\Delta G_{coop} = -3.6 \text{ kJ mol}^{-1}$ ). There thus appears to be a negative cooperativity ( $\Delta G_{coop} > 0$ ) in energy coupling of Gua binding to MtPNP on  $P_i$  binding to the binary complex, whereas  $P_i$  binding to MtPNP to form the binary complex shows a positive cooperativity ( $\Delta G_{coop} < 0$ ) in energy coupling upon Gua binding and ensuing ternary complex formation [52]. It is thus tempting to suggest that Gua release from MtPNP:Gua binary complex would facilitate  $P_i$  binding to MtPNP for the forward reaction. On the other hand, as cellular  $P_i$  concentration is in the millimolar range [53] and it is likely that a proportion of MtPNP would be present as MtPNP: $P_i$  binary complex, an increase in affinity of Gua for MtPNP: $P_i$  binary complex would result in formation of a non-productive complex, which could play a role in controlling MtPNP enzyme activity in response to changes in the intracellular concentration of 6-oxopurine nucleosides. In short, MtPNP activity would rely on a balance between free 6-oxonucleosides and bases.

The initial velocity and product inhibition patterns and equilibrium binding results are consistent with a steady-state ordered bi bi kinetic mechanism where  $P_i$  is the first substrate to bind to the enzyme, followed by the binding of 2dGuo to form the ternary complex capable of undergoing catalysis, and R1P is the first product to dissociate from the enzyme, followed by dissociation of Gua



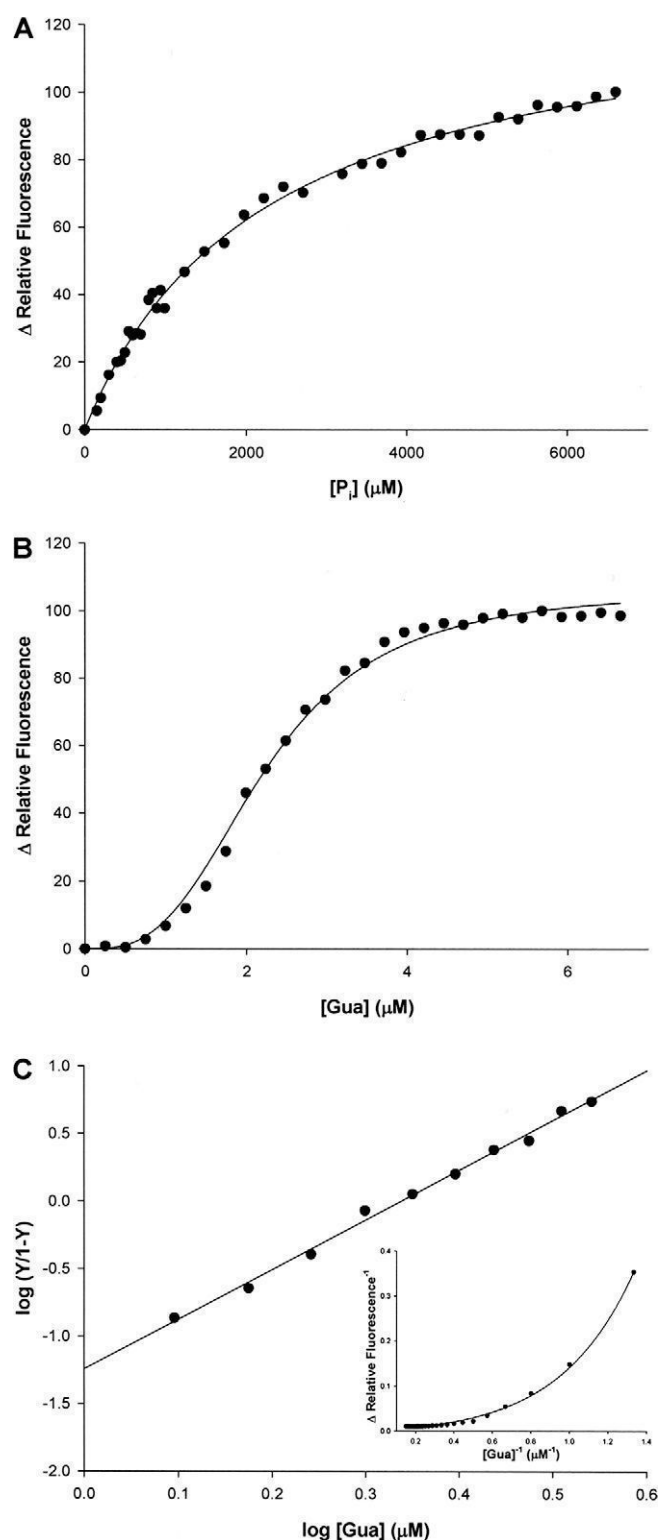


**Fig. 3.** Overall dissociation constant for MtPNP: $P_i$  (A) and MtPNP:Gua (B) binary complex formation monitoring changes in intrinsic protein fluorescence. (C) Hill logarithmic plot of the data between 10% and 90% active site saturation with Gua. Inset represents the fit of double-reciprocal plot of the fluorescence data to an exponential growth equation.

(Fig. 5). A similar order of substrate addition was proposed for Guo phosphorolysis by calf spleen PNP [16], while a random order was suggested for Ino arsenolysis (nonreversible phosphorolysis catalyzed by PNP upon replacement of  $P_i$  by arsenate) by the same en-

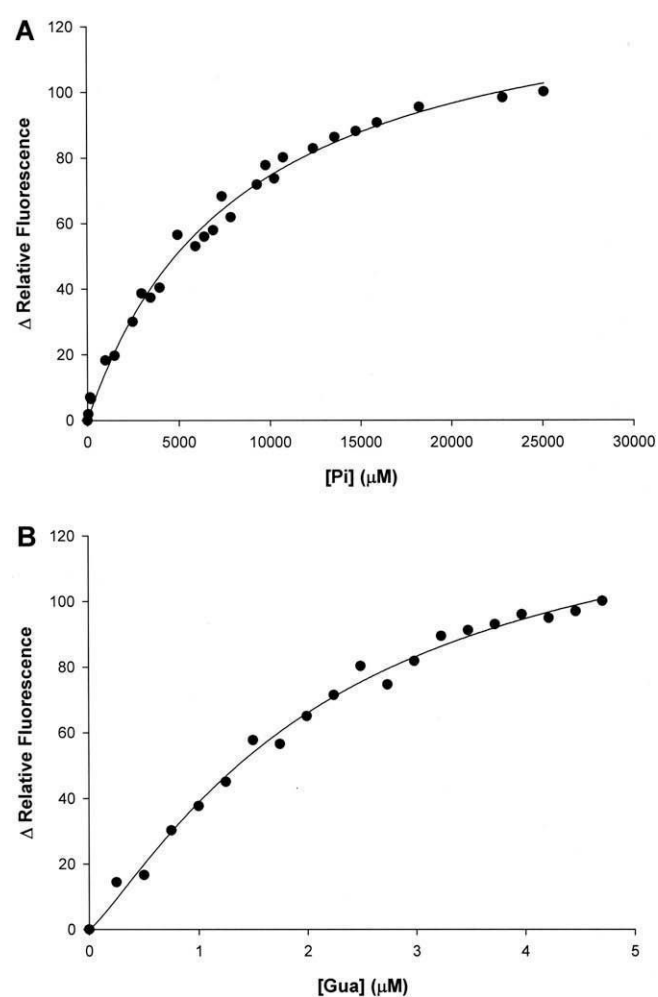


**Fig. 4.** Overall dissociation constant for ternary complex formation upon (A)  $P_i$  binding to MtPNP:Gua, and (B) Gua binding to MtPNP: $P_i$  monitoring changes in intrinsic protein fluorescence.

zyme [54]. In both cases, however, the order of product release was the same as proposed in the present work.

#### SPR measurements

In order to test the possibility that 2dGuo was able to bind to the free enzyme but induced no change in protein fluorescence, SPR measurements were carried out. There was no observable increase in RU upon increasing 2dGuo concentration, which is consistent with the proposed enzyme mechanism in which 2dGuo cannot bind to free MtPNP enzyme.

#### pH-rate profiles

The pH dependence of  $k_{cat}$  and  $k_{cat}/K_M$  for both 2dGuo and  $P_i$  were determined to probe acid/base chemistry in MtPNP mode of action. The pH-rate profiles (Fig. 6) were bell-shaped, and the data were best fitted to Eq. (5), which describes decreases in the parameter values on both acidic and basic limbs with slopes of 1 and  $-1$ , respectively. However, it should be pointed out that no data could be collected below pH 6.0 due to enzyme instability and thus only a rough estimate of the apparent  $pK_a$  values on the acidic limb could be obtained. The  $k_{cat}$  (Fig. 6A) and  $k_{cat}/K_{2dGuo}$  (Fig. 6C) profiles indicate that one group must be protonated for both catalytic activity ( $pK_a = 8.9 \pm 0.4$ ) and binding of 2dGuo ( $pK_a = 8.5 \pm 0.3$ ). It



Fig. 5. Proposed kinetic mechanism for MtPNP with 2'-deoxyguanosine.

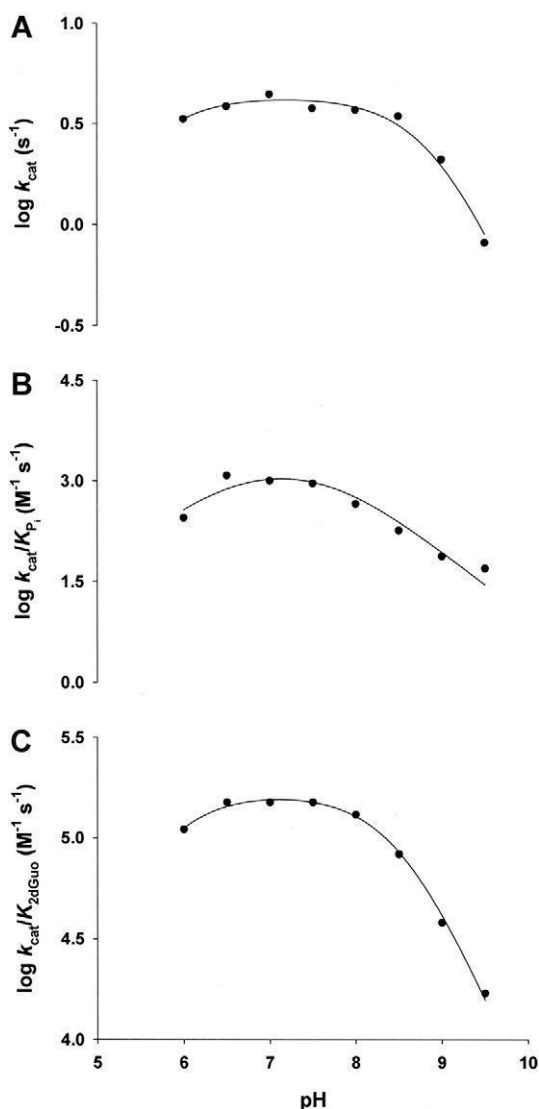


Fig. 6. pH dependence of MtPNP kinetic parameters. Plots: (A)  $\log k_{cat}$ , (B)  $\log k_{cat}/K_{P_i}$ , and (C)  $\log k_{cat}/K_{2dGuo}$ . Experimental data were fitted to Eq. (5).

is likely that both profiles are reporting on the same group. The nucleoside has no dissociating groups with  $pK_a$  values in the pH range tested here, indicating that this group is probably an amino acid side chain of the enzyme.

A comparison between the three-dimensional structures of ternary complexes of either MtPNP or bovine spleen PNP in complex with a transition state analogue (ImmH) and  $P_i$  showed that the contacts in their catalytic sites are similar but not identical [18]. Most strikingly, is a 2.8 Å hydrogen bond between Tyr188 and O5' in MtPNP that is prevented by a phenylalanine in this position in the mammalian enzymes. Since the structure of MtPNP indicates that the substrate-assisted catalysis involves the oxocarbenium transition state stabilization for phosphorolysis of nucleosides by an interaction with 5'-OH group, it is thus tempting to suggest that the Tyr188 hydroxyl group is the general acid catalyst whose deprotonation abolishes binding and catalytic activity. However, there are other groups such as Tyr180 hydroxyl that participates

in  $P_i$  binding which could also account for the acid–base catalysis identified in the pH–rate profiles. Interestingly, Tyr188 is the only residue that interacts directly with bound ImmH inhibitor that is not conserved in the mammalian PNPs [18], which could be exploited to design inhibitors more specific for MtPNP.

Analysis of the  $k_{cat}/K_{P_i}$  profile indicates that deprotonation of a group with an apparent  $pK_a$  value of  $7.8 \pm 0.4$  abolishes  $P_i$  binding (Fig. 6B). The Henderson–Hasselbalch's equation predicts that the concentration of the basic form of  $P_i$  ( $pK = 7.2$ ) at pH 6.0 would be approximately 3 mM, which is well above the  $K_{P_i}$  value (1.37 mM). Determination of the three-dimensional structures of MtPNP:ImmH: $P_i$  ternary complex [18] and MtPNP: $P_i$  binary complex [55] showed that side chains of Arg88 and His90 hydrogen bond to O1 of the bound  $P_i$ , while Ser36 interacts with both O4 and O3 through side chain and backbone atoms. The  $P_i$  O2 oxygen is anchored by a direct hydrogen bond with the side chain of Ser208 and a water-mediated hydrogen bond with the backbone amide of Ala120 and the hydroxyl group of Tyr180. It is thus tempting to suggest that the imidazole side chain of His90 is the group whose deprotonation abolishes binding and catalysis, since the nitrogen with the hydrogen atom in the nonionized form of the imidazole ring could be the hydrogen bond donor for  $P_i$  binding and/or catalysis. Notwithstanding, site-directed mutagenesis analysis will be required to assign any role to this residue.

#### Temperature effects

The data on dependence of  $k_{cat}$  on temperature (Fig. 7) were fitted to Eq. (6), yielding a value of 4.7 kcal mol<sup>-1</sup> for the energy of activation of MtPNP-catalyzed reaction. It should be pointed out that the pre-exponential factor (A) was considered as temperature-independent in the temperature range used here. Thus, the value of 4.7 kcal mol<sup>-1</sup> represents the minimal amount of energy required to initiate the MtPNP-catalyzed chemical reaction, since we measured the enzyme activity at saturating concentrations of substrates. Moreover, the linearity of the Arrhenius plot (Fig. 7) indicates that there is no change in the rate-limiting step over the temperature range utilized here.

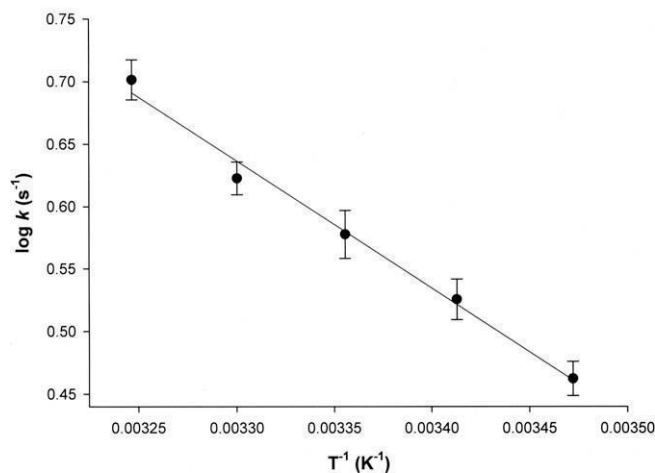
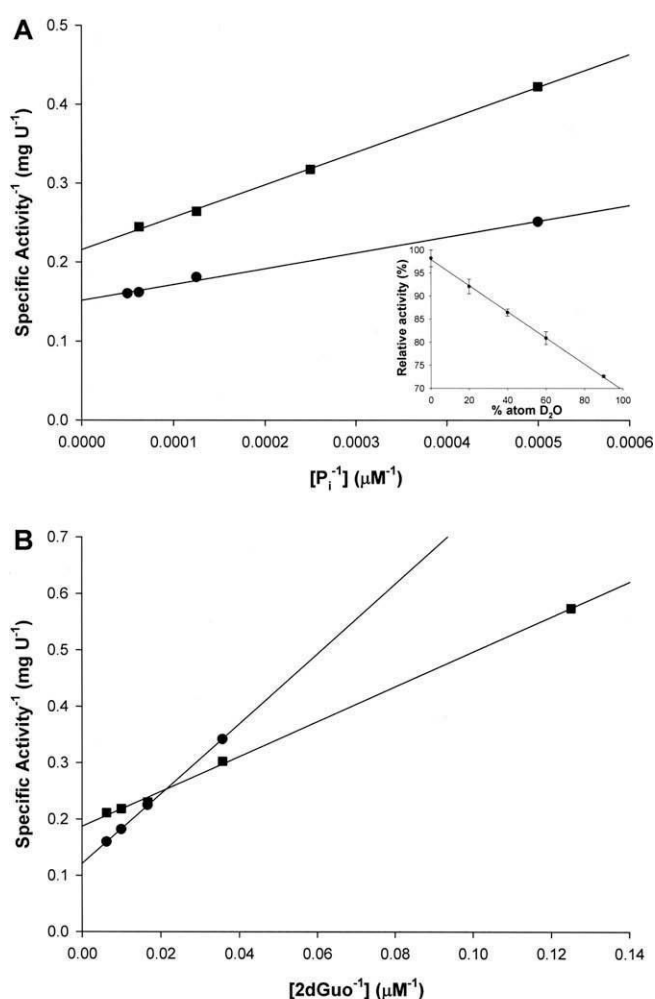


Fig. 7. Temperature dependence of the  $\log k_{cat}$ . Saturating conditions of substrates were determined and used at each temperature. The line is a fit to Eq. (6).

## Solvent kinetic isotope effects and proton inventory

Solvent kinetic deuterium isotope effects were evaluated to assess the contribution of solvent proton transfer to a step in the MtPNP-catalyzed reaction (Fig. 8). Solvent isotope effects on  $V$  arise from solvent-exchangeable protons being transferred during events following the formation of the ternary complex capable of undergoing catalysis, which include the chemical steps, possible enzyme conformational changes and product release. Solvent isotope effects on  $V/K$  arise from solvent-exchangeable protons being transferred during steps in the reaction mechanism from the binding of substrates to the first irreversible step, usually considered to be the release of the first product. Hence,  $V/K$  isotope effects are a combination of binding and catalytic isotope effects [56]. The value of  $1.6 \pm 0.1$  for the solvent kinetic deuterium isotope effect on  $V$  ( $^{D_2}V$ ) indicates that any proton transfer occurring after the formation of the ternary complex capable of undergoing catalysis contributes modestly to the rate-limiting step of the reaction. The value of  $2.2 \pm 0.2$  for the solvent effect on  $P_i$   $V/K$  ( $^{D_2}V/K_{P_i}$ ) suggests that proton transfer steps taking place from binding of  $P_i$  up to release of the first product (R1P) contribute to the reaction rate-limiting step. The different values for  $^{D_2}V$  and  $^{D_2}V/K_{P_i}$  suggest that they are reporting on distinct portions of the reaction sequence.



**Fig. 8.** Solvent isotope effects for MtPNP. Plots: (A)  $P_i$  and (B) 2dGuo as the varied substrate, with saturating concentration of the co-substrate. The reaction mix contained either 0 (●) or 90 (■) atom%  $D_2O$ . Inset represents the proton inventory on MtPNP, with both substrates at saturating concentrations.

An inverse solvent kinetic isotope effect was observed for  $V/K_{2dGuo}$  ( $0.5 \pm 0.1$ ), showing that any proton transfer taking place from 2dGuo binding to the MtPNP: $P_i$  binary complex up to product release does not occur in a rate-limiting step. This result indicates that proton transfer does not dominate the prominent energetic barriers in the reaction coordinate, since transfers at energetic barriers result in normal solvent deuterium kinetic isotope effects [57]. Inverse solvent kinetic isotope effects may originate in protons being transferred from cysteine or from metal-bound water [58]; however, these cannot account for the inverse effect observed here since MtPNP is not a metalloenzyme and no cysteine has been proposed to play any role in binding or catalysis [18]. Low barrier hydrogen bonds between acceptor and donor groups with similar  $pK_a$  values may also give rise to inverse solvent isotope effects [59]. However, whether this compressed hydrogen bond arrangement between acceptor and donor groups with similar  $pK_a$  values exists in MtPNP will have to await three-dimensional structure determination of MtPNP in complex with 2dGuo. A mixture of proton transfer and inverse equilibrium isotope effects may also be invoked to interpret some observed inverse solvent isotope effects, depending on their magnitudes and provided that the equilibrium effects dominate [57]. It would thus imply inverse solvent equilibrium isotope effect only on 2dGuo binding to MtPNP: $P_i$  binary complex, as the effects on  $V$  and  $V/K_{P_i}$  are normal. However, further experimental results are needed to confirm or discard this possibility. At any rate, a simple qualitative interpretation is that the inverse  $V/K_{2dGuo}$  solvent isotope effect indicates that bonds to the isotopic label are tighter in the bound complex as compared to the free reactant state, which indicates that intramolecular or intermolecular restraints render motion more energy demanding in the bound state.

To assess the number of protons being transferred during phosphorylation of 2dGuo catalyzed by MtPNP that give rise to the solvent isotope effects, a proton inventory was performed on the maximal velocity of the reaction (inset in Fig. 8). The linear relationship between  $V$  and the mole fraction of  $D_2O$  indicates that a single proton is transferred in the step that exhibits the solvent isotope effect on  $V$ .

## Pre-steady-state kinetics

In order to assess whether product release contributes to the rate-limiting step, measurement of pre-steady-state product formation was carried out. It should be pointed out that 2dGuo and  $P_i$  concentrations were above  $K_M$  values and in excess as compared to MtPNP concentration, so that any burst in product formation could be reliably assessed [60,61]. Fitting the pre-steady-state trace showing a single exponential decay (Fig. 9) to Eq. (10) yielded a value of  $8.91 \pm 0.05$  s<sup>-1</sup> for the apparent first-order rate constant for product formation (1 cm pathlength), in agreement with the catalytic rate constant value for 2dGuo. There was no apparent accumulation of observable product on the enzyme active site (Fig. 9) when high concentration of MtPNP (20 μM) was mixed with saturating concentrations of 2dGuo (150 μM) and  $P_i$  (20 mM). However, part of the signal could not be detected because it occurred in the dead time of the equipment (1.37 ms). The change in absorbance lost in the dead time corresponds to approximately 23 μM of product formation, which thus indicates that there is a burst in product formation that occurred in the dead time of the equipment since the mixing chamber enzyme concentration is 20 μM. Accordingly, the transient kinetics of enzyme-product compound formation indicates that microscopic rate constants involved in product release contributed to the rate-limiting step for the steady-state turnover. The modest solvent isotope effect on  $V$  is likely due to product release rather than chemical steps or possible enzyme conformational changes preceding the latter. In

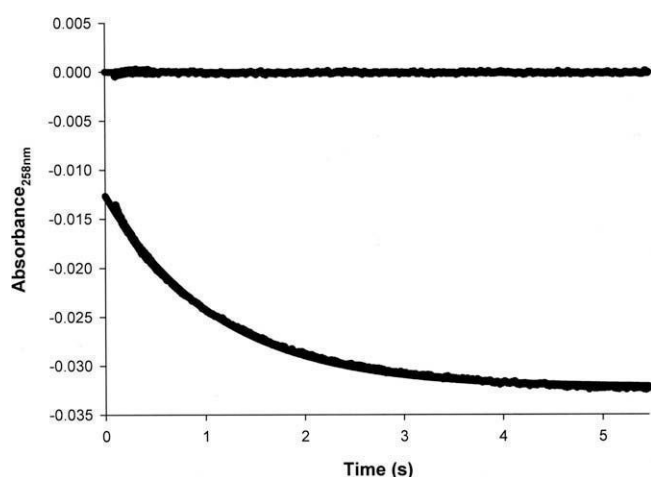


**Fig. 9.** Representative stopped-flow trace for product formation. The exponential decay yielded a value of  $8.91 \text{ s}^{-1}$  for the apparent first-order rate constant of product formation.

agreement with our results, the pre-steady-state kinetic mechanism of hydrolysis of Ino by calf spleen PNP has been shown to include a burst of product formation, in which release of hypoxanthine is the rate-limiting step [62].

### Summary

In the present report, we have shown that MtPNP is more specific to 2dGuo and no phosphorolysis of adenosine could be detected. Initial velocity, product inhibition and equilibrium binding data indicate that MtPNP catalyzes phosphorolysis of 2dGuo by a steady-state ordered bi bi kinetic mechanism, in which  $P_i$  binds first to the enzyme followed by the binding of 2dGuo to form the catalytically competent ternary complex, and R1P is the first product to dissociate from the enzyme followed by dissociation of Gua. The pH-dependence of  $k_{\text{cat}}$  and  $k_{\text{cat}}/K_{2\text{dGuo}}$  indicated a general acid as being essential for both catalysis and 2dGuo binding. In addition, pH-rate profiles showed that deprotonation of a group abolishes  $P_i$  binding ( $\text{p}K_a = 7.8$ ), suggesting that His90 may be involved in binding and catalysis. Proton inventory and solvent deuterium isotope effects on  $V$  and  $V/K$  indicate that a single solvent proton transfer makes a modest contribution to the rate-limiting step. Pre-steady-state kinetic data indicate that product release contributes to the rate-limiting step for the MtPNP-catalyzed reaction. It is hoped that the results here described may be useful to the rational design of anti-TB agents and that they may contribute to our understanding of the biology of *M. tuberculosis*.

### Acknowledgments

This work is dedicated to a lifetime of achievement in academia by Tuiskon Dick, who died on December 8th, 2008.

### References

- [1] J.B. Bass Jr., L.S. Farer, P.C. Hopewell, R. O'Brien, R.F. Jacobs, F. Ruben, D.E. Snider Jr., G. Thornton, *J. Respir. Crit. Care Med.* 149 (1994) 1359–1374.
- [2] S.K. Sharma, A. Mohan, *J. Indian. Med. Assoc.* 101 (2003) 157–158.
- [3] C. Dye, S. Scheele, P. Dolin, V. Pathania, M.C. Raviglione, *J. Am. Med. Assoc.* 282 (1999) 677–686.
- [4] Centers for Disease Control and Prevention, *Morb. Mortal. Wkly. Rep.* 55 (2006) 301–305.
- [5] Centers for Disease Control and Prevention, *Morb. Mortal. Wkly. Rep.* 56 (2007) 250–253.
- [6] M. Jassal, W.R. Bishai, *Lancet Infect. Dis.* 9 (2009) 19–30.
- [7] S.M. Hingley-Wilson, V.K. Sambandamurthy, W.R. Jacobs Jr., *Nat. Immunol.* 4 (2003) 949–955.

- [8] C. Nathan, *Science* 322 (2008) 1337–1338.
- [9] D. Avarbock, J. Salem, L.S. Li, Z.M. Wang, H. Rubin, *Gene* 233 (1999) 261–269.
- [10] M. Cashel, D.R. Gentry, V.J. Hernandez, D. Vinella, in: F.C. Neidhardt (Ed.), *Escherichia coli and Salmonella: Cellular and Molecular Biology*, ASM Press, Washington, 1996, pp. 1458–1496.
- [11] A.K. Ojha, T.K. Mukherjee, D. Chatterji, *Infect. Immun.* 68 (2000) 4084–4091.
- [12] T.P. Primm, S.J. Andersen, V. Mizrahi, D. Avarbock, H. Rubin, C.E. Barry III, *J. Bacteriol.* 182 (2000) 4889–4898.
- [13] J.L. Dahl, C.N. Kraus, H.I. Boshoff, B. Doan, K. Foley, D. Avarbock, G. Kaplan, V. Mizrahi, H. Rubin, *Proc. Natl. Acad. Sci. USA* 100 (2003) 10026–10031.
- [14] H. Zheng, L. Lu, B. Wang, S. Pu, X. Zhang, G. Zhu, W. Shi, L. Zhang, H. Wang, S. Wang, G. Zhao, Y. Zhang, *PLoS ONE* 3 (2008) e2375.
- [15] L.A. Basso, D.S. Santos, W. Shi, R.H. Furneaux, P.C. Tyler, V.L. Schramm, *J.S. Blanchard, Biochemistry* 40 (2001) 8196–8203.
- [16] D.J. Porter, *J. Biol. Chem.* 267 (1992) 7342–7351.
- [17] H.M. Kalckar, *J. Biol. Chem.* 167 (1947) 429–443.
- [18] W. Shi, L.A. Basso, D.S. Santos, P.C. Tyler, R.H. Furneaux, J.S. Blanchard, S.C. Almo, V.L. Schramm, *Biochemistry* 40 (2001) 8204–8215.
- [19] E.A. Taylor Ringia, P.C. Tyler, G.B. Evans, R.H. Furneaux, A.S. Murkin, V.L. Schramm, *J. Am. Chem. Soc.* 128 (2006) 7126–7127.
- [20] S.S. Poletto, I.O. da Fonseca, L.P. de Carvalho, L.A. Basso, D.S. Santos, *Protein Expr. Purif.* 34 (2004) 118–125.
- [21] K.C. Kelley, K.J. Huestis, D.A. Austen, C.T. Sanderson, M.A. Donoghue, S.K. Stickle, E.S. Kawasaki, M.S. Osburne, *Gene* 156 (1995) 33–36.
- [22] U.K. Laemmli, *Nature* 227 (1970) 680–685.
- [23] M.M. Bradford, *Anal. Biochem.* 72 (1976) 248–254.
- [24] M.R. Webb, *Proc. Natl. Acad. Sci. USA* 89 (1992) 4884–4887.
- [25] A. Bzowska, E. Kulikowska, D. Shugar, *Z. Naturforsch.* 45 (1990) 59–70.
- [26] D.W. Parkin, V.L. Schramm, *Biochemistry* 34 (1995) 13961–13966.
- [27] E. Kulikowska, A. Bzowska, J. Wierchowski, D. Shugar, *Biochim. Biophys. Acta* 874 (1986) 355–363.
- [28] W.B. Parker, P.W. Allan, A.E.A. Hassan, J.A. Secrist III, E.J. Sorscher, W.R. Waud, *Cancer Gene Ther.* 10 (2003) 23–29.
- [29] P.F. Cook, W.W. Cleland, *Enzyme Kinetics and Mechanisms*, Garland Science, London, New York, 2007, pp. 325–366.
- [30] V. Henri, Hermann, Paris, 1903.
- [31] L. Michaelis, M.L. Menten, *Biochem. Zeitschr.* 49 (1913) 333–369.
- [32] A.V. Hill, *Biochem. J.* 7 (1913) 471–480.
- [33] K.F. Jensen, *Eur. J. Biochem.* 61 (1976) 377–386.
- [34] J.D. Stoeckler, in: R.J. Glazer (Ed.), *Developments in Cancer Chemotherapy*, CRC Press, Boca Raton, FL, 1984, pp. 35–60.
- [35] P.A. Ropp, T.W. Traut, *Arch. Biochem. Biophys.* 288 (1991) 614–620.
- [36] W.J. Hennen, C.-H. Wong, *J. Org. Chem.* 54 (1989) 4692–4695.
- [37] R.G. Silva, J.H. Pereira, F. Canduri, W.F. de Azevedo Jr., L.A. Basso, D.S. Santos, *Arch. Biochem. Biophys.* 442 (2005) 49–58.
- [38] A. Bzowska, E. Kulikowska, D. Shugar, *Pharmacol. Ther.* 88 (2000) 349–425.
- [39] T.P. Zimmerman, N.B. Gersten, A.F. Ross, R.P. Miech, *Can. J. Biochem.* 49 (1971) 1050–1054.
- [40] J.D. Stoeckler, A.F. Poirot, R.M. Smith, R.E. Parks Jr., S.E. Ealick, K. Takabayashi, M.D. Erion, *Biochemistry* 36 (1997) 11749–11756.
- [41] W.B. Parker, E.W. Barrow, P.W. Allan, S.C. Shaddix, M.C. Long, W.W. Barrow, N. Bansal, J.A. Maddry, *Tuberculosis (Edinb)* 84 (2004) 327–336.
- [42] K.F. Jensen, P. Nygaard, *Eur. J. Biochem.* 51 (1975) 253–265.
- [43] K.F. Jensen, *Biochim. Biophys. Acta* 525 (1978) 346–356.
- [44] H. Lineweaver, D. Burk, *J. Am. Chem. Soc.* 56 (1934) 658–666.
- [45] M.D. Erion, J.D. Stoeckler, W.C. Guida, R.L. Walter, S.E. Ealick, *Biochemistry* 36 (1997) 11735–11748.
- [46] C. Mao, W.J. Cook, M. Zhou, A.A. Federov, S.C. Almo, S.E. Ealick, *Biochemistry* 37 (1998) 7135–7146.
- [47] J. Tebbe, A. Bzowska, B. Wielgus-Kutrowska, W. Schröder, Z. Kazimierzczuk, D. Shugar, W. Saenger, G. Koellner, *J. Mol. Biol.* 294 (1999) 1239–1255.
- [48] M. Ghanem, S. Saen-oon, N. Zhadin, C. Wing, S.M. Cahill, S.D. Schwartz, R. Callender, V.L. Schramm, *Biochemistry* 47 (2008) 3202–3215.
- [49] W.W. Cleland, *Adv. Enzymol. Relat. Areas Mol. Biol.* 45 (1977) 273–387.
- [50] I.H. Segel, *Enzyme Kinetics. Behavior and Analysis of Rapid Equilibrium and Steady-State Enzyme Systems*, John Wiley and Sons, Inc., New York, 1975, pp. 560–590.
- [51] I.H. Segel, *Enzyme Kinetics. Behavior and Analysis of Rapid Equilibrium and Steady-State Enzyme Systems*, John Wiley and Sons, Inc., New York, 1975, pp. 346–464.
- [52] G. Weber, *Adv. Protein Chem.* 29 (1975) 1–83.
- [53] T.W. Traut, *Mol. Cell. Biochem.* 140 (1994) 1–22.
- [54] P.C. Kline, V.L. Schramm, *Biochemistry* 32 (1993) 13212–13219.
- [55] D.O. Nolasco, F. Canduri, J.H. Pereira, J.R. Cortinóz, M.S. Palma, J.S. Oliveira, L.A. Basso, W.F. de Azevedo Jr., D.S. Santos, *Biochem. Biophys. Res. Commun.* 324 (2004) 789–794.
- [56] V.L. Schramm, *Curr. Opin. Chem. Biol.* 11 (2007) 529–536.
- [57] D.J. Merkler, V.L. Schramm, *Biochemistry* 32 (1993) 5792–5799.
- [58] D.M. Quinn, L.D. Sutton, in: P.F. Cook (Ed.), *Enzyme Mechanism from Solvent Isotope Effects*, CRC Press, Boca Raton, FL, 1991, pp. 73–126.
- [59] W.W. Cleland, *Biochemistry* 31 (1992) 317–319.
- [60] K. Hiromi, *Kinetics of Fast Enzyme Reactions: Theory and Practice*, Kodansha Ltd., Tokyo, 1979, pp. 187–253.
- [61] L.A. Basso, P.C. Engel, A.R. Walmsley, *Eur. J. Biochem.* 234 (1995) 603–615.
- [62] P.C. Kline, V.L. Schramm, *Biochemistry* 31 (1992) 5964–5973.

## 5. DISCUSSÃO

Após uma triagem de condições ideais de crescimento bacteriano para expressão da proteína recombinante, foi verificado que o nível mais alto de produção de MtPNP pôde ser alcançado 50,7 h após indução por isopropil  $\beta$ -D-tiogalactopiranosídeo (IPTG), utilizando *E. coli* BL21(DE3)NH contendo o vetor pET-23a(+):*deoD*. A proteína recombinante foi purificada com êxito a partir do estabelecimento de um protocolo de purificação contendo quatro passos cromatográficos, capaz de produzir 140 mg de MtPNP, pura e funcional, a partir de 20 g de cultura celular, o que representa um aumento de aproximadamente 600% no nível de recuperação protéica quando comparado ao protocolo previamente publicado (BASSO *et al.*, 2001).

A análise dos parâmetros cinéticos e eficiências catalíticas aparentes em estado estacionário obtidas para os compostos naturais e sintéticos testados com MtPNP estão dispostos na Tabela 1 do Artigo 2 (Table 1). Cabe notar que as curvas cinéticas para  $P_i$  ou qualquer dos nucleosídeos nos intervalos de concentração aqui testados apresentaram um melhor ajuste à função hiperbólica de Michaelis-Menten (HENRI, 1903; MICHAELIS & MENTEN, 1913), como pode ser observado na Figura 8.

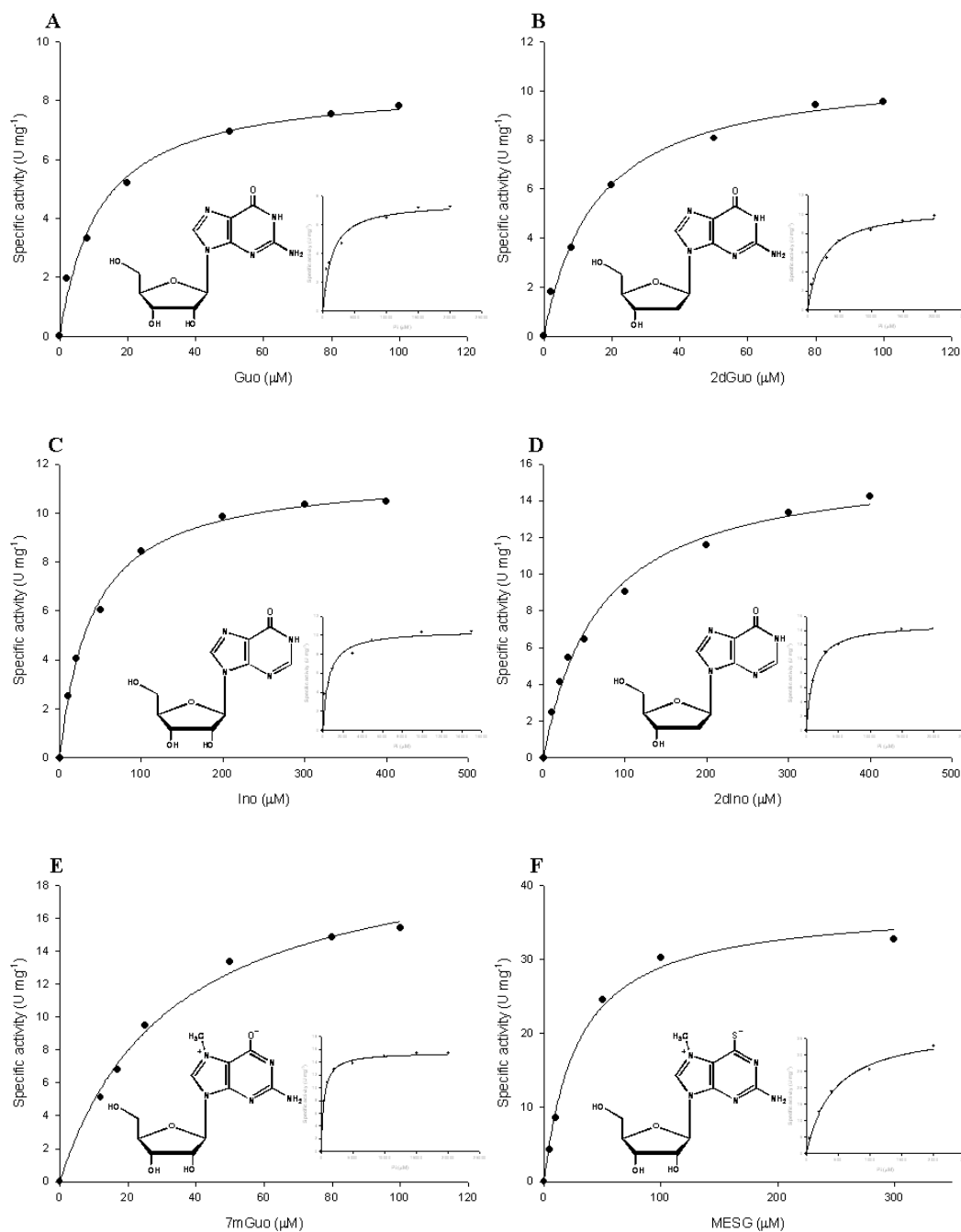


**Figura 8.** Curvas de saturação para os substratos testados com MtPNP. (A) Guo; (B) 2dGuo; (C) Ino; (D) 2dIno; (E) 7mGuo; e (F) MESG. Cada gráfico contém a estrutura química do nucleosídeo correspondente e uma inserção que corresponde à curva para  $P_i$ .

Os maiores valores de constante catalítica ( $k_{cat}$ ) ocorreram com 7-metil-6-tio-guanosina (MESG) e 7-metilguanosina (7mGuo), sendo a reação essencialmente

irreversível no sentido da fosforólise com estes dois substratos (HENNEN & WONG, 1989; WEBB, 1992). Verificou-se também que a especificidade de MtPNP por  $P_i$  é uma ordem de grandeza maior para estes mesmos dois substratos, reflexo de valores de  $k_{cat}$  maiores e valores de constante de dissociação global ( $K_M$ ) menores. A enzima mostrou-se mais específica por MESG e 7mGuo que por qualquer outro nucleosídeo natural testado, o que se deve basicamente aos seus valores aumentados de  $k_{cat}$ , dada a similaridade entre seus valores de  $K_M$ . Estes resultados estão em contraste com os observados para HsPNP, que mostrou-se mais específica por substratos naturais como inosina (Ino) e guanosina (Guo) que por MESG (SILVA *et al.*, 2005). Ainda, o valor de  $K_M$  de MtPNP obtido para MESG foi aproximadamente 12 vezes menor que para HsPNP. Estas diferenças observadas entre a enzima humana e a micobacteriana indicam que inibidores enzimáticos com maior especificidade por MtPNP podem ser desenhados baseados nas substituições nos grupos funcionais químicos de MESG, particularmente o enxofre na posição 6 da base purínica.

As PNPs triméricas são conhecidas pela alta especificidade à catálise de 6-oxopurinas naturais, seus nucleosídeos [Ino, 2'-desoxiinosina (2dIno), Guo e 2'-desoxiguanosina (2dGuo)] e alguns análogos, enquanto PNPs hexaméricas adicionalmente aceitam 6-aminopurinas (Ade), seus nucleosídeos e muitos análogos (BZOWSKA *et al.*, 2000). Entre as PNPs triméricas, as taxas de fosforólise e/ou síntese de Ado, quando detectáveis, são insignificantes (ZIMMERMAN *et al.*, 1971; STOECKLER *et al.*, 1997). Apesar de MtPNP ter sido claramente classificada dentro da classe das PNPs triméricas, não existe nenhum estudo publicado que tenha descrito o metabolismo de Ado em células de *M. tuberculosis* (PARKER *et al.*, 2004) ou mesmo dados experimentais que tenham avaliado a especificidade de MtPNP por Ado. De fato, MtPNP é um homotrímero em solução (BASSO *et al.*, 2001), da mesma forma que as PNPs de mamíferos, mas

diferentemente das enzimas hexaméricas procarióticas (JENSEN, 1978; TRAUT, 1994). Entretanto, não há nenhuma publicação reportando a capacidade de MtPNP em catalisar a fosforólise de Ado, um nucleosídeo 6-oxopurínico. Desta forma, passamos a investigar a especificidade de MtPNP por Ado como um possível substrato; nossos resultados indicam claramente que a taxa de fosforólise de Ado por MtPNP é indetectável ou, na melhor das hipóteses, insignificante. Estes resultados estão de acordo com a literatura, que afirma que PNPs triméricas não têm a capacidade de catalisar a fosforólise de nucleosídeos 6-aminopurínicos a uma extensão mensurável. Desta forma, estes resultados demonstram que MtPNP, assim como outras PNPs triméricas, catalisa a fosforólise de nucleosídeos com substituintes do tipo 6-oxo (ou outros substituintes com propriedades eletrônicas análogas, como S ou Se) (STOECKLER, 1984) e um N protonado na posição 1. Os análogos de Guo metilados no N7 (7mGuo e MESG) se mostraram, como esperado (KULIKOWSKA *et al.*, 1986), excelentes substratos na direção da fosforólise, ainda que sintéticos. Todos os experimentos subseqüentes aqui descritos foram realizados com 2dGuo, um substrato que apresentou uma alta eficiência catalítica, além de se mostrar mais apropriado para ensaios enzimáticos.

Os padrões de velocidade inicial foram determinados utilizando tanto 2dGuo como  $P_i$  como substrato variável para distinguir o mecanismo entre seqüencial e *ping-pong*. A análise dos gráficos de duplo-recíproco (LINEWEAVER & BURK, 1934) revelaram padrões de intersecção para ambos os substratos [Figura 2 do Artigo 2 (Fig. 2)], o que é consistente com a formação de complexo ternário e um mecanismo seqüencial. A existência de complexos ternários também foi descrita para outras PNPs triméricas, como a bovina, de eritrócitos humanos e de *Cellulomonas sp.* (ERION *et al.*, 1997; MAO *et al.*, 1998; TEBBE *et al.*, 1999). O mecanismo ordenado de equilíbrio rápido também pôde ser



descartado, visto que neste mecanismo a família de linhas do segundo substrato a se ligar a enzima deveria ter o ponto de intersecção no eixo das ordenadas. A partir da aplicação dos dados à equação 2 do Artigo 2 (Eq. (2)), foi possível estimar os seguintes valores às constantes cinéticas verdadeiras, em estado estacionário:  $k_{\text{cat}} = 4.4 \pm 0.1 \text{ s}^{-1}$ ,  $K_{2\text{dGuo}} = 47 \pm 4 \text{ }\mu\text{M}$ ,  $K_{\text{P}_i} = 1372 \pm 105 \text{ }\mu\text{M}$ ,  $k_{\text{cat}}/K_{2\text{dGuo}} = 9.4 (\pm 0.8) \times 10^4 \text{ M}^{-1} \text{ s}^{-1}$  e  $k_{\text{cat}}/K_{\text{P}_i} = 3.2 (\pm 0.3) \times 10^3 \text{ M}^{-1} \text{ s}^{-1}$ . O valor de  $k_{\text{cat}}$  para MtPNP utilizando 2dGuo como substrato é aproximadamente 6 vezes menor que para HsPNP utilizando Guo como substrato; entretanto, seus valores de  $K_M$  são similares (GHANEM *et al.*, 2008).

Os estudos de inibição por produto [Gua e ribose 1-fosfato (R1P)] foram conduzidos para elucidar a ordem de adição dos substratos à enzima. Os dados foram ajustados à equações de inibição competitiva [equação 3 do Artigo 2 (Eq. (3))] ou não-competitiva [equação 4 do Artigo 2 (Eq. (4))]. Os resultados obtidos, resumidos na Tabela 2 do Artigo 2 (Table 2), demonstram um padrão de inibição de três não-competitivas e uma competitiva, o que está consistente com um mecanismo cinético ordenado em estado estacionário do tipo bi bi (SEGEL, 1975; CLELAND, 1977), onde  $\text{P}_i$  é o primeiro substrato a ser ligar a enzima, seguido pela ligação de 2dGuo para formar o complexo ternário cataliticamente competente.

Experimentos de ligação foram empregados com o objetivo de confirmar, ou não, o mecanismo cinético proposto. Houve aumento na fluorescência intrínseca de MtPNP tanto na ligação de  $\text{P}_i$  quanto de Gua. A titulação de MtPNP foi hiperbólica com  $\text{P}_i$  [Figura 3A do Artigo 2 (Fig. 3A)] e sigmoideal com Gua [Figura 3B do Artigo 2 (Fig. 3B)]. O ajuste dos dados do primeiro a uma função hiperbólica [equação 1 do Artigo 2 (Eq. (1))] e do segundo à equação de Hill (HILL, 1913) [equação 8 do Artigo 2 (Eq. (8))] deu origem aos valores de  $2232 \pm 86 \text{ }\mu\text{M}$  para a constante de dissociação global ( $K_d$ ) de  $\text{P}_i$  e de  $11 \pm 1 \text{ }\mu\text{M}$

para Gua ( $K'$ ). O valor de  $K_d$  de  $P_i$  para MtPNP é 12 vezes maior do que o para HsPNP (GHANEM *et al.*, 2008). O valor para  $K'$  representa a constante de dissociação média para formação do complexo binário MtPNP:Gua, que compreende fatores de interação e a constante de dissociação intrínseca (SEGEL, 1975; WEBER, 1975). O gráfico de Hill destes dados [Figura 3C do Artigo 2 (Fig. 3C)], ajustados à equação 9 do Artigo 2 (Eq. (9)), geraram um valor de  $11 \pm 1 \mu\text{M}$  para  $K'$  e um valor maior que 1 para  $h$  ( $3.2 \pm 0.2$ ), o coeficiente de Hill. Este último valor indica forte cooperatividade homotrópica positiva na ligação de Gua à MtPNP trimérica, fato que é reforçado pela curvatura para cima do gráfico de duplo-recíproco [inserção na Figura 3C do Artigo 2 (inset in Fig. 3C)]. Foi recentemente determinado um valor de  $0,4 \mu\text{M}$  para a ligação de Gua à HsPNP. Cabe notar que a titulação de HsPNP livre de cromóforo (onde os resíduos de triptofano nas posições 16, 94 e 178 foram substituídos por tirosinas) com Gua gerou um valor de constante de dissociação global similar quando comparado a HsPNP tipo selvagem (GHANEM *et al.*, 2008). Assim, a titulação de MtPNP com Gua aqui apresentada demonstra claramente a ligação da base à enzima livre. Não foi observada qualquer mudança na fluorescência intrínseca da proteína durante a adição tanto de 2dGuo quanto de R1P, o que sugere que nenhum destes compostos consegue se ligar à MtPNP livre.

Os padrões de velocidade inicial e inibição por produto e os resultados de ligação em equilíbrio estão consistentes com um mecanismo cinético ordenado em estado estacionário do tipo bi bi onde  $P_i$  é o primeiro substrato a se ligar a enzima, seguido da ligação de 2dGuo para formar o complexo ternário capaz de sofrer catálise, e R1P é o primeiro produto a se dissociar da enzima, seguido pela dissociação de Gua. O mecanismo proposto está ilustrado na Figura 5 do Artigo 2 (Fig. 5). Uma ordem similar de adição de substrato foi proposta para a fosforólise de Guo pela PNP bovina (PORTER, 1992),

enquanto uma ordem randômica foi sugerida para a arsenólise de Ino (fosforólise irreversível catalisada pela PNP resultante da substituição de  $P_i$  por arsenato) pela mesma enzima (KLINE & SCHRAMM, 1993). Entretanto, em ambos os casos, a ordem de liberação dos produtos foi a mesma à proposta no presente estudo.

Medidas de SPR foram conduzidas com o objetivo de testar a possibilidade de 2dGuo ter capacidade de se ligar a enzima livre sem induzir mudança na fluorescência da proteína. Nesta análise, não foi observado qualquer aumento nas unidades de resposta durante o aumento da concentração de 2dGuo, o que é consistente com o mecanismo enzimático proposto, que afirma que 2dGuo não consegue se ligar à MtPNP livre.

A dependência de  $k_{cat}$  e  $k_{cat}/K_M$  pelo pH foi determinada tanto para 2dGuo como para  $P_i$  para investigar a química ácido/base no modo de ação de MtPNP. Os perfis de pH [Figura 6 do Artigo 2 (Fig. 6)] foram do tipo *bell-shape* (em forma de sino), e os dados foram melhor ajustados à equação 5 do Artigo 2 (Eq. (5)), que descreve decréscimos nos valores dos parâmetros tanto na extremidade acídica quanto na extremidade básica, com inclinações de 1 e -1, respectivamente. Entretanto, cabe salientar que não foi possível coletar dados abaixo de pH 6,0 devido a instabilidade enzimática e, portanto, foi realizada apenas uma estimativa dos valores aparentes de  $pK_a$  na extremidade acídica. Os perfis de  $k_{cat}$  [Figura 6A do Artigo 2 (Fig. 6A)] e de  $k_{cat}/K_{2dGuo}$  [Figura 6C do Artigo 2 (Fig. 6C)] indicam que um grupo necessita estar protonado para que haja atividade catalítica ( $pK_a = 8.9 \pm 0.4$ ) e ligação de 2dGuo ( $pK_a = 8.5 \pm 0.3$ ). É provável que estes dois perfis estejam reportando o mesmo grupo. Uma vez que o nucleosídeo não apresenta grupos de dissociação com valores de  $pK_a$  no intervalo de pH testado, é provável que este grupo seja uma cadeia lateral de um aminoácido da proteína.

Uma comparação entre as estruturas tridimensionais de complexos ternários de MtPNP e PNP bovina em complexo com ImmH e  $P_i$  mostrou que os contatos em seus sítios catalíticos são similares, mas não são idênticos (SHI *et al.*, 2001). Ainda mais impressionante é o fato de que uma ligação de hidrogênio de 2,8 Å entre Tyr188 e o O5' de MtPNP que é impedida por uma fenilalanina nesta posição nas enzimas de mamíferos. Uma vez que a estrutura de MtPNP indica que a catálise auxiliada pelo substrato envolve a estabilização do oxocarbênio do estado de transição para a fosforólise de nucleosídeos a partir de uma interação com o grupo OH5', é tentador sugerir que o grupo hidroxil de Tyr188 é o grupamento ácido cuja deprotonação abole tanto a ligação quanto a atividade catalítica. Entretanto, existem outros grupos como o hidroxil de Tyr180 que participa da ligação de  $P_i$  e que também poderia ser responsável pela catálise ácido/base identificada nos perfis de pH. É interessante notar que Tyr188 é o único resíduo que interage diretamente com o inibidor ImmH ligado que não está conservado nas PNPs de mamíferos (SHI *et al.*, 2001), o que poderia ser explorado para o desenho de inibidores mais específicos por MtPNP.

A análise do perfil de  $k_{cat}/K_{P_i}$  indica que a deprotonação de um grupo com um valor aparente de  $pK_a$  de  $7.8 \pm 0.4$  abole a ligação de  $P_i$  [Figura 6B do Artigo 2 (Fig. 6B)]. A equação de Henderson-Hasselbalch prediz que a concentração da forma básica de  $P_i$  ( $pK = 7.2$ ) em pH 6,0 seria de aproximadamente 3 mM, o que está consideravelmente acima do valor de  $K_{P_i}$  (1,37 mM). A determinação das estruturas tridimensionais do complexo ternário MtPNP:ImmH: $P_i$  (SHI *et al.*, 2001) e do complexo binário MtPNP: $P_i$  (NOLASCO *et al.*, 2004) mostrou que as cadeias laterais de Arg88 e His90 formam ligações de hidrogênio com O1 do  $P_i$  ligado, enquanto Ser36 interage tanto com O4 quanto com O3 a partir de átomos da cadeia lateral e da cadeia polipeptídica. O

O<sub>2</sub> de P<sub>i</sub> é ancorado por uma ligação de hidrogênio com a cadeia lateral de Ser208 e uma ligação de hidrogênio mediada pela água com a amida peptídica de Ala120 e o grupo hidroxil de Tyr180. Portanto, é tentador sugerir que a cadeia lateral imidazol de His90 é o grupo cuja deprotonação abole a ligação e a catálise, visto que o nitrogênio com o átomo de hidrogênio na forma não-ionizada do anel imidazol poderia ser o eletrófilo ou doador de ligação de hidrogênio para a ligação do P<sub>i</sub> e/ou catálise. Contudo, análises por mutagênese sítio direcionada serão necessárias para que seja possível atribuir qualquer papel a este resíduo.

Os dados relativos à dependência de  $k_{cat}$  em função da temperatura, apresentados na [Figura 7 do Artigo 2 \(Fig. 7\)](#) foram ajustados à [equação 6 do Artigo 2 \(Eq. \(6\)\)](#), gerando um valor de 4,7 kcal mol<sup>-1</sup> para a energia de ativação da reação catalisada pela MtPNP. Cabe notar que o fator pré-exponencial ( $A$ ) foi considerado como independente de temperatura no intervalo de temperatura estudado. Portanto, o valor obtido representa a quantidade mínima de energia necessária para iniciar a reação química catalisada por MtPNP, visto que foi medida a atividade enzimática em concentrações saturantes de substratos. Além disso, a linearidade do gráfico de Arrhenius [[Figura 7 do Artigo 2 \(Fig. 7\)](#)] indica que não há mudança no passo limitante da velocidade dentro do intervalo de temperatura estudado.

Foram realizados estudos de efeitos isotópicos cinéticos de deutério de solvente para avaliar a contribuição da transferência de prótons do solvente a um passo na reação catalisada pela MtPNP [[Figura 8 do Artigo 2 \(Fig. 8\)](#)]. Efeitos isotópicos de solvente em  $V$  podem ser originados a partir de prótons intercambiáveis do solvente que são transferidos durante eventos subsequentes a formação do complexo ternário capaz de sofrer catálise, que incluem passos químicos, possíveis modificações conformacionais da enzima e a

liberação de produto. Efeitos isotópicos de solvente em  $V/K$  podem ser originados a partir de prótons intercambiáveis do solvente que são transferidos durante passos no mecanismo de reação desde a ligação dos substratos até o primeiro passo irreversível, geralmente considerado como a liberação do primeiro produto. Assim, efeitos isotópicos em  $V/K$  constituem uma combinação de efeitos isotópicos de ligação e catálise (SCHRAMM, 2007). O valor de  $1,6 \pm 0,1$  para os efeitos isotópicos cinéticos de deutério de solvente em  $V$  ( $^{D_2O}V$ ) indicam que qualquer transferência de prótons que ocorra após a formação do complexo ternário capaz de sofrer catálise contribui modestamente ao passo limitante da velocidade da reação. O valor de  $2,2 \pm 0,2$  para o efeito de solvente em  $V/K$  de  $P_i$  ( $^{D_2O}V/K_{P_i}$ ) sugere que os passos de transferência de prótons que ocorrem desde a ligação de  $P_i$  até a liberação do primeiro produto (R1P) contribuem para o passo limitante da velocidade da reação. Os valores diferentes para  $^{D_2O}V$  e  $^{D_2O}V/K_{P_i}$  sugerem que estes estão reportando em porções distintas da seqüência da reação.

Um efeito isotópico cinéticos de deutério de solvente inverso foi observado para  $V/K_{2dGuo}$  ( $0,5 \pm 0,1$ ), mostrando que qualquer transferência de próton que ocorra desde a ligação de 2dGuo ao complexo binário MtPNP: $P_i$  até a liberação de produto não ocorre em um passo limitante da velocidade de reação. Este resultado indica que a transferência de próton não domina as barreiras energéticas proeminentes na coordenação da reação, visto que as transferências em barreiras energéticas resultam em efeitos isotópicos cinéticos de deutério de solvente normais (MERKLER & SCHRAMM, 1993). Efeitos isotópicos cinéticos de solvente podem ser originados a partir da transferência de prótons de cisteína ou de água associada a metal (QUINN & SUTTON, 1991); entretanto, estes não podem ser responsáveis pelo efeito inverso observado, visto que MtPNP não é uma metaloenzima e nunca foi proposto que cisteína desempenhe qualquer papel na ligação (SHI *et al.*, 2001).

Ligações de hidrogênio que podem ser formadas/quebradas com baixa energia (*low barrier*) entre grupos aceptores e doadores com valores similares de  $pK_a$  também podem dar origem a efeitos isotópicos de solvente inversos (CLELAND, 1992). Entretanto, para que seja possível afirmar que este arranjo comprimido de ligações de hidrogênio entre grupos aceptores e doadores com valores similares de  $pK_a$  existam em MtPNP, será necessário determinar a estrutura tridimensional de MtPNP em complexo com 2dGuo. Uma mistura de transferência de próton e efeitos isotópicos inversos em equilíbrio também pode ser levada em consideração para interpretar alguns efeitos isotópicos de solvente inversos observados, dependendo das suas magnitudes e na condição de que efeitos de equilíbrio dominem (MERKLER & SCHRAMM, 1993). Isto implicaria em um efeito isotópico de solvente inverso em equilíbrio apenas na ligação de 2dGuo ao complexo binário MtPNP:P<sub>i</sub>, já que os efeitos em  $V$  e  $V/K_{P_i}$  são normais. Entretanto, fazem-se necessários mais resultados experimentais para confirmar ou descartar esta possibilidade. De qualquer forma, uma simples interpretação qualitativa permite afirmar que o efeito isotópico de solvente inverso em  $V/K_{2dGuo}$  indica que as ligações às marcações isotópicas são mais fortes no complexo ligado quando comparadas ao estado de reagente livre, o que indica que limitações intra ou intermoleculares fazem com que o movimento tenha um custo energético mais elevado no estado ligado.

Um inventário de prótons foi realizado na velocidade máxima da reação catalisada pela MtPNP para avaliar o número de prótons que são transferidos durante a fosforólise de 2dGuo [inserção na Figura 8A do Artigo 2 (inset in Fig. 8A)]. A relação linear entre  $V$  e a porcentagem em número de moles (*mole fraction*) de D<sub>2</sub>O indica que um único próton é transferido no passo que exhibe o efeito isotópico de solvente em  $V$ .

Medidas de formação de produto em estado pré-estacionário foram conduzidas para avaliar se a liberação de produto constitui o passo limitante da velocidade. O ajuste do decaimento exponencial simples à [equação 10 do Artigo 2 \(Eq. \(10\)\)](#) gerou um valor de  $8.91 \pm 0.05 \text{ s}^{-1}$  para a constante de velocidade aparente de primeira ordem para a formação de produto (caminho óptico de 1 cm), em acordo com o valor de  $k_{\text{cat}}$  nos experimentos de velocidade inicial. Não foi observada a presença de rápida formação de produto (*burst*) no sítio ativo da enzima [[Figura 9 do Artigo 2 \(Fig. 9\)](#)] quando uma alta concentração de MtPNP (20  $\mu\text{M}$ ) foi misturada a concentrações saturantes de 2dGuo (150  $\mu\text{M}$ ) e  $\text{P}_i$  (20 mM). Cabe notar que as concentrações de 2dGuo and  $\text{P}_i$  estavam acima dos respectivos valores de  $K_M$  e em excesso se comparadas à concentração de enzima, de forma que qualquer *burst* na formação de produto poderia ser confiantemente avaliada ([HIROMI, 1979; BASSO et al., 1995](#)). Entretanto, parte do sinal não pôde ser detectada por ter ocorrido no *dead time* do equipamento (1,37 ms). A mudança na absorbância que foi perdida no *dead time* corresponde a aproximadamente 23  $\mu\text{M}$  de formação de produto, o que indica a ocorrência de *burst* na formação de produto (dentro do *dead time* do equipamento), visto que a concentração de enzima na câmara de mistura é de 20  $\mu\text{M}$ . Assim, a cinética transiente de formação de produto por via enzimática indica que o passo limitante da velocidade para a reação catalisada pela enzima (*turnover*) em estado estacionário é a liberação de produto. Desta forma, é provável que o modesto efeito isotópico de solvente em  $V$  esteja relacionado à liberação do produto do que aos passos químicos ou possíveis mudanças conformacionais da enzima. Foi demonstrado que o mecanismo cinético em estado pré-estacionário da hidrólise de Ino pela PNP bovina inclui um *burst* na formação de produto, onde a liberação de Hx constitui o passo limitante da velocidade ([KLINE & SCHRAMM, 1992](#)).



## 6. CONCLUSÕES E PERSPECTIVAS

A TB constitui uma ameaça a saúde pública no mundo, acometendo milhões de pessoas há séculos. A geração de cepas resistentes às drogas instituídas no tratamento da doença exige que novas estratégias sejam adotadas no combate ao *M. tuberculosis*. A identificação de singularidades do patógeno é fundamental, pois pode revelar alvos potenciais para o desenho de drogas de ação seletiva contra o mesmo. A latência micobacteriana é um fenômeno fisiológico central e indispensável ao sucesso da infecção no hospedeiro humano. A validação de alvos moleculares ativos durante essa fase da doença representam, portanto, um avanço significativo em busca de uma quimioterapia mais eficiente contra a TB. Ainda, a caracterização do mecanismo cinético e químico de reações catalisadas por enzimas essenciais à viabilidade do bacilo representa uma excelente forma de abordagem neste sentido.

O tema principal desta Tese é o estudo da especificidade de substrato e do mecanismo cinético de MtPNP, uma enzima chave da rota de salvamento de purinas que, segundo a literatura, é essencial ao *M. tuberculosis* e está envolvida em seu processo de latência. Com o objetivo de aprofundar o conhecimento sobre esta enzima, o presente trabalho experimental pôde concluir que: MtPNP é mais específica por 2dGuo e não tem capacidade de fosforilar Ado; os dados de velocidade inicial, inibição por produto e ligação em equilíbrio indicam que MtPNP catalisa a fosforólise de 2dGuo a partir de um mecanismo cinético ordenado em estado estacionário do tipo bi bi, onde P<sub>1</sub> é o primeiro substrato a se ligar à enzima livre, seguido da ligação de 2dGuo para formar o complexo ternário cataliticamente competente, e R1P é o primeiro produto a se dissociar da enzima, seguido da dissociação de Gua; a dependência de  $k_{cat}$  e  $k_{cat}/K_{2dGuo}$  pelo pH indicou um

grupamento ácido como sendo essencial tanto para a catálise quanto para a ligação de 2dGuo; ainda, os perfis de pH mostraram que a deprotonação de um grupo abole a ligação de  $P_i$ , sugerindo que His90 possa estar envolvido na ligação e catálise; o inventário de prótons e os efeitos isotópicos de deutério de solvente em  $V$  e  $V/K$  indicam que uma única transferência de próton do solvente contribui modestamente ao passo limitante de velocidade; e, finalmente, os dados de cinética em estado pré-estacionário indicam que a liberação de produto é o passo limitante da velocidade para a reação catalisada pela MtPNP.

Espera-se que os resultados descritos neste trabalho possam contribuir para a melhor compreensão da biologia de *M. tuberculosis*, requisito fundamental para o desenho racional de drogas com ação seletiva contra sua viabilidade. Esta classe de compostos deve alvejar a infecção latente, além de ser ativa contra cepas do bacilo resistentes às drogas atualmente utilizadas no tratamento da doença. A curto prazo, dentre os experimentos que podem dar continuidade ao trabalho aqui descrito estão: efeitos isotópicos de solvente de ligação em equilíbrio, mutagênese sítio direcionada, cinética em estado pré-estacionário e o estudo de oligomerização em diferentes valores de pH.

## 7. REFERÊNCIAS BIBLIOGRÁFICAS

- AVARBOCK, D.; SALEM, J.; LI, L. S.; WANG, Z. M. & RUBIN, H. Cloning and characterization of a bifunctional RelA/SpoT homologue from *Mycobacterium tuberculosis*, *Gene* 233: 261-269, 1999.
- BARCLAY, R. & WHEELER, P. R. Metabolism of mycobacteria in tissues, *Biol. Mycobacter.* 3: 37-94, 1989.
- BASSO, L. A.; ENGEL, P. C. & WALMSLEY, A. R. The mechanism of substrate and coenzyme binding to clostridial glutamate dehydrogenase during reductive amination, *Eur. J. Biochem.* 234: 603-615, 1995.
- BASSO, L. A.; SANTOS, D. S.; SHI, W.; FURNEAUX, R. H.; TYLER, P. C.; SCHRAMM, V. L. & BLANCHARD, J. S. Purine nucleoside phosphorylase from *Mycobacterium tuberculosis*. Analysis of inhibition by a transition-state analogue and dissection by parts, *Biochemistry* 40: 8196-8203, 2001.
- BLOOM, B. R. & MURRAY, C. J. L. Tuberculosis: commentary on a reemergent killer, *Science* 257: 1055-1064, 1992.
- BLOOM, B. R. & SMALL, P. M. The evolving relation between humans and *Mycobacterium tuberculosis*, *N. Engl. J. Med.* 338: 677-678, 1998.
- BRAEKEN, K.; MORIS, M.; DANIELS, R.; VANDERLEYDEN, J. & MICHIELS J. New horizons for (p)ppGpp in bacterial and plant physiology, *Trends Microbiol.* 14(1): 45-54, 2006.
- BRENNAN, P. J. & NIKAIDO, H. The envelope of mycobacteria, *Annu. Rev. Biochem.* 64: 29-63, 1995.
- BRENNAN, P.J. Tuberculosis in the context of emerging and reemerging diseases, *FEMS Immunol. Med. Microbiol.* 18: 263-269, 1997.
- BZOWSKA, A.; KULIKOWSKA, E. & SHUGAR, D. Purine nucleoside phosphorylases: properties, functions, and clinical aspects, *Pharmacol. Ther.* 88: 349-425, 2000.
- CALMETTE, A. La vaccination préventive contre la tuberculose par BCG, 1er édition, Masson et Cie, Paris, 1927.
- CASHEL, M.; GENTRY, D. R.; HERNANDEZ, V. J. & VINELLA, D. The Stringent Response, in: *Escherichia coli and Salmonella: Cellular and Molecular Biology* (NEIDHARDT, F. C., Ed.), pp 1458-1496, ASM Press, Washington, DC, 1996.
- CASTIGLIONI, A. History of tuberculosis, Medical Life Press, New York, 1993.
- CAWS, M. & DROBNIOWSKI, F. A. Molecular techniques in the diagnosis of *Mycobacterium tuberculosis* and the detection of drug resistance, *Ann. NY Acad. Sci.* 953: 138-145, 2001.
- CENTERS FOR DISEASE CONTROL AND PREVENTION Emergence of *Mycobacterium tuberculosis* with extensive resistance to second-line drugs - worldwide, 2000-2004, *Morb. Mortal. Wkly. Rep.* 55: 301-305, 2006.
- CENTERS FOR DISEASE CONTROL AND PREVENTION Extensively drug-resistant tuberculosis - United States, 1993-2006, *Morb. Mortal. Wkly. Rep.* 56: 250-253, 2007.
- CHATTERJI, D. & OJHA, A. K. Revisiting the stringent response, ppGpp and starvation signaling, *Curr. Opin. Microbiol.* 4: 160-165, 2001.
- CLELAND, W. W. Determining the chemical mechanisms of enzyme-catalyzed reactions by kinetic studies, *Adv. Enzymol. Relat. Areas Mol. Biol.* 45: 273-387, 1977.
- CLELAND, W. W. Low-barrier hydrogen bonds and low fractionation factor bases in enzymatic reactions, *Biochemistry* 31: 317-319, 1992.

- COLDITZ, G. A.; BREWER, T. F.; BERKEY, C. S.; WILSON, M. E.; BURDICK, E.; FINEBERG, H. V. & MOSTELLER, F. Efficacy of BCG vaccine in the prevention of tuberculosis. Meta-analysis of the published literature, *JAMA* 271: 698-702, 1994.
- COLE, S. T.; BROSCHE, R.; PARKHILL, J.; GARNIER, T.; CHURCHER, C.; HARRIS, D.; GORDON, S. V.; EIGLMEIER, K.; GAS, S.; BARRY, C. E., III; TEKAIA, F.; BADCOCK, K.; BASHAM, D.; BROWN, D.; CHILLINGWORTH, T.; CONNOR, R.; DAVIES, R.; DEVLIN, K.; FELTWELL, T.; GENTLES, S.; HAMLIN, N.; HOLROYD, S.; HORNSBY, T.; JAGELS, K.; KROGH, A.; MCLEAN, J.; MOULE, S.; MURPHY, L.; OLIVER, K.; OSBORNE, J.; QUAIL, M. A.; RAJANDREAM, M. A.; ROGERS, J.; RUTTER, S.; SEEGER, K.; SKELTON, J.; SQUARES, R.; SQUARES, S.; SULSTON, J. E.; TAYLOR, K.; WHITEHEAD, S. & BARRELL, B. G. Deciphering the biology of *Mycobacterium tuberculosis* from the complete genome sequence, *Nature* 393: 537-544, 1998.
- DAHL, J. L.; KRAUS, C. N.; BOSHOFF, H. I.; DOAN, B.; FOLEY, K.; AVARBOCK, D.; KAPLAN, G.; MIZRAHI, V.; RUBIN, H. & BARRY, C. E., III The role of RelMtb-mediated adaptation to stationary phase in long-term persistence of *Mycobacterium tuberculosis* in mice, *Proc. Natl. Acad. Sci. USA* 100: 10026-10031, 2003.
- DANIEL, T. M. Captain of death: the story of tuberculosis, 1st edition, University of Rochester Press, New York, 1997.
- EHLERS, S. Immunity to tuberculosis: a delicate balance between protection and pathology, *FEMS Immunol. Med. Microbiol.* 23: 149-158, 1999.
- ENARSON, D. A. & MURRAY, J. F. Global epidemiology of tuberculosis, in: *Tuberculosis* (ROM, W. M. & GARAY, S., Eds.), pp 57-75, Little, Brown and Co., Boston, MA, 1996.
- ERION, M. D.; STOECKLER, J. D.; GUIDA, W. C.; WALTER, R. L. & EALICK, S. E. Purine nucleoside phosphorylase. 2. Catalytic mechanism, *Biochemistry* 36: 11735-11748, 1997.
- FARKAS, D. H. Molecular diagnostics: the best is yet to come, *Trends Mol. Med.* 8: 245, 2002.
- FÄTKENHEUER, G.; TAELEMAN, H.; LEPAGE, P.; SCHWENK, A. & WENZEL, R. The return of tuberculosis, *Diagn. Microbiol. Infect. Dis.* 34: 139-146, 1999.
- FISCHL, M. A.; DAIKOS, G. L.; UTTAMCHANDANI, R. B.; POBLETE, R. B.; MORENO, J. N.; REYES, R. R.; BOOTA, A. M.; THOMPSON, L. M.; CLEARY, T. J.; OLDHAM, S. A. Clinical presentation and outcome of patients with HIV infection and tuberculosis caused by multiple-drug-resistant bacilli, *Ann. Intern. Med.* 117: 184-190, 1992.
- GHANEM, M.; SAEN-OON, S.; ZHADIN, N.; WING, C.; CAHILL, S. M.; SCHWARTZ, S. D.; CALLENDER, R. & SCHRAMM, V. L. Tryptophan-free human PNP reveals catalytic site interactions, *Biochemistry* 47: 3202-3215, 2008.
- GILBERT, G. L. Molecular diagnostics in infectious diseases and public health microbiology: cottage industry to postgenomics, *Trends Mol. Med.* 8: 280-287, 2002.
- GLICKMAN, M. S. & JACOBS, W. R., JR Microbial pathogenesis of *Mycobacterium tuberculosis*: dawn of a discipline, *Cell* 104: 477-485, 2001.
- GRANGE, J. M.; STANFORD, J. L. & ROOK, G. A. Tuberculosis and cancer: parallels in host responses and therapeutic approaches?, *Lancet* 345: 1350-1352, 1995.

- HENNEN, W. J. & WONG, C. -H. A new method for the enzymatic synthesis of nucleosides using purine nucleoside phosphorylase, *J. Org. Chem.* 54: 4692-4695, 1989.
- HENRI, V. Lois Générales de l'Action des Diástases, Hermann, Paris, 1903.
- HESS, J. & KAUFMANN, S. H. Development of novel tuberculosis vaccines. *C. R. Acad. Sci. III* 322: 953-958, 1999.
- HILL, A. V. The Combinations of Haemoglobin with Oxygen and with Carbon Monoxide. I., *Biochem. J.* 7: 471-480, 1913.
- HIROMI, K. Analysis of fast enzyme reactions: transient kinetics, in: *Kinetics of fast enzyme reactions*, pp 187-253, Kodansha Ltd, Tokyo, 1979.
- JAGIRDAR, J. & ZAGZAG, D. Pathology and insights into pathogenesis of tuberculosis, in: *Tuberculosis* (ROM, W. M. & GARAY, S., Eds.), pp 467-482, Little, Brown and Co., Boston, MA, 1996.
- JARLIER, V. & NIKAIDO, H. Mycobacterial cell wall: structure and role in natural resistance to antibiotics, *FEMS Microbiol. Lett.* 123: 11-18, 1994.
- JASSAL, M. & BISHAI, W. R. Extensively drug-resistant tuberculosis, *Lancet Infect. Dis.* 9(1): 19-30, 2009.
- JENSEN, K. F. Two purine nucleoside phosphorylases in *Bacillus subtilis*. Purification and some properties of the adenosine-specific phosphorylase, *Biochim. Biophys. Acta* 525: 346-356, 1978.
- KALCKAR, H. M. Differential spectrophotometry of purine compounds by means of specific enzymes. I. Determination of hydroxypurine compounds, *J. Biol. Chem.* 167: 429-443, 1947.
- KLINE, P. C. & SCHRAMM, V. L. Purine nucleoside phosphorylase. Catalytic mechanism and transition-state analysis of the arsenolysis reaction, *Biochemistry* 32: 13212-13219, 1993.
- KLINE, P. C. & SCHRAMM, V. L. Purine nucleoside phosphorylase. Inosine hydrolysis, tight binding of the hypoxanthine intermediate, and third-the-sites reactivity, *Biochemistry* 31: 5964-5973, 1992.
- KOCH, R. The aetiology of tuberculosis, *Berlin Klin. Wochenschr.* 19: 221-230, 1882.
- KULIKOWSKA, E.; BZOWSKA, A.; WIERZCHOWSKI, J. & SHUGAR, D. Properties of two unusual, and fluorescent, substrates of purine-nucleoside phosphorylase: 7-methylguanosine and 7-methylinosine, *Biochim. Biophys. Acta* 874: 355-363, 1986.
- LABIDI, A. H.; ESTES, R. C.; DAVID, H. L. & BOLLON, A. P. Mycobacterium recombinant vaccines, *Tunis. Med.* 79: 65-81, 2001.
- LINEWEAVER, H. & BURK, D. The Determination of Enzyme Dissociation Constants, *J. Am. Chem. Soc.* 56: 658-666, 1934.
- MAGNUSSON, L. U.; FAREWELL, A. & NYSTRÖM, T. ppGpp: a global regulator in *Escherichia coli*, *Trends Microbiol.* 13(5): 236-42, 2005.
- MAO, C.; COOK, W. J.; ZHOU, M.; FEDEROV, A. A.; ALMO, S. C. & EALICK, S. E. Calf spleen purine nucleoside phosphorylase complexed with substrates and substrate analogues, *Biochemistry* 37: 7135-7146, 1998.
- MERKLER, D. J. & SCHRAMM, V. L. Catalytic mechanism of yeast adenosine 5'-monophosphate deaminase. Zinc content, substrate specificity, pH studies, and solvent isotope effects, *Biochemistry* 32: 5792-5799, 1993.
- MICHAELIS, L. & MENTEN, M. L. The kinetics of invertase activity, *Biochem. Zeitschr.* 49: 333-369, 1913.

- NARAIN, J. P.; RAVIGLIONE, M. C. & KOCHI, A. HIV-associated tuberculosis in developing countries: epidemiology and strategies for prevention, *Tuber. Lung Dis.* 73: 311-321, 1992.
- NOLAN, C. M. Nosocomial multidrug-resistant tuberculosis: global spread of the third epidemic, *J. Infect. Dis.* 176: 748-751, 1997.
- NOLASCO, D. O.; CANDURI, F.; PEREIRA, J. H.; CORTINÓZ, J. R.; PALMA, M. S.; OLIVEIRA, J. S.; BASSO, L. A.; DE AZEVEDO, W. F., JR & SANTOS, D. S. Crystallographic structure of PNP from *Mycobacterium tuberculosis* at 1.9 Å resolution, *Biochem. Biophys. Res. Commun.* 324: 789-794, 2004.
- NSB EDITORIAL COMMENT Taming tuberculosis-again, *Nat. Struct. Biol.* 7: 87-88, 2000.
- OJHA, A. K.; MUKHERJEE, T. K. & CHATTERJI, D. High intracellular level of guanosine tetraphosphate in *Mycobacterium smegmatis* changes the morphology of the bacterium, *Infect. Immun.* 68: 4084-4091, 2000.
- ORME, I. M. The search for new vaccines against tuberculosis, *J. Leukoc. Biol.* 70: 1-10, 2001.
- ORME, I. M.; MCMURRAY, D. N. & BELISLE, J. T. Tuberculosis vaccine development: recent progress, *Trends Microbiol.* 9: 115-118, 2001.
- PABLOS-MENDEZ, A.; RAVIGLIONE, M. C.; LASZLO, A.; BINKIN, N.; RIEDER, H. L.; BUSTREO, F.; COHN, D. L.; LAMBREGTS-VAN WEEZENBEEK, C. S.; KIM, S. J.; CHAULET, P. & NUNN, P. Global surveillance for antituberculosis-drug resistance, 1994-1997, *N. Engl. J. Med.* 338: 1641-1649, 1998.
- PARKER, W. B. & LONG, M. C. Purine metabolism in *Mycobacterium tuberculosis* as a target for drug development, *Curr. Pharm. Des.* 13(6): 599-608, 2007.
- PARKER, W. B.; BARROW, E. W.; ALLAN, P. W.; SHADDIX, S. C.; LONG, M. C.; BARROW, W. W.; BANSAL, N. & MADDRY, J. A. Metabolism of 2-methyladenosine in *Mycobacterium tuberculosis*, *Tuberculosis (Edinb)* 84: 327-336, 2004.
- PARKS, R. E., JR & AGARWAL, R. P. Purine Nucleoside Phosphorylase, in: *The Enzymes* (BOYER, P. D., Ed.), 3rd edition, pp 483-514, Academic Press, New York, 1972.
- PARRISH, N. M.; DICK, J. D. & BISHAI, W. R. Mechanisms of latency in *Mycobacterium tuberculosis*, *Trends Microbiol.* 6: 107-112, 1998.
- PASQUALOTO, K. F. M. & FERREIRA, E. I. An approach for the rational design of new antituberculosis agents, *Curr. Drug Targets* 2: 427-437, 2001.
- PETRINI, B. & HOFFNER, S. Drug-resistant and multidrug-resistant tubercle bacilli, *Int. J. Antimicrob. Agents* 13: 93-97, 1999.
- PORTER, D. J. Purine nucleoside phosphorylase. Kinetic mechanism of the enzyme from calf spleen, *J. Biol. Chem.* 267: 7342-7351, 1992.
- PRIMM, T. P.; ANDERSEN, S. J.; MIZRAHI, V.; AVARBOCK, D.; RUBIN, H. & BARRY, C. E., III The stringent response of *Mycobacterium tuberculosis* is required for long-term survival, *J. Bacteriol.* 182: 4889-4898, 2000.
- QUINN, D. M. & SUTTON, L. D. Theoretical basis and mechanistic utility of solvent isotope effects, in: *Enzyme Mechanism from Solvent Isotope Effects* (COOK, P. F., Ed.), 1st edition, pp 73-126, CRC Press, Boca Raton, FL, 1991.
- RILEY, L. W. Drug-resistant tuberculosis, *Clin. Infect. Dis.* 17: S442-446, 1993.
- ROBERTSON, J. G. Enzymes as a special class of therapeutic target: clinical drugs and modes of action, *Curr. Opin. Struct. Biol.* 17: 674-679, 2007.

- RUFFINO-NETTO, A. Tuberculosis: the neglected calamity, *Rev. Soc. Bras. Med. Trop.* 35: 51-58, 2002.
- SCHRAMM, V. L. Binding isotope effects: boon and bane, *Curr. Opin. Chem. Biol.* 11: 529-536, 2007.
- SCHROEDER, E. K.; DE SOUZA, N.; SANTOS, D. S.; BLANCHARD, J. S. & BASSO, L. A. Drugs that inhibit mycolic acid biosynthesis in *Mycobacterium tuberculosis*, *Curr. Pharm. Biotechnol.* 3(3): 197-225, 2002.
- SEGEL, I. H. Ordered Bi Bi System, in: *Enzyme Kinetics. Behavior and Analysis of Rapid Equilibrium and Steady-State Enzyme Systems*, pp 560-590, John Wiley and Sons, Inc., New York, 1975.
- SHI, W.; BASSO, L. A.; SANTOS, D. S.; TYLER, P. C.; FURNEAUX, R. H.; BLANCHARD, J. S.; ALMO, S. C. & SCHRAMM, V. L. Structures of purine nucleoside phosphorylase from *Mycobacterium tuberculosis* in complexes with immucillin-H and its pieces, *Biochemistry* 40: 8204-8215, 2001.
- SILVA, R. G.; PEREIRA, J. H.; CANDURI, F.; DE AZEVEDO, W. F., JR; BASSO, L. A. & SANTOS, D. S. Kinetics and crystal structure of human purine nucleoside phosphorylase in complex with 7-methyl-6-thio-guanosine, *Arch. Biochem. Biophys.* 442: 49-58, 2005.
- STOECKLER, J. D. Purine nucleoside phosphorylase: a target for chemotherapy, in: *Developments in Cancer Chemotherapy* (GLAZER, R. J., Ed.), pp 35-60, CRC Press, Boca Raton, FL, 1984.
- STOECKLER, J. D.; CAMBOR, C. & PARKS, R. E., JR Human erythrocytic purine nucleoside phosphorylase: reaction with sugar-modified nucleoside substrates, *Biochemistry* 19(1): 102-107, 1980.
- STOECKLER, J. D.; POIROT, A. F.; SMITH, R. M.; PARKS, R. E., JR; EALICK, S. E.; TAKABAYASHI, K. & ERION, M. D. Purine nucleoside phosphorylase. 3. Reversal of purine base specificity by site-directed mutagenesis, *Biochemistry* 36: 11749-11756, 1997.
- SWARTZ, M. N. Impact of antimicrobial agents and chemotherapy from 1972 to 1998, *Antimicrob. Agents Chemother.* 44: 2009-2016, 2000.
- TAYLOR RINGIA, E. A.; TYLER, P. C.; EVANS, G. B.; FURNEAUX, R. H.; MURKIN, A. S. & SCHRAMM, V. L. Transition state analogue discrimination by related purine nucleoside phosphorylases, *J. Am. Chem. Soc.* 128: 7126-7127, 2006.
- TEBBE, J.; BZOWSKA, A.; WIELGUS-KUTROWSKA, B.; SCHRÖDER, W.; KAZIMIERCZUK, Z.; SHUGAR, D.; SAENGER, W. & KOELLNER, G. Crystal structure of the purine nucleoside phosphorylase (PNP) from *Cellulomonas sp.* and its implication for the mechanism of trimeric PNPs, *J. Mol. Biol.* 294: 1239-1255, 1999.
- TELENTI, A. & ISEMAN, M. Drug-resistant tuberculosis: what do we do now?, *Drugs* 59: 171-179, 2000.
- TRAUT, T. W. Physiological concentrations of purines and pyrimidines, *Mol. Cell. Biochem.* 140: 1-22, 1994.
- VILLEMEN, J. A. C. R. Acad. Sci. 61: 1012, 1865.
- WEBB, M. R. A continuous spectrophotometric assay for inorganic phosphate and for measuring phosphate release kinetics in biological systems, *Proc. Natl. Acad. Sci. USA* 89: 4884-4887, 1992.
- WEBER, G. Energetics of ligand binding to proteins, *Adv. Protein Chem.* 29: 1-83, 1975.

- WHEELER, P. R. Enzymes for purine synthesis and scavenging in pathogenic mycobacteria and their distribution in *Mycobacterium leprae*, *J. Gen. Microbiol.*; 133: 3013-3018, 1987.
- WORLD HEALTH ORGANIZATION Global Tuberculosis Control, WHO Report 1998, Geneva, Switzerland, WHO/TB/98.237, 1998.
- YOUNG, D. B. Blueprint for the white plague, *Nature* 393: 515-516, 1998.
- YOUNG, D. Letting the genome out of the bottle: prospects for new drug development, *Ann. NY Acad. Sci.* 953: 146-150, 2001.
- ZALKIN, H. & NYGAARD, P. Biosynthesis of purine nucleotides, in: *Escherichia coli and Salmonella: Cellular and Molecular Biology* (NEIDHARDT, F. C., Ed.), 2nd edition, ASM Press, Washington, DC, 1996.
- ZHENG, H.; LU, L.; WANG, B.; PU, S.; ZHANG, X.; ZHU, G.; SHI, W.; ZHANG, L.; WANG, H.; WANG, S.; ZHAO, G. & ZHANG, Y. Genetic basis of virulence attenuation revealed by comparative genomic analysis of *Mycobacterium tuberculosis* strain H37Ra versus H37Rv, *PLoS ONE* 3, e2375, 2008.
- ZIMMERMAN, T. P.; GERSTEN, N. B.; ROSS, A. F. & MIECH, R. P. Adenine as substrate for purine nucleoside phosphorylase, *Can. J. Biochem.* 49, 1050-1054, 1971.



## **8. APÊNDICES**

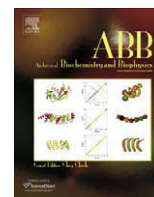
Nesta seção estão apresentados, como Apêndices, todos os trabalhos que foram desenvolvidos durante o período de doutorado em atividades realizadas pelo presente autor em projetos paralelos, não fazendo, portanto, parte do corpo principal da Tese.

**8.1. ARTIGO 3:** TIMMERS, L. F.; CACERES, R. A.; VIVAN, A. L.; GAVA, L. M.; DIAS, R.; DUCATI, R. G.; BASSO, L. A.; SANTOS, D. S. & DE AZEVEDO, W. F., JR  
Structural studies of human purine nucleoside phosphorylase: towards a new specific empirical scoring function. *Arch. Biochem. Biophys.*, 479(1): 28-38, 2008.



Contents lists available at ScienceDirect

## Archives of Biochemistry and Biophysics

journal homepage: [www.elsevier.com/locate/yabbi](http://www.elsevier.com/locate/yabbi)

## Structural studies of human purine nucleoside phosphorylase: Towards a new specific empirical scoring function

Luis Fernando Saraiva Macedo Timmers<sup>a,1</sup>, Rafael Andrade Caceres<sup>a,b,1</sup>, Ana Luiza Vivan<sup>a</sup>, Lisandra Marques Gava<sup>c</sup>, Raquel Dias<sup>a</sup>, Rodrigo Gay Ducati<sup>d,e</sup>, Luiz Augusto Basso<sup>b,e</sup>, Diogenes Santiago Santos<sup>b,e,\*</sup>, Walter Filgueira de Azevedo Jr.<sup>a,b,\*</sup>

<sup>a</sup> Faculdade de Biociências, Laboratório de Bioquímica Estrutural, Pontifícia Universidade Católica do Rio Grande do Sul, Porto Alegre, RS, Brazil

<sup>b</sup> Programa de Pós-Graduação em Medicina e Ciências da Saúde, Pontifícia Universidade Católica do Rio Grande do Sul, Porto Alegre, RS, Brazil

<sup>c</sup> Universidade Estadual de Campinas, Campinas, SP, Brazil

<sup>d</sup> Programa de Pós-Graduação em Biologia Celular e Molecular, Universidade Federal do Rio Grande do Sul, Porto Alegre, RS, Brazil

<sup>e</sup> Centro de Pesquisas em Biologia Molecular e Funcional, Instituto de Pesquisas Biomédicas, Pontifícia Universidade Católica do Rio Grande do Sul, Porto Alegre, RS, Brazil

## ARTICLE INFO

## Article history:

Received 23 May 2008

and in revised form 20 August 2008

Available online 30 August 2008

## Keywords:

Empirical scoring functions

Docking

Virtual screening

Quinazolinone

Enzymology

Molecular dynamics

## ABSTRACT

Human purine nucleoside phosphorylase (*HsPNP*) is a target for inhibitor development aiming at T-cell immune response modulation. In this work, we report the development of a new set of empirical scoring functions and its application to evaluate binding affinities and docking results. To test these new functions, we solved the structure of *HsPNP* and 2-mercapto-4(3H)-quinazolinone (*HsPNP*:MQU) binary complex at 2.7 Å resolution using synchrotron radiation, and used these functions to predict ligand position obtained in docking simulations. We also employed molecular dynamics simulations to analyze *HsPNP* in two conditions, as apoenzyme and in the binary complex form, in order to assess the structural features responsible for stability. Analysis of the structural differences between systems provides explanation for inhibitor binding. The use of these scoring functions to evaluate binding affinities and molecular docking results may be used to guide future efforts on virtual screening focused on *HsPNP*.

© 2008 Elsevier Inc. All rights reserved.

Purine nucleoside phosphorylase (PNP)<sup>2</sup> (EC 2.4.2.1) is a key enzyme of the purine salvage pathway, responsible for the inter-conversion between (deoxy)nucleosides and bases, which in turn may be converted to uric acid for excretion or reused in nucleic acid biosynthesis [1]. This enzyme catalyzes the reversible cleavage, in the presence of inorganic phosphate (P<sub>i</sub>), of *N*-glycosidic bonds of purine nucleosides and deoxynucleosides, except adenosine, to generate alpha-ribose 1-phosphate and the corresponding purine base [2]. The reaction proceeds with inversion of configuration, from beta-nucleosides to alpha-ribose 1-phosphate [3].

\* Corresponding authors. Address: Centro de Pesquisas em Biologia Molecular e Funcional, PUCRS, Av. Ipiranga, 6681 Prédio, 92A, Porto Alegre 90619-900, RS, Brazil. Fax: +55 51 33203629.

E-mail addresses: [diogenes@pucrs.br](mailto:diogenes@pucrs.br) (D.S. Santos), [walter.junior@pucrs.br](mailto:walter.junior@pucrs.br) (W.F. de Azevedo).

<sup>1</sup> L.F.S.M.T. and R.A.C. contributed equally to this work.

<sup>2</sup> Abbreviations used: PNP, purine nucleoside phosphorylase; P<sub>i</sub>, inorganic phosphate; *HsPNP*, homo sapiens PNP; MHC, major histocompatibility complex; dGuo, deoxyguanosine; dGTP, deoxyguanosine triphosphate; dCyK, deoxycytidine kinase; dCTP, deoxycytidine triphosphate; dGMP, deoxyguanosine monophosphate; NP-I, class I of nucleoside phosphorylases; MQU, 2-mercapto-4(3H)-quinazolinone; MD, molecular dynamics; SPC/E, simple point charge extended; RMSD, root mean-square deviation; RMSF, root mean-square fluctuation; RDS, rigid-body docking simulations; HB, hydrogen bonds; DMSO, dimethyl sulfoxide.

0003-9861/\$ - see front matter © 2008 Elsevier Inc. All rights reserved.

doi:10.1016/j.ab.2008.08.015

Interest in this enzyme stems from the discovery that mutations in the locus encoding for *Homo sapiens* PNP (*HsPNP*) cause T-cell impairment in human beings, though keeping normal levels of B-cells [4,5]. The activation of helper T-cells requires that they recognize a complex formed between an antigen and a class II MHC (Major Histocompatibility Complex) protein on the surface of antigen-presenting cells with appropriate costimulation. These results in interleukin-2 release which, in turn, leads to T-cell clonal expansion with activity against cells exhibiting the stimulatory antigen. However, most naive T-cells receive no antigenic signal and undergo apoptosis. Cellular nucleic acids from the apoptosed cells are recycled. Naive T-cells have the ability to transport and phosphorylate deoxyguanosine (dGuo) to deoxyguanosine triphosphate (dGTP), which accumulates relative to normal cells [6]. There are two enzymes that utilize dGuo as a substrate in humans, PNP and deoxycytidine kinase (dCyK). PNP catalyzes the phosphorolysis of dGuo to guanine and ribose 1-phosphate. The normal role of dCyK in dividing T-cells is the salvage of deoxycytidine to form deoxycytidine triphosphate (dCTP), and dGuo predominantly undergoes phosphorolysis by PNP because dGuo has a higher affinity for PNP than for dCyK [7]. When dGuo accumulates beyond normal levels, dCyK catalyzes the conversion of dGuo to deoxyguanosine monophosphate (dGMP), which is then converted to dGTP. Accumulated dGTP inhibits ribonucleotide reductase, thus

preventing the conversion of ribonucleoside diphosphates to corresponding deoxyribonucleoside diphosphates. Depletion of deoxyribonucleotides ultimately results in the inhibition of DNA synthesis and cell replication, leading to suppression of proliferation of immature T-cells [8–10]. Inhibition of PNP enzyme activity leads to an increase in dGuo concentration that will, in turn, trigger that cascade of events ultimately leading to inhibition of cell proliferation [6]. Accordingly, HsPNP has been proposed as a target for drug design, aiming the enzyme inhibition for treatment of immunological disorders [11], which include type IV autoimmune disorders such as rheumatoid arthritis, psoriasis, inflammatory bowel disorders, and multiple sclerosis [12], and T-cell proliferative disorders such as organ transplant rejection, T-cell lymphoma, and T-cell leukemia [6]. Moreover, PNP inhibitors can also be used to avoid cleavage of anticancer and antiviral drugs, since many of these drugs mimic natural purine nucleosides and can thereby be cleaved by HsPNP before accomplishing their therapeutic role [13,14]. HsPNP is classified, based on substrate specificity and structural characteristics, as belonging to the class I of Nucleoside Phosphorylases (NP-I) [15]. The crystallographic structure is a trimer and analysis of HsPNP in solution, using SAXS, confirmed that the crystallographic trimer is conserved in solution [16,17].

The 2-mercapto-4(3H)-quinazolinone (MQU, Fig. 1) is a derivative of quinazolinone. Quinazolinones are good lead compounds for design of inhibitors of human erythrocyte PNP. Quinazolinone-based inhibitors irreversibly inactivate human erythrocyte PNP, probably by reductive addition and cross-linking of Glu201 and Glu259, both of which are active site residues [18].

In the present work, we describe the crystallographic structure of HsPNP in complex with MQU, which was resolved at 2.7 Å, using recombinant HsPNP and synchrotron radiation. We also present molecular dynamics simulations to give detailed information on the dynamics properties of the crystallographic structures of HsPNP in apo form and in complex with MQU. The analysis of molecular dynamics trajectory indicated that functionally an important motif has both a very stable structure and tertiary arrangement. In addition, this structural data together with previously published crystallographic structures of HsPNP were employed to propose a set of specific empirical scoring functions. These scoring functions were able to estimate  $pK_d$  and also identify the best results obtained from molecular docking, which provides for the first time a set of reliable and specific empirical scoring functions, which were developed for analysis of interaction of ligands with HsPNP. In addition, experimental determination of  $K_d$  for MQU confirmed the predicted low affinity of this ligand for HsPNP.

## Materials and methods

### Crystallization and data collection

Recombinant HsPNP was expressed and purified as previously described [19]. HsPNP:MQU was crystallized using the experimental conditions described elsewhere [20,21]. Rhombohedral-shaped

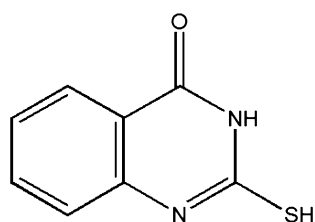


Fig. 1. Molecular formula of 2-mercapto-4(3H)-quinazolinone.

crystals with dimensions up to 0.5 mm were obtained overnight. In brief, a PNP solution was concentrated to 13 mg mL<sup>-1</sup> potassium phosphate buffer (pH 7.1) and incubated in presence of 0.6 mM ligand (Sigma). Hanging drops were equilibrated by vapor diffusion at 25 °C against reservoir containing 17% saturated ammonium sulfate solution in 0.05 M citrate buffer (pH 5.3).

In order to increase the resolution of the HsPNP:MQU crystal, data were collected from a flash-cooled crystal at 100 K. Prior to flash cooling, up to 50% by volume of glycerol was added to the crystallization drop. X-ray diffraction data were collected at a wavelength of 1.431 Å using the Synchrotron Radiation Source (Station PCr, Laboratório Nacional de Luz Síncrotron, LNLS, Campinas, SP, Brazil) and a CCD detector (MARCCD) with an exposure time of 30 s per image at a crystal to detector distance of 120 mm. X-ray diffraction data were processed to 2.7 Å resolution using the program MOSFLM and scaled with the program SCALA [22].

Upon cooling the cell parameters shrank from  $a = b = 142.90$  Å, and  $c = 165.20$  Å to  $a = b = 138.66$  Å, and  $c = 159.37$  Å. Volume of the unit cell for HsPNP:MQU binary complex was  $2.65 \times 10^{-6}$  Å<sup>3</sup>, which is in accordance with one monomer in the asymmetric unit with a  $V_m$  value of  $4.70$  Å<sup>3</sup> Da<sup>-1</sup> (the values for unit cell and  $V_m$  were calculated with the Matthews Probabilities online [23]). Assuming a value  $0.26$  cm<sup>3</sup> g<sup>-1</sup> for the protein partial specific volume, the calculated solvent content in the crystal is 74% and the calculated crystal density is  $1.10$  g cm<sup>-3</sup>.

### Crystal structure

The crystal structure of the HsPNP:MQU was determined by standard molecular replacement methods using the program AMoRe [24], incorporated in the CCP4 program package [22], using as search model the structure of HsPNP apoenzyme (PDB accession code: 1M73) [25,26]. Structure refinement was performed using REFMAC [22]. The atomic positions obtained from molecular replacement were used to initiate the crystallographic refinement. The overall stereochemical quality of the final model for HsPNP:MQU complex was assessed by the program PARMODEL [27]. The trimeric structure and atomic models were superposed using the program LSQKAB from CCP4 [22].

### Molecular dynamics simulation protocol

HsPNP is biologically active as a trimer. Hence, to better understand HsPNP structural and dynamics features, molecular dynamics (MD) simulation was carried out. The trimeric structure of HsPNP was built following the crystallographic HsPNP (PDB access code: 1PF7). Attempts to simulate the dynamics behavior of HsPNP as a monomeric system generated unreliable results, since Phe159 from the adjacent monomer is part of the active site, as previously described [28].

MD simulations were performed with the GROMACS [29] package using the Gromos 96.1 (53A6) [30] force field. The MQU topology was generated with the PRODRG program [31]. Accurate force fields are essential for reproducing the conformational and dynamic behavior of condensed-phase systems. Gromos 96.1 force fields are well parameterized for proteins but the parameters for small molecules are still limited for simulation of more complicated biological systems. Thus, for the atomic charges in the MQU molecules GAMESS [32] was employed, and the ligand (MQU) was submitted to single-point *ab initio* calculations at RHF 6-31G\* level in order to obtain Lowdin derived charges. Manipulation of structures was performed with Pymol program [33]. The first system was composed by apoenzyme HsPNP (system A) and the second by HsPNP enzyme and MQU ligand (system B). The simulations for these systems were performed by a time period of 4 ns.

In both systems were added  $\text{Na}^+$  counter ions (24  $\text{Na}^+$  ions on the system A and twenty seven  $\text{Na}^+$  ions on the system B) using Genion Program of the GROMACS simulation suite to neutralize the negative charge density of these systems.

Each structure was placed in the center of a truncated cubic box filled with Simple Point Charge Extended (SPC/E) water molecules [34], containing 42265 water molecules for the system A and 40855 for the system B. The initial simulation cell dimensions were  $89.52 \text{ \AA} \times 85.86 \text{ \AA} \times 49.24 \text{ \AA}$  for the system A and  $89.78 \text{ \AA} \times 84.11 \text{ \AA} \times 50.13 \text{ \AA}$  for the system B, and had the protein solvated by a layer of water molecules of at least  $10 \text{ \AA}$  in all directions in both systems. During the simulations, bond lengths within the proteins were constrained by using LINCS algorithm [35]. The SETTLE algorithm was used to constrain the geometry of water molecules [36]. In the MD simulation protocol, the binary complex, ions, and water molecules were first subjected to 1500 steps of energy minimization by steepest descent followed by 1500 steps of conjugate gradient to remove close van der Waals contacts. The systems were then submitted to a short molecular dynamic without restraints. The temperature of the system was then increased from 50 K to 300 K in 5 steps (50 K to 100 K, 100 K to 150 K, 150 K to 200 K, 200 K to 250 K, and 250 K to 300 K), and velocities at each step were reassigned according to the Maxwell–Boltzmann distribution at that temperature and equilibrated for 10 ps except the last part of thermalization phase, which was for 40 ps. Energy minimization and MD simulations were carried out under periodic boundary conditions. The simulation was computed in the NPT ensemble at 300 K with the Berendsen temperature coupling and constant pressure of 1 atm with isotropic molecule-based scaling [37]. The LINCS algorithm, with  $10^{-5} \text{ \AA}$  tolerance, was applied to fix all bonds containing a hydrogen atom, allowing the use of a time step of 2.0 fs in the integration of the equations of motion. No extra restraints were applied after the equilibration phase. The electrostatic interactions between non-ligand atoms were evaluated by the particle-mesh Ewald method [38] with a charge grid spacing of  $\sim 1.0 \text{ \AA}$  and the charge grid was interpolated on a cubic grid with the direct sum tolerance set to  $1.0 \times 10^{-5}$ . The Lennard-Jones interactions were evaluated using a  $9.0 \text{ \AA}$  atom-based cutoff [39].

All analysis were performed on the ensemble of system configurations extracted at 0.5-ps time intervals from the simulation, and MD trajectory collection was initiated after 1 ns of dynamics to guarantee a completely equilibrated evolution. The MD simulation and analysis of results were performed in a personal computer with an Intel Core 2 Duo E6300 CPU of 1.86 GHz clock speed and with 4 Gb of RAM.

The convergence of the different simulations were analyzed in terms of the secondary structure, root mean-square deviation (RMSD) from the initial model structures, and root mean-square fluctuation (RMSF) to estimate the B-factor. For the B-factor calculation, the RMSFs were calculated relative to the last 2 ns averaged backbone structures, and all coordinate frames from the trajectories were first superimposed on the initial conformation to remove any effect of overall translation and rotation. Atomic isotropic B-factors were calculated from trajectories using the following equation:

$$B - \text{factor}_i = (8\pi^2/3)(\langle r_i^2 \rangle - \langle r_i \rangle^2) \quad (1)$$

where  $(\langle r_i^2 \rangle - \langle r_i \rangle^2)$  is the mean-square positional fluctuation of atom  $i$  [40,41].

#### Molecular docking protocol

Rigid-body docking simulations (RDS) were performed using ZDOCK 2.3 [42], which is used for the prediction of the three-

dimensional structure of a protein–protein complex from the coordinates of its component structures; it is classified as bound docking or unbound docking [43]. This method is important for the development of new drugs because RDS is based on three basic tasks, which are: (1) characterization of the binding site; (2) positioning of the ligand into the binding site; and (3) evaluating the strength of interaction for a specific ligand–receptor complex [44].

The RDS was performed with 13 different compounds for HsPNP, and these ligands were built using a molecular mechanics force field and minimized with conjugated gradient algorithm method for 1000 steps with RMS Gradient  $0.1 \text{ kcal \AA}^{-1} \text{ mol}^{-1}$ . These docked structures, together with 2 crystallographic structures (PNP in complex with either acyclovir (1PWY) or inosine (1RCT)) compose our test set to be used to validate a specific empirical scoring function to estimate ligand-binding affinities. For docking of the present crystallographic structure before the RDS the ligand was rotated  $180^\circ$  along  $z$ -axis and translated 1 (fractional coordinates) along the three axis, using the program LSQKAB [22]. This docking simulation was carried out in order to test the ability of our new empirical scoring function to evaluate docking results. A total of 99 docked structures were generated, and RMSDs were calculated against the crystallographic structure (HsPNP:MQU).

#### Evaluation of binding affinity

The analysis of the interaction between a ligand and a protein target is still an important scientific tool to predict new potential drugs. The affinity and specificity between a ligand and its protein target depends on several structural features such as directional hydrogen bonds (HB) and ionic interactions, as well as on shape complementarity of the contact surfaces of both partners [45]. Attempts to use the empirical scoring functions available in the program XSCORE (HPScore, HMScore and HSScore) [46] and program Drugscore [47] to evaluate the binding affinity of the ligands against HsPNP generated unsatisfactory results, with low correlation coefficient between experimental and predicted affinities.

Therefore, in order to improve the results for computational determined binding affinities, we developed a novel empirical scoring function [48]. In spite of many problems in the understanding of the structural features important for binding affinity, most of the experimentally available data indicates that additive functions for protein–ligand interactions might be a good approach to the development of empirical scoring functions. With atomic coordinates  $(x, y, z)$  available for protein–ligand complexes, the analysis of the binding can be estimated as a sum of interactions multiplied by weighting coefficients ( $c_j$ ), as indicated by the following equation:

$$pK_d = c_0 + \sum_{j=1}^N c_j f_j(x, y, z) \quad (2)$$

$pK_d$  is the  $-\log K_d$  where  $K_d$  could be either an estimate of overall dissociation constant ( $K_M$  or  $K_d$ ) or dissociation constant for an enzyme activity inhibitor ( $K_i$ ),  $c_0$  is a regression constant,  $f_j$ s are functions that account for van der Waals interactions, intermolecular HBs, deformation, hydrophobic effect and others that may be included.

Most of the empirical functions use the size of the contact surface at the protein–ligand interface to estimate the hydrophobic interaction. A reasonable correlation between experimental affinities can be obtained with contact areas ( $A_1$ ) alone. We have recently proposed the use of a novel set of scoring functions which are based on the observation that the major determinants to ligand specificity are intermolecular HBs and hydrophobic contacts [49–51]. The present set of scoring functions contains 25 polynomial functions described in Table 1, comprising terms up to degree 2, which may involve cross-terms (HB and A). Determination of the

**Table 1**  
Polynomial empirical scoring functions

pK <sub>d</sub> T	Functions
1	1.21082 + 0.290938 * HB + 3.01849 * A
2	2.55586 + 0.284172 * HB + 1.52129 * A * A
3	1.62730692439939 + 0.134428282118786 * HB + 0.011564243645413 * HB * HB + 2.95047720180332 * A * A
4	2.96661 + 0.118486 * HB + 0.0122541 * HB * HB + 1.48312 * A * A
5	0.354505 + 0.141384 * HB + 0.0115682 * HB * HB + 6.09996 * A - 1.74406 * A * A
6	-0.061829 + 0.297946 * HB + 6.16727 * A - 1.74366 * A * A
7	0.805447 + 0.0211133 * HB * HB + 5.96296 * A - 1.70141 * A * A
8	2.02696 + 0.0206507 * HB * HB + 2.89337 * A
9	3.29656 + 0.0202696 * HB * HB + 1.45802 * A * A
10	3.88331 + 0.0048745 * HB + 0.318024 * HB * A
11	3.11326 + 1.20067 * A + 0.274646 * HB * A
12	4.30244 - 0.170762 * HB + 0.0136116 * HB * HB + 0.308455 * HB * A
13	0.704576 + 0.367881 * HB + 3.58451 * A - 0.0862137 * HB * A
14	1.1138 + 0.211753 * HB + 0.0116538 * HB * HB - 0.0879995 * HB * A + 3.52769 * A
15	2.0286 + 0.02062 * HB * HB + 2.89022 * A + 0.000509408 * HB * A
16	3.89706 + 0.00330052 * HB * HB + 0.288261 * HB * A
17	-0.376415 + 0.23806 * HB + 0.0116799 * HB * HB - 0.109449 * HB * A + 7.04613 * A - 1.87046 * A * A
18	-0.784559 + 0.394502 * HB - 0.10763 * HB * A + 7.09836 * A - 1.86796 * A * A
19	2.23253 + 3.43884 * A + 0.277792 * HB * A - 1.25123 * A
20	3.33866 + 0.0161386 * HB * HB + 0.0693682 * HB * A + 1.23337 * A * A
21	0.770528 + 0.0216618 * HB * HB - 0.00904417 * HB * A + 6.0334 * A - 1.70945 * A * A
22	3.63791 + 0.281169 * HB * A + 0.55785 * A * A
23	3.89467 + 0.321571 * HB * A
24	2.67982 + 0.248414 * HB + 0.0407366 * HB * A + 1.38177 * A * A
25	3.07883 + 0.0864079 * HB + 0.012179 * HB * HB + 0.0377019 * HB * A + 1.35423 * A * A

intermolecular HBs and  $A_1$  of 100 binary complexes available at PDBBIND [52] were used to propose this set of functions (Supplementary material). No HsPNP structures were included in this dataset. This novel function is based exclusively on the HBs,  $A_1$  and accessible surface area for the ligand ( $A_2$ ). The additive nature of the empirical scoring functions generally leads to large ligands obtaining high scores. This effect is undesirable. Owing to the overestimation of the  $A_1$  contribution to the empirical scoring function we devised a simple scheme to reduce this contribution. We introduced a penalty term that diminishes the dependence of the score on molecular size. We divided the  $A_1$  by the term  $A_2 - A_1$ , which presents the highest values for complexes with  $A_1$  much smaller than  $A_2$ . This scheme reduces the contribution of the  $A_1$  term in the empirical function for those ligands with relatively small  $A_1$ . The empirical function 17 presents the highest correlation coefficient between empirical and predicted binding affinities. This function is composed of a polynomial involving the number of intermolecular HBs and the modified contact area ( $A$ ), as follows:

$$pK_d = c_0 + c_1 HB + c_2 HB^2 + c_3 HBA + c_4 A + c_5 A^2 \quad (3)$$

where  $c_0$  is the regression constant, and  $c_j$ s are the weights for the other terms present in the above equation. The term  $A$  is determined by the following equation:

$$A = A_1 / (A_2 - A_1) \quad (4)$$

The terms  $A_1$  and  $A_2$  were calculated using a modified version of Lee and Richards' algorithm [53] implemented in the AREAIMOL [22]. The intermolecular HBs were determined using a method previously described [48]. Standard multivariate regression was carried out on the whole training set. This approach has been previously used in the study of PNP from *Streptococcus agalactiae* [48].

#### Enzymatic assay for HsPNP

All chemicals used here were of analytical or reagent grade and required no further purification. MQU was solubilized in dimethyl sulfoxide (DMSO). All enzyme activity assays were performed at 25 °C and 50 mM Tris at pH 7.6. The phosphorolysis of 2-amino-6-mercapto-7-methylpurine ribonucleoside (MESG) to 2-amino-6-mercapto-7-methylpurine ( $\epsilon = 11000 \text{ M}^{-1} \text{ cm}^{-1}$  at 360 nm) was

monitored spectrophotometrically by the change in absorbance in the presence of  $P_i$  and HsPNP. Both substrates (MESG and  $P_i$ ) were used at fixed non-saturating concentrations in the absence or presence of MQU in the reaction mixture in order to evaluate its inhibitory effect.

#### Fluorescence spectroscopy

Fluorescence titration of HsPNP by MQU was carried out at 25 °C by making microliter additions of 2.0 mM MQU (final concentration ranging from 1.0 to 9.96  $\mu\text{M}$ ) to 2 mL of 3  $\mu\text{M}$  HsPNP in 50 mM Tris at pH 7.6, keeping the dilution to a maximum of 0.50%. Measurements of intrinsic protein fluorescence of HsPNP employed excitation wavelength at 296 nm and emission wavelength ranging from 305 to 420 nm (maximum  $\lambda_{EM} = 330 \text{ nm}$ ). The slits for excitation and emission wavelengths were, respectively, 3.0 and 10 nm. To account for the inner filter effect due to MQU absorption of excitation light, two cuvettes were placed in series so that the contents of the first cuvette (either buffer or MQU) acted as a filter of the excitation light and the light from the second cuvette detected.

#### Experimental data analysis

Data from equilibrium fluorescence spectroscopy were fitted to Eq. (5), the Hill equation [54], in which  $F$  is the observed fluorescence signal,  $F_{max}$  is the maximal fluorescence,  $F/F_{max}$  ratio is the degree of saturation,  $n$  represents the total number of binding sites, and  $K'$  is the mean dissociation constant for HsPNP:MQU binary complex formation, which is comprised of interaction factors and the intrinsic dissociation constant.

$$F/F_{max} = A^n / (K' + A^n) \quad (5)$$

## Results and discussion

#### Molecular replacement and crystallographic refinement

The standard procedure of molecular replacement using AMoRe [24] was used to solve the structure. Function computation corre-

lation was of 76.1% and the  $R_{\text{factor}}$  of 35.4% after rotation and translation of the model. The highest magnitude of the correlation coefficient function obtained for the Euler angles were  $\alpha = 113.57^\circ$ ,  $\beta = 58.49^\circ$ , and  $\gamma = 157.90^\circ$ . The fractional coordinates are  $T_x = 0.496$ ,  $T_y = 0.2909$ , and  $T_z = 0.1989$ . At this stage  $2F_{\text{obs}} - F_{\text{calc}}$  omit maps were calculated. These maps showed clear electron density for the MQU in the complex. Fig. 2A shows the electron density ( $F_{\text{obs}} - F_{\text{calc}}$ ) map where we clearly see the bound ligand. Atomic coordinates for MQU have been included in the model and all crystallographic refinement using Refmac5 [22] continued with maximum likelihood protocol, followed by alternate cycles of positional refinement and manual rebuilding using MIFit 3.1.0 [55]. Finally, the positions of MQU, water, and sulfate molecules were checked and corrected in  $F_{\text{obs}} - F_{\text{calc}}$  maps. The final model has an  $R_{\text{factor}}$  of 21.5% and  $R_{\text{free}}$  of 27.1%, with 69 water molecules, three sulfate ions, and MQU. The average B-factor for main chain atoms is  $41.61 \text{ \AA}^2$ , whereas that for side chain atoms is  $44.54 \text{ \AA}^2$  (Table 2).

#### Overall description

The structural model of the HsPNP in complex with MQU indicates a trimeric structure. Each PNP monomer displays an alpha-/beta-fold consisting of a mixed beta-sheet surrounded by alpha-helices. The model contains an eight-stranded mixed beta-sheet and a five-stranded mixed beta-sheet, which join to form a distorted beta-barrel. The residues making up the eight-stranded sheet are 26–31, 46–48, 67–73, 76–82, 110–120, 128–138, 188–195, and 234–242. The five-stranded mixed sheet consists of 116–120, 128–133, 188–193, 215–218, and 238–242 residues. Seven alpha-helices surround the beta-sheet structure. The alpha-helices are composed of residues 8–19, 99–103, 139–142, 168–180, 203–212, 222–231, and 263–281. The model of HsPNP in complex with MQU consists of 288 amino acids with a molecular mass of 32016.7 Da and a theoretical pI value of 6.50. Analysis of the electron density maps at final stages of crystallographic refinement reveals the presence of MQU in the active site of HsPNP. Fig. 2B shows schematic drawings of the HsPNP:MQU complex.

#### Ligand-binding conformational changes

The structure presents conformational changes upon MQU binding to HsPNP active site. The superimposition of the structures of PNP apoenzyme and PNP complexed with MQU shows relatively small changes, with a value of  $0.8 \text{ \AA}$  for RMSD in the coordinates of all C $\alpha$  after superimposition of HsPNP:MQU on the PNP apoenzyme (data not shown). The largest movement was observed for residues 240–260, which act as a gate that opens during substrate binding. This gate is anchored near the central beta-sheet at one end and is

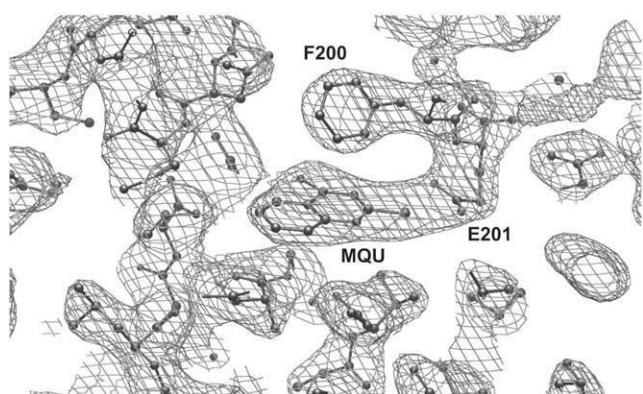


Fig. 2A. Electron density ( $2F_{\text{obs}} - F_{\text{calc}}$ ) map of MQU in binding-pocket.

Table 2

Data collection and refinement statistic

Cell parameters	$a = b = 142.9 \text{ \AA}$ , $c = 165.2 \text{ \AA}$ $\alpha = \beta = 90.0^\circ$ , $\gamma = 120.0^\circ$
Space group	R32
Number of measurements with $I > 2\sigma(I)$	79943
Number of independent reflections	16197
Completeness of data (%)	98.76
$R_{\text{sym}}^\dagger$ (%)	6.7
High resolution shell (Å)	2.85–2.70
Completeness in the highest resolution shell (%)	99.9
$R_{\text{sym}}^\dagger$ in the highest resolution shell (%)	35.6
$R_{\text{factor}}^\ddagger$ (%)	21.5%
$R_{\text{free}}^\ddagger$ (%)	27.1%
B values* ( $\text{Å}^2$ )	
Main chain	41.61
Side chains	44.54
2-Mercapto-4(3H)-quinazolinone	51.02
Waters	34.08
Sulfate groups	33.9
Observed RMSD from ideal geometry	
Bond lengths (Å)	0.013
Bond angles (degrees)	2
Dihedral (degrees)	25.04
No. of water molecules	69
No. of sulfate groups	3

\*  $R_{\text{sym}} = 100 \sum |I(h) - \langle I(h) \rangle| / \sum I(h)$  with  $I(h)$ , observed intensity and  $\langle I(h) \rangle$ , mean intensity of reflection  $h$  overall measurement of  $I(h)$ .

†  $R_{\text{factor}} = 100 \times \sum |F_{\text{obs}} - F_{\text{calc}}| / \sum (F_{\text{obs}})$ , the sums being taken overall reflection with  $F/\Sigma(F) > 2$  cutoff.

‡  $R_{\text{free}}$  =  $R_{\text{factor}}$  for 10% of the data, which were not included during crystallographic refinement.

\* B values = average B values for all non-hydrogens atoms.



Fig. 2B. Schematic drawings of the HsPNP:MQU complex.

responsible for controlling access to the active site. The gate movement involves a helical transformation of residues 257–265 in the transition apoenzyme complex [28].

#### Interactions with 2-mercapto-4(3H)-quinazolinone

The present complexed structure differs from previously reported HsPNP structures since it was co-crystallized with MQU. Structural comparison of the final binary complex (HsPNP:MQU) with HsPNP in the apo form indicates that the binding of MQU induces conformational changes mainly in the region comprised by residues 240–260. In the apo structure this region is disordered, presenting relatively high B-factors, when compared with the rest of the structure. The binary complex for HsPNP:MQU presents a helix in this region, which indicates that ligand binding promotes further stability for this region. This behavior was confirmed in the molecular dynamics simulations described below.

The specificity and affinity between enzyme and a ligand depend on directional HBs and ionic interactions, as well as on shape complementarity of the contact surfaces of both partners [56]. Analysis of the HBs between MQU and HsPNP reveals a 3.1 Å intermolecular HB involving the residue Asn243.

#### Molecular dynamics simulations

To obtain an estimate of the MD trajectory quality convergence, the backbone RMSD from the starting crystallographic structures and the radius of gyration were calculated (Fig. 3), suggesting stability of quaternary structure. After rapid increase during the first 100 ps, the protein backbone RMSD average and standard deviation over the last 2 ns of the system A trajectory was  $2.4 \pm 0.1$  Å and the system B was  $2.1 \pm 0.1$  Å. A plateau of RMSDs for the system A was achieved within 160 ps and for the system B was achieved within 120 ps of unrestrained simulation, suggesting that 4000 ps unrestrained simulation were sufficient for stabilizing fully relaxed models. This analysis suggests that the systems are stable and the radius of gyration centered on the center of mass of the trimeric HsPNP remains essentially constant indicating that the monomers of HsPNP structure remain in the trimeric state.

The superimposition of the average structure of the system A with the initial model (data not shown) does not show major conformational changes in comparison to the initial model, which is consistent with the relatively low RMSD value. The flexibility of the proteins was assessed by the B-factor from MD trajectory. In a typical B-factor pattern, low B-factor values indicate the well-structured regions while the high values indicate the loosely structured loop regions or terminal domains [57]. A comparison between HsPNP apoenzyme and HsPNP:MQU binary complex shows that regions R1–R3 (Fig. 4) have large B-factor values, mainly in the binding-pocket. Fig. 5 presents the B-factors for each monomer (HsPNP is a homotrimer which is constituted by three monomers herein named subunit A, B and C) during the simulation. Regions R2 and R3 (Fig. 4) are comprised of residues involved in, respectively, the phosphate binding site and the purine binding site. The presence of MQU (Fig. 5, dashed line) leads to stability of loops in R2 and R3 regions, which are involved in substrate entrance and exit. The R2 region is composed of one loop (181–187) between two beta-sheets and the R3 is composed of one loop (243–264).

The Phe159 is the only residue in the catalytic site of PNP that is located in an adjacent subunit, and this residue is responsible for the hydrophobic interactions with the substrate bound to an adjacent monomer.

#### Empirical scoring function

A novel set of empirical scoring functions has been described in Materials and methods. These functions use only two terms to evaluate the binding affinity, involving intermolecular HBs and contact surface; these empirical scoring functions are fast to calculate and may be used in virtual screening projects focused on HsPNP. Polynomial function 17 shows the highest correlation coefficient against the training set. A correlation coefficient of 0.73 and a standard deviation of 1.8 in  $pK_d$  units were obtained, which are close to the ones obtained by XSCORE empirical scoring function, 0.74 and 1.71, respectively. Previously published comparison studies involving 14 empirical scoring functions indicated that XSCORE [58] was able to obtain the best results in evaluation of binding affinities, therefore the program XSCORE was chosen as comparison for this new set of scoring functions. Table 1 shows all 25 functions. Fig. 6 shows the dispersion plot for the predicted and experimental  $pK_d$ s used in the training set.

The true value of a novel empirical scoring function lies in its predictive capability. This is especially useful when one is trying to use a specific empirical scoring function for a protein. It has been demonstrated that dividing up a set of known inhibitors into clusters of chemically similar molecules and then deriving a specific scoring function for each molecule increases the accuracy of the scoring function [48,59,60]. We previously illustrated this application on the study of a new empirical function for complexes involving PNP from *Streptococcus agalactiae* [48]. In the present study we have used 15 binary complexes involving HsPNP and different ligands as a test set (Table 3). The main reason to choose these complexes as test set are the following: (1) we are interested in testing the ability of our novel function to predict the affinity of ligands for HsPNP; (2) there is experimental information for the affinities of these ligands; and (3) no HsPNP complexes were used in the training set. Therefore, this test set tends to be a challenge and a validation method for our scoring function. Analysis of the binding affinity of the complexes present in the test set generates a corre-

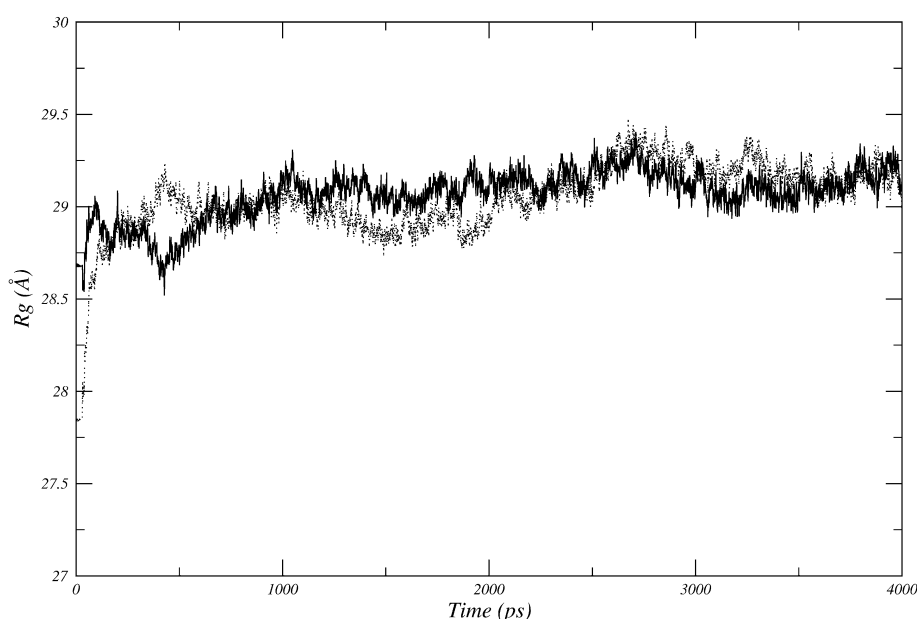
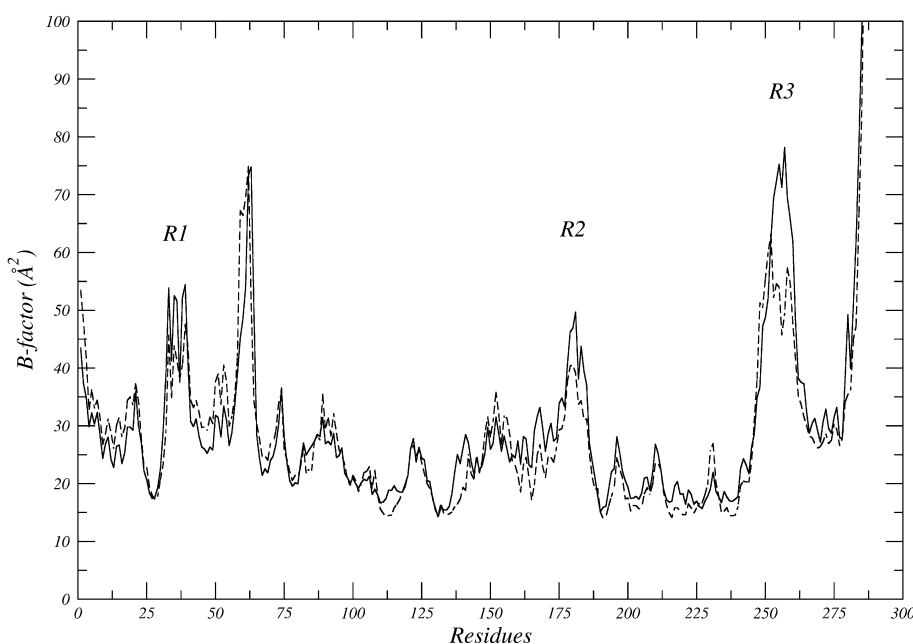
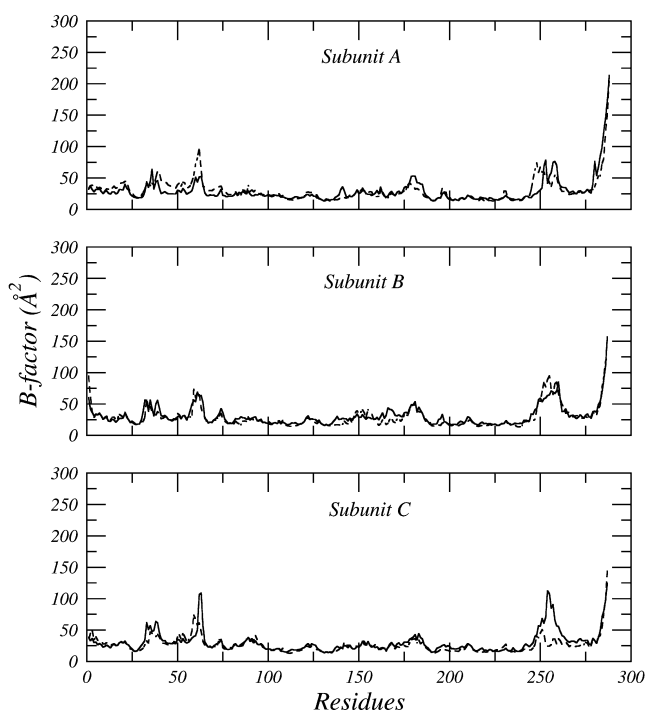


Fig. 3. Radius of gyration of the HsPNP apoenzyme (solid line) and HsPNP:MQU (dashed line).





**Fig. 4.** B-factor average of the trimeric structure during the molecular dynamics. The solid line shows the values of HsPNP apoenzyme and dashed line gives the calculation of complex HsPNP:MQU.



**Fig. 5.** B-factor for each monomer, subunit A, B and C (HsPNP apoenzyme and HsPNP:MQU) during the simulation. The solid line shows the values of HsPNP apoenzyme and dashed line gives the calculation of complex HsPNP:MQU.

lation coefficient of 0.67 for function 12, considerably better than the one obtained using XSCORE for each function present in this program (HPScore, HMScore and HSScore), 0.29, 0.39 and 0.39, respectively, and Drugscore,  $-0.0017$ . Fig. 7 shows the dispersion plot for  $pK_d$  estimated using our empirical scoring function.

Empirical scoring functions that decompose the binding free energy into a sum of terms present an intrinsic problem in physical sense, since this decomposition is not allowed. Free energy of binding is a state function but its terms are not [61]. Furthermore, addi-

tive methods are not able to describe subtle cooperative effects [62]. We partially overcome this problem introducing cross-terms involving HBs and contact surface.

To further validate this specific scoring function for HsPNP we used it to predict the best result for docking simulation. We used the present crystallographic structure (HsPNP:MQU) to test the ability of the polynomial empirical scoring functions to predict the best molecular docking result, when compared with crystallographic structure. Empirical scoring functions have been used to analyze the results of molecular docking, generating better results than the native docking functions [52]. We used the polynomial empirical scoring functions to predict the best docking result and compared our results with the results obtained using HPScore, HMScore and HSScore present in the program XSCORE [52] and Drugscore [47].

The main goal in the analysis of the molecular docking results is to identify the lowest RMSDs between the docked structure and the crystallographic structure. It is expected that the best results will generate the lowest estimated  $K_d$ . Using this approach we applied the polynomial empirical scoring functions and XSCORE (Supplementary material). To verify the correlation between RMSD and estimated  $K_d$ s we used Spearman's rank order correlation coefficient ( $\rho$ ), as shown below, since there is no direct relationship between both variables (RMSD and  $pK_d$ ).

$$\rho = 1 - \left\{ 6 \sum_{j=1}^N [r(\text{RMSD}_j) - r(K_{d_j})]^2 / N^3 - N \right\} \quad (6)$$

where  $r(\text{RMSD}_j)$  and  $r(K_{d_j})$  are the ranks for RMSD and  $K_d$ , respectively, and  $N$  is the number of pairs ( $n = 99$ , in our case). The Spearman's rank order correlation coefficient between the predicted  $K_d$  and RMSD for XSCORE is  $-0.39$ , and the best result for the polynomial scoring functions generated a correlation coefficient of 0.55, obtained using function 12. These results strongly indicate the predictive capability of the polynomial empirical scoring functions when employed in the analysis of docking results for HsPNP. The value obtained ( $\rho = 0.55$ ) is higher than 0.329, the critical value at the 0.0005 level of significance. It implies that polynomial empirical scoring function 12 can be used for prediction of the best results obtained in molecular docking against HsPNP.

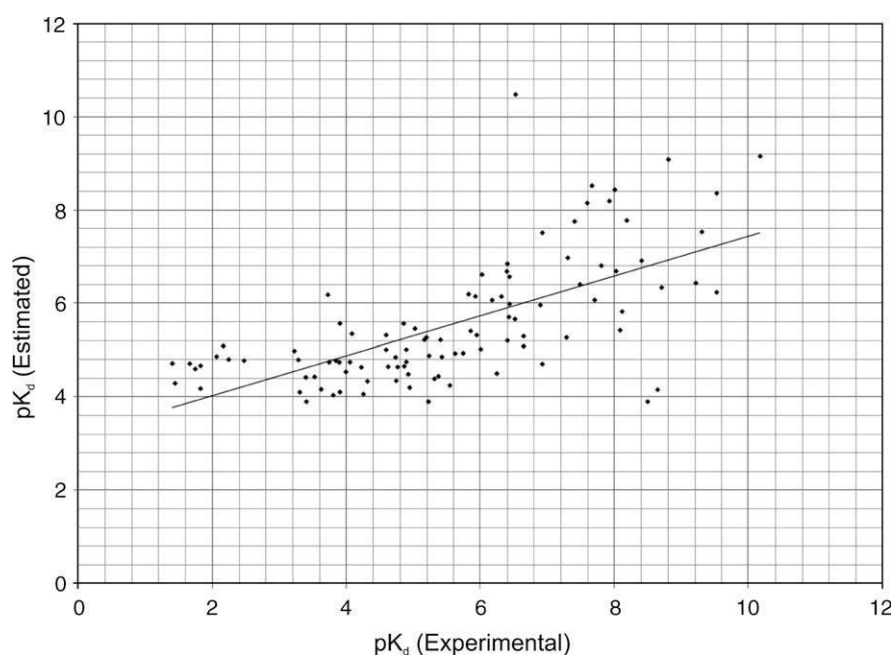


Fig. 6. Dispersion plot for the training set.

Table 3

Test set for empirical scoring function

Ligand	$pK_d$ exp	$pK_d$ T12	HP score	HM score	HS score	Drug score (pairsurf/pdb)
2-Amino-6-methylthiopurine	3.52	4.30	4.86	4.92	4.77	-523568
5-Chloro-5-deoxy-8-aminoguanosine	6.4	5.54	5.34	5.58	5.26	-525628
6-Mercaptoguanosine	3.78	4.59	5.23	5.41	5.11	-407960
6-Mercaptopurine	4.13	4.61	4.55	4.68	4.44	-523681
Acyclovir	4.04	4.80	5.09	5.12	4.88	-525155
Hipoxanthine	4.41	4.92	4.43	4.57	4.33	-525598
Methylthioinosine	4.92	5.31	5.45	5.58	5.36	-526452
Oxallopurinol	3.09	4.74	4.7	4.85	4.49	-525148
Quinazolinone	3.49	4.51	5.12	5.42	5.02	-525590
Xanthine	3.42	4.51	4.59	4.76	4.5	-525268
Allopurinol	3.01	4.60	4.54	4.67	4.33	-525588
8-Amino-5-deoxy-5-iodoguanosine	5.48	4.85	4.51	4.94	4.57	-524011
7-Methylinosine	3.43	4.98	5.08	5.23	4.94	-526463
Inosine	4.39	4.30	5.67	5.92	5.58	-525084
6-Mercaptoguanosine-riboside	4.15	4.80	5.49	5.66	5.38	-407960

The dispersion plot for the RMSD and  $K_d$  for function 12 is shown in Fig. 8, which clearly demonstrates concentration of RMSD results around 0–1 Å and 18–20 Å. The first region indicates the correct binding site for HsPNP. Fig. 9 shows this region and the 3 best docking results obtained using our empirical scoring function. The second region may indicate an alternative binding site (Fig. 10) involving residues Asn3, Trp94, Gln144, Pro146, Arg148, and Gly149. The crystallographic structure of HsPNP in complex with guanine [17] identified 4 potential phosphate binding sites. The third identified phosphate group makes HBs involving residues Gln144 and Arg148 from an adjacent subunit, which was also identified in the present docking simulations. Although these residues are not part of the active site, they are close, allowing binding of phosphates, which have been proposed to be involved in the modulation of HsPNP affinity [17,63–65].

#### Assessment of MQU upon HsPNP activity

Enzymatic assays revealed a low inhibitory effect of MQU on HsPNP activity. The use of fixed substrate concentrations near the  $K_M$  values ( $K_{MESG} = 358 \mu\text{M}$  and  $K_{Pi} = 94 \mu\text{M}$ , [66]) for HsPNP in

the presence of MQU up to 200  $\mu\text{M}$  resulted in a relative specific activity of 97.7% with respect to the same assay conditions in the absence of the latter. It should be pointed that MQU was solubilized in DMSO, and the effect of the latter on HsPNP enzyme activity was taken into account. The low MQU inhibitory effect on HsPNP experimentally obtained indicates that the empirical scoring function here described detects, not surprisingly, compounds with low overall dissociation constant for HsPNP:MQU binary complex formation (which indicates that this enzyme has a high affinity for binding to this compound), not necessarily inhibitors. Note that the demonstration of binding does not necessarily correspond to inhibition, and inhibitors might have by definition a high/low binding constant (low/high affinity) [67].

#### Equilibrium binding of MQU to HsPNP

The enhancement in intrinsic protein fluorescence upon MQU binding to HsPNP was sigmoidal (Fig. 11) and fitting the data to the Hill equation yielded values of 11 ( $\pm 3$ )  $\mu\text{M}$  for  $K'$  and 1.8 ( $\pm 0.3$ ) for  $n$ . This result is in agreement with the prediction that MQU should be able to bind to HsPNP.

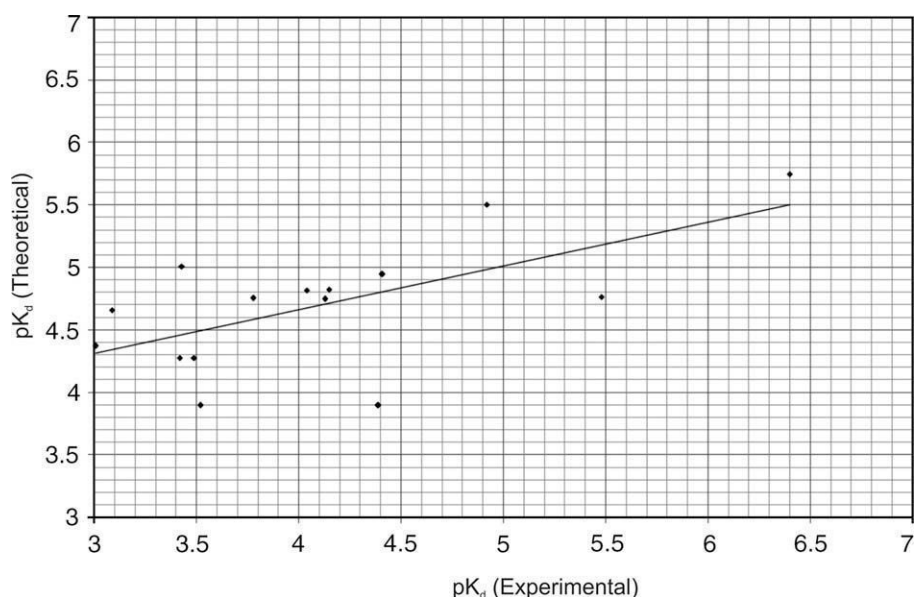


Fig. 7. Dispersion plot for the test set.

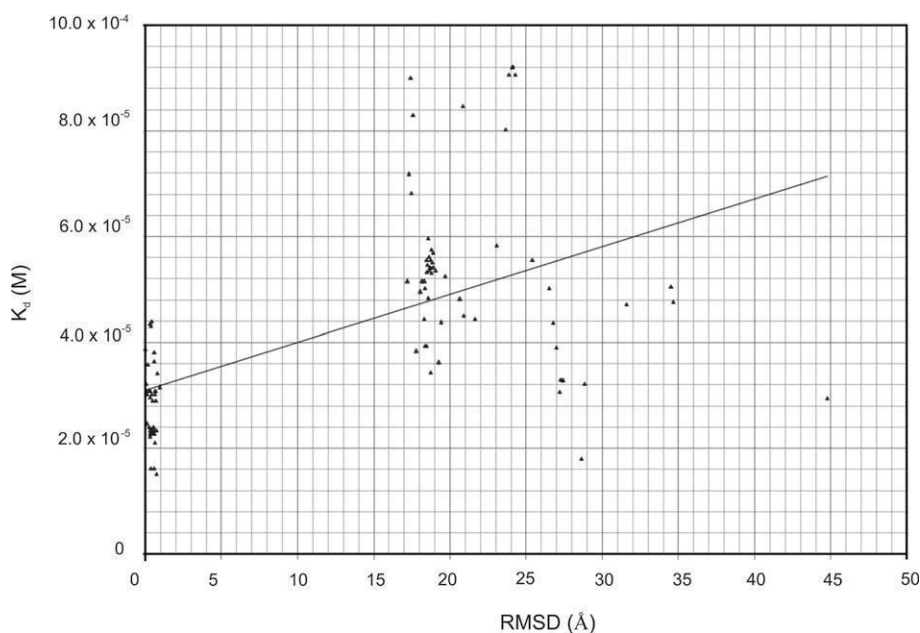


Fig. 8. Dispersion plot for the docking set (99 structures).

## Conclusions

Analysis of the structure of *Hs*PNP in complex with MQU provides additional information for the structure-based design of drugs and improvement of already identified lead compounds. The structural analysis of the model *Hs*PNP:MQU shows conformational changes in the regions comprised by residues 240–260, such as *Hs*PNP structures in complex with other ligands. However, the analysis with the HPScore, HMScore, HSScore and a novel empirical scoring function showed that MQU is not a good inhibitor for *Hs*PNP. Furthermore, the novel empirical scoring function was able to identify that 5-chloro-5-deoxy-8-aminoguanosine presents high affinity against *Hs*PNP, suggesting a possible new lead compound.

Analysis of the MD simulation indicated that structural models of *Hs*PNP apoenzyme and *Hs*PNP:MQU complex display a stable tri-

mer during all dynamics simulation. Analysis of the B-factor graphics shows that *Hs*PNP complexed with MQU present more stability than *Hs*PNP apoenzyme, mainly in the regions 2 and 3 (R2 and R3) showed in Fig. 4, and the same graphics confirms the movement in the loop (240–260) observed on the model analysis, which is important for the binding-pocket. These regions are involved in the binding sites, the R2 involved the phosphate binding site and the R3 involved the purine binding site.

Testing of our set of empirical scoring functions indicates that they are able to predict the ligand-binding affinities against *Hs*PNP, superior to the ones obtained using HPScore, HMScore, HSScore and Drugscore. Furthermore, the use of the empirical scoring function 12, which ranks better for *Hs*PNP (Table 3), to analyze molecular docking results, indicates that the use of this methodology gives better results than XSCORE. This altogether strongly indicates

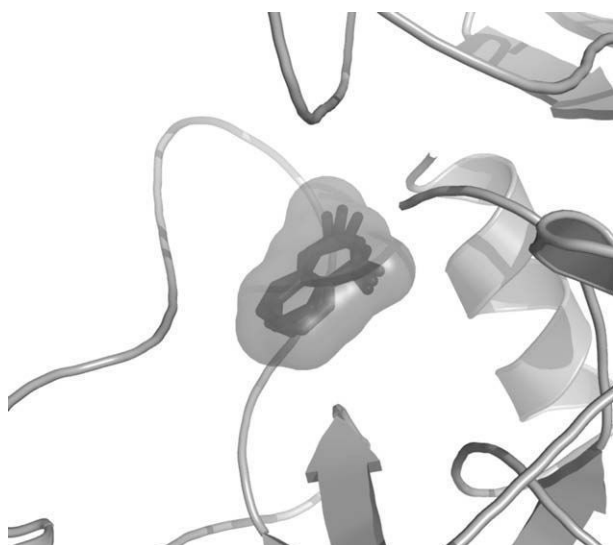


**Fig. 9.** Superposition of the 3 best dockings obtained with our empirical scoring function.

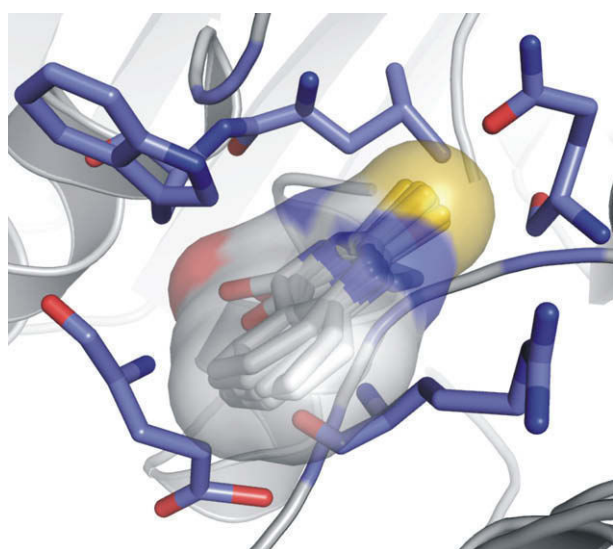


**Fig. 10.** Region that may indicate an alternative binding site.

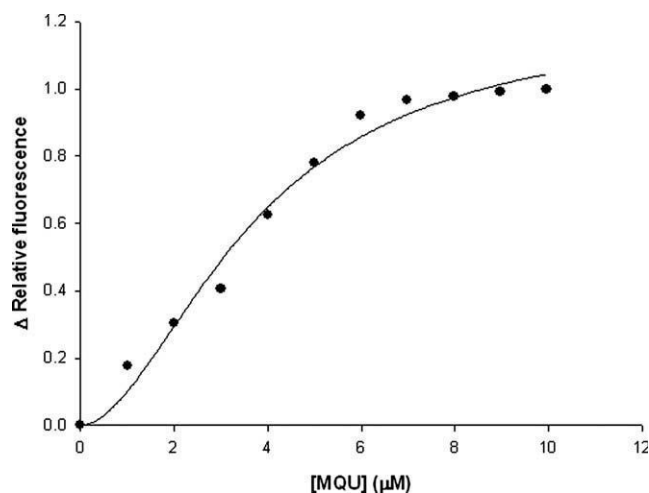


**Fig. 11.** Overall dissociation constant for HsPNP:MQU binary complex formation monitoring changes in intrinsic protein fluorescence.

that this methodology may be used to speed-up virtual screening projects focused on searching new inhibitors of HsPNP enzyme activity.

### Deposit

The atomic coordinates and structure factors for the HsPNP:MQU structure have been deposited at the Protein Data Bank, access code: 3D1 V.

### Acknowledgments

This article is dedicated to the memory of Prof. Icaro de Sousa Moreira (1953–2008).

This work was supported by grants from CNPq, CAPES and Instituto do Milênio (CNPq-MCT). W.F.A., D.S.S., and L.A.B. are senior researchers of CNPq (Conselho Nacional de Pesquisas, Brazil).

### Appendix A. Supplementary data

Supplementary data associated with this article can be found, in the online version, at doi:10.1016/j.abb.2008.08.015.

### References

- [1] R.E. Parks Jr., R.P. Agarwal, The Enzymes, in: P.D. Boyer (Ed.), Academic Press, New York, 1972, pp. 483–514.
- [2] H.M. Kalckar, J. Biol. Chem. 167 (1943) 429–443.
- [3] D.J.T. Porter, J. Biol. Chem. 267 (1992) 7342–7351.
- [4] E.R. Giblett, A.J. Ammann, D.W. Wara, R. Sandman, L.K. Diamond, Lancet 1 (1975) 1010–1013.
- [5] W.B.J. Stoop, M. Zegers, G.F.M. Hendrickx, L.H.S. van Heukelom, G.E.J. Staal, P.K. de Bree, S.K. Wadman, R.E. Ballieux, N. Engl. J. Med. 296 (1977) 651–655.
- [6] S. Bantia, J.A. Montgomery, H.G. Johnson, G.M. Walsh, Immunopharmacology 35 (1996) 53–63.
- [7] T.A. Krenitsky, J.V. Tuttle, G.W. Koszalka, I.S. Chen, L.M. Beacham, J.L. Rideout, G.B. Elion, J. Biol. Chem. 251 (1976) 4055–4061.
- [8] M.L. Market, Immunodef. Rev. 3 (1991) 45–81.
- [9] I.S. Kazmers, B.S. Mitchell, P.E. DaDonna, L.L. Wotring, L.B. Townsend, W.N. Kelly, Science 214 (1981) 1137–1139.
- [10] S. Eriksson, L. Thelander, M. Kaerman, Biochemistry 18 (1979) 2948–2952.
- [11] J.D. Stoeckler, Developments in Cancer Chemotherapy, in: R.I. Glazer (Ed.), CRC Press, Boca Raton, 1984, pp. 35–60.
- [12] V.L. Schramm, Biochim. Biophys. Acta 1578 (2002) 107–117.
- [13] S.E. Ealick, S.A. Rule, D.C. Carter, T.J. Greenhough, Y.S. Babu, W.J. Cook, J. Habash, J.R. Helliwell, J.D. Stoeckler, R.E. Parks Jr., J. Biol. Chem. 265 (1990) 1812–1820.
- [14] S.E. Ealick, Y.S. Babu, C.E. Bugg, M.D. Erion, W.C. Guida, J.A. Secrist III, J.A. Montgomery, Proc. Natl. Acad. Sci. USA 88 (1991) 11540–11544.
- [15] M.J. Pugmire, S.E. Ealick, Biochem. J. 361 (2002) 1–25.
- [16] W.F. de Azevedo, G.C. Santos, D.M. dos Santos, R.R. Olivieri, F. Canduri, R.G. Silva, L.A. Basso, M.A. Mendes, M.S. Palma, D.S. Santos, Biochem. Biophys. Res. Commun. 309 (2003) 928–933.
- [17] W.F. de Azevedo, F. Canduri, D.M. dos Santos, J.H. Pereira, R.G. Silva, M.A. Mendes, L.A. Basso, M.S. Palma, D.S. Santos, Biochem. Biophys. Res. Commun. 312 (2003) 767–772.
- [18] A. Bzowska, E. Kulikowska, D. Shugar, Pharmacol. Ther. 88 (2000) 349–425.
- [19] R.G. Silva, L.P. Carvalho, J.S. Oliveira, C.A. Pinto, M.A. Mendes, M.S. Palma, L.A. Basso, D.S. Santos, Protein Expr. Purif. 27 (2003) 158–164.
- [20] W.F. de Azevedo, F. Canduri, W.F. dos Santos, W.F. Pereira, W.F. Dias, R.G. Silva, M.A. Mendes, L.A. Basso, M.S. Palma, D.S. Santos, Biochem. Biophys. Res. Commun. 309 (2003) 922–927.
- [21] S.E. Ealick, Y.S. Babu, C.E. Bugg, M.D. Erion, W.C. Guida, J.A. Montgomery, J.A. Secrist III, Proc. Natl. Acad. Sci. USA 91 (1991) 11540–11544.
- [22] Collaborative Computational Project, Number 4, Acta Crystallogr. D 50 (1994) 760–763.
- [23] K.A. Kantardjiev, B. Rupp, Protein Sci. 12 (2003) 1865–1871.
- [24] J. Navaza, Acta Crystallogr. A 50 (1994) 157–163.
- [25] F. Canduri, D.M. dos Santos, R.G. Silva, M.A. Mendes, L.A. Basso, M.S. Palma, W.F. de Azevedo, D.S. Santos, Biochem. Biophys. Res. Commun. 313 (2004) 907–914.
- [26] D.M. Santos, F. Canduri, J.H. Pereira, M.V.B. Dias, R.G. Silva, M.A. Palma, M.S. Mendes, L.A. Basso, W.F. de Azevedo, D.S. Santos, Biochem. Biophys. Res. Commun. 308 (2003) 553–559.
- [27] H.B. Uchoa, G.E. Jorge, N.J.F. da Silveira, J.C. Câmara Jr., F. Canduri, W.F. de Azevedo Jr., Biochem. Biophys. Res. Commun. 325 (2004) 1481–1486.

- [28] W.F. de Azevedo, F. Canduri, D.M. dos Santos, R.G. Silva, J.S. de Oliveira, L.P. de Carvalho, L.A. Basso, M.A. Mendes, M.S. Palma, D.S. Santos, *Biochem. Biophys. Res. Commun.* 308 (2003) 545–552.
- [29] D. van der Spoel, E. Lindahl, B. Hess, G. Groenhof, A.E. Mark, H.J. Berendsen, *Comp. Chem.* 26 (2005) 1701–1718.
- [30] C. Oostenbrink, T.A. Soares, N.F. van der Vegt, W.F. van Gunsteren, *Eur. Biophys. J.* 34 (2005) 273–284.
- [31] D.M.F. van Aalten, B. Bywater, J.B.C. Findlay, M. Hendlich, R.W.W. Hooft, G. Vriend, *J. Comput. Aided Mol., Des.* 10 (1996) 255–262.
- [32] M.W. Schmidt, K.K. Baldrige, J.A. Boatz, S.T. Elbert, M.S. Gordon, J.H. Jensen, S. Koseki, N. Matsunaga, K.A. Nguyen, S.J. Su, T.L. Windus, M. Dupuis, J.A. Montgomery, *J. Comput. Chem.* 14 (1993) 1347–1363.
- [33] W.L. Delano, J.W. Lam, *Abstr. Pap. Am. Chem. Soc.* 230 (2005) 1371–1372.
- [34] H.J.C. Berendsen, J.P.M. Postma, W.F. van Gunsteren, J. Hermans, *Interaction models for water in relation to protein hydration*, in: B. Pullman, D. Reidel (Eds.), *Intermolecular Forces*, Publishing Company, Dordrecht, The Netherlands, 1981, p. 331.
- [35] B. Hess, H. Bekker, H.J.C. Berendsen, J.G.E.M. Fraaije, *J. Comput. Chem.* 18 (1997) 1463–1472.
- [36] S. Miyamoto, P.A. Kollman, *J. Comput. Chem.* 13 (1992) 952–962.
- [37] S. Chowdhuri, Ming-Liang. Tan, T. Ichiye, *J. Chem. Phys.* 125 (2006) 144513–1–144513–8.
- [38] T. Darden, D. York, L.A. Pedersen, *J. Chem. Phys.* 98 (1993) 10089–10092.
- [39] O.N. de Souza, R.L. Ornstein, *J. Biomol. Struct. Dyn.* 16 (1999) 1205.
- [40] P.H. Hünenberger, A.E. Mark, W.F. van Gunsteren, *J. Mol. Biol.* 252 (1995) 492–503.
- [41] W.F. van Gunsteren, A.E. Mark, *J. Chem. Phys.* 108 (1998) 6109–6116.
- [42] R. Chen, L. Li, Z. Weng, *Proteins* 52 (2003) 80–87.
- [43] R. Chen, Z. Weng, *Proteins: Struct. Funct. Genet.* 47 (2002) 281–294.
- [44] P.E. Bourne, H. Weissig, *Structural bioinformatics*, in: P.E. Bourne (Ed.), *California*, 2003, pp. 448–452.
- [45] W.F. de Azevedo, J.H. Mueller-Dieckmann, U. Schulze-Gahmen, P.J. Worland, E. Sausville, S.H. Kim, *Proc. Natl. Acad. Sci. USA* 93 (1996) 2735–2740.
- [46] R. Wang, L. Lai, S. Wang, *J. Comput. Aided Mol. Des.* 16 (2002) 11–26.
- [47] H. Gohlke, M. Hendlich, G. Klebe, *J. Med. Biol.* 295 (2000) 337–356.
- [48] R.A. Caceres, L.F.S. Timmers, R. Dias, L.A. Basso, D.S. Santos, W.F. de Azevedo, *Bioorg. Med. Chem.* 16 (2008) 4984–4993.
- [49] G. Klebe, H.-J. Böhm, *Angew. Chem., Int. Ed. Engl.* 35 (1996) 2588–2614.
- [50] M. Matsumara, W.J. Becktel, B.W. Matthews, *Nature* 4 (1988) 406–410.
- [51] V. Nauchatel, M.C. Villaverde, F. Sussman, *Protein Sci.* 4 (1995) 1356–1364.
- [52] R. Wang, X. Fang, Y. Lu, C.Y. Yang, S. Wang, *J. Med. Chem.* 48 (2005) 4111–4119.
- [53] B. Lee, F.M. Richards, *J. Mol. Biol.* 55 (1971) 379–400.
- [54] A.V. Hill, *Biochem. J.* 7 (1913) 471–480.
- [55] D.E. McRee, *Acta Crystallogr. D* 60 (2004) 2276–2279.
- [56] F. Canduri, L.G. Teodoro, V. Fadel, C.C. Lorenzi, V. Hial, R.A. Gomes, J. Ruggiero Neto, W.F. de Azevedo, *Acta Crystallogr. D* 57 (2001) 1560–1570.
- [57] A.C. Saladino, Y. Xu, P. Tang, *Biophys. J.* 88 (2005) 1009–1017.
- [58] R. Wang, Y. Lu, X. Fang, S. Wang, *J. Chem. Inf. Comput. Sci.* 44 (2004) 2114–2125.
- [59] H.-J. Böhm, *Prediction of non-bonded interactions in drug design*, in: H.-J. Böhm, G. Schneider (Eds.), *Protein–Ligand Interactions*, Wiley-VCH Verlag GmbH & Co. KGaA, Weinheim, Germany, 2003, pp. 3–17.
- [60] R.C. Rizzo, M. Udier-Blagovic, D.P. Wang, E.K. Watkins, M.B.K. Smith, R.H. Smith, J. Tirado-Rives, W.L.J. Jorgensen, *J. Med. Chem.* 45 (2002) 2970–2987.
- [61] A.E. Mark, W.F. van Gunsteren, *J. Mol. Biol.* 240 (1994) 167–176.
- [62] D.H. Williams, B. Bardsley, *Perspect. Drug Discov. Des.* 17 (1999) 43–59.
- [63] W.F. de Azevedo Jr., F. Canduri, L.A. Basso, M.S. Palma, D.S. Santos, *Cell. Biochem. Biophys.* 44 (2006) 405–411.
- [64] F. Canduri, V. Fadel, L.A. Basso, M.S. Palma, D.S. Santos, W.F. de Azevedo Jr., *Biochem. Biophys. Res. Commun.* 327 (2005) 646–649.
- [65] F. Canduri, V. Fadel, M.V. Dias, L.A. Basso, M.S. Palma, D.S. Santos, W.F. de Azevedo Jr., *Biochem. Biophys. Res. Commun.* 326 (2005) 335–338.
- [66] R.G. Silva, J.H. Pereira, F. Canduri, W.F. de Azevedo Jr., L.A. Basso, D.S. Santos, *Arch. Biochem. Biophys.* 442 (2005) 49–58.
- [67] B.K. Schoichet, *Nature* 432 (2004) 862–865.

**8.2. ARTIGO 4:** DUCATI, R. G.; BASSO, L. A. & SANTOS, D. S. Mycobacterial shikimate pathway enzymes as targets for drug design. *Curr. Drug Targets*, 8(3): 423-435, 2007.

## Mycobacterial Shikimate Pathway Enzymes as Targets for Drug Design

R.G. Ducati<sup>§†</sup>, L.A. Basso<sup>§\*</sup> and D.S. Santos<sup>§\*</sup>

<sup>§</sup>Centro de Pesquisas em Biologia Molecular e Funcional, Faculdade de Farmácia, Instituto de Pesquisas Biomédicas, Pontifícia Universidade Católica do Rio Grande do Sul, Porto Alegre, RS, Brazil and <sup>†</sup>Programa de Pós-Graduação em Biologia Celular e Molecular, Universidade Federal do Rio Grande do Sul, Porto Alegre, RS, Brazil

**Abstract:** The aetiological agent of tuberculosis (TB), *Mycobacterium tuberculosis*, is responsible for millions of deaths annually. The increasing prevalence of the disease, the emergence of multidrug-resistant strains, and the devastating effect of human immunodeficiency virus co-infection have led to an urgent need for the development of new and more efficient antimycobacterial drugs. Since the shikimate pathway is present and essential in algae, higher plants, bacteria, and fungi, but absent from mammals, the gene products of the common pathway might represent attractive targets for the development of new antimycobacterial agents. In this review we describe studies on shikimate pathway enzymes, including enzyme kinetics and structural data. We have focused on mycobacterial shikimate pathway enzymes as potential targets for the development of new anti-TB agents.

**Key Words:** 3-deoxy-D-arabino-heptulosonate-7-phosphate synthase; 3-dehydroquinate synthase; 3-dehydroquinate dehydratase; shikimate 5-dehydrogenase; shikimate kinase; 5-enolpyruvylshikimate-3-phosphate synthase; chorismate synthase; antimycobacterial drug design.

### TUBERCULOSIS

Infectious diseases have represented a global concern throughout centuries of human history, claiming for millions of lives every year. Tuberculosis (TB) pictures as a main player among these. Epidemiological studies have indicated that approximately one third of the world's population is infected with *Mycobacterium tuberculosis* (Mt), the aetiological agent of human TB, which is responsible for more human deaths than any other single infectious agent, accounting for 26% of all preventable deaths and 7% of all deaths [1]. Approximately 95% of TB cases occur in developing nations, which account for 98% of the deaths worldwide [2]. These statistics are inevitable, as a reflect of national regions where very few resources are available to ensure proper treatment and where human immunodeficiency virus (HIV) infection is common, which wanes immunity, thereby reactivating the contained, but not eradicated, mycobacterial infection, both forging a deadly synergy [3, 4]. The demographical concentration of TB deaths among developing nations and higher mortality for rates among ages ranging from 25 to 54 years, the most economically fruitful years of life, causes substantial losses in productivity and contributes to the impoverishment of third-world countries [5]. Several countries have been reaching treatment success's substantially below average due, in part, to the complications caused by HIV/AIDS epidemic and the widespread emergence of multidrug-resistant tuberculosis (MDR-TB) strains [3, 6].

Among existing therapeutic agents, isoniazid and rifampicin stand as the most effective first-line antimycobacterial drugs [7] prescribed. However, MDR-TB, which comprises strains resistant to at least isoniazid and rifampicin, is more difficult and expensive to treat, and more likely to be fatal [8], thus leading to the use of second-line drugs, which are less effective, more toxic and more expensive [8-10]. It is important to point out that 79% of MDR-TB cases are represented by "super strains," resistant to at least

three of the four main drugs used to treat TB [9]. The emergence of MDR strains of pathogenic bacteria has become a worldwide concern, leading to a requirement for new antimicrobial agents, which in turn demands the identification of suitable drug targets. Unfortunately, no new first-line antimycobacterial agents have been identified in the last 25 years to replace the currently used drugs [11]. Although bacille Calmette-Guérin (BCG) still remains the most widely prophylactic strategy used against TB, reactivation of latent infection in adults cannot be prevented in a satisfactory way [12]. Therefore, there is an urgent need for the development of both better vaccines and new and more efficient antimycobacterial agents. Future drugs should present selective toxicity, be active against drug-resistant and non-resistant strains, and shorten short-course treatment duration in order to improve patient compliance. However, little interest has been shown by the pharmaceutical industry, which has not been necessarily attributed to the high investment needed to develop a new anti-TB compound, but to the small financial return awaited, since most TB cases occur in developing countries [13].

### SHIKIMATE PATHWAY

The biosynthesis of aromatic rings from carbohydrate precursors in microorganisms and plants involves a range of extraordinary chemical transformations that together constitute the shikimate pathway; through seven enzymatic steps, phosphoenolpyruvate (PEP) and D-erythrose 4-phosphate (E4P) are condensed to the branch point compound chorismate (endproduct), which leads to several additional terminal pathways [14]. With exception of the first and the fifth enzymes of the common pathway, all others are synthesized constitutively [15]. Although intermediates of the pathway seem to be identical for both prokaryotic and eukaryotic organisms, great differences can sometimes be found in the primary structure and properties of homologous enzymes. One of the remarkable features of this pathway is the very different molecular organization and structure of the enzymes in bacteria and fungi. Most bacteria present all the pathway reaction steps catalyzed by seven separate monofunctional enzymes, encoded by separate genes [16-19], except for *Bacillus subtilis*, which has a trifunctional multienzyme complex (which contains activities for the first, fifth and seventh reaction steps) [20, 21]. Fungi feature a singular system where the first and last reactions are catalyzed by monofunctional

\*Address correspondence to these authors at the Centro de Pesquisas em Biologia Molecular e Funcional, Faculdade de Farmácia, Instituto de Pesquisas Biomédicas, Pontifícia Universidade Católica do Rio Grande do Sul, Porto Alegre, RS, Brazil; Tel: +55-51-33203629; Fax, +55-51-33203629; E-mail, diogenes@puccs.br and luiz.basso@puccs.br

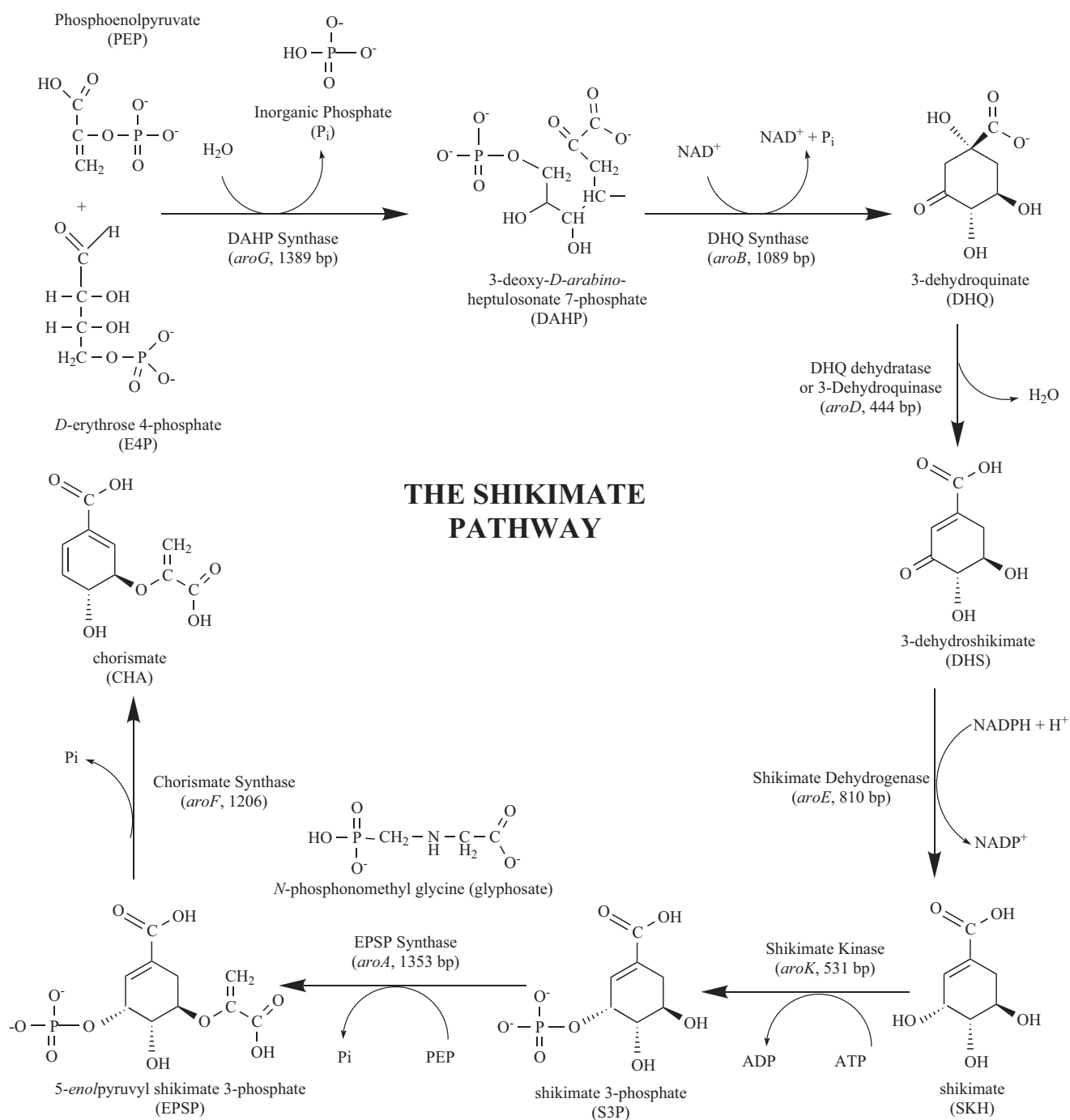


**Fig. (1).** The shikimate pathway (main trunk).

enzymes, and the five central steps are displayed by a single pentafunctional polypeptide called the multifunctional AROM complex [22-26]. Evidence from DNA sequence analysis strongly suggests that the pentafunctional product of this singular gene has evolved through a series of fusions of the ancestral sequences corresponding to the five separate genes present in prokaryotes [27].

The shikimate pathway is an attractive target for herbicide and antimicrobial agent development due to its essentiality in algae, higher plants, bacteria, and fungi, and absence from mammals [28], which have to derive their aromatic compounds from diet. Moreover, biochemical, genetic, and chemotherapeutic evidence presented

for the existence of a functional shikimate pathway in apicomplexan parasites should also provide attractive targets for the development of new antiparasite agents [29, 30].

The complete genome sequence determination of *M. tuberculosis* H37Rv [31] allowed the identification of genes involved in metabolic pathways for the pathogen, by sequence homology. The identification and validation of microbial essential pathways that are absent in its host are important as a first step towards specific inhibitor design with low toxicity [32]. Homologues to enzymes in the shikimate pathway (Fig. (1)) have been identified in the genome sequence of *M. tuberculosis* H37Rv; these genes are located as



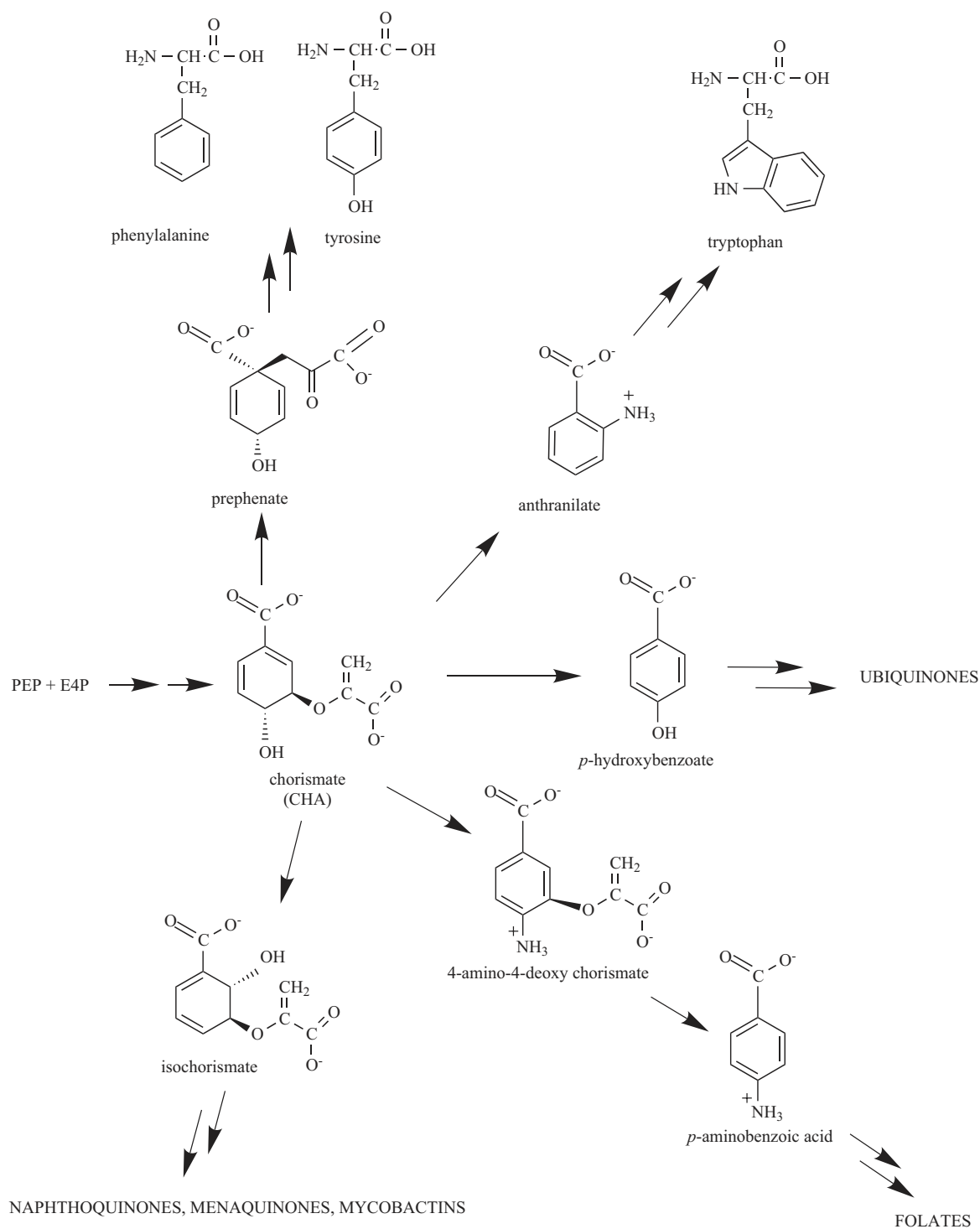


**Fig. (2).** Chorismate is a key precursor of mycobacterial biosynthesis of aromatic amino acids, ubiquinones, folates, naphthoquinones, menaquinones and mycobactins.

follows: *aroD* (Rv2537c), *aroB* (Rv2538c), *aroK* (Rv2539c), *aroF* (Rv2540c) form one cluster of genes, whereas *aroG* (Rv2178c), *aroE* (Rv2552c), *aroA* (Rv3227) do not [31]. These genes have been further shown to be essential for mycobacterial viability, even in the presence of exogenous supplementation [33]. In *M. tuberculosis*, this pathway also leads to the biosynthesis of chorismic acid (Fig. (2)), which is a precursor for the synthesis of aromatic amino acids, ubiquinones, folates, naphthoquinones, menaquinones, and mycobactins [34]. Both essentiality and absence from its human

host validate the shikimate pathway component enzymes as potential target candidates for the development of non-toxic antimycobacterial agents. These reasons have attracted scientific interest for almost three decades in the shikimate pathway enzymes as potential targets for the design of herbicides and antimicrobial compounds [35].

Several approaches are used to identify compounds that inhibit the activity of a particular gene product. An interesting approach relies on the high throughput screening of natural and synthetic

compounds; however, an alternative rational approach can be achieved based on detailed information of target-ligand interactions, usually obtained through tridimensional structure [32]. In order to design new inhibitors, crystal structures of several enzymes of the shikimate pathway have been recently elucidated [36-62]. All of the pathway enzymic steps are of potential interest, and the availability of structures for all of the pathway enzymes should allow rational inhibitor design to progress more rapidly.

Potent compounds have already been identified with inhibitory potential for several enzymes of this pathway. The commercial success of glyphosate as a broad-spectrum post emergence herbicide has already established that the shikimate pathway enzymes are excellent targets for herbicides [63]. These enzymes have also been proposed as targets for antimicrobial agents [64], since shikimate analog compounds such as (6*S*)-6-fluoroshikimic acid have already proven to act as a broad-spectrum antibacterial agent, active against aromatic biosynthesis [65]. Shikimate and other intermediates of the pathway are small, densely functionalized structures that seem to offer options for skeletal modification (analogs) [66]. Synthesis of structural mimics of both putative reactive intermediates and transition states found along enzyme reaction coordinates has proven to be a highly effective strategy for discovery of potent enzyme inhibitors [67]. When stable mimics of reactive intermediates and transition states are synthesized and the extent of enzyme inhibition which is achieved with these mimics is quantitated, insights can be gleaned into enzyme mechanism [68].

In order to pave the way for structural and functional efforts currently under way in our laboratory, and assess the feasibility of utilizing shikimate pathway enzymes as potential targets for antimycobacterial agent development, the genes from *M. tuberculosis* H37Rv were cloned, and their recombinant encoded-proteins expressed in *Escherichia coli* host-cells. The expression and purification of all mycobacterial enzymes will provide protein for crystallization trials aiming at three-dimensional structure determination by X-ray diffraction, which may in turn give a framework on which to base the design of new agents with antitubercular activity with, hopefully, selective therapeutic action. Knowledge of the molecular structure of the active site, as well as the enzymes mechanism of action will undoubtedly aid in the design of useful inhibitors that may be used as antimycobacterial agents. The already published structures should facilitate screening of experimental conditions to obtain crystals of mycobacterial proteins and may provide templates for structure determination by molecular replacement. It is hoped that such inhibitors will eventually give rise to new antimycobacterial drugs. It should be pointed out that the introduction of new drugs into inefficient health programs will accelerate the emergence of resistance to these new compounds. Thereby, these agents shall be used in an intelligent and efficient system manner, avoiding them to turn useless.

### **3-Deoxy-D-Arabino-Heptulosonate-7-Phosphate Synthase (EC 4.1.2.15)**

**(systematic name: 2-dehydro-3-deoxy-D-arabino-heptonate-7-phosphate D-erythrose-4-phosphate-lyase or phospho-2-dehydro-3-deoxyheptonate aldolase)**

The shikimate pathway starting point involves the stereospecific aldol-like condensation of the pentose phosphate pathway intermediate, E4P, and the glycolytic intermediate, PEP, to yield the seven carbon keto acid 3-deoxy-D-arabino-heptulosonate-7-phosphate (DAHP) and release of inorganic phosphate (Pi) from PEP. The reaction is catalyzed by DAHP synthase enzyme and was first demonstrated experimentally in 1959 [69, 70] in *E. coli* cellular extracts. It constitutes the first committed step in the biosynthesis of aromatic amino acids in bacteria, fungi and plants, from which phenylalanine, tyrosine, tryptophan, and various aromatic cofactors and secondary metabolites are derived.

As most microorganisms, wild-type *E. coli* possesses three structural genes - *aroF*, *aroG* and *aroH* - coding for three feedback inhibitor-sensitive DAHP synthase isoenzymes - DAHP synthase (TYR), DAHP synthase (PHE) and DAHP synthase (TRP) - respectively inhibited by their endproducts - tyrosine, phenylalanine and tryptophan; and all by their pathway intermediate, chorismate [28, 71, 72]. The presence of isofunctional enzymes with differentially regulated activities provides the cell with a unique ability to modulate the overall rate of synthesis in response to the availability of the individual aromatic amino acids [36]. Thereby, feedback inhibition of *E. coli* isoenzymes represents the principal means by which metabolite flow into aromatic synthesis is regulated [73]. All three genes were identified by mutation and mapped [74], and sequence analysis suggested a common evolutionary origin, since they have a high degree of sequence similarity and undoubtedly arose by gene duplication and divergence [75].

Inhibition studies have demonstrated that, whereas DAHP synthase (TYR) and DAHP synthase (PHE) inhibition by their respective feedback endproducts reaches 95%, tryptophan does not exceed 60% DAHP synthase (TRP) inhibition [76]. The partial DAHP synthase (TRP) tryptophan-inhibition may constitute a metabolic mechanism which evolved to ensure a basal level of DAHP synthesis under conditions of aromatic amino acid sufficiency. Since inhibition of the DAHP synthase (TYR) and DAHP synthase (PHE) isoenzymes by their respective feedback effectors is essentially complete, the partial inhibition of DAHP synthase (TRP) could provide for the continued synthesis of folates, quinones, and other aromatic derivatives of the shikimate pathway [77]. However, DAHP synthases are, in most microorganisms, but not all, the target for pathway regulation by negative feedback inhibition, which controls carbon flow into the shikimate pathway. Among these exceptions are the hyperthermophilic *Thermotoga maritima*'s thermostable DAHP synthase, which is inhibited by both phenylalanine and tyrosine, but not by tryptophan [78], and the *Pyrococcus furiosus*'s enzyme, which is not inhibited by neither of its pathway endproducts [79]. Furthermore, like the bacterial enzymes, which are regulated at the transcriptional level by repression and at the protein level by aromatic feedback-inhibition of DAHP synthase, plant homologues are also subject to metabolic regulation, although feedback inhibition does not occur for any aromatic amino acid [80]; regulation occurs preferentially at the genetic level [81]. Interestingly, it has been demonstrated that the administration of glyphosate, the inhibitor of the penultimate enzyme of the pathway, in sublethal doses can increase DAHP synthase activity *in vivo* [82], possibly due to a decrease in chorismate production, which leads to an increased carbon flow into the pathway through an increase in DAHP synthase activity. Parallel studies have demonstrated that the reaction can be inhibited by fructose 1,6-diphosphate, sedoheptulose, 1,7-diphosphate, and 3-deoxy-D-arabino-hexonic acid 7-phosphate [70] and a model for the mechanism of allosteric inhibition suggests a loss in the enzyme's binding ability for E4P and a flipped orientation binding for PEP upon phenylalanine binding [83]. Although little has been published involving DAHP synthase inhibition, the first mechanism-based inhibitor for this enzyme has recently been designed and synthesized, and seems to be a very slow binding inhibitor for *E. coli*'s enzyme [84]. The purification of the isoenzymes to homogeneity demonstrated that they are oligomers; the less abundant isoforms, DAHP synthase (TYR) and DAHP synthase (TRP) are 35 kDa and 39 kDa homodimers in solution, respectively [85-87], whereas the major isoform, DAHP synthase (PHE) is a 38 kDa homotetramer of two tight dimers [36, 88]. Further kinetic studies of highly purified *E. coli* DAHP synthase (TYR) and DAHP synthase (PHE) revealed an ordered and sequential mechanism, in which PEP is the first enzyme-binding substrate [86, 89].

There has been an ongoing controversy in the literature regarding the nature of the metal ion at the active site of this enzyme. A

variety of metal ions have been proposed to reside at the active site of DAHP synthase under physiological conditions. The current dogma concerning its identity is that the metal ion giving the highest rate is more likely to be the one assisting the catalytic reaction [90]. Although there are conflicting reports as to which metal is essential for activity maintenance *in vivo*, there is a consensus agreement that all three DAHP synthases are metalloenzymes [91] that have a common requirement for a metal cofactor [92], and which seem to be inactivated upon removal of endogenous metal by treatment with chelating agents [91]. Although homogeneous protein analyses have demonstrated that metal requirement can be satisfied by several divalent cations [92], the native-enzymes' metal preference is still not clear. Different growth conditions seem to play a role in its metal content variation, as copper [93], iron or zinc metalloenzymes, though the last two are the ones preferred *in vivo* [92]. The metal is clearly intimately required at the active site and might play a role in catalysis, and, perhaps, in structural integrity [94].  $\text{Fe}^{+2}$  and, perhaps,  $\text{Zn}^{+2}$ , might actually be the preferred metal cofactors *in vivo*, based on the presence of these two metals in the purified isoenzymes, on the high apparent affinity of DAHP synthase (PHE) for these ions *in vitro*, and on their relatively high bioavailability [92]. However, today, after more than 30 years of research, the nature of the physiological metal ion at the active site of DAHP synthase remains an open question [90]. Furthermore, the metal-enzyme stoichiometries of reactivated DAHP synthase (PHE) apoenzyme indicates that a single metal ion is associated with each enzyme monomer [92], as was previously concluded from the results of similar analyses of DAHP synthase (TRP) [87] and DAHP synthase (TYR) [93].

Sulfhydryl group modification studies on DAHP synthases from different microorganisms have suggested that at least one cysteine residue is essential for catalytic activity [80, 95, 96]; two cysteine residues, cysteine-61 and cysteine-328, have been shown to be highly conserved among all members of the DAHP synthase super family [97]. Mutational analysis of these two residues has demonstrated that cysteine-61 is essential for metal binding and catalytic activity, whereas cysteine-328 is nonessential, although conservative replacements at this position did have significant negative effects on the kinetic properties of the enzyme, suggesting that the latter lies near the active site [98]. However, other mutagenic and spectroscopic studies imply that cysteine-61 is not directly involved in metal binding in DAHP synthase (PHE), but that it might be near the metal binding site or in some way influencing the geometry of the metal binding site [99].

Although most microorganisms and some plants have three DAHP synthase encoding-genes, *M. tuberculosis* genome sequence-homology analysis revealed a single open reading frame (ORF), Rv2178c, identified as the *aroB* gene (1389 bp), coding for a 462 amino acid polypeptide [31]. We have cloned the *aroG* gene from *M. tuberculosis* H37Rv and expressed the recombinant enzyme in its soluble form using electrocompetent *E. coli* Rosetta-gami<sup>TM</sup>(DE3) host-cells (Novagen) grown at 37°C for 24 hours in Luria Bertani (LB) medium. Enzyme activity measurements demonstrated a 92-fold increase in specific activity for cloned extracts in contrast to control, and steady-state velocity analysis revealed a linear dependence on cellular extract volume added to the reaction mixture. Recombinant MtDAHP synthase has been purified approximately 3-fold to electrophoretic homogeneity through an anion exchange, gel filtration and another anion exchange chromatography step. The purification protocol yields 5 mg of homogeneous protein from 6 L of culture (36 g of cells). Electrospray ionization mass spectrometry (ESI-MS) studies determined the subunit molecular mass of active MtDAHP synthase as 50,510.38 Da, and also revealed no peak at the expected mass for the three *E. coli* enzyme isoforms, thus providing evidence for both identity and purity of the recombinant protein. A value of  $253 \pm 25$  kDa was determined for the molecular mass of native MtDAHP synthase homogeneous

protein by analytical gel filtration chromatography, suggesting that the enzyme is stable as a homopentamer in solution [100].

The three-dimensional structure determination of *E. coli* and *T. maritima* DAHP synthases [36-39, 83] provided a better understanding of protein folding and catalytic/regulatory structural details for this DAHP synthase enzyme type. Taking advantage of the fact that the reaction rate of the above mentioned hyperthermophilic enzyme is negligible at 4 °C [78], it was possible to determine the first structure of a DAHP synthase containing both substrates and metal cofactor bound at the active site. The DAHP synthase-Cd-PEP-E4P complex is the first example of such enzyme's structure - containing all reaction components: metal cofactor and both substrates - which have clarified the enzymes' reaction mechanism [39]. More recently, a type II DAHP synthase three-dimensional structure was finally elucidated (from *M. tuberculosis*), revealing an evident evolutionary relationship between the, previously apparently unrelated, type II and I DAHP synthases. Although they share minimal sequence identity and significant differences in quaternary structure, there is a remarkable similarity in protein fold and function, and key residues are completely conserved and closely positioned among the two enzyme types, which indicates a possible common ancestry [40]. Altogether, these structures might aid in the complete elucidation of the enzyme's catalytic mechanism. It becomes important to notice that the structural similarities recently revealed among the DAHP synthase types may suggest that the same inhibitors designed for other DAHP synthase enzymes (type I) could be useful lead compounds for the development of new antimycobacterial agents; the above mentioned type II structure may also be useful for selective inhibitor design for type II enzyme based on key differences revealed among both enzyme types.

### 3-Dehydroquinase Synthase (EC 4.6.1.3)

(systematic name: 3-deoxy-arabino-heptulosonate-7-phosphatase)

The second step in the shikimate pathway, involving the conversion of the seven-carbon keto acid DAHP to 3-dehydroquinase (DHQ), the first carbocyclic metabolite in the pathway, is catalyzed by DHQ synthase. Srinivasan and coworkers were the first group to report the enzymatic reaction in a partially purified preparation from *E. coli* [101]. This enzyme is essential for the synthesis of ring-containing compounds in the common pathway; the reaction assembles the carbocyclic ring that ultimately becomes the benzene ring of aromatic amino acids, coenzyme Q, folic acid, and a range of aromatic secondary metabolites.

DHQ synthase has attracted considerable mechanistic interest and has long been regarded as a catalytic marvel due to its ability to perform several consecutive chemical reactions in one active site during each catalyzed turnover of substrate into product [68, 101-104]. In this sequence, which is mechanistically unusually diverse for a single enzyme, it appears to mediate five sequential transformations: (i) the oxidation of the secondary alcohol at C-5; (ii) the  $\beta$ -elimination of inorganic phosphate across C-6 and C-7; (iii) the reduction of the resulting enone at C-5; (iv) the ring opening of the enol pyranose; and (v) the final intramolecular aldol-like reaction that produces DHQ [101]. The molecular mechanism of the overall reaction has been extensively studied through substrate analogue use [103, 105] and, more recently, by crystal structure analysis [41, 42]. An everlasting debate as to whether DHQ synthase is actively involved in all these steps [101], or whether several steps occur spontaneously, making DHQ synthase a spectator in its own mechanism [102, 103] has ruled for decades. However, DHQ synthase active site arrangement indicates that the enzyme is not just a spectator in catalysis but stabilizes intermediates and prevents side reactions through its entire reaction pathway [41]. This enzyme is mechanistically distinguished by its catalytic requirement and use of  $\text{NAD}^+$  cofactor; reduction of  $\text{NAD}^+$  to NADH during the first step of the enzyme-catalyzed reaction is followed by reoxidation of

NADH to NAD<sup>+</sup> at a later enzyme-catalyzed step prior to release of DHQ from the active site [106].

Increasing attention has recently been paid to the catalytic role of the metal at the active site [107, 108]. There has been considerable disagreement as to whether the native form of DHQ synthase binds Co<sup>+2</sup> or Zn<sup>+2</sup> at its active site. Although the Co<sup>+2</sup>-form of the enzyme has been reported to be more stable and has a higher specific activity [108], the bioavailability of Zn<sup>+2</sup> in nature seems to be much greater [104]; in this sense, DHQ synthase might naturally be a Zn<sup>+2</sup>-metalloenzyme as previously proposed [104]. Experimental data has shown that *Salmonella typhimurium* and *Aspergillus nidulans* enzymes have a second zinc binding site, and that binding of the second Zn<sup>+2</sup> ion to the fungal enzyme is inhibitory [109], as was noted for the bacterial enzyme [107]; such an inhibitory site may potentially regulate the activity of DHQ synthase *in vivo* [109]. Despite the nature of the metal *in vivo*, treatment of the isolated metalloenzyme with ethylenediaminetetraacetic acid (EDTA) results in the rapid formation of inactive apoenzyme, which may be reconstituted by the addition of a variety of different divalent metal cations. The identity of the metal ion not only influences the enzyme's catalytic activity but also affects the rate of NAD<sup>+</sup> dissociation from the active site during turnover. Moreover, substrate binding prevents the removal of Co<sup>+2</sup> by EDTA. Taken together, these results demonstrate a central role for the metal ion in the catalytic mechanism [107]. Hasan and Nester have determined *B. subtilis* enzyme kinetic constants as 5.5 x 10<sup>-5</sup> M for Co<sup>+2</sup>, 5.5 x 10<sup>-5</sup> for NAD<sup>+</sup>, and 1.32 x 10<sup>-4</sup> M for DAHP [110].

A few inhibition studies have been carried out with *E. coli* DHQ synthase activity. The enzyme can be inhibited by NADase, EDTA, tris(hydroxymethyl)aminomethane, and 5,5-diethylbarbiturate [101]. Carbacyclic phosphonate, a DAHP analogue, inhibits DHQ synthase enzyme with a K<sub>i</sub> of 0.8 nM [102]; the nanomolar level, slowly reversible inhibitor amply represents most of the structural features known to be essential to inhibition of DHQ synthase [102, 111]. The strong inhibition associated with carbaphosphonate has been attributed to tight interactions between active site residues and the C-4 ketocarbaphosphonate formed by oxidation of DHQ synthase-bound carbaphosphonate by bound NAD<sup>+</sup> [103]. Carbaphosphonate has been particularly useful for understanding the early steps of the catalyzed reaction [103], as well as identifying critical interactions in the first high-resolution crystal structure of the enzyme [41]. However, the development of potent DHQ synthase inhibitors demands a further detailed characterization of its catalytic mechanism [109].

In prokaryotes, DHQ synthases are encoded by single function genes denoted *aroB* [28]. However, great differences can be found among microorganisms; evidence suggests that *B. subtilis* DHQ synthase forms a trifunctional enzyme complex together with the seventh enzyme of the shikimate pathway and NADPH flavin reductase [110], and in some microbial eukaryotes such as *Neurospora crassa*, *A. nidulans* and *Saccharomyces cerevisiae*, DHQ synthase is active as the N-terminal domain of a penta-domain enzyme (AROM), catalyzing reactions 2 through 6 of the prechorismate part of the pathway [112]. Carpenter and coworkers determined the crystal structure of the DHQ synthase domain of the AROM protein from *A. nidulans* at 1.8 Å resolution with Zn<sup>+2</sup>, NAD<sup>+</sup> and the high-affinity inhibitor, carbaphosphonate, bound at the active site. The crystal structure showed that the enzyme assembles as a functional homodimer, with two domains in each monomer [41]. The *E. coli* DHQ synthase is a monomer with 362 amino acids and a molecular weight (MW) of 38.8 kDa [16].

*M. tuberculosis* genome sequence-homology analysis revealed a single ORF, Rv2538c, identified as the *aroB* gene (1089 bp), coding for a 362 amino acid polypeptide [31]. The mycobacterial gene has been cloned and sequenced, and deduced protein sequence analyses demonstrated that the MtDHQ synthase enzyme is closely related to its equivalent fungal and prokaryotic shikimate pathway

homologues [113]. We have cloned the *aroB* gene from *M. tuberculosis* H37Rv and expressed the recombinant enzyme in its soluble form using electrocompetent *E. coli* BL21<sup>TM</sup>(DE3) host-cells (Novagen) grown at 37°C for 18 hours in LB medium. Enzyme activity measurements and steady-state mechanism studies of MtDHQ synthase are currently underway. Recombinant MtDHQ synthase enzyme has been purified to electrophoretic homogeneity through an anion exchange, hydrophobic interaction and gel filtration chromatography step. The purification protocol is still undergoing optimization in order to obtain higher protein yield. We surely hope to soon determine the stable native enzyme oligomeric state in solution, and mass spectrometry analyses shall determine the subunit molecular mass of active MtDHQ synthase [Mendonça et al. (manuscript in preparation)].

### 3-Dehydroquininate Dehydratase (EC 4.2.1.10)

(systematic name: 3-dehydroquininate hydro-lyase)

Formerly known as dehydroquinase (DHQase), 3-dehydroquininate dehydratase catalyses the third step in the shikimate pathway, the dehydration of DHQ to give 3-dehydroshikimate (DHS), introducing the first double bond of the aromatic ring. The enzymatic reaction of this single-substrate enzyme was first studied by Mitsuhashi and Davis with a partially purified enzyme preparation from both *Aerobacter aerogenes* and *E. coli*, where they also demonstrated the reversibility of the reaction [114]. Interestingly, although most conversion-reactions require a catalytic component, such as an enzyme, various do not; one such case is DHQ, which can be chemically convertible to DHS by heat at an acidic pH [115].

DHQase belongs to an integral part of two metabolic pathways which are characterized by two classes of enzymes - type I and II. Type I DHQase, which is a typified biosynthetic form, is associated exclusively with chorismate biosynthesis in fungi, plants, and some bacteria, catalyzing a *cis(syn)*-dehydration of DHQ with loss of the pro-*R* hydrogen from C-2 via a covalent imine intermediate (Schiff base mechanism) [44]; type II DHQase, which is found in the catabolic quinate pathway of fungi and in the shikimate pathway of many bacteria [116-118] catalyzes a *trans(anti)*-dehydration of DHQ with loss of the more acidic axial pro-*S* hydrogen from C-2 via an enolate intermediate [44]. The biosynthetic type I DHQase consists of three known, constitutively expressed subtypes: a monofunctional form, of which the *E. coli* enzyme has been the most widely studied [19, 22, 119, 120]; a bifunctional form found in plants, which is partnered by the following shikimate pathway enzyme [121-123]; and finally a multifunctional form in which the DHQase activity is located in one domain of the large pentafunctional polypeptide present in fungi [124]. Some fungi possess both DHQase types, although each one fulfills a singular role: type I enzyme is considered the anabolic form of the shikimate pathway, whereas type II constitutes the catabolic form in the pathway that soil organisms employ to degrade the abundant plant metabolite quinate [125]. Type II DHQases have a much smaller subunit molecular mass (16-18 kDa) and they typically oligomerize into a heat-stable homododecameric structure [116, 126]; among some exceptions is the *Streptomyces hygroscopicus* enzyme, which oligomerizes as a homoheptamer [127]. The catabolic quinate pathway, which occurs in saprophytic fungi such as *N. crassa* and *A. nidulans*, provides a route for the conversion of the abundant plant storage compound quinic acid (or its esters) into *p*-hydroxybenzoic acid, which is subsequently degraded to acetyl-CoA and succinyl-CoA by the β-ketoadipate pathway [126, 128, 129] for use as a major source of carbon and energy.

It is generally believed that enzymes have evolved to catalyze reactions by optimal mechanisms, being extremely unusual to find two mechanistically distinct enzymes that catalyze the same reaction. The structures of enzymes catalyzing the reactions in central metabolic pathways are generally well conserved as are their cata-

lytic mechanisms. Therefore, the two DHQase types are somewhat unusual as they are unrelated at the sequence level and utilize completely different mechanisms and stereochemistries [116, 130] to catalyze the same overall reaction, besides having completely different subunit architectures [44], representing an interestingly uncommon example of convergent or parallel evolution [27, 116]. Moreover, little is known about the mechanism of type II DHQases, and all attempts to speculate the role of metal ions as electrophilic catalysts for DHQase have failed; neither a metal nor a tightly bound cofactor seem to be involved in the enzymatic mechanism [131].

*E. coli* type I DHQase [132] is a homodimer encoded by the *aroD* structural gene, which encodes a 240 amino acid polypeptide with a calculated subunit MW of 28 kDa [19, 133]. Type II DHQases, on the other hand, were found only as highly multimeric monofunctional proteins, such as dodecamers of approximately 190 kDa [134], and were first identified as components of the fungal quinate catabolic pathway [118, 128]. Until recently, biosynthetic DHQases were found to be type I in phylogeny, whereas the only examples of type II DHQases were found in the catabolic quinate-utilization pathway; however, they were more recently found as a biosynthetic shikimate pathway component in *Streptomyces coelicolor* [135] and *M. tuberculosis* [113, 134], and as a component of both pathways in *Amycolatopsis methanolica* [129]. Over the past few years it has become clear that classification of type I and type II DHQases as biosynthetic and catabolic-like, respectively, is inappropriate [127].

*M. tuberculosis* has only a single DHQase, type II, involved in the biosynthetic shikimate pathway [113], which is extremely heat-stable, and has the lowest reported  $K_m$  value of any type II DHQase [134]. Interestingly, the MtDHQase has higher similarity both in deduced amino acid sequence and physiological features to the quinate catabolic enzyme from filamentous fungi than to the biosynthetic shikimate pathway prokaryotic ones; thereby, MtDHQase was designated *aroQ* (for quinate) [113]; more recently, however, the structural gene that codes for MtDHQase was also designated *aroD* [31]. Like *Helicobacter pylori* type II DHQase [46], MtDHQase forms a dodecamer of 23 symmetry, with each of the four trimers occupying the face of a tetrahedron. Each subunit has a flavodoxin-like fold, comprised of a central five-stranded parallel  $\beta$ -sheet, which is flanked by two  $\alpha$ -helices on one side and three  $\alpha$ -helices on the other [44], being the minimum size of the active unit a trimer [136]. It seems important to point out that in *S. coelicolor*, arginine-23 might not be simply involved in substrate recognition but must have a catalytic role, and tyrosine-28 has been identified as a residue in or near the active site. Both residues are conserved in all type II DHQases, and the corresponding residues in MtDHQase have been found to be essential for enzyme activity [137].

Very few studies have been performed reporting DHQase structure, all of which representing somewhat preliminary data. Among them, there were type II DHQase structure [47] and in complex with a transition state analog 2,3-anhydro-quinic acid [45], and the crystallization of *M. tuberculosis* enzyme type [138]. A high-throughput screen of hundreds of thousands of compounds recently tested by Robinson and co-workers against purified type II DHQase from *H. pylori* provided a series of compounds with little or no structural similarity to DHQ with considerable inhibitory effect. Although type II DHQases from *H. pylori* and *M. tuberculosis* are extremely similar in active site topology, none of these compounds had equivalent activity against the mycobacterial enzyme [139]. A number of selective inhibitors have been synthesized by Frederickson and co-workers for type II DHQase [140], including 2,3-quinic acid and the above mentioned transition state analog. These inhibitors contain all the structural features of the substrate and transition state, respectively, with the exception of the C-3 carbonyl which is absent [141]. As stated, 2,3-anhydro-quinic acid inhibitor mimics a proposed transition state, and it has been shown that inhibitors with

a double bond between C-2 and C-3 bind significantly more tightly than those lacking this bond [140], as it has a  $K_i$  of 30  $\mu$ M for this enzyme, 20-fold lower than the  $K_m$  for substrate [45]; this was the first report of inhibitors of type II DHQase [140]. More recent studies with a series of analogues of the known inhibitor (1*R*,3*R*,4*R*)-1,3,4-trihydroxycyclohex-5-en-1-carboxylic acid revealed the most potent inhibitor reported to date for type II enzyme from *M. tuberculosis*, the 3-nitrophenyl derivative, with a  $K_i$  of 54 nM, more than 700 times lower than the  $K_m$  of the substrate [142].

*M. tuberculosis* genome sequence-homology analysis revealed a single ORF, Rv2537c, identified as the *aroD* gene (444 bp), coding for a 147 amino acid polypeptide [31], with a subunit MW of approximately 15.8 kDa. We have cloned the *aroD* gene from *M. tuberculosis* H37Rv and overexpressed the recombinant enzyme in its soluble form using electrocompetent *E. coli* BL21<sup>TM</sup>(DE3) host-cells (Novagen) grown at 37°C for 24 hours in LB medium. Enzyme kinetics studies, isotope effects, and crystal structure determination efforts are currently underway.

### Shikimate 5-Dehydrogenase (EC 1.1.1.25)

(systematic name: shikimate:NAD<sup>+</sup> 5-oxido reductase)

The fourth step in the shikimate pathway, involving the reversible conversion of DHS and NADPH to yield shikimate, a 3, 4, 5-trihydroxycyclohexene-1-carboxylic acid, and NADP<sup>+</sup>, is catalyzed by shikimate 5-dehydrogenase (SD), originally called DHS reductase [17, 28, 143]. The NADPH-dependent reduction of DHS was first demonstrated in extracts of *E. coli* by Yaniv and Gilvarg in 1955 [143].

This enzyme belongs to a superfamily of NAD(P)H-dependent oxidoreductases that act in anabolic and catabolic pathways [48]. *E. coli* expresses two SD paralogs, the NADP-dependent AroE and a putative YdiB enzyme; these enzymes are the only two proteins from the SD family present in this microorganism. YdiB is a dual specificity quinate/shikimate dehydrogenase that can utilize either NAD<sup>+</sup> or NADP<sup>+</sup> as a cofactor. Like all presently known NAD-dependent quinate/shikimate dehydrogenases, these two enzymes are involved in the catabolic quinate pathway, which allows growth of microorganisms with quinate as the sole carbon source by its conversion into protocatechuate and subsequent metabolism by the  $\beta$ -ketoacid pathway [49]. The presence of two SD isoforms in *E. coli* raises intriguing questions concerning their specific biological roles. The existence of a second SD also affects the design of any potential drugs, because YdiB might compensate for AroE inhibition, although it is not yet clear if YdiB participates in the shikimate pathway or has another biological function. A systematic analysis of the bacterial genomes revealed that 14 species possess at least two SD isoenzymes, showing that this phenomenon is not only limited to *E. coli* or related species [49].

Although dehydrogenases usually form oligomers, SDs, encoded by the *aroE* structural gene, are present as a monomer in most bacteria [17, 144]; *E. coli* *aroE* structural gene codes for a 272 amino acid polypeptide which behaves as a 30 kDa monomer [17, 144] with 56  $\mu$ M and 65  $\mu$ M Michaelis constants for NADP<sup>+</sup> and shikimate, respectively [49]. SD structures have been recently solved for *E. coli* [49] and *Haemophilus influenzae* [52], as well as the structure of SD paralog YdiB from *E. coli* [48, 49], among a few others. Like the *E. coli* AroE [49], *Methanococcus jannaschii* SD structure determination revealed an enzyme with a deep cleft, which contains the active site, formed at the junction of two domains, responsible for binding the NADP<sup>+</sup> cofactor. The C-terminal domain is easily recognizable as a Rossmann fold dinucleotide binding domain, responsible for binding the NADP<sup>+</sup> cofactor; the N-terminal substrate binding and dimerization domain, an  $\alpha$ - $\beta$ - $\alpha$  sandwich, represents a unique topological fold [50, 51]. The crystal structures of AroE from *H. influenzae* both in its apo form and in complex with NADPH, also revealed a molecule with two domains,

a catalytic domain with a novel open twisted  $\alpha/\beta$  motif and an NADPH binding domain with a typical Rossmann fold [52].

The very few inhibition studies performed to date have revealed that 1,6-dihydroxy-2-oxoisonicotinic acid, a novel DHS analogue synthesized as a potential herbicide, proved to be a competitive inhibitor when the enzyme was assayed in the direction of DHS formation (0.12 mM), but showed no inhibition in the reverse direction, even at very low DHS concentrations. This differential inhibition was particularly surprising as the structure resembles DHS more than it does shikimate. Other inhibitor compounds in the same series also display this anomalous behavior [145, 146].

Although some microorganisms have two SD encoding-genes, *M. tuberculosis* genome sequence-homology analysis revealed a single ORF, Rv2552c, identified as the *aroE* gene (810 bp), coding for a 269 amino acid polypeptide [31]. We have cloned the *aroE* gene from *M. tuberculosis* H37Rv and expressed the recombinant enzyme in its soluble form using electrocompetent *E. coli* BL21<sup>TM</sup>(DE3) host-cells (Novagen) grown at 37°C for 24 hours in LB medium [147]. A simple method of releasing cytoplasmic proteins without cell lysis by repeated cycles of freezing and thawing [148] has been shown to be essential for some recombinant protein solubility. SDS-PAGE protein band densitometric quantification analysis showed that MtSD constitutes approximately 8% of total protein present in the soluble cell extract under the experimental conditions used. Enzyme activity measurements demonstrated a 5-fold increase in specific activity for cloned extracts in contrast to control, and steady-state velocity analysis revealed a linear dependence on cellular extract volume added to the reaction mixture [147]. Recombinant MtSD has been purified approximately 8.5-fold to electrophoretic homogeneity through an anion exchange, hydrophobic interaction, gel filtration, and another anion exchange chromatography step. The purification protocol yields 11 mg of homogeneous protein (98% purity) with a specific activity value of approximately 3.90 U mg<sup>-1</sup> from 49 g of cells. The enzyme appears to be a dimer of approximately 58 kDa in solution with subunit molecular mass value of 27,076 Da (ESI-MS). Apparent  $K_m$  values for DHS, NADPH, shikimate and NADP<sup>+</sup> are 31  $\mu$ M, 10  $\mu$ M, 50  $\mu$ M, and 22  $\mu$ M, respectively [149].

### **Shikimate Kinase (EC 2.7.1.71)**

#### **(systematic name: ATP:shikimate 3-phosphotransferase)**

The second half of the shikimate pathway initiates (fifth step) with the reaction catalyzed by shikimate kinase (SK). The enzyme catalyzes a phosphate transfer from ATP co-substrate to the carbon-3 hydroxyl group of shikimate resulting in the formation of shikimate-3-phosphate (S3P) and ADP.

Both *S. typhimurium* [22, 150] and *E. coli* [22, 151] have two SK enzyme isoforms, *aroK*-encoded type I (SKI) [152, 153] and *aroL*-encoded type II (SKII) [18, 151, 154], which share 30% identity and 46% similarity over their entire length. *E. coli aroK*-encoded SKI [151, 153, 155] and *aroL*-encoded SKII [18] are monomeric proteins with a MW of 19.5 kDa containing 173 amino acid residues; their similar size and homology suggest a common origin [153]. The presence of two enzymes explains the failure to isolate bacterial mutants lacking this activity, since independent mutations would be required in two separate genes. Enzyme activity is dependent on the presence of a divalent cation as a cofactor; Mg<sup>2+</sup> has been shown to be the most effective one, although significant activity was obtained with all of the other divalent cations tested [156]. Inhibition studies have demonstrated that neither one is inhibited by their endproducts [156].

Isofunctional enzymes are usually observed catalyzing leader (branch) reactions of pathways that display a further endproduct ramification; these are the ones whose encoding genes are frequently affected through specific regulation. It is therefore unusual for there to be two isoforms in the middle of a metabolic pathway,

and the reason for the existence of two SK isoenzymes is not known; however, it has been proposed that shikimate may be a branch-point intermediate for two different pathways [157]. It should be pointed out that, among all the genes of the common pathway, *aroF*, *aroG*, *aroH*, and *aroL* are the only ones subjected to control [158]. However, as to whether the *E. coli* observed gene regulation system is somewhat similar among prokaryotes remains to be established, since no SK activity regulation has been observed in *S. typhimurium*, in the conditions tested [158]. Interestingly, the only known function for which a shikimate pathway gene had not been identified was SKI [151]; some years of research allowed the identification [159] and assignment [152] of an ORF as the gene encoding SKI in *E. coli*, designated *aroK*.

Although they seem to catalyze the same reaction, SKII isoform appears to play a dominant role in the shikimate pathway in *E. coli*, being the principal enzyme which phosphorylates shikimate in the cell [156, 160]; its expression is controlled by the *tyrR* regulator, and it is repressed by tyrosine and tryptophan [151, 160]. However, the physiological role of SKI is much less clear, as the enzyme seems to be expressed constitutively and has a much lower affinity for shikimate ( $K_m$  of 20 mM compared with 0.2 mM for SKII) [156]. Since expression deficiency caused by mutations in the *aroK* gene are associated with sensitivity to the antibiotic mecillinam [161], it has been suggested that SKI may have an alternative biological role in which it phosphorylates shikimate only fortuitously [156]. Hence, SKI might phosphorylate (or otherwise modify) some substrate other than shikimate and this product results in a lower division potential [161]. Evidence also suggests that SKI might have a function in the transport of amino acids, at least in *Lactobacillus* [162]. Contrary to the presence of isoenzymes in *E. coli*, complete genome sequences of a number of bacteria, for example, *H. influenzae* and *M. tuberculosis*, have revealed the presence of only one SK-coding gene. Most of these SKs appear to be encoded by *aroK* rather than *aroL* because their amino acid sequences have higher degree of identity with *E. coli* SKI. The kinetic parameters for *aroK*-encoded MtSK ( $K_m$  shikimate = 410  $\mu$ M /  $K_m$  ATP = 83  $\mu$ M) [55, 163] are more similar to those of *aroL*-encoded *E. coli* SKII than to those of *aroK*-encoded *E. coli* SKI [55].

MtSK belongs to the family of nucleoside monophosphate (NMP) kinases, which are composed of three domains: (1) the CORE domain containing the five stranded parallel  $\beta$ -sheet and the P-loop (residues 9-17), which forms the binding site for nucleotides; (2) the LID domain (residues glycine-112 to aspartate-124), which closes over the active site and has residues that are essential for the binding of ATP; and the NMP-binding domain (residues threonine-33 to glutamate-61), which functions to recognize and bind shikimate [53, 55, 57, 164-166]. The residue glutamate-61 is conserved in both *aroK*- and *aroL*-encoded SK enzymes and has been implicated in shikimate binding [54-56]. It plays an important role in positioning a shikimate molecule, even though it is not directly involved in substrate binding [57]. Several reports have suggested that the enzyme undergoes conformational changes during catalysis [53, 54, 57, 164], and the regions responsible for this movement are the NMP-binding site and the LID domain. Kinases should undergo large movements during catalysis to shield their active center from water in order to avoid ATP hydrolysis [166]. Although several SK structures have been solved, such as the *Erwinia chrysanthemi* [54], *E. coli* (SKI) [56], *Campylobacter jejuni* (unpublished, PDB accession code 1VIA) and MtSK [55], among others, Pereira and co-workers were the first group to solve the three-dimensional structure of any SK complexed with shikimate. In MtSK, the glutamate-61 residue that is strictly conserved among SKs forms a hydrogen bond and salt bridge with arginine-58 and assists in positioning the guanidinium group of arginine-58 for shikimate binding [163]. The more recently published crystal structure of MtSK in complex with shikimic acid and an ATP analogue should also help the elucidation of the enzymological conforma-

tional changes upon substrate (both) binding and structure-based inhibitor design [58]. Detailed data on SK structural analysis will be provided in an accompanying paper in this issue by Pereira *et al.*

Very few inhibition studies have been performed with SK enzyme. An and co-workers [66] have proposed cyclopentylideneacetates, as well as cyclopentenyl structures, as ring contracted analogues of shikimic acid, although these five-membered ring shikimate analogues were designed in the absence of any knowledge of the structure of substrate-bound SK. Notwithstanding, elucidation of MtSK crystal structures may now allow improvement of efficacy of previous shikimate analogues.

Although a few microorganisms have more than one SK encoding-gene, *M. tuberculosis* genome sequence-homology analysis revealed a single ORF (as above stated), Rv2539c, identified as the *aroK* gene (531 bp), coding for a 176 amino acid polypeptide [31]. We have cloned the *aroK* gene from *M. tuberculosis* H37Rv and expressed the recombinant enzyme in its soluble form using electrocompetent *E. coli* BL21<sup>TM</sup>(DE3) host-cells (Novagen) grown at 37°C for 23 hours in LB medium. SDS-PAGE protein band densitometric quantification analysis showed that MtSK constitutes approximately 30% of total protein present in the soluble cell extract under the experimental conditions used. Enzyme activity measurements demonstrated a 328-fold increase in specific activity for cloned extracts in contrast to control, and steady-state velocity analysis revealed a linear dependence on cellular extract volume added to the reaction mixture [167]. The development of purification protocols to obtain homogeneous recombinant protein allowed determination of the three-dimensional structure of MtSK [163].

#### 5-Enolpyruvylshikimate-3-Phosphate Synthase (EC 2.5.1.19)

(systematic name: phosphoenolpyruvate: 3-phosphoshikimate 5-O-(1-carboxyvinyl)-transferase)

The sixth (penultimate) step in the shikimate pathway, involving the entry of a second PEP in the pathway, and which is, along with S3P, condensed to yield 5-enolpyruvylshikimate-3-phosphate (EPSP) and P<sub>i</sub>, is catalyzed by EPSP synthase. Levin and Sprinson were the first ones to demonstrate EPSP formation as a product of *E. coli* EPSP synthase activity [168, 169]. As was previously proposed in *E. coli* [169], it has been actually demonstrated in *S. typhimurium* that the reaction mechanism involves the unusual transfer of the enolpyruvyl moiety from PEP apparently unchanged to the acceptor molecule [170]. *E. coli* EPSP synthase subunit MW was estimated to be 49 kDa by SDS-PAGE, and the native MW was estimated to be 55 kDa by gel filtration, indicating that the enzyme is monomeric [171].

The enzyme is the cellular target for N-[phosphonomethyl]-glycine, the active ingredient of the broad-spectrum, nonselective herbicide glyphosate [172]. Inhibition of the EPSP synthase reaction by glyphosate is competitive with respect to PEP, with a K<sub>i</sub> of 1.1 μM, and uncompetitive with respect to S3P [173]. Although the binding of the potent reversible inhibitor glyphosate is competitive with PEP, the ternary complex EPSP synthase-S3P-glyphosate may not be a transition state analog, because PEP and glyphosate binding is apparently not identical [174, 175]. It has long been known that glyphosate inhibits bacterial growth *in vitro* [176, 177]. The inhibition of the growth of apicomplexan parasites *in vitro* by glyphosate provided the first evidence of the occurrence of the shikimate pathway in this important group of mammalian pathogens; the glyphosate therapeutic potential success has been demonstrated in mice as an efficient agent against the pathogenic protozoans that cause diseases like toxoplasmosis or malaria [29]. However, its efficacy displays great variations among different organisms, as much as three orders of magnitude inhibitor-constant variations may be found when some plant and bacterial enzymes are compared; generally, plant EPSP synthases have lower K<sub>i</sub> values for glyphosate than their bacterial homologues [125]. Efforts have been

made towards elucidating the herbicide-enzyme interaction [178] and to seek other compounds with similar inhibitory capabilities. Insight into the reason for glyphosate potency through formation of a dead-end ternary complex of enzyme, shikimate phosphate and glyphosate was provided by Boocock and Coggins [173]. Subsequent mechanistic, kinetic and structural studies on EPSP synthase have extended our understanding [59, 60, 179, 180], but interestingly no more commercially important inhibitors of this enzyme have emerged.

A few research groups discovered some transition state analogs through benzene ring substitution of the shikimate ring, which show potent EPSP synthase inhibition [181-183]. It is important to point out that enzyme inhibition requires very small concentrations (nM) of some of these inhibitors, and they are readily accessible through organic synthesis; thereby, these may represent the next generation of commercial herbicides that also function through inhibition of the shikimate pathway. Further detailed data on EPSP synthase will be provided in an accompanying paper in this issue by Marques *et al.*

*M. tuberculosis* genome sequence-homology analysis revealed a single ORF, Rv3227, identified as the *aroA* gene (1353 bp), coding for a 450 amino acid polypeptide, with a 46.43 kDa predicted MW [31]. Although Garbe and co-workers cloned *M. tuberculosis* *aroA* gene, their focus relied on gene characterization (sequencing) and MtEPSP synthase immunochemical analysis [184]. We have cloned the *aroA* gene from *M. tuberculosis* H37Rv and expressed the recombinant enzyme in its soluble form using electrocompetent *E. coli* BL21<sup>TM</sup>(DE3) host-cells (Novagen) grown at 37°C for 14.7 hours in LB medium. SDS-PAGE protein band densitometric quantification analysis showed that MtEPSP synthase constitutes approximately 40% of total protein present in the soluble cell extract under the experimental conditions used. Enzyme activity measurements demonstrated a 101-fold increase in specific activity for cloned extracts in contrast to control, and steady-state velocity analysis revealed a linear dependence on cellular extract volume added to the reaction mixture [167]. Recombinant MtEPSP synthase has been purified approximately 2.8-fold to electrophoretic homogeneity through a simple one-step purification protocol using an anion exchange column. The purification protocol yields 53 mg of homogeneous protein from 1 L of culture, with a specific activity value of approximately 18 U mg<sup>-1</sup> [185]. Steady-state kinetics, isotope effects, pre-steady-state kinetics and crystal structure determination studies are currently underway in our laboratory. Recent results in our group suggested that the presence of P<sub>i</sub> induces conformational changes (closure movement) in MtEPSP synthase [186].

#### Chorismate Synthase (EC 4.6.1.4)

(systematic name: 5-O-(1-Carboxyvinyl)-3-phosphoshikimate phosphate-lyase)

The seventh and final reaction in the main trunk of the shikimate pathway introduces another (second) double bond into the aromatic ring system and gives chorismic acid and P<sub>i</sub> through a *trans*-1,4 elimination of phosphate from EPSP [187, 188]. The reaction is catalyzed by chorismate synthase (CS) and requires reduced flavin mononucleotide (FMN) as a coenzyme for activity, even though, like DHQ synthase, the overall reaction is redox neutral; it is an unusual reaction in that the redox state of the functional cofactor flavin remains unchanged. After the establishment of chorismate chemical structure, it was shown that it could be formed from EPSP by cell extracts of *E. coli* [189].

The *E. coli* CS subunit MW is 38 kDa and the native enzyme has shown to be a tetramer [190], which seems to have its activity inhibited by iron chelators and by high Fe<sup>+2</sup> levels [189]. CS activity has been shown to vary among different organisms; it is monofunctional in *E. coli* and higher plants, bifunctional in *N. crassa* (the best-studied bifunctional CS), and trifunctional heterotrimeric in

*B. subtilis*. Monofunctional CS requires reduced flavin addition to *in vitro* enzyme assays; bifunctional enzyme has an associated NADP-driven flavin reductase within the same polypeptide chain [125]. A more thorough description on CS may be found in an accompanying paper in this issue by Dias *et al.*

*M. tuberculosis* genome sequence-homology analysis revealed a single ORF, Rv2540c, identified as the *aroF* gene (1206 bp), coding for a 401 amino acid polypeptide [31]. We have cloned the *aroF* gene from *M. tuberculosis* H37Rv and expressed the recombinant enzyme in its soluble form using electrocompetent *E. coli* Rosetta™(DE3) host-cells (Novagen) grown at 37°C for 18h hours in LB medium. Enzyme activity measurements and steady-state velocity of MtCS are currently underway. Recombinant MtCS has been purified to electrophoretic homogeneity through an anion exchange and hydrophobic interaction chromatography step, and proven to be a homodimer in solution. The purification protocol yields 170 mg of homogeneous protein from 6 L of culture (25 g of cells). ESI-MS determined the subunit molecular mass of active MtCS as 41,804.04 Da, and N-terminal sequencing revealed that the first methionine was not removed [Ely *et al.* (manuscript submitted to BBRC)]. Crystallization and X-ray crystallographic analyses [191], structural modeling (MtCS with FMN and EPSP) [Fernandes *et al.* (*in press*)] and structure determination (in the apo state) [62] have been performed in our laboratory in order to elucidate MtCS substrate requirements and enzyme mechanism of action.

#### CONCLUDING REMARKS

The TB Structural Genomics Consortium is an organization devoted to encouraging, coordinating, and facilitating the determination and analysis of structures of proteins from *M. tuberculosis* [192]. Studies being conducted by the TB Structural Genomics Consortium will make available the structures of many potential target proteins and should provide important information such as the biological function of proteins harboring no homology to any known protein. A number of these proteins must be selected for further analysis and computational chemistry techniques applied to identify leads. It is hoped that an understanding of the enzyme and chemical mechanisms of action of mycobacterial shikimate pathway enzymes as well as their three-dimensional structures will provide a framework on which to base the rational design of antimycobacterial agents.

#### ACKNOWLEDGEMENTS

Financial support for this work was provided by Millennium Initiative Program MCT-CNPq, Ministry of Health - Secretary of Health Policy (Brazil) to DSS and LAB. DSS (304051/1975-06) and LAB (520182/99-5) are research career awarded from the National Research Council of Brazil (CNPq).

#### ABBREVIATIONS

AIDS	=	acquired immune deficiency syndrome
BCG	=	bacille Calmette-Guérin
CS	=	chorismate synthase
DAHP phosphate	=	3-deoxy-D-arabino-heptulosonate-7-phosphate
DHQ	=	3-dehydroquininate
DHQase	=	dehydroquininate dehydratase
DHS	=	3-dehydroshikimate
E4P	=	D-erythrose 4-phosphate
EDTA	=	ethylenediaminetetraacetic acid
EPSP	=	5-enolpyruvylshikimate-3-phosphate
ESI-MS	=	electrospray ionization mass spectrometry

LB	=	Luria Bertani
MDR-TB	=	multidrug-resistant tuberculosis
Mt	=	<i>Mycobacterium tuberculosis</i>
MW	=	molecular weight
NMP	=	nucleoside monophosphate
ORF	=	open reading frame
PEP	=	phosphoenolpyruvate
P <sub>i</sub>	=	inorganic phosphate
S3P	=	shikimate-3-phosphate
SD	=	shikimate 5-dehydrogenase
SK	=	shikimate kinase
TB	=	tuberculosis

#### REFERENCES

- [1] Enarson, D.A. and Murray, J.F. (1996) *in Tuberculosis* (Rom, W.M. and Garay, S., Eds.), Little, Brown and Co., Boston, MA, pp. 57-75.
- [2] World Health Organization (1998) WHO/TB/98.237.
- [3] World Health Organization (2004) WHO/HTM/TB/2004.331.
- [4] Young, D.B. (1998) *Nature*, **393**, 515-516.
- [5] Murray, C.J.L. (1994) *in Tuberculosis: Pathogenesis, Protection, and Control* (Bloom, B.R., Ed.), ASM, Washington, pp. 583-622.
- [6] Bloom, B.R. and Murray, C.J.L. (1992) *Science*, **257**, 1055-1064.
- [7] Basso, L.A. and Blanchard, J.S. (1998) *Adv. Exp. Med. Biol.*, **456**, 115-144.
- [8] WHO Global tuberculosis programme - Tuberculosis Fact Sheet, 1998. [<http://www.who.int/gtb/publications/index.htm#Reports>].
- [9] World Health Organization (2004) *Saudi. Med. J.*, **25**, 1139-1140.
- [10] Stokstad, E. (2000) *Science*, **287**(5462), 2391.
- [11] Petrini, B. and Hoffner, S. (1999) *Int. J. Antimicrob. Agents*, **13**, 93-97.
- [12] Colditz, G.A.; Brewer, T.F.; Berkey, C.S.; Wilson, M.E.; Burdick, E.; Fineberg, H.V. and Mosteller, F. (1994) *J. Am. Med. Assoc.*, **271**, 698-702.
- [13] Ruffino-Netto, A. (2002) *Rev. Soc. Bras. Med. Trop.*, **35**, 51-58.
- [14] Pittard, A.J. (1996) *in Escherichia coli and Salmonella: Cellular and Molecular Biology*, (Neidhardt, F.C., Ed.), ASM Press, Washington, DC, pp. 458-484.
- [15] Tribe, D.E.; Camakaria, H. and Pittard, J. (1976) *J. Bacteriol.*, **127**, 1085-1097.
- [16] Millar, G. and Coggins, J.R. (1986) *FEBS Lett.*, **200**(1), 11-17.
- [17] Anton, I.A. and Coggins, J.R. (1988) *Biochem. J.*, **249**(2), 319-326.
- [18] Millar, G.; Lewendon, A.; Hunter, M.G. and Coggins, J.R. (1986) *Biochem. J.*, **237**(2), 427-437.
- [19] Duncan, K.; Chaudhuri, S.; Campbell, M.S. and Coggins, J.R. (1986) *Biochem. J.*, **238**(2), 475-483.
- [20] Nakatsukasa, W.M. and Nester, E.W. (1972) *J. Biol. Chem.*, **247**(18), 5972-5979.
- [21] Huang, L.; Montoya, A.L. and Nester, E.W. (1975) *J. Biol. Chem.*, **250**(19), 7675-7681.
- [22] Berlyn, M.B. and Giles, N.H. (1969) *J. Bacteriol.*, **99**(1), 222-230.
- [23] Kinghorn, J.R. and Hawkins, A.R. (1982) *Mol. Gen. Genet.*, **186**(1), 145-152.
- [24] Charles, I.G.; Keyte, J.W.; Brammar, W.J. and Hawkins, A.R. (1985) *Nucleic Acids Res.*, **13**(22), 8119-8128.
- [25] Charles, I.G.; Keyte, J.W.; Brammar, W.J.; Smith, M. and Hawkins, A.R. (1986) *Nucleic Acids Res.*, **14**(5), 2201-2213.
- [26] Coggins, J.R.; Boocock, M.R.; Chaudhuri, S.; Lambert, J.M.; Lumsden, J.; Nimmo, G.A. and Smith, D.D. (1987) *Methods Enzymol.*, **142**, 325-341.
- [27] Hawkins, A.R. (1987) *Curr. Genet.*, **11**(6-7), 491-498.
- [28] Bentley, R. (1990) *Crit. Rev. Biochem. Mol. Biol.*, **25**(5), 307-384.
- [29] Roberts, F.; Roberts, C.W.; Johnson, J.J.; Kyle, D.E.; Krell, T.; Coggins, J.R.; Coombs, G.H.; Milhous, W.K.; Tzipori, S.; Ferguson, D.J.; Chakrabarti, D. and McLeod, R. (1998) *Nature*, **393**(6687), 801-805.
- [30] McConkey, G.A. (1999) *Antimicrob. Agents Chemother.*, **43**(1), 175-177.
- [31] Cole, S.T.; Brosch, R.; Parkhill, J.; Garnier, T.; Churcher, C.; Harris, D.; Gordon, S.V.; Eiglmeier, K.; Gas, S.; Barry, C.E. 3rd;



- Tekaia, F.; Badcock, K.; Basham, D.; Brown, D.; Chillingworth, T.; Connor, R.; Davies, R.; Devlin, K.; Feltwell, T.; Gentles, S.; Hamlin, N.; Holroyd, S.; Hornsby, T.; Jagels, K. and Barrel, B.G. (1998) *Nature*, **393**(6685), 537-544.
- [32] Duncan, K. (2003) *Tuberculosis (Edinb)*, **83**(1-3), 201-207.
- [33] Parish, T. and Stoker, N.G. (2002) *Microbiology*, **148**(Pt 10), 3069-3077.
- [34] Ratledge, C. (1982) in *The Biology of the Mycobacteria* (Ratledge, C. and Stanford, J.L., Eds.), Academic Press, London, pp. 185-271.
- [35] Coggins, J.R.; Abell, C.; Evans, L.B.; Frederickson, M.; Robinson, D.A.; Roszak, A.W. and Laphorn, A.P. (2003) *Biochem. Soc. Trans.*, **31**(Pt 3), 548-552.
- [36] Shumilin, I.A.; Kretsinger, R.H. and Bauerle, R. (1999) *Struct. Folding Des.*, **7**(7), 865-875.
- [37] Wagner, T.; Shumilin, I.A.; Bauerle, R. and Kretsinger, R.H. (2000) *J. Mol. Biol.*, **301**, 389-399.
- [38] Shumilin, I.A.; Bauerle, R. and Kretsinger, R.H. (2003) *Biochemistry*, **42**, 3766-3776.
- [39] Shumilin, I.A.; Bauerle, R.; Wu, J.; Woodard, R.W. and Kretsinger, R.H. (1998) *J. Mol. Biol.*, **341**(2), 455-466.
- [40] Webby, C.J.; Baker, H.M.; Lott, J.S.; Baker, E.N. and Parker, E.J. (2005) *J. Mol. Biol.*, **354**(4), 927-939.
- [41] Carpenter, E.P.; Hawkins, A.R.; Frost, J.W. and Brown, K.A. (1998) *Nature*, **394**(6690), 299-302.
- [42] Nichols, C.E.; Hawkins, A.R. and Stammers, D.K. (2004) *Acta Crystallogr. D Biol. Crystallogr.*, **60**(Pt 5), 971-973.
- [43] Sugahara, M.; Nodake, Y.; Sugahara, M. and Kunishima, N. (2005) *Proteins*, **58**(1), 249-252.
- [44] Gourley, D.G.; Shrive, A.K.; Polikarpov, I.; Krell, T.; Coggins, J.R.; Hawkins, A.R.; Isaacs, N.W. and Sawyer, L. (1999) *Nat. Struct. Biol.*, **6**(6), 521-525.
- [45] Roszak, A.W.; Robinson, D.A.; Krell, T.; Hunter, I.S.; Fredrickson, M.; Abell, C.; Coggins, J.R. and Laphorn, A.J. (2002) *Structure (Camb)*, **10**(4), 493-503.
- [46] Lee, B.I.; Kwak, J.E. and Suh, S.W. (2003) *Proteins*, **51**(4), 616-617.
- [47] Maes, D.; Gonzalez-Ramirez, L.A.; Lopez-Jaramillo, J.; Yu, B.; De Bondt, H.; Zegers, I.; Afonina, E.; Garcia-Ruiz, J.M. and Gulnik, S. (2004) *Acta Crystallogr. D Biol. Crystallogr.*, **60**(Pt 3), 463-471.
- [48] Benach, J.; Lee, I.; Edstrom, W.; Kuzin, A.P.; Chiang, Y.; Acton, T.B.; Montelione, G.T. and Hunt, J.F. (2003) *J. Biol. Chem.*, **278**(21), 19176-19182.
- [49] Michel, G.; Roszak, A.W.; Sauve, V.; Maclean, J.; Matte, A.; Coggins, J.R.; Cygler, M. and Laphorn, A.J. (2003) *J. Biol. Chem.*, **278**(21), 19463-19472.
- [50] Padyana, A.K. and Burley, S.K. (2003) *Structure (Camb)*, **11**(8), 1005-1013.
- [51] Vogan, E. (2003) *Structure (Camb)*, **11**(8), 902-903.
- [52] Ye, S.; Von Delft, F.; Brooun, A.; Knuth, M.W.; Swanson, R.V. and McRee, D.E. (2003) *J. Bacteriol.*, **185**(14), 4144-4151.
- [53] Vonnrhein, C.; Schlauderer, G.J. and Schulz, G.E. (1995) *Structure*, **3**(5), 483-490.
- [54] Krell, T.; Coggins, J.R. and Laphorn, A.J. (1998) *J. Mol. Biol.*, **278**(5), 983-997.
- [55] Gu, Y.; Reshetnikova, L.; Li, Y.; Wu, Y.; Yan, H.; Singh, S. and Ji, X. (2002) *J. Mol. Biol.*, **319**(3), 779-789.
- [56] Romanowski, M.J. and Burley, S.K. (2002) *Proteins*, **47**(4), 558-562.
- [57] Pereira, J.H.; Oliveira, J.S.; Canduri, F.; Dias, M.V.; Palma, M.S.; Basso, L.A.; de Azevedo, W.F. Jr and Santos, D.S. (2004) *Biochem. Biophys. Res. Commun.*, **325**(1), 10-17.
- [58] Gan, J.; Gu, Y.; Li, Y.; Yan, H. and Ji, X. (2006) *Biochemistry*, **45**(28), 8539-8545.
- [59] Stallings, W.C.; Abdel-Meguid, S.S.; Lim, L.W.; Shieh, H.S.; Dayringer, H.E.; Leimgruber, N.K.; Stegeman, R.A.; Anderson, K.S.; Sikorski, J.A.; Padgett, S.R. and Kishore, G.M. (1991) *Proc. Natl. Acad. Sci. USA*, **88**(11), 5046-5050.
- [60] Schonbrunn, E.; Eschenburg, S.; Shuttleworth, W.A.; Schloss, J.V.; Amrhein, N.; Evans, J.N. and Kabsch, W. (2001) *Proc. Natl. Acad. Sci. USA*, **98**(4), 1376-1380.
- [61] Maclean, J. and Ali, S. (2003) *Structure (Camb)*, **11**(12), 1499-1511.
- [62] Dias, M.V.; Borges, J.C.; Ely, F.; Pereira, J.H.; Canduri, F.; Ramos, C.H.; Frazzon, J.; Palma, M.S.; Basso, L.A.; Santos, D.S. and de Azevedo, W.F. Jr (2006) *J. Struct. Biol.*, **154**(2), 130-143.
- [63] Mousdale, D.M. and Coggins, J.R. (1991) in *Target sites for herbicide action* (Kirkwood, R.C., Ed.), Plenum Press, New York, pp. 29-56.
- [64] Balasubramanian, S.G.M.; Davies, G.M.; Coggins, J.R. and Abell, C. (1991) *J. Am. Chem. Soc.*, **113**, 8945-8946.
- [65] Davies, G.M.; Barrett-Bee, K.J.; Jude, D.A.; Lehan, M.; Nichols, W.W.; Pinder, P.E.; Thain, J.L.; Watkins, W.J. and Wilson, R.G. (1994) *Antimicrob. Agents Chemother.*, **38**(2), 403-406.
- [66] An, M.; Toochinda, T. and Bartlett, P.A. (2001) *J. Org. Chem.*, **66**(4), 1326-1333.
- [67] Montchamp, J.-L. and Frost, J.W. (1994) *J. Org. Chem.*, **59**, 7596-7601.
- [68] Montchamp, J.-L. and Frost, J.W. (1997) *J. Am. Chem. Soc.*, **119**(33), 7645-7653.
- [69] Srinivasan, P.R.; Katagiri, M. and Sprinson, D.B. (1959) *J. Biol. Chem.*, **234**(4), 713-715.
- [70] Srinivasan, P.R. and Sprinson, D.B. (1959) *J. Biol. Chem.*, **234**(4), 716-722.
- [71] Blattner, F.R.; Plunkett, G. 3rd; Bloch, C.A.; Perma, N.T.; Burland, V.; Riley, M.; Collado-Vides, J.; Glasner, J.D.; Rode, C.K.; Mayhew, G.F.; Gregor, J.; Davis, N.W.; Kirkpatrick, H.A.; Goeden, M.A.; Rose, D.J.; Mau, B. and Shao, Y. (1997) *Science*, **277**(5331), 1453-1474.
- [72] Herrmann, K.M. (1995) *Plant Physiol.*, **107**, 7-12.
- [73] Ogino, T.; Garner, C.; Markley, J.L. and Herrmann, K.M. (1982) *Proc. Natl. Acad. Sci. USA*, **79**(19), 5828-5832.
- [74] Wallace, B.J. and Pittard, J. (1967) *J. Bacteriol.*, **93**(1), 237-244.
- [75] Ray, J.M.; Yanofsky, C. and Bauerle, R. (1988) *J. Bacteriol.*, **170**(12), 5500-5506.
- [76] Pittard, J. and Gibson, B.J. (1970) *Curr. Top. Cell Regul.*, **2**, 29-63.
- [77] Herrmann, K.M. (1983) in *Amino Acids: Biosynthetic and Genetic Regulation* (Herrmann, K.M. and Somerville, R.L., Eds.), Addison-Wesley Publishing Co., Inc., Reading, MA, pp 301-322.
- [78] Wu, J.; Howe, D.L. and Woodard, R.W. (2003) *J. Biol. Chem.*, **278**(30), 27525-27531.
- [79] Schofield, L.R.; Patchett, M.L. and Parker, E.J. (2004) *Protein Expr. Purif.*, **34**(1), 17-27.
- [80] Huisman, O.C. and Kosuge, T. (1974) *J. Biol. Chem.*, **249**(21), 6842-6848.
- [81] Suzich, J.A.; Dean, J.F.D. and Herrmann, K.M. (1985) *Plant Physiol.*, **79**, 765-770.
- [82] Pinto, J.E.B.P.; Dyer, W.E.; Weller, S.C. and Herrmann, K.M. (1988) *Plant. Physiol.*, **87**, 891-893.
- [83] Shumilin, I.A.; Zhao, C.; Bauerle, R. and Kretsinger, R.H. (2002) *J. Mol. Biol.*, **320**, 1147-1156.
- [84] Walker, S.R. and Parker, E.J. (2006) *Bioorg. Med. Chem. Lett.*, **16**(11), 2951-2954.
- [85] Hu, C.Y. and Sprinson, D.B. (1977) *J. Bacteriol.*, **129**(1), 177-183.
- [86] Schoner, R. and Herrmann, K.M. (1976) *J. Biol. Chem.*, **251**(18), 5440-5447.
- [87] Ray, J.M. and Bauerle, R. (1991) *J. Bacteriol.*, **173**(6), 1894-1901.
- [88] McCandliss, R.J.; Poling, M.D. and Herrmann, K.M. (1978) *J. Biol. Chem.*, **253**(12), 4259-4265.
- [89] Simpson, R.J. and Davidson, B.E. (1976) *Eur. J. Biochem.*, **70**(2), 501-507.
- [90] Furdui, C.; Zhou, L.; Woodard, R.W. and Anderson, K.S. (2004) *J. Biol. Chem.*, **279**(44), 45618-45625.
- [91] McCandliss, R.J. and Herrmann, K.M. (1978) *Proc. Natl. Acad. Sci. USA*, **75**(10), 4810-4813.
- [92] Stephens, C.M. and Bauerle, R. (1991) *J. Biol. Chem.*, **266**(31), 20810-20817.
- [93] Baasov, T. and Knowles, J.R. (1989) *J. Bacteriol.*, **171**(11), 6155-6160.
- [94] Jordan, P.A.; Bohle, D.S.; Ramilo, C.A. and Evans, J.N. (2001) *Biochemistry*, **40**(28), 8387-8396.
- [95] Staub, M. and Denes, G. (1969) *Biochim. Biophys. Acta*, **178**(3), 599-608.
- [96] Sugimoto, S. and Shiio, I. (1980) *J. Biochem. (Tokyo)*, **87**(3), 881-890.
- [97] Subramaniam, P.S.; Xie, G.; Xia, T. and Jensen, R.A. (1998) *J. Bacteriol.*, **180**(1), 119-127.
- [98] Stephens, C.M. and Bauerle, R. (1992) *J. Biol. Chem.*, **267**(9), 5762-5767.
- [99] Sundaram, A.K.; Howe, D.L.; Sheflyan, G.Y. and Woodard, R.W. (1998) *FEBS Lett.*, **441**(2), 195-199.

- [100] Rizzi, C.; Frazzoni, J.; Ely, F.; Weber, P.G.; Fonseca, I.O.; Gallas, M.; Oliveira, J.S.; Mendes, M.A.; Souza, B.M.; Palma, M.S.; Santos, D.S. and Basso, L.A. (2005) *Protein Expr. Purif.*, **40**(1), 23-30.
- [101] Srinivasan, P.R.; Rothschild, J. and Sprinson, D.B. (1963) *J. Biol. Chem.*, **238**, 3176-3182.
- [102] Widlanski, T.; Bender, S.L. and Knowles, J.R. (1989) *J. Am. Chem. Soc.*, **111**, 2299-2300.
- [103] Bender, S.L.; Widlanski, T. and Knowles, J.R. (1989) *Biochemistry*, **28**(19), 7560-7572.
- [104] Lambert, J.M.; Boocock, M.R. and Coggins, J.R. (1985) *Biochem. J.*, **226**(3), 817-829.
- [105] Widlanski, T.; Bender, S.L. and Knowles, J.R. (1989) *Biochemistry*, **28**(19), 7572-82.
- [106] Chandran, S.S. and Frost, J.W. (2001) *Bioorg. Med. Chem. Lett.*, **11**(12), 1493-1496.
- [107] Bender, S.L.; Mehdi, S. and Knowles, J.R. (1989) *Biochemistry*, **28**(19), 7555-7560.
- [108] Moore, J.D.; Skinner, M.A.; Swatman, D.R.; Hawkins, A.R. and Brown, K.A. (1998) *J. Am. Chem. Soc.*, **120**(28), 7105-7106.
- [109] Skinner, M.A.; Gunel-Ozcan, A.; Moore, J.; Hawkins, A.R. and Brown, K.A. (1997) *Biochem. Soc. Trans.*, **25**(4), S609.
- [110] Hasan, N. and Nester, E.W. (1978) *J. Biol. Chem.*, **253**(14), 4999-5004.
- [111] Piehler, L.T.; Montchamp, J.-L.; Frost, J.W. and Manly, C.J. (1991) *Tetrahedron*, **47**, 2423.
- [112] Moore, J.D.; Coggins, J.R.; Viriden, R. and Hawkins, A.R. (1994) *Biochem. J.*, **301**(Pt 1), 297-304.
- [113] Garbe, T.; Servos, S.; Hawkins, A.; Dimitriadis, G.; Young, D.; Dougan, G. and Charles, I. (1991) *Mol. Gen. Genet.*, **228**(3), 385-392.
- [114] Mitsuhashi, S. and Davis, B.D. (1954) *Biochim. Biophys. Acta*, **15**(1), 54-61.
- [115] Davis, B.D. and Weiss, U. (1953) *Arch. Exp. Pathol. Pharmacol.*, **220**(Suppl), 1-15.
- [116] Kleanthous, C.; Deka, R.; Davis, K.; Kelly, S.M.; Cooper, A.; Harding, S.E.; Price, N.C.; Hawkins, A.R. and Coggins, J.R. (1992) *Biochem. J.*, **282**(Pt 3), 687-695.
- [117] Harris, J.M.; Gonzalez-Bello, C.; Kleanthous, C.; Hawkins, A.R.; Coggins, J.R. and Abell, C. (1996) *Biochem. J.*, **319**, 333-336.
- [118] Giles, N.H.; Case, M.E.; Baum, J.; Geever, R.; Huiet, L.; Patel, V. and Tyler, B. (1985) *Microbiol. Rev.*, **49**(3), 338-358.
- [119] Chaudhuri, S.; Lambert, J.M.; McColl, L.A. and Coggins, J.R. (1986) *Biochem. J.*, **239**(3), 699-704.
- [120] Chaudhuri, S.; Duncan, K. and Coggins, J.R. (1987) *Methods Enzymol.*, **142**, 320-324.
- [121] Polley, L.D. (1978) *Biochim. Biophys. Acta*, **526**(1), 259-266.
- [122] Koshiya, T. (1978) *Biochim. Biophys. Acta*, **522**(1), 10-18.
- [123] Mousdale, D.M.; Campbell, M.S. and Coggins, J.R. (1987) *Phytochem.*, **26**, 2665-2670.
- [124] Gaertner, F.H. and Cole, K.W. (1977) *Biochem. Biophys. Res. Commun.*, **75**(2), 259-264.
- [125] Herrmann, K.M. and Weaver, L.M. (1999) *Annu. Rev. Plant Physiol. Plant Mol. Biol.*, **50**, 473-503.
- [126] Hautala, J.A.; Jacobson, J.W.; Case, M.E. and Giles, N.H. (1975) *J. Biol. Chem.*, **250**(15), 6008-6014.
- [127] Florova, G.; Denoya, C.D.; Morgenstern, M.R.; Skinner, D.D. and Reynolds, K.A. (1998) *Arch. Biochem. Biophys.*, **350**(2), 298-306.
- [128] Hawkins, A.R.; Giles, N.H. and Kinghorn, J.R. (1982) *Biochem. Genet.*, **20**(3-4), 271-286.
- [129] Euverink, G.J.; Hessels, G.I.; Vrijbloed, J.W.; Coggins, J.R. and Dijkhuizen, L. (1992) *J. Gen. Microbiol.*, **138**(Pt 11), 2449-2457.
- [130] Harris, J.; Kleanthous, C.; Coggins, J.R.; Hawkins, A.R. and Abell, C. (1993) *J. Chem. Soc. Chem. Commun.*, **13**, 1080-1081.
- [131] Bottomley, J.R.; Hawkins, A.R. and Kleanthous, C. (1996) *Biochem. J.*, **319**(Pt 1), 269-278.
- [132] Deka, R.K.; Kleanthous, C. and Coggins, J.R. (1992) *J. Biol. Chem.*, **267**, 22237-22242.
- [133] Chaudhuri, S.; Duncan, K.; Graham, L.D. and Coggins, J.R. (1991) *Biochem. J.*, **275**(Pt 1), 1-6.
- [134] Moore, J.D.; Lamb, H.K.; Garbe, T.; Servos, S.; Dougan, G.; Charles, I.G. and Hawkins, A.R. (1992) *Biochem. J.*, **287**(Pt 1), 173-181.
- [135] White, P.J.; Young, J.; Hunter, I.S.; Nimmo, H.G. and Coggins, J.R. (1990) *Biochem. J.*, **265**(3), 735-738.
- [136] Price, N.C.; Boam, D.J.; Kelly, S.M.; Duncan, D.; Krell, T.; Gourley, D.G.; Coggins, J.R.; Viriden, R. and Hawkins, A.R. (1999) *Biochem. J.*, **338**, 195-202.
- [137] Krell, T.; Horsburgh, M.J.; Cooper, A.; Kelly, S.M. and Coggins, J.R. (1996) *J. Biol. Chem.*, **271**(40), 24492-24497.
- [138] Gourley, D.G.; Coggins, J.R.; Isaacs, N.W.; Moore, J.D.; Charles, I.G. and Hawkins, A.R. (1994) *J. Mol. Biol.*, **241**, 488-491.
- [139] Robinson, D.A.; Stewart, K.A.; Price, N.C.; Chalk, P.A.; Coggins, J.R. and Laphorn, A.J. (2006) *J. Med. Chem.*, **49**(4), 1282-1290.
- [140] Frederickson, M.; Parker, E.J.; Hawkins, A.R.; Coggins, J.R. and Abell, C. (1999) *J. Org. Chem.*, **64**, 2612-2613.
- [141] Evans, L.D.; Roszak, A.W.; Noble, L.J.; Robinson, D.A.; Chalk, P.A.; Matthews, J.L.; Coggins, J.R.; Price, N.C. and Laphorn, A.J. (2002) *FEBS Lett.*, **530**(1-3), 24-30.
- [142] Sanchez-Sixto, C.; Prazeres, V.F.; Castedo, L.; Lamb, H.; Hawkins, A.R. and Gonzalez-Bello, C. (2005) *J. Med. Chem.*, **48**(15), 4871-4881.
- [143] Yaniv, H. and Gilvarg, C. (1955) *J. Biol. Chem.*, **213**(2), 787-795.
- [144] Chaudhuri, S. and Coggins, J.R. (1985) *Biochem. J.*, **226**(1), 217-223.
- [145] Baillie, A.C.; Corbett, J.R.; Dowsett, J.R. and McCloskey, P. (1972) *Biochem. J.*, **126**(3), 21P.
- [146] Baillie, A.C.; Corbett, J.R.; Dowsett, J.R. and McCloskey, P. (1972) *Pesticide Sci.*, **3**, 113-120.
- [147] Magalhaes, M.L.; Pereira, C.P.; Basso, L.A. and Santos, D.S. (2002) *Protein Expr. Purif.*, **26**(1), 59-64.
- [148] Johnson, B.H. and Hecht, M.H. (1994) *Biotechnology (NY)*, **12**(13), 1357-1360.
- [149] Fonseca, I.O.; Magalhaes, M.L.; Oliveira, J.S.; Silva, R.G.; Mendes, M.A.; Palma, M.S.; Santos, D.S. and Basso, L.A. (2006) *Protein Expr. Purif.*, **46**(2), 429-437.
- [150] Morell, H. and Sprinson, D.B. (1968) *J. Biol. Chem.*, **243**(3), 676-677.
- [151] Ely, B. and Pittard, J. (1979) *J. Bacteriol.*, **138**(3), 933-943.
- [152] Lobner-Olesen, A. and Marinus, M.G. (1992) *J. Bacteriol.*, **174**(2), 525-529.
- [153] Whipp, M.J. and Pittard, A.J. (1995) *J. Bacteriol.*, **177**(6), 1627-1629.
- [154] DeFeyter, R.C. and Pittard, J. (1986) *J. Bacteriol.*, **165**(1), 226-232.
- [155] Griffin, H.G. and Gasson, M.J. (1995) *DNA Seq.*, **5**(3), 195-197.
- [156] DeFeyter, R.C. and Pittard, J. (1986) *J. Bacteriol.*, **165**(1), 331-333.
- [157] Weiss, U. and Edwards, J.M. (1980) *The biosynthesis of aromatic compounds*, John Wiley and Sons, New York, pp. 103-133.
- [158] Gollub, E.; Zalkin, H. and Sprinson, D.B. (1967) *J. Biol. Chem.*, **242**(22), 5323-5328.
- [159] Lobner-Olesen, A.; Boye, E. and Marinus, M.G. (1992) *Mol. Microbiol.*, **6**(13), 1841-1851.
- [160] DeFeyter, R.C.; Davidson, B.E. and Pittard, J. (1986) *J. Bacteriol.*, **165**(1), 233-239.
- [161] Vinella, D.; Gagny, B.; Joseleau-Petit, D.; D'Ari, R. and Cashel, M. (1996) *J. Bacteriol.*, **178**(13), 3818-3828.
- [162] Griffin, H.G. and Gasson, M.J. (1995) *Mol. Gen. Genet.*, **246**(1), 119-127.
- [163] Pereira, J.H.; Oliveira, J.S.; Canduri, F.; Dias, M.V.; Palma, M.S.; Basso, L.A.; Santos, D.S. and de Azevedo, W.F. Jr (2004) *Acta Crystallogr. D Biol. Crystallogr.*, **60**(Pt 12 Pt 2), 2310-2319.
- [164] Dhaliwal, B.; Nichols, C.E.; Ren, J.; Lockyer, M.; Charles, I.; Hawkins, A.R. and Stammers, D.K. (2004) *FEBS Lett.*, **574**(1-3), 49-54.
- [165] de Azevedo, W.F. Jr; Canduri, F.; Oliveira, J.S.; Basso, L.A.; Palma, M.S.; Pereira, J.H. and Santos, D.S. (2002) *Biochem. Biophys. Res. Commun.*, **295**(1), 142-148.
- [166] Jencks, W.P. (1975) *Adv. Enzymol. Relat. Areas Mol. Biol.*, **43**, 219-410.
- [167] Oliveira, J.S.; Pinto, C.A.; Basso, L.A. and Santos, D.S. (2001) *Protein Expr. Purif.*, **22**(3), 430-435.
- [168] Levin, J.G. and Sprinson, D.B. (1960) *Biochem. Biophys. Res. Commun.*, **3**, 157-163.
- [169] Levin, J.G. and Sprinson, D.B. (1964) *J. Biol. Chem.*, **239**, 1142-1150.
- [170] Bondinell, W.E.; Vnek, J.; Knowles, P.F.; Sprecher, M. and Sprinson, D.B. (1971) *J. Biol. Chem.*, **246**(20), 6191-6196.
- [171] Lewendon, A. and Coggins, J.R. (1983) *Biochem. J.*, **213**(1), 187-191.
- [172] Steirnücken, H.C. and Amrhein, N. (1980) *Biochem. Biophys. Res. Commun.*, **94**(4), 1207-1212.

- [173] Boocock, M.R. and Coggins, J.R. (1983) *FEBS Lett.*, **154**(1), 127-133.
- [174] Sammons, R.D.; Gruys, K.J.; Anderson, K.S.; Johnson, K.A. and Sikorski, J.A. (1995) *Biochemistry*, **34**, 6433-6440.
- [175] McDowell, L.M.; Klug, C.A.; Beusen, D.D. and Schaefer, J. (1996) *Biochemistry*, **35**, 5395-5403.
- [176] Jaworski, E.G. (1972) *J. Agr. Food Chem.*, **20**, 1195-1198.
- [177] Rogers, S.G.; Brand, L.A.; Holder, S.B.; Sharps, E.S. and Brackin, M.J. (1983) *Appl. Environ. Microbiol.*, **46**, 37-43.
- [178] Funke, T.; Han, H.; Healy-Fried, M.L.; Fischer, M. and Schonbrunn, E. (2006) *Proc. Natl. Acad. Sci. USA*, **103**(35), 13010-13015.
- [179] Padgett, S.R.; Re, D.B.; Gasser, C.S.; Eichholtz, D.A.; Frazier, R.B.; Hironaka, C.M.; Levine, E.B.; Shah, D.M.; Fraley, R.T. and Kishore, G.M. (1991) *J. Biol. Chem.*, **266**(33), 22364-22369.
- [180] Anderson, K.S., and Johnson, K.A. (1990) *Chem. Rev.*, **90**, 1131-1149.
- [181] Miller, M.J.; Braccolino, D.S.; Cleary, D.G.; Ream, J.E.; Walker, M.C. and Sikorski, J.A. (1994) *Bioorg. Med. Chem. Lett.*, **21**, 2605-2608.
- [182] Miller, M.J.; Cleary, D.G.; Ream, J.E.; Snyder, K.R. and Sikorski, J.A. (1995) *Bioorg. Med. Chem.*, **3**, 1685-1692.
- [183] Shah, A.; Font, J.L.; Miller, M.J.; Ream, J.E.; Walker, M.C. and Sikorski, J.A. (1997) *Bioorg. Med. Chem.*, **5**, 323-334.
- [184] Garbe, T.; Jones, C.; Charles, I.; Dougan, G. and Young, D. (1990) *J. Bacteriol.*, **172**(12), 6774-6782.
- [185] Oliveira, J.S.; Mendes, M.A.; Palma, M.S.; Basso, L.A. and Santos, D.S. (2003) *Protein Expr. Purif.*, **28**(2), 287-292.
- [186] Borges, J.C.; Pereira, J.H.; Vasconcelos, I.B.; dos Santos, G.C.; Olivieri, J.R.; Ramos, C.H.; Palma, M.S.; Basso, L.A.; Santos, D.S. and de Azevedo, W.F. Jr (2006) *Arch. Biochem. Biophys.*, **452**(2), 156-164.
- [187] Balasubramanian, S.; Abell, C. and Coggins, J.R. (1990) *J. Am. Chem. Soc.*, **112**, 8581-8583.
- [188] Hawkes, T.R.; Lewis, T.; Coggins, J.R.; Mousedale, D.M.; Lowe, D.J. and Thorneley, R.N.F. (1990) *Biochem. J.*, **265**, 899-902.
- [189] Morell, H.; Clark, M.J.; Knowles, P.F. and Sprinson, D.B. (1967) *J. Biol. Chem.*, **242**(1), 82-90.
- [190] White, J.; Millar, G. and Coggins, J.R. (1988) *Biochem. J.*, **251**, 313-322.
- [191] Dias, M.V.; Ely, F.; Canduri, F.; Pereira, J.H.; Frazzon, J.; Basso, L.A.; Palma, M.S.; de Azevedo, W.F. Jr and Santos, D.S. (2004) *Acta Crystallogr. D Biol. Crystallogr.*, **60**(Pt 11), 2003-2005.
- [192] Terwilliger, T.C.; Park, M.S.; Waldo, G.S.; Berendzen, J.; Hung, L.W.; Kim, C.Y.; Smith, C.V.; Sacchettini, J.C.; Bellinzoni, M.; Bossi, R.; De Rossi, E.; Mattevi, A.; Milano, A.; Riccardi, G.; Rizzi, M.; Roberts, M.M.; Coker, A.R.; Fossati, G.; Mascagni, P.; Coates, A.R.; Wood, S.P.; Goulding, C.W.; Apostol, M.I.; Anderson, D.H.; Gill, H.S.; Eisenberg, D.S.; Taneja, B.; Mande, S.; Pohl, E.; Lamzin, V.; Tucker, P.; Wilmanns, M.; Colovos, C.; Meyer-Klaucke, W.; Munro, A.W.; McLean, K.J.; Marshall, K.R.; Leys, D.; Yang, J.K.; Yoon, H.J.; Lee, B.I.; Lee, M.G.; Kwak, J.E.; Han, B.W.; Lee, J.Y.; Baek, S.H.; Suh, S.W.; Komen, M.M.; Arcus, V.L.; Baker, E.N.; Lott, J.S.; Jacobs, W. Jr.; Alber, T. and Rupp, B. (2003) *Tuberculosis (Edinb)*, **83**(4), 223-249.

## 9. CURRICULUM VITAE resumido

DUCATI, R. G.

### 1. DADOS PESSOAIS

**Nome:** Rodrigo Gay Ducati

**Local e data de nascimento:** Strasbourg, França - 09/05/1980

**Endereço profissional:** Avenida Ipiranga, 6681 - Prédio 92A - Partenon  
Porto Alegre, RS - Brasil CEP 90619-900 Caixa Postal 1429.

**Telefone profissional:** (51)33203629

**E-mail:** rodrigoducati@yahoo.com.br

### 2. FORMAÇÃO:

2005-2009: Doutorado em Biologia Celular e Molecular pela Universidade Federal do Rio Grande do Sul (UFRGS). *Título tese:* Especificidade de substrato e mecanismo cinético da enzima fosforilase de nucleosídeos purínicos de *Mycobacterium tuberculosis*. *Orientador:* Luiz Augusto Basso. *Agência de fomento:* Coordenação de Aperfeiçoamento de Pessoal de Nível Superior (CAPES) e Conselho Nacional de Desenvolvimento Científico e Tecnológico (CNPq).

2003-2005: Mestrado em Genética e Biologia Molecular pela Universidade Federal do Rio Grande do Sul (UFRGS). *Título dissertação:* Caracterização do gene hisD de *Mycobacterium tuberculosis* H37Rv: clonagem, seqüenciamento, superexpressão e medidas de atividade enzimática do seu produto - a proteína histidinol desidrogenase. *Orientador:* Diógenes Santiago Santos e Luiz Augusto Basso. *Agência de fomento:* Coordenação de Aperfeiçoamento de Pessoal de Nível Superior (CAPES).

1998-2004: Graduação em Licenciatura em Ciências Biológicas pela Universidade Federal do Rio Grande do Sul (UFRGS).

1998-2002: Graduação em Bacharelado em Ciências Biológicas pela Universidade Federal do Rio Grande do Sul (UFRGS). *Título monografia:* *Mycobacterium tuberculosis*: o mensageiro da morte. *Orientador:* Diógenes Santiago Santos.

### 3. ESTÁGIOS:

2001-2003: Aluno de iniciação científica do Grupo de Microbiologia Molecular e Funcional do Departamento de Biologia Molecular e Biotecnologia da Universidade Federal do Rio Grande do Sul (UFRGS). *Atividades desenvolvidas:* aperfeiçoamento de técnicas laboratoriais e aprofundamento de conhecimentos em microbiologia, biologia molecular e bioquímica. *Orientadores:* Prof. Dr. Diógenes Santiago Santos e Prof. Dr. Luiz Augusto Basso.

2000-2001: Bolsista de iniciação científica do Laboratório de Crustáceos do Departamento de Zoologia e do Laboratório de Ecotoxicologia do Centro de Ecologia da Universidade Federal do Rio Grande do Sul (UFRGS). *Atividades desenvolvidas:* Executante do projeto Avaliação da sensibilidade de *Aegla platensis*, uma espécie nativa do Rio Grande do Sul, visando seu uso como organismo-teste em testes de toxicidade. *Orientadores:* Profa. Dra. Georgina Bond-Buckup e Dr. Alexandre Arenzon (co-orientador). *Agência de fomento:* Fundação de Amparo à Pesquisa do Rio Grande do Sul (FAPERGS).

#### 4. ARTIGOS COMPLETOS PUBLICADOS

- DUCATI, R. G.; SANTOS, D. S. & BASSO, L. A. Substrate specificity and kinetic mechanism of purine nucleoside phosphorylase from *Mycobacterium tuberculosis*. *Arch. Biochem. Biophys.* (no prelo).
- TIMMERS, L. F.; CACERES, R. A.; VIVAN, A. L.; GAVA, L. M.; DIAS, R.; DUCATI, R. G.; BASSO, L. A.; SANTOS, D. S. & DE AZEVEDO, W. F., JR Structural studies of human purine nucleoside phosphorylase: towards a new specific empirical scoring function. *Arch. Biochem. Biophys.*, 479(1): 28-38, 2008.
- DUCATI, R. G.; BASSO, L. A. & SANTOS, D. S. Mycobacterial shikimate pathway enzymes as targets for drug design. *Curr. Drug Targets*, 8(3): 423-435, 2007.
- DUCATI, R. G.; RUFFINO-NETTO, A.; BASSO, L. A. & SANTOS, D. S. The resumption of consumption - a review on tuberculosis. *Mem. Inst. Oswaldo Cruz*, 101(7): 697-714, 2006.

#### 5. RESUMOS E TRABALHOS APRESENTADOS EM CONGRESSOS

- 2008: TIMMERS, L. F.; CACERES, R. A.; VIVAN, A. L.; GAVA, L. M.; DIAS, R.; DUCATI, R. G.; BASSO, L. A.; SANTOS, D. S. & DE AZEVEDO, W. F., JR Estudo estrutural da Purina Nucleosídeo Fosforilase Humana e uma nova função escore empírica específica, IX Salão de Iniciação Científica da Pontifícia Universidade Católica do Rio Grande do Sul (PUCRS), Porto Alegre, RS.
- 2006: KERSCHKE, P. L. C.; DUCATI, R. G.; FONSECA, I. O.; SCHNEIDER, C. Z.; BASSO, L. A. & SANTOS, D.S. Characterization of the *tyrA* Gene from *Mycobacterium tuberculosis* H37Rv: Cloning, Sequencing and Expression of Its Product - the Prephenate Dehydrogenase Enzyme, XXXV Reunião Anual da Sociedade Brasileira de Bioquímica e Biologia Molecular (SBBq), Águas de Lindóia, SP.
- 2005: DUCATI, R. G.; BASSO, L. A. & SANTOS, D. S. Molecular Cloning and Expression of Functional Histidinol Dehydrogenase (EC 1.1.1.23) from *Mycobacterium tuberculosis* H37Rv, XXXIV Reunião Anual da Sociedade Brasileira de Bioquímica e Biologia Molecular (SBBq), Águas de Lindóia, SP.
- 2004: VIVAN, A. L.; SCHNEIDER, C. Z.; DUCATI, R. G.; BASSO, L. A.; SANTOS, D. S. Expression of Functional Prephenate Dehydratase from *Mycobacterium tuberculosis* H37Rv, XXXIII Reunião Anual da Sociedade Brasileira de Bioquímica e Biologia Molecular (SBBq), Caxambu, MG.
- 2003: DUCATI, R. G.; VIVAN, A. L.; SCHNEIDER, C. Z.; BASSO, L. A. & SANTOS, D. S. Cloning, Sequencing and Overexpression of the *tyrA* Gene from *Mycobacterium tuberculosis* H37Rv, XXII Congresso Brasileiro de Microbiologia, Florianópolis, SC.
- 2003: VIVAN, A. L.; SCHNEIDER, C. Z.; DUCATI, R. G.; BASSO, L. A. & SANTOS, D. S. Cloning of the *pheA* Gene from *Mycobacterium tuberculosis* H37Rv and Overexpression of the Prephenate Dehydratase Enzyme, XXII Congresso Brasileiro de Microbiologia, Florianópolis, SC.
- 2003: DUCATI, R. G.; SCHNEIDER, C. Z.; BASSO, L. A. & SANTOS, D. S. Amplification, Cloning and Sequencing of the *tyrA* Gene from *Mycobacterium tuberculosis* H37Rv, XXXII Reunião Anual da Sociedade Brasileira de Bioquímica e Biologia Molecular (SBBq), Caxambu, MG.